Active

roject #: E-16-X11   Cost share #: E-16-373   Rev #: 4
enter # : 10/24-6-R7955-0A0   Center shr #: 10/22-1-F7955-0A0   OCA file #:
                                                                Work type : RES
ontract#: OSP-92-10-668-007   Mod #: 2   Document : SUBCONT
rime   #: DAAL03-92-G-0380   Contract entity: GTRC

ubprojects ? : N   CFDA: N/A
lain project #:   PE #: N/A

roject unit: AERO ENGR   Unit code: 02.010.110
roject director(s):
   ARMANIOS E A   AERO ENGR   (404)894-8202

ponsor/division names: CLARK ATLANTA UNIVERSITY   / ATLANTA, GA
ponsor/division codes: 400   / 094

ward period: 930101   to   950927 (performance)   950927 (reports)

ponsor amount   New this change   Total to date
     Contract value   47,590.00   137,350.00
     Funded   47,590.00   137,350.00
ost sharing amount   11,779.00

loes subcontracting plan apply ?: N

itle: ADVANCED COMPOSITES AND SMART STRUCTURES RESEARCH

PROJECT ADMINISTRATION DATA

)CA contact: Ina R. Lashley   894-4820

Sponsor technical contact   Sponsor issuing office

DR. LEBONE MOETI   VANNESSA DANIELS
(404)880-8907   (404)880-6071

CLARK ATLANTA UNIVERSITY   CLARK ATLANTA UNIVERSITY
221 JAMES P BRAWLEY DR., S.W.   OFFICE OF SPONSORED PROGRAMS
ATLANTA, GA 30324   221 JAMES P BRAWLEY DR., S.W.
                                       ATLANTA, GA 30324

ecurity class (U,C,S,TS) : U   ONR resident rep. is ACO (Y/N): N
)efense priority rating   :   N/A   N/A supplemental sheet
:quipment title vests with: Sponsor   GIT
   NONE PROPOSED. PRIOR APPROVAL REQUIRED IF ANY PURCHASED.
\dministrative comments -
   AMENDMENT #2 ADDS $47,590 NEW FUNDS ($4,082 COST-SHARE REQUIRED), AND EXTENDS
' PERIOD OF PERFORMANCE TO 9/27/95.

GEORGIA INSTITUTE OF TECHNOLOGY
OFFICE OF CONTRACT ADMINISTRATION

NOTICE OF PROJECT CLOSEOUT

Closeout Notice Date 11/08/95

Project No. E-16-X11_____   Center No. 10/24-6-R7955-0A0_

Project Director ARMANIOS E A_____   School/Lab AERO ENGR_____

Sponsor CLARK ATLANTA UNIVERSITY/ATLANTA, GA_____

Contract/Grant No. OSP-92-10-668-007_____   Contract Entity GTRC

Prime Contract No. DAAL03-92-G-0380_____

Title ADVANCED COMPOSITES AND SMART STRUCTURES RESEARCH_____

Effective Completion Date 950927 (Performance) 950927 (Reports)

Closeout Actions Required:	Y/N	Date Submitted
Final Invoice or Copy of Final Invoice	Y	_____
Final Report of Inventions and/or Subcontracts	Y	_____
Government Property Inventory & Related Certificate	Y	_____
Classified Material Certificate	N	_____
Release and Assignment	N	_____
Other _____	N	_____

Comments_____

Subproject Under Main Project No. _____

Continues Project No. _____

Distribution Required:

Project Director	Y
Administrative Network Representative	Y
GTRI Accounting/Grants and Contracts	Y
Procurement/Supply Services	Y
Research Property Managment	Y
Research Security Services	N
Reports Coordinator (OCA)	Y
GTRC	Y
Project File	Y
Other _____	N
_____	N

NOTE: Final Patent Questionnaire sent to PDPI.

STATUS REPORT

ADVANCED COMPOSITES AND SMART STRUCTURES RESEARCH

GRANT : DAAL03-92-G-380
GEORGIA TECH PROJECT: E16-X11

PRINCIPAL INVESTIGATOR
E. A. Armanios
School of Aerospace Engineering
Georgia Institute of Technology
Atlanta GA 30332-0150

Sponsor Technical Contact: DR. LEBONE MOETI
Clark Atlanta University
221 James P. Brawley Dr., S.W.
Atlanta, GA 30324

Problem studied

The primary objective of this research is the development of analytical tools, testing methods and smart concepts for advanced composite structures.

Progress during this reporting period

During this reporting period progress was made on the development of testing methods for elastically tailored laminated composites with extension-twist coupling.

Background: Elastically tailored composite laminates offer structural designers new degrees of freedom. With the use of materials that exhibit a coupled behavior such as extension-twist or bend-twist coupling, new, more efficient structural designs can be produced. However, while such laminates can be easily designed, testing can be a challenging task. Commonly available universal testing machines are not equipped to handle a second degree of freedom and bi-axial testing machines are quite expensive and less frequently available.

Test Methods: Four different methods of testing extension-twist coupled specimens are being developed. The first, is a rotational transducer to be used in a universal testing machine as a substitute for a loading grip. The transducer gives rotational angle as an output voltage proportional to the angle of twist. A schematic of this design appears in Figure 1. This design was found to induce a torsional restraining moment as the applied load was increased. This issue is addressed in some detail in the following section.

The second method is modified version of the rotational transducer that use an air bearing design in order to eliminate any torsional restraint. The third, is a dynamic loading frame which allows a completely free end condition for the test coupon during the loading sequence while accurate measurements of twist angle are taken. This design is suitable for isolating the aerodynamic contribution to the loading and simulates helicopter rotor blade behavior for closed cross section composites. The fourth method is a stand-alone apparatus that applies a known rotation to a composite laminate while the change in specimen length is measured.
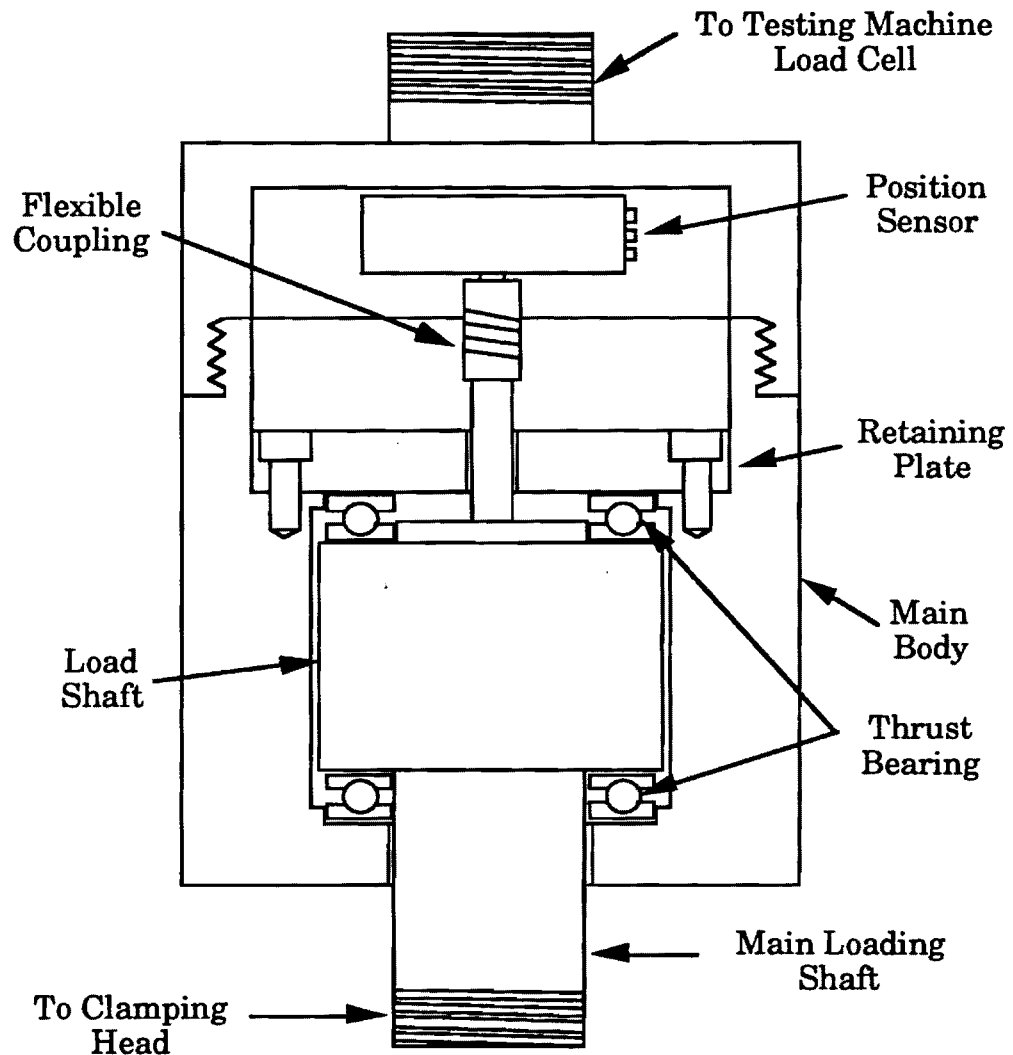
Figure 1. Transducer cross-section

Rotational Transducer Design and Test

This design provides an economical and a reliable and repeatable means for testing elastically tailored composite specimens without the need for an expensive bi-axial loading platform. The transducer is unique in that it allows freedom of twist at the end of the specimen while undergoing

axial load, yielding an instrument that is capable of accurately measuring the specimen end twist angle. One end of the specimen is clamped to the transducer while the other is fixed in a standard, Instron produced serrated clamp. A schematic of the transducer cross section appears in Figure 1.

Specimen Fabrication

The specimens for all the tests were made with Hercules AS4/3502 graphite/epoxy pre-impregnated sheets. After curing and trimming, final specimen dimensions were 0.9" x 11.75". The stacking sequence is given by

$$[\theta/(\theta-90)_2/\theta/-\theta/(90-\theta)_2/-\theta]_T \qquad (1)$$

with angle θ varying from 10° to 80° at 10° intervals. Four specimens were fabricated for each value of θ.

Test Results

Tests showed that a sample size of four specimens gives closely grouped data without excess scatter. Therefore, the results of each configuration tested herein are the average of the results of four specimens. The material constants, E_{11}, E_{22}, G_{12}, v_{12}, and v_{21} were determined by measuring strains in $[0]_8$, $[90]_8$, and $[45]_8$ specimens. The measured material properties are summarized in Table I.

Table I. Material properties

$E_{11} = 19$ Msi

$E_{22} = 1.54$ Msi

$G_{12} = 0.86$ Msi

$v_{12} = 0.33$

In the testing procedure, the specimen is placed in the test machine and any initial offsets are removed. Data acquisition is accomplished via a Keithley Series 500 analog to digital converter and amplifier system connected to an IBM PC-AT. The test procedure is to manually apply a constant end lengthening until a pre-determined load is reached. When this load is reached, the computer samples the load and the end twist of the specimen. This procedure is then repeated until a number of data points are taken. For the tests presented here, the maximum load applied is 350 lb.

The resulting data are shown in Figures 2 and 3. Figure 2 shows the laminate with $\theta=30°$. The slope of the least squares line through the data is

3

150.9 lb/°/in. This slope is the average of the slopes of the least squares fit lines through each of the four data sets. Figure 3 shows the extension-twist coupling as a function of angle θ .
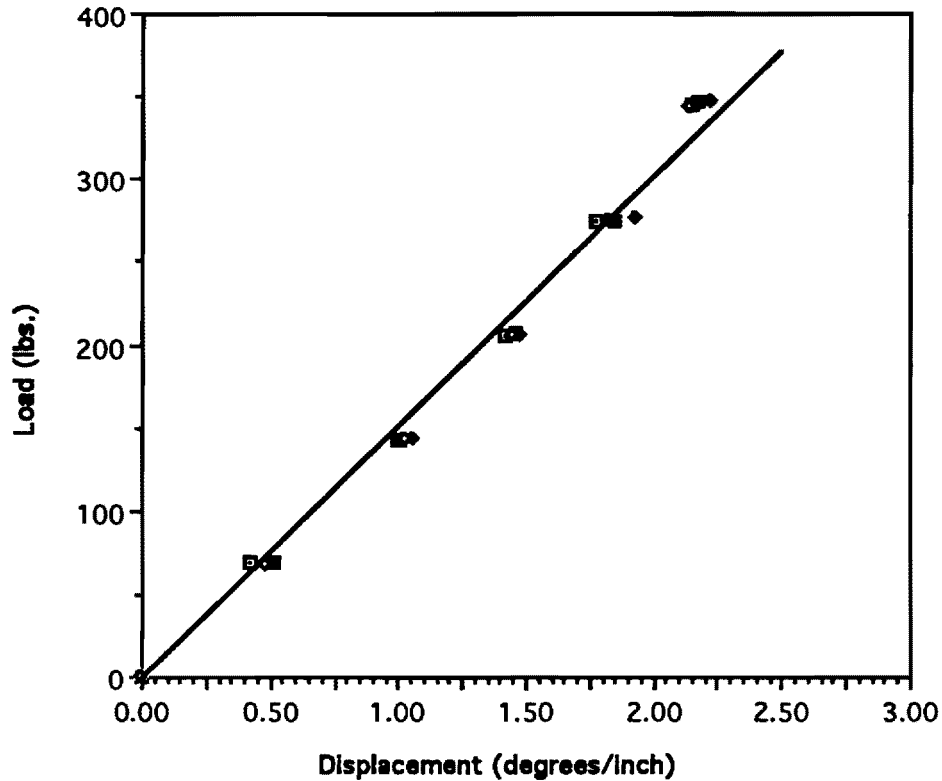

Figure 2 Extension-twist for laminate with θ=30°

The least square fit equations are provided along with the R^2 values·

Comparison of Predictions

Initial tests of the laminate showed that the experimental coupling was less than the theoretical prediction by a significant amount. Errors in manufacture of the specimens were considered as were proper calibration and set-up of the transducer. However, none of these considerations would have the large effect at hand. The transducer was then checked for a torsional restraining moment as the load was increased through the range used in testing. While the restraining moment is small, the effects are not negligible when compared to the torsional rigidity of the test specimen. Therefore the restraining moment was measured and plotted as a function of applied tensile load. The resulting plot, appearing in Figure 4, is linear and the slope of the least squares fit line through the data can be used in the theoretical analysis where the transducer is modeled as a torsional spring. The magnitude of the restraining moment at zero tensile load is due to the resistance of the position sensor.
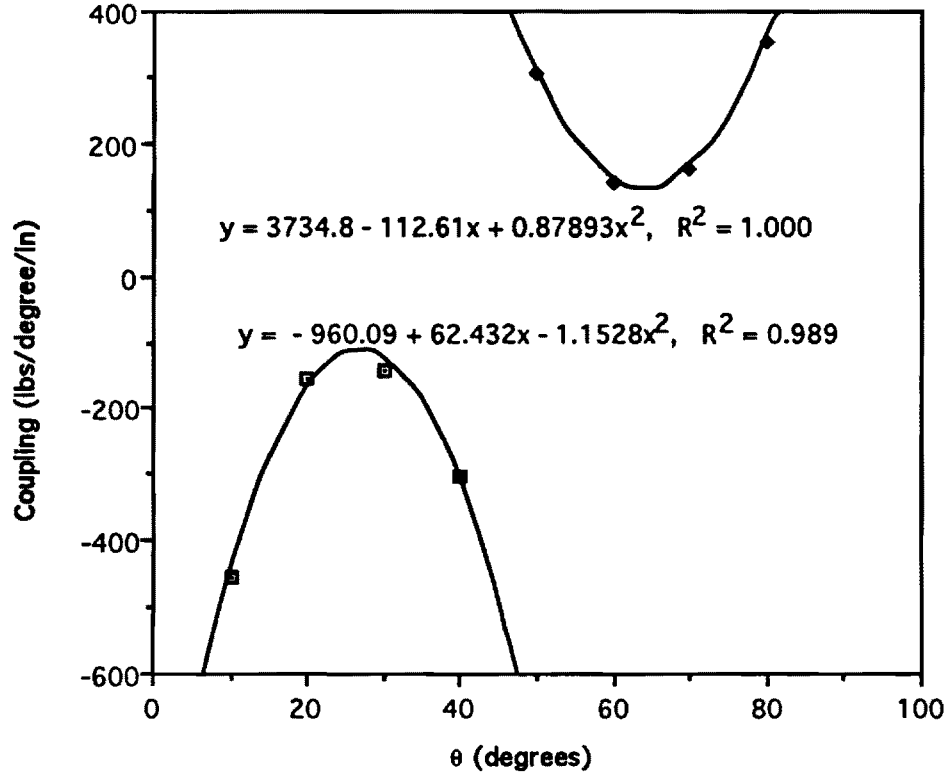
4

Figure 3. Extension-twist data at various angle θ.

The boundary conditions applied to the tested specimens are modified to reflect the restraining torsional moment proportional to the applied tensile load. From the test data of Figure 4, the coefficient of proportionality, ψ, between the applied axial load and restraining moment is ±0.001705 inch. The Shear Deformation Theory (SDT) of Reference 1 is modified to reflect this influence when predicting the extension-twist coupling.

For the class of laminates given in Eq.(1), ψ is negative for $0<\theta<45°$ and positive for $45°<\theta<90°$. A comparison between the predictions of the SDT [1] and Classical Lamination Theory (CLT) for $\theta=10°$ to $80°$ at $10°$ intervals is provided in Table II.

Table II. Predictions of extension-twist coupling from SDT and CLT

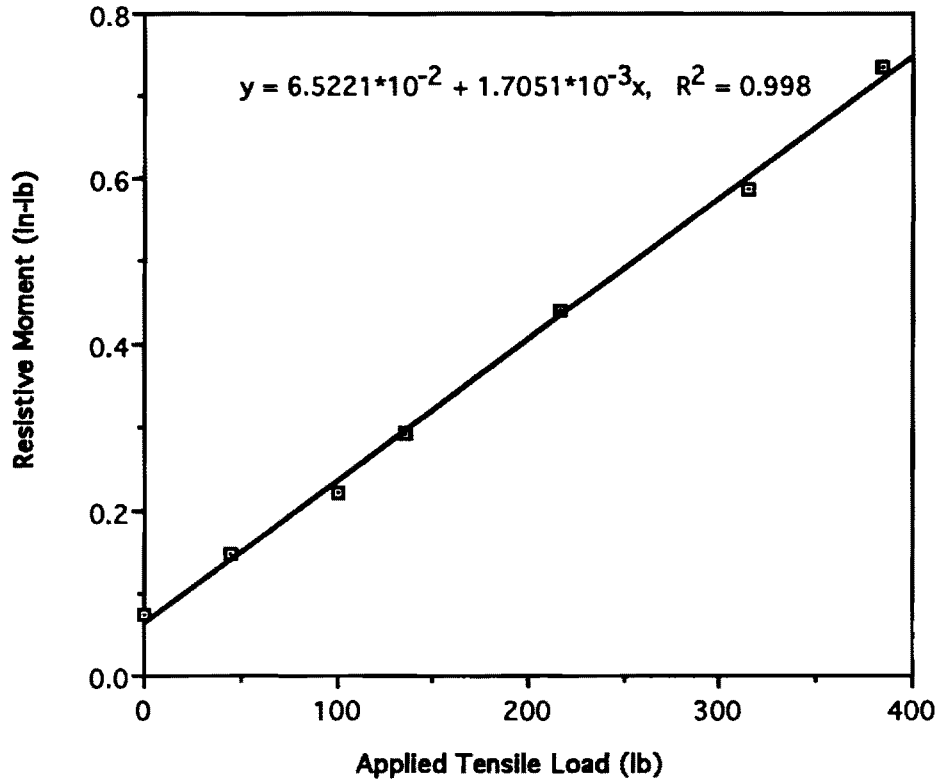| θ	10°	20°	30°	40°	50°	60°	70°	80°
SDT	0.00676	0.01603	0.01676	0.00715	-0.00715	-0.01676	-0.01603	-0.00676
CLT	0.00702	0.01622	0.01691	0.00728	-0.00728	-0.01691	-0.01622	-0.00702

Figure 4. Plot of restraining torsional moment versus applied tensile load

It is seen that the shear deformation contribution to the extension-twist coupling is negligible in this class of laminates.

The CLT predictions along with test data are shown in Figure 5. Also appearing in the figure is the CLT prediction which neglects the effect of the torsional restraining moment denoted by "CLT-Unrestrained." It is seen that the torsional restraining moment has a significant effect on extension-twist coupling. Good agreement between test results and the CLT solution is also observed.

<u>Conclusion</u>

The three other methods being developed aim at reducing the restraining moment associated with increasing applied axial loading. A comparison of test data using each of the testing methods to those results from CLT, SDT and finite element method will show the effectiveness of each method in measuring extension-twist coupling. This investigation will be the subject of the work of Reference 2.
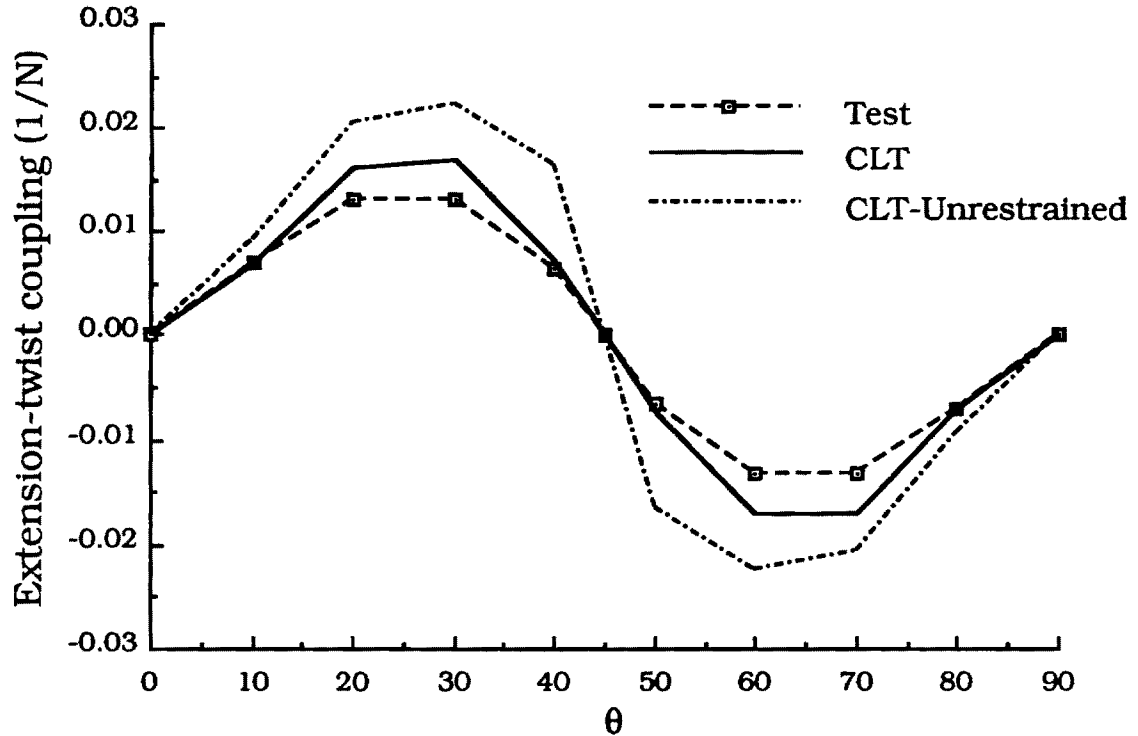
Figure 5. Comparison of Extension-twist coupling at Various angle θ.

References

[1] Armanios, E. A. and Li, J., "Interlaminar Fracture Analysis of Unsymmetrical Laminates," Composite Materials: Fatigue and Fracture, Fourth Volume, ASTM STP 1156, W. W. Stinchcomb and N. E. Ashbaugh, Eds., American Society for Testing and Materials, Philadelphia, 1993, pp. 341-360.

[2] Hooke, D. A. and Armanios, E. A., "Examination of Three Methods for Testing Extension-twist Coupled Laminates," accepted for presentation, 12th Symposium on Composite Materials: Testing and Design, May 16-17, 1994, Montreal, Quebec, Canada.

STATUS REPORT

ADVANCED COMPOSITES AND SMART STRUCTURES RESEARCH

GRANT : DAAL03-92-G-380
GEORGIA TECH PROJECT: E16-X11

PRINCIPAL INVESTIGATOR
E. A. Armanios
School of Aerospace Engineering
Georgia Institute of Technology
Atlanta GA 30332-0150

Sponsor Technical Contact: DR. LEBONE MOETI
Clark Atlanta University
221 James P. Brawley Dr., S.W.
Atlanta, GA 30324

Problem studied

The primary objective of this research is the development of analytical tools, testing methods and smart concepts for advanced composite structures.

Progress during this reporting period

During this reporting period progress was made on the design of four testing methods for measuring the extension-twist coupling in advanced elastically tailored laminates. Results for three of these methods were compared and challenges and suggestions for testing methods were provided.

It is seen that the testing method chosen can greatly influence the results, and therefore experimental methods must be well thought out prior to the actual test.

A damage study was performed to show the effects of free-edge delamination on extension-twist coupling. The experimental reduction in coupling was compared with a theoretical model.

This work was presented as part of the American Helicopter Society (AHS) Student Lichten Award and won the competition. Attached in the Appendix is a paper submitted for publication in the Proceedings of the 1994 AHS Forum. The paper presents a detailed description of the four test methods and provides the results of the damage study.

Appendix

Lichten Award Student Paper
To be published in the Proceedings of the 1994 AHS Forum

Testing Methods for Advanced Elastically Tailored Composite Laminates

David A. Hooke
Georgia Institute of Technology
Atlanta, GA 30332

Abstract

Elastically tailored composite laminates are those laminates which have been designed with specifically tailored stiffness parameters. These parameters can be sized to give an out-of-plane response to in-plane loading, resulting in deformation modes not found in conventional, homogeneous materials.

This paper will discuss four different testing methods that may be used to determine the extension-twist coupling coefficient. Results for three of these methods will be compared and challenges and suggestions for testing methods will be provided.

It will be seen that the testing method chosen can greatly influence the results, and therefore experimental methods must be well thought out prior to the actual test.

A damage study is also presented to show the effects of free-edge delamination on extension-twist coupling. The experimental reduction in coupling is then compared with a theoretical model.

Introduction

By using elastically tailored composite materials, the structural engineer has an extra degree of freedom during the design stage of an aircraft. Generally speaking, using elastically tailored laminates instead of conventional materials can reduce part count and increase efficiency of the whole structure.

Two popular examples of elastically tailored composite laminates are those that exhibit bend-twist coupling and extension-twist coupling. Bend-twist coupling has a use in wing structures where an increase in wing loading may produce a wing-tip wash-in to help prevent tip stall. Extension-twist coupling has a use in rotor blades, where an increase in centrifugal load can result in an increase or decrease in the pitch angle of the rotor blade. For the concerns of this paper, it will be assumed that a laminate has been designed to exhibit some predicted extension-twist coupling. The focus is now on testing for verification of theory and determination of material properties.

Generally speaking, manufacturing extension-twist coupled laminates is no more difficult than any other laminate. The challenges are in the design and testing. In the design stage, the engineer must specify the elastic response, analyze the curing stresses, and consider failure modes. Therefore there must be a very clear understanding of the complete structural problem. After a rigorous analysis has been made, the laminate can be manufactured. The testing engineer must then accurately test the material properties. With conventional materials this may include an axial, flexure, temperature, or fatigue test. This basic idea is also true for elastically tailored composite laminates with the exception that the desired deformation modes must be unrestrained. In the specific case of extension-twist coupled laminates, the laminate must be free to twist under axial loading. The major challenge is to develop a testing method that satisfies this free end condition while being accurate, repeatable, adaptable, and cost effective.

A previous test performed by Chandra[1] incorporated a device that applied a one pound suspended load through a cable, pulley, and thrust bearing mechanism. The resultant twist of the specimen was then measured at intervals along the length using a reflected light beam. Testing laminates at higher loads requires a new method of applying

the load. Conventional bi-axial testing machines may be used by applying a known load or extension while ensuring that the resulting torque is zero. However, this requires a great deal of accuracy in the torsion load cell due to the low torsional rigidity of the laminate under test. In addition, the cost of such equipment is sometimes prohibitive.

Two of the methods presented in this work, namely the rotating frame and air bearing transducers, ensure that the free edge condition is met to the highest degree. The rotating frame testing apparatus guarantees that the free end condition is met. The air bearing transducer meets the requirement to the same degree of accuracy, but allows for rapid testing of the specimens and is designed for production use. Furthermore, the air bearing design is adaptable to common universal testing machines with a minimum of parts and requires no external computer support. Using this method, a database of material constants can be developed for a specific material system or lay-up sequence. These constants can then be compared to either production values during manufacturing or to values throughout a life cycle. As will be seen, the change in elastic extension-twist coupling relates to damage in the laminate.

The other two methods, the moment-extension method and the ball-thrust bearing transducer, discussed in this work provide some restraint to the motion of the laminate. The effects of the restraint vary for the two methods, but may be modeled in the analysis as some additional external loading.

Analysis

The constitutive equations relating stress resultants and in-plane strains and curvatures for a laminated plate with arbitrary lay-up are the following.

$$
\begin{bmatrix}
\alpha_1 & \alpha_{12} & \alpha_{16} & \beta_{11} & \beta_{12} & \beta_{16} \\
\alpha_{21} & \alpha_{22} & \alpha_{26} & \beta_{21} & \beta_{22} & \beta_{26} \\
\alpha_{61} & \alpha_{62} & \alpha_{66} & \beta_{61} & \beta_{62} & \beta_{66} \\
\beta_{11} & \beta_{12} & \beta_{16} & \delta_{11} & \delta_{12} & \delta_{16} \\
\beta_{21} & \beta_{22} & \beta_{26} & \delta_{21} & \delta_{22} & \delta_{26} \\
\beta_{61} & \beta_{62} & \beta_{66} & \delta_{61} & \delta_{62} & \delta_{66}
\end{bmatrix}
\begin{Bmatrix}
N_{xx} \\ N_{yy} \\ N_{xy} \\ M_{xx} \\ M_{yy} \\ M_{xy}
\end{Bmatrix}
=
\begin{Bmatrix}
\varepsilon_{xx} \\ \varepsilon_{yy} \\ \gamma_{xy} \\ \kappa_{xx} \\ \kappa_{yy} \\ \kappa_{xy}
\end{Bmatrix}
\tag{1}
$$

The extension-twist coupling is governed by parameter β_{16} which is a function of the laminate geometry and axial, bending, and coupling stiffnesses. Explicit expressions for β_{16} for a laminate with and without free edge delamination is provided in Ref.[2].

The analogous equations for a closed section laminate are:[3]

$$
\begin{Bmatrix}
N \\ M_x \\ M_y \\ M_z
\end{Bmatrix}
=
\begin{bmatrix}
C_{11} & C_{12} & C_{13} & C_{14} \\
C_{12} & C_{22} & C_{23} & C_{24} \\
C_{13} & C_{23} & C_{33} & C_{34} \\
C_{14} & C_{24} & C_{34} & C_{44}
\end{bmatrix}
\begin{Bmatrix}
U_1' \\ \varphi' \\ U_3'' \\ U_2''
\end{Bmatrix}
\tag{2}
$$

Where U_1, U_2, and U_3 are average displacements along coordinates x, y, z, respectively and φ is the twist angle. A prime in Eq.(2) denotes differentiation with respect to x. The extension-twist coefficients are governed by C_{12} which is defined as:

$$C_{12} = \frac{\oint \dfrac{B(s)}{C(s)} ds}{\oint \dfrac{1}{C(s)} ds} Ae \qquad (3)$$

Where Ae is the enclosed area of the cross-section and $A(s)$, $B(s)$, and $C(s)$ are the reduced axial, coupling, and shear stiffnesses. These are related to the axial stiffness coefficients A_{ij} $(i,j = 1,2, 6)$[4].

$$A(s) = A_{11} - \frac{(A_{12})^2}{A_{22}}$$

$$B(s) = 2\left[A_{16} - \frac{A_{12}A_{26}}{A_{22}} \right] \qquad (4)$$

$$C(s) = 4\left[A_{66} - \frac{(A_{26})^2}{A_{22}} \right]$$

Extension-twist coupling in laminated composite plates results from in-plane extension-shear coupling of the off-axis plies. By stacking a set of plies at $+\theta$ and $-\theta$ a twisting behavior results from applied extension as shown schematically in Figure 1a. For a closed cell, extension-twist can be produced by wrapping off-axis plies around a mandrel resulting in a shear flow around the closed section as illustrated in Figure 1b.
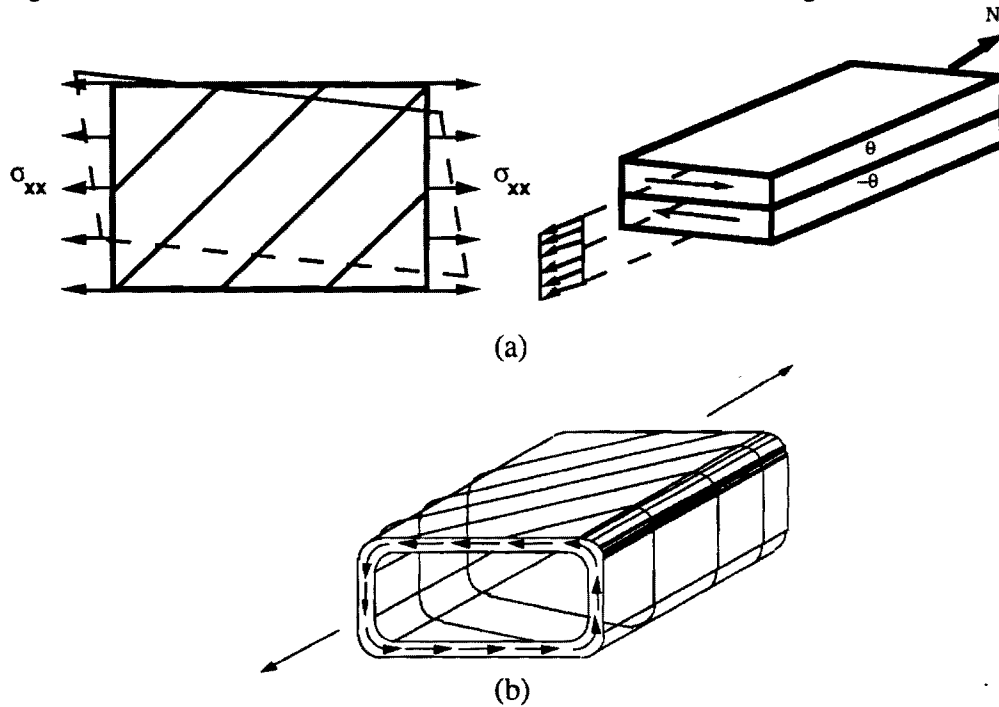

(a)

(b)

Figure 1. Coupling Mechanism in (a) Laminated Plates and (b) Closed Sections.

Testing

The goals to be achieved by testing extension-twist coupled laminates are to verify the theoretical prediction of β_{16}, quantify the effects of known damage to the laminate, and determine the failure modes. Completing such an experimental study will build a database of material constants, coupling degradation due to damage, and failure load limits. This information is essential in order to design safe, high performance structures.

Four testing methods will be explained here. The first testing method uses a thrust bearing to achieve the free-rotating end condition. The load is applied through the transducer, and the resultant twist of the laminate is measured by the change in voltage across a linear precision potentiometer. By measuring the twist angle and the applied load, β_{16} can be found. This design is easily produced, supplies repeatable results, and is easily interfaced with computer data acquisition systems. The overall accuracy of the test changes throughout the load sequence, however. Due to friction in the ball-thrust bearing the resultant measured twist may be less than would occur in a truly free state. This effect has been quantified in Figure 2 where the restraining moment associated with the bearing friction is plotted against axial load. The restraining moment due to friction is small, but not negligible.
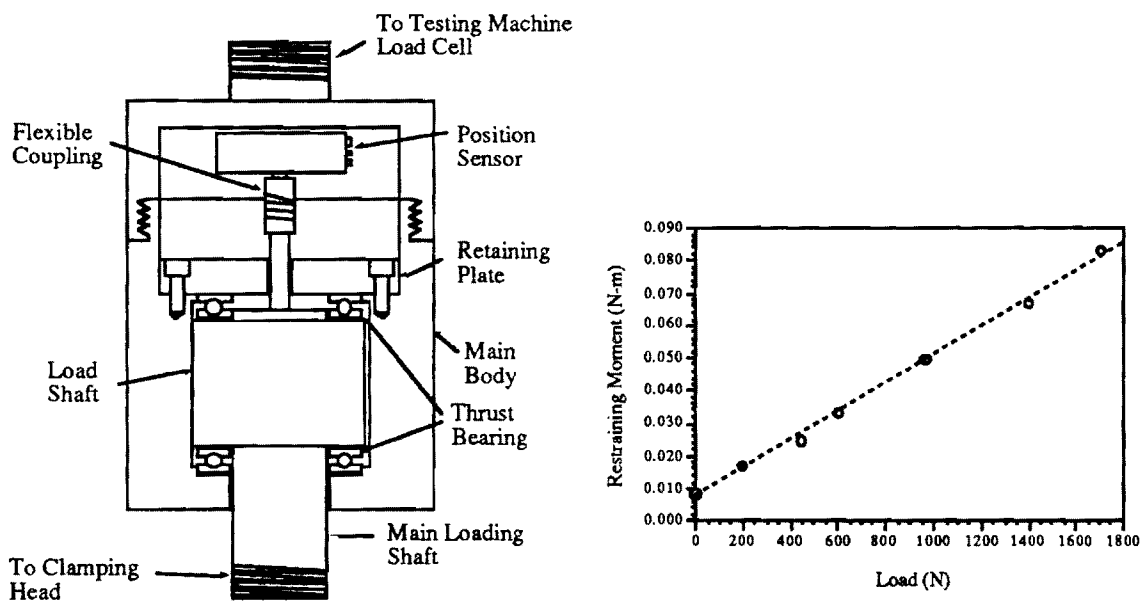

Figure 2. Ball Thrust Bearing Transducer and Restraining Moment Graph

The second testing method uses the fact that the stiffness matrix is symmetric. Here one end of the laminate under test is clamped uniformly as shown in Figure 3. The other free end is fitted with a fixture that maintains the displacement in the vertical and horizontal direction. The only degrees of freedom for the end are then axial displacement and rotation. A torsional load is then applied to the laminate and the corresponding axial displacement measured. The axial strain is estimated based on precise measurements and the corresponding coupling coefficient, β_{16}, can be determined. This design is easily produced, supplies repeatable results, and is readily interfaced with computer data acquisition systems. However, measurement of the low applied torque present an

instrumentation hurdle, the testing method is not easily adaptable to any existing equipment, and failure testing may be difficult.
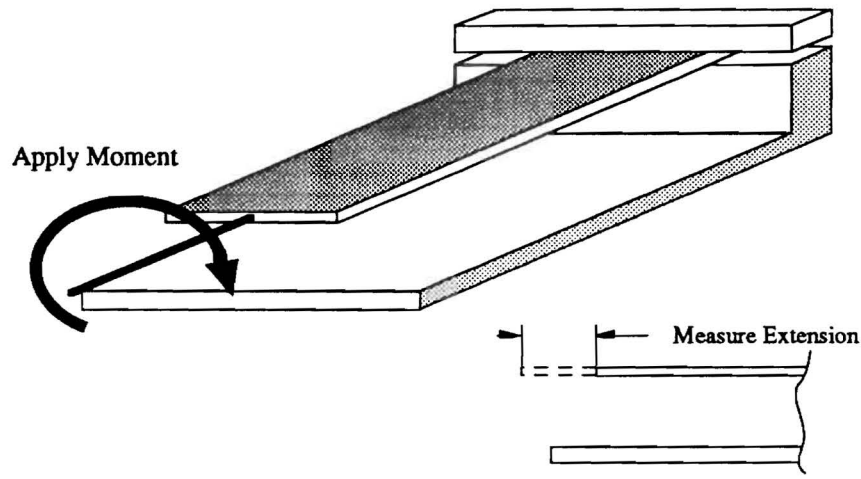

Figure 3. Moment-Extension Testing Schematic

A third testing method uses a rotating testing frame as shown schematically in Figure 4. The laminate under test is clamped at one end to a fixture which rotates in a vacuum chamber. The advantages to this testing method are that the free edge condition is met exactly. Because of this, the results are repeatable, and dynamic measurements and flow visualization can be made with closed sections. However, failure testing using this method would be unsafe. Because the end is indeed free and the high levels of load required to fracture laminates, a failure test would lead to high speed projectiles. Data logging from such a method is also difficult. A load cell would become part of the rotating mass, and measurements would be taken through either slip rings, which are susceptible to electrical noise or through the use of video. While video measurements are quite accurate, the amount of post-processing becomes a hindrance to the overall testing procedure. Fixturing and balancing also become a challenge for each test.
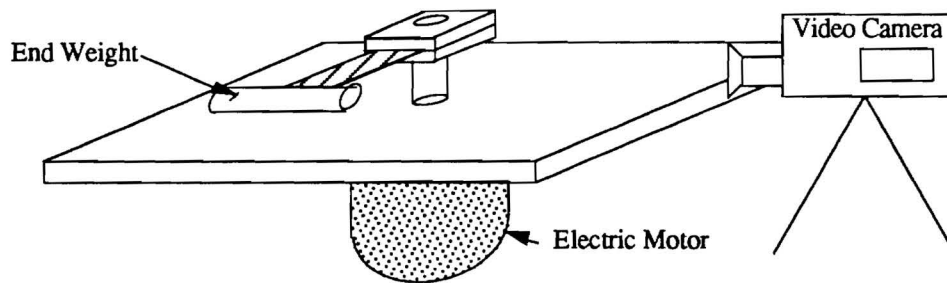

Figure 4. Rotating Frame Apparatus

The final testing method proposed is an air-bearing based transducer. Much like the thrust bearing transducer described above, the air bearing transducer is easily producible, gives repeatable results, is accurate, maintains the free end condition, is adaptable to existing universal testing machines, and allows for safe failure testing. Furthermore, a

very precise non-contact method for measuring the angle of twist is incorporated within the transducer so that external computers are not required for operation.

Results and Discussion

In the case of testing extension-twist coupled laminates, the rotating frame testing apparatus will yield the benchmark for which all other methods will be measured. However, as stated earlier, this is not the preferred method of testing due to set-up time and data acquisition. Quantitative results for this method are shown in the Table I. The corresponding plot of the data generated from the rotating frame, air bearing and ball thrust bearing is shown in Figure 5. The load on the specimen was calculated using the mass of the end weight, angular speed, and radius of rotation. As shown in Figure 5, the coupling observed in this preliminary test is actually *lower* than observed using the other testing methods. This is because the test chamber is not under complete vacuum and there is still enough air present to cause some aerodynamic loading on the specimen and the end weight. Because the torsional rigidity of the laminate is relatively low, the small resultant aerodynamic forces can have a large effect as does the frictional force in the ball-thrust bearing design. It is quite clear, however, that the fundamental method does work. Using a specimen length of approximately 8 inches, and a 0.293 lb (133 g) weight, a rotation on the of 5° has been measured using a strobe light, video camera, and video post processing techniques.

The benchmark must still be made. Future tests using this method will incorporate a tube which will enclose the specimen and end weight. The tube will be sealed at the root and capped with a clear piece of Lucite with scribed angle lines. The specimen will fit inside the tube with a circular end weight mounted on the free end. At rest the end weight will lie on the inner diameter of the tube. With the increase in RPM during the test, the end weight will lift off and 'float' inside the tube. A scribed line on the end weight can then be viewed using a strobe light, and its angle measured with reference to the scribed lines on the end cap. The specimen will thus be in a sealed environment and the aerodynamic effects negated.

At this time a second air-bearing transducer has been designed and is in the manufacturing stage. The data presented from the first transducer are for comparison of testing methods and should be used only as an indication of the state of the available technology. It was designed solely as a proof-of-concept device, but is able to produce some very encouraging results. The transducer under manufacture is sized for higher loads and is equipped with an onboard, digital, non contact method of angle measurement.

The basic principle used in the transducer is that air pressure applied to a piston produces a force. However, the piston is not sealed in any way to the cylinder. Therefore the efficiency of the device depends on the clearance between the piston and the cylinder. The device used for these tests applied a maximum of 70 lb. to the specimen. The resultant twist was measured using a fixed scale mounted off board, and a long pointer mounted on the free end clamp. After the transducer was mounted and aligned in the testing machine, data was produced and is shown in Figure 5.

The last transducer in the test is the ball-thrust bearing based transducer. Because of the ease of use of this transducer, it will be used to measure the coupling of the standard undamaged laminate and the coupling in a series of damaged laminates. This transducer is connected to the load cell of the universal testing machine. The load is then applied in the same manner as with any other test, by moving the cross-head. The resultant twist is converted to a voltage via a precision potentiometer. This voltage can be read manually or

by a computer data acquisition system. The results of the test on the undamaged laminate appear in Figure 5.
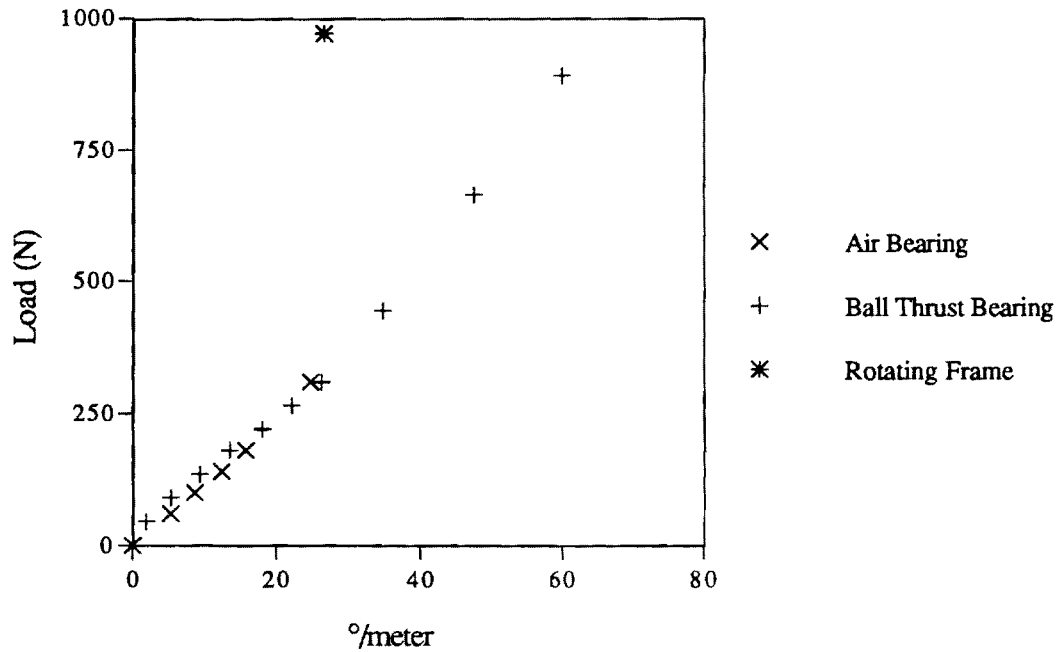
Figure 5. Coupling Measured with Three Different Methods

Comparison of Results

Table I shows the measured coupling for a single laminate using the different methods. The far right column is a measurement of the inverse ratio of coupling to the benchmark coupling measurement.

Table I. Comparison of Test Results

Testing Method	Measured Coupling (N/°/m)	% of Benchmark
Rotating Frame	36.38	100 %
Air Bearing	12.43	292 %
Ball Thrust Bearing (<315N)	11.30	322 %
Ball Thrust Bearing (>315N)	17.49	208 %

As indicated earlier, the aerodynamic levels may have a significant influence on the rotating specimen. Future tests using the enclosed tube method is bound to reduce these effects and truly establish an accurate benchmark. It is worth noting that the coupling measured by the two other transducers is quite close at low loads. At higher loads, though, the effects of friction become apparent in the results from the ball thrust bearing data.

Results from a Damage Study

The following results were obtained from a damage study that included twelve specimens. The lay-up for each of the specimens was $[\theta/((\theta-90)_2/\theta/-\theta/(90-\theta)_2/-\theta]$ with $\theta=30°$. This lay-up produces extension-twist coupling as a result of mechanical load but is hygrothermally stable.[5] Three classes of laminates were tested. The first class were undamaged, including no built in delaminations. The second class had imbedded edge delaminations at the mid-plane as shown schematically in Figure 6(a). The third class had imbedded edge delaminations between off-axis plies as shown in Figure 6(b). Four specimens were manufactured for each of the classes. The results of the test for each of the classes were then averaged.
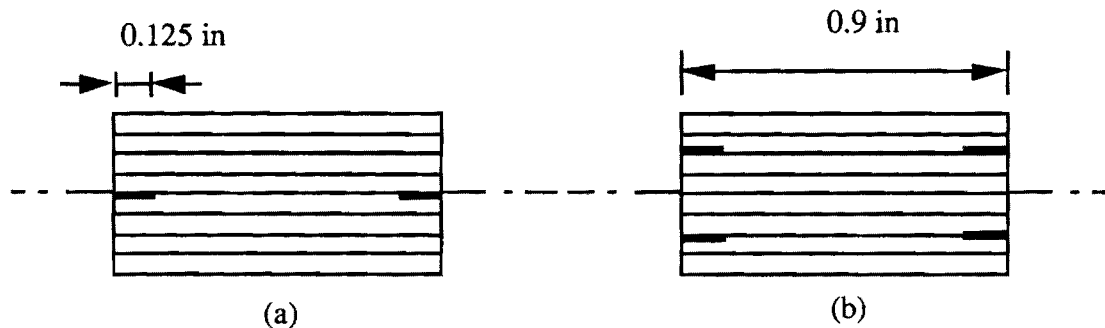
Figure 6. (a) Mid-Plane Delamination (b) Off-Axis Delamination

Influence of Boundary Conditions

The effect of boundary conditions has been addressed by checking the unit twist of the specimens by two methods. First, the overall angle of twist of the free end is divided by the length between the grips. Secondly, the twist between two points in an interior region is measured, then divided by its length.

Results show that the boundary conditions have a negligible affect on the overall behavior of the specimen. Under a tensile load of 1334N (300 lbs), end twist was 19.8° ± 0.2° over a length of 25.4 cm (10 in.), yielding a twist per length of 0.78°/cm ± 0.008°/cm (1.98°/in. ± 0.02°/in). Under the same load, the interior region measured 2° over a region of 2.54 cm (1 in) yielding a twist per length of 0.79°/cm (2°/in), or up to 1% difference compared to the first method.

Specimen Fabrication

The specimens for all the tests were made with Hercules AS4/3502 graphite/epoxy pre-impregnated sheets. After curing and trimming, final specimen dimensions were 2.3 cm x 29.9 cm (0.9" x 11.75").

Test Results

Tests showed that a sample size of four specimens gives closely grouped data. Therefore, the results of each configuration tested herein are the average of the results of four specimens. The material constants, E_{11}, E_{22}, G_{12}, v_{12}, and v_{21} were determined by measuring strains in $[0]_8$, $[90]_8$, and $[45]_8$ specimens. From the 0° laminate, E_{11} and

v_{12} are determined. Similarly, E_{22} and v_{21} are found from the 90° laminate measurements, and G_{12} is found from the 45° laminate measurements. The material properties are summarized in Table II.

Table II. Material Properties

$$E_{11} = 131 \text{ GPa } (19 \text{ Msi})$$
$$E_{22} = 10.62 \text{ GPa } (1.54 \text{ Msi})$$
$$G_{12} = 5.93 \text{ GPa } (0.86 \text{ Msi})$$
$$v_{12} = 0.33$$

In the testing procedure, the specimen is placed in the test machine and any initial offsets are removed. Data acquisition is accomplished via a Keithley Series 500 analog to digital converter and amplifier system connected to an IBM PC-AT. The test procedure is to manually apply a constant extension deformation until a pre-determined load is reached. When this load is reached, the computer samples the load and the end twist of the specimen. This procedure is then repeated until a number of data points are taken. For the tests presented here, the maximum load applied is 1557N (350 lbs).

Data for undamaged laminates is shown in the following figures. Figure 7 shows the laminate with $\theta=30°$. The slope of the least squares line through the data is 17.05 N/°/m (150.9 lbs/°/in). Figure 8 shows the extension-twist coupling as a function of θ along with the least square fit through the data.
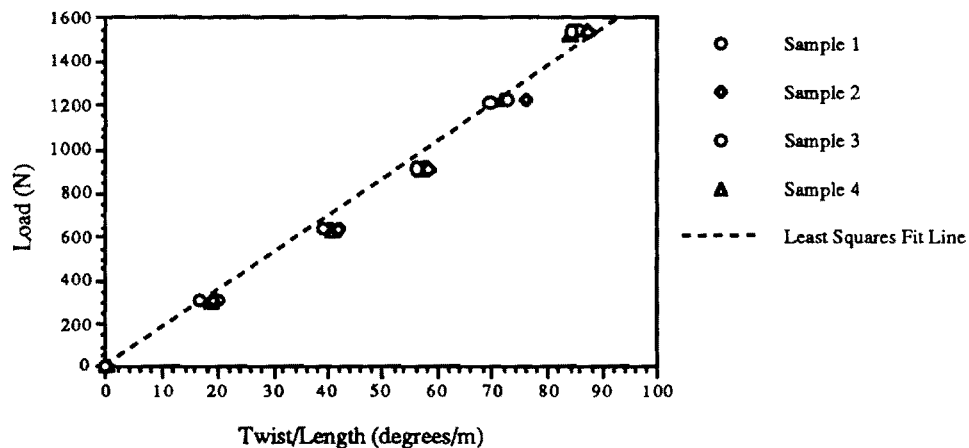
Figure 7. Extension-twist Coupling for laminate with $\theta=30°$
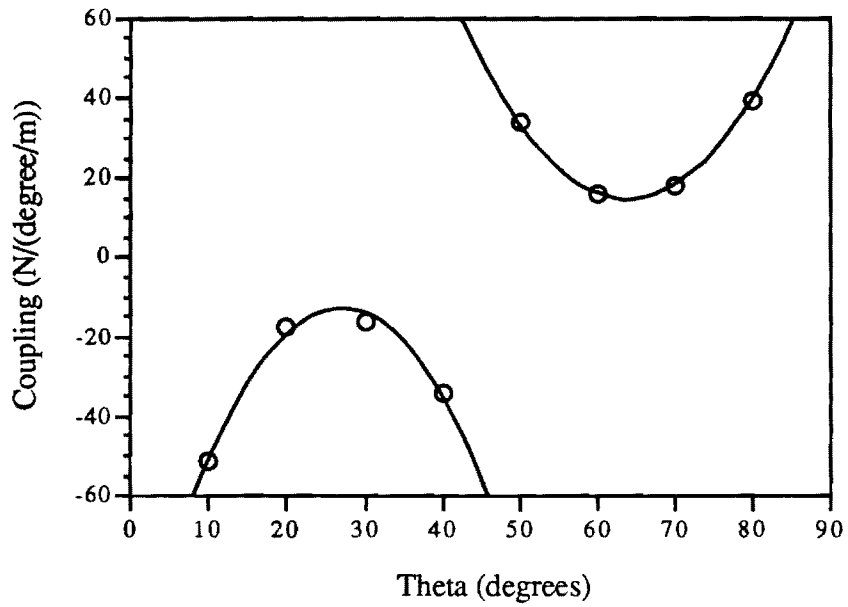
Figure 8. Extension-twist data for varying θ.

The twist vanishes for laminates with θ=0°, 90°, and 45°. In the case of θ=45°, the extension twist coupling vanishes since the in-plane extension shear coupling of each half of the laminate is zero.

The reduction in coupling associated with damage are summarized in Figure 9. A clear reduction in coupling is seen from the graphs. This reduction is indicative of the presence of damage and could be the basis of a non-destructive evaluation technique.
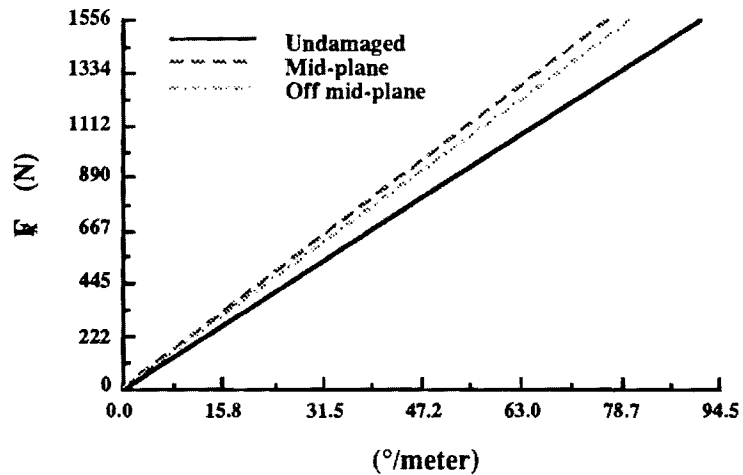
Figure 9. Extension-twist Coupling Reduction for Laminates with θ=30°

Comparison with Predictions

Initial tests of the laminate showed that the experimental coupling was less than the theoretical prediction by a significant amount. The transducer was then checked for a torsional restraining moment as the load was increased through the range used in testing. While the restraining moment is small, its effect is not negligible when compared to the torsional rigidity of the test specimen. The restraining moment was measured and plotted as a function of applied tensile load. The resulting plot, appearing in Figure 10, is linear and the slope of the least squares fit line through the data can be used in the theoretical analysis where the transducer is modeled as a torsional spring. The magnitude of the restraining moment at zero tensile load is due to the resistance of the position sensor.
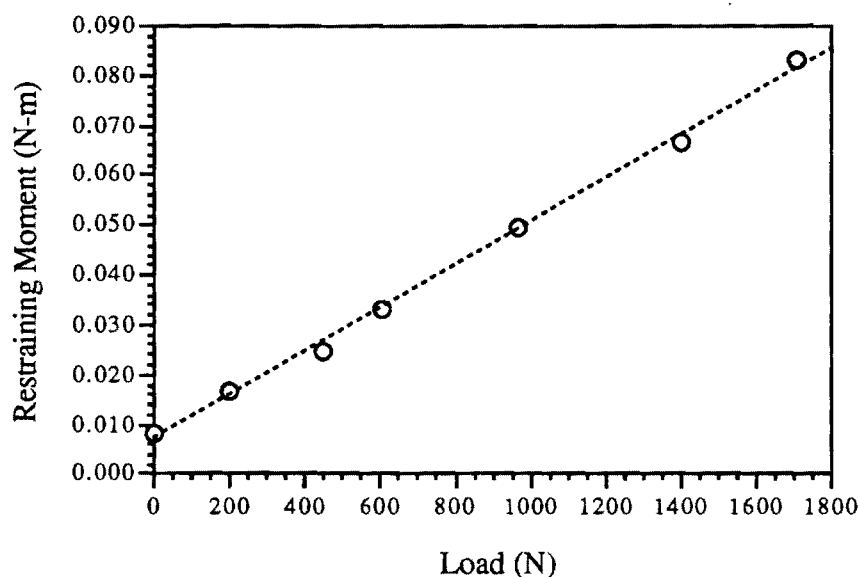
Figure 10. Restraining Moment as function of Axial Load

A comparison between theoretical predictions[6] and test data found in Table III.

Table III. Comparison of Theoretical Predictions with Test Data

Damage Location	Theoretical % Coupling Reduction	Experimental % Coupling Reduction
Mid-Plane	18.0 %	18.5 %
Off-Axis	16.7 %	13.1 %

For mid-plane delamination, the analytical prediction shows a reduction of 18% which is 2.7% lower than the test data. However, for off mid-plane delamination, the analysis predicts a 27.5% lower reduction than the test result. This is because the analytical model did not account for the compressive transverse normal stress effects.

Conclusion

Four methods to test extension-twist coupling have been presented. Results for three of the four methods have been provided. Preliminary results show that a properly sized air bearing transducer will greatly enhance the accuracy of results.

A series of test have been run to show the effects of internal edge delamination on extension-twist coupling. The results show that there is a measurable decrease in coupling which depends on the location of the delamination in the stacking sequence. The benefits of the non-destructive testing method are that it may be used as a quality check during manufacturing or as a monitoring technique during the life cycle of a composite structure.

Acknowledgment

References

[1] Chandra, Stemple, and Chopra, "Thin Walled Composite Beams Under Bending, Torsional, and Extensional Load", *Journal of Aircraft*, Vol. 27, No. 7, July 1990.

[2] Armanios, E.A., Hooke, D., Kamat, M., Palmer, D., and Li, J., "Design and Testing of Composite Laminates for Optimum Extension-Twisting Coupling," *Composite Materials: Testing and Design (Eleventh Volume), ASTM STP 1206*, E.T. Camponeschi, Jr., Ed., American Society for Testing and Materials, Philadelphia, 1993, pp.249-262

[3] Berdichevsky, V., Armanios, E. A. and Badir, A., "Theory of Anisotropic Thin-walled Closed-cross-section Beams," *Composites Engineering*, Vol. 2, Nos. 5-7, pp. 411-432, 1992.

[4] Vinson, J. R. and Sierakowski, R. L. *The Behavior of Structures Composed of Composite Materials*, Martinus Nijhoff, Dordecht, The Netherlands, 1987, p. 54.

[5] Winckler, S. I., "Hygrothermally Curvature Stable Laminates with Tension-Torsion Coupling," *Journal of the American Helicopter Society*, Vol. 31, No. 7, July 1985, pp. 56-58

[6] Armanios, E. A., Hooke, D., and Li, J., "Interlaminar Fracture Testing and Analysis of Composite Laminates with Extension-Twist Coupling," in *Developments in Theoretical and Applied Mechanics, Volume XVI, Sixteenth Southeastern Conference on Theoretical and Applied Mechanics (SECTAM)*, Nashville, Tennessee, April 12-14, 1992, pp. II.15-21-II.15-27

STATUS REPORT

ADVANCED COMPOSITES AND SMART STRUCTURES RESEARCH

GRANT : DAAL03-92-G-380
GEORGIA TECH PROJECT: E16-X11

PRINCIPAL INVESTIGATOR
E. A. Armanios
School of Aerospace Engineering
Georgia Institute of Technology
Atlanta GA 30332-0150

Sponsor Technical Contact: DR. LEBONE MOETI
Clark Atlanta University
221 James P. Brawley Dr., S.W.
Atlanta, GA 30324

Problem studied

The primary objective of this research is the development of analytical tools, testing methods and smart concepts for advanced composite structures.

Progress during this reporting period

The progress made during this reporting period is provided in the attached paper entitled: "Examination of Three Methods for Testing Extension-twist Coupled Laminates." The paper was presented at the Twelfth Symposium on Composite Materials: Testing and Design and was submitted for publication in an ASTM Special Technical Publication.

EXAMINATION OF THREE METHODS FOR TESTING EXTENSION-TWIST COUPLED LAMINATES

By

David A. Hooke and Erian A. Armanios
School of Aerospace Engineering
Georgia Institute of Technology
Atlanta, Georgia 30332-0150

ABSTRACT

Elastically tailored composite laminates are those laminates which have been designed with specifically tailored stiffness parameters. These parameters can be sized to give an out-of-plane response to in-plane loading, resulting in deformation modes not found in conventional homogeneous materials.

Three different methods of testing extension-twist coupled specimens are discussed. The benefits and limitations of each of the methods are highlighted. Quantitative results for each of the testing methods using a hygrothermally stable specimen are shown and compared to determine the applicability and suitability of each of the methods.

A comparison of data with predictions from a shear deformation sublaminate plate theory and Finite Element Method are presented.

KEY WORDS: laminated composites, elastic tailoring, test methods

Introduction

Elastically tailored composite materials provide an extra degree of freedom to meet design requirements efficiently and economically. Using elastically tailored laminates can reduce part count and weight and increase performance of the whole structure.

Two popular examples of elastically tailored composite laminates are those that exhibit bend-twist coupling and extension-twist coupling. Bend-twist coupling has a use in fixed wing structures where an increase in wing loading may produce a wing-tip wash-in to help prevent tip stall. Extension-twist coupling has a use in rotary wings, where an increase in centrifugal load can result in an increase or decrease in the pitch angle of the rotor blade.

This paper is concerned with laminated composites designed to exhibit extension-twist coupling. Emphasis is given on the development of testing methods to characterize the behavior of the laminates, provide a data base, and verify analytical predictions.

When testing an elastically tailored composite, the desired deformation modes must be unrestrained. In the specific case of extension-twist coupled laminates, the laminate must be free to twist under axial loading. The major challenge is to develop a testing method that satisfies this free end condition while being accurate, repeatable, adaptable, and cost effective.

A previous test performed by Chandra [1] incorporated a device that applied a one pound suspended load through a cable, pulley, and thrust bearing mechanism. The resultant twist of the specimen was then measured at intervals along its length using a reflected light beam. Testing laminates at higher loads requires a new method of applying the load. Conventional bi-axial testing machines may be used by applying a known load or extension while ensuring that the resulting torque is zero. However, the torsion load cell

should be designed to accommodate the low torsional rigidity of the laminate. In addition, the cost of such equipment is sometimes prohibitive.

This paper presents three alternative methods. The first testing apparatus discussed, the ball-thrust bearing transducer introduced in Ref. 2, provides some restraint to the rotational motion of the laminate. The effect of the restraint could be modeled in the analysis as a torsional loading proportional to axial load.

The other two testing apparatuses presented in this work, namely the rotating frame and improved thrust bearing apparatus, ensure that the free edge condition is met to the highest degree. The rotating frame testing apparatus guarantees that the free end condition is met. The improved thrust bearing design meets the requirement to the same degree of accuracy, but allows for rapid testing of laminates and is designed for production use. Furthermore, the improved design is adaptable to common universal testing machines with a minimum of parts and requires no external computer support. Using this method, a database of material constants can be developed for a specific material system or lay-up sequence. These constants can then be compared to either production values during manufacturing or to values throughout a life cycle.

In the following, a derivation of the analytical prediction for the extension-twist coupling is presented along with a finite element simulation. This is followed by a description of the design and manufacturing of each of the test methods and experimental procedures. The characteristics of each method are illustrated through test data. Comparison of analytical predictions with test results is presented.

Analysis

Shear Deformation Laminated Plate Theory

The sublaminate shear deformation analysis of Ref. 3 is used in order to predict the twist associated with extension load in a $[\alpha/(\alpha-90)_2/\alpha/-\alpha/(90-\alpha)_2/-\alpha]_T$ laminate. This unsymmetrical lay-up ensures hygrothermal stability of the laminate [4] and eliminates initial warping which results from the curing stresses. A summary of the governing equations and solution procedure is presented for convenience.

The governing equations are written for the generic sublaminate shown in Fig. 1. A sublaminate is a ply or group of plies from the original laminate that is treated as a single laminated unit with equivalent effective properties. The in-plane stress resultants are denoted by N_{xx}, N_{yy}, and N_{xy} while M_{xx}, M_{yy}, and M_{xy} denote the bending in the x-z and y-z planes and the torsional moment respectively. The shear resultants in the y-z and x-z planes are denoted by Q_x and Q_y respectively. The interlaminar shear and peel stresses at the laminate upper and lower surfaces are denoted by t_{ux}, t_{uy}, p_u, and t_{lx}, t_{ly}, p_l, respectively. In the present case the entire laminate cross section is modeled as one sublaminate. The displacement field is given by

$$u(x,y,z) = \varepsilon_o x + \kappa xz + U(y) + z\beta_x(y)$$

$$v(x,y,z) = \frac{\theta}{L}xz + V(y) + z\beta_y(y) \tag{1}$$

$$w(x,y,z) = -\frac{\kappa}{2}x^2 - \frac{\theta}{L}xy + W(y)$$

where u, v, and w denote displacements relative to the x, y, and z axes, respectively. The origin of the Cartesian coordinate system coincides with the center of the laminate. The laminate length is denoted by L and the axial extension strain is ε_o. The twisting rotation

and bending curvature are denoted by θ and κ, respectively. These result from the coupling effects associated with unsymmetrical lay-ups. Mid-plane displacements in the x, y, and z directions are represented by $U(y)$, $V(y)$, and $W(y)$ respectively.

Shear deformation is recognized through the rotation β_x and β_y. Bending about the z axis is neglected since the laminate thickness is small compared to its width.

The corresponding strains are

$$\varepsilon_{xx} = \varepsilon_{xx}^o + z\kappa_{xx} \quad \varepsilon_{yy} = \varepsilon_{yy}^o + z\kappa_{yy} \quad \varepsilon_{zz} = 0$$

$$\gamma_{xy} = \gamma_{xy}^o + z\kappa_{xy} \quad \gamma_{yz} = \gamma_{yz}^o \qquad \gamma_{xz} = \gamma_{xz}^o \tag{2}$$

The strain components associated with the reference surface are denoted by superscript o. These and the associated curvatures are defined as

$$\varepsilon_{xx}^o = \varepsilon_o \quad \varepsilon_{yy}^o = V_{,y} \quad \gamma_{xy}^o = U_{,y}$$

$$\kappa_{xx} = \kappa \quad \kappa_{yy} = \beta_{y,y} \quad \kappa_{xy} = \beta_{x,y} + \frac{\theta}{L} \tag{3}$$

$$\gamma_{yz}^o = \beta_y + W_{,y} \qquad \gamma_{xz}^o = \beta_x - \frac{\theta}{L} y$$

where partial differentiation is denoted by a comma.

The constitutive relationships for the hygrothermally stable lay-up considered, take the following uncoupled form

$$\begin{Bmatrix} N_{xx} \\ N_{yy} \\ M_{xy} \end{Bmatrix} = \begin{bmatrix} A_{11} & A_{12} & B_{16} \\ A_{12} & A_{11} & -B_{16} \\ B_{16} & -B_{16} & D_{66} \end{bmatrix} \begin{Bmatrix} \varepsilon_{xx}^o \\ \varepsilon_{yy}^o \\ \kappa_{xy} \end{Bmatrix} \tag{4}$$

$$\begin{Bmatrix} N_{xy} \\ M_{xx} \\ M_{yy} \end{Bmatrix} = \begin{bmatrix} A_{66} & B_{16} & -B_{16} \\ B_{16} & D_{11} & D_{12} \\ -B_{16} & D_{12} & D_{22} \end{bmatrix} \begin{Bmatrix} \gamma_{xx}^o \\ \kappa_{xx} \\ \kappa_{xy} \end{Bmatrix} \tag{5}$$

$$\begin{Bmatrix} Q_y \\ Q_x \end{Bmatrix} = \begin{bmatrix} A_{44} & 0 \\ 0 & A_{44} \end{bmatrix} \begin{Bmatrix} \gamma_{yz}^o \\ \gamma_{xz}^o \end{Bmatrix} \tag{6}$$

For a sublaminate of thickness h, the stiffness coefficients are defined as

$$(A_{ij}, B_{ij}, D_{ij}) = \int_{-h/2}^{h/2} \overline{Q_{ij}}(1, z, z^2) dz \tag{7}$$

where $\overline{Q_{ij}}$ are the transformed reduced stiffnesses as defined in Ref. 5. Since the upper and lower surface of the sublaminate are stress free, the equilibrium equations reduce to

.

$$N_{xy,y} = N_{yy,y} = Q_{y,y} = 0 \tag{8}$$

$$M_{yy,y} - Q_y = 0 \tag{9}$$

$$M_{xy,y} - Q_x = 0 \tag{10}$$

From the boundary conditions

$$N_{yy}\big|_{y=\pm b} = N_{xy}\big|_{y=\pm b} = Q_y\big|_{y=\pm b} = M_{yy}\big|_{y=\pm b} = 0 \tag{11}$$

where b denotes the laminate semi-width, Eq(s) 8 and 9 reduce to

$$N_{yy} = N_{xy} = M_{yy} = Q_y = 0 \tag{12}$$

Substitution of Eq(s) 3 and 12 into Eq(s) 4 and 5 yields

$$M_{xx} = \frac{B_{16}^2(D_{11} - D_{22} - 2D_{12}) + A_{66}(D_{11} - D_{12}^2)}{D_{22}A_{66} - B_{16}^2} \kappa \tag{13}$$

$$\begin{Bmatrix} N_{xx} \\ M_{xy} \end{Bmatrix} = \begin{bmatrix} \alpha_{11} & \alpha_{12} \\ \alpha_{12} & \alpha_{22} \end{bmatrix} \begin{Bmatrix} \varepsilon_o \\ \beta_{x,y} + \dfrac{\theta}{L} \end{Bmatrix} \tag{14}$$

where

$$\alpha_{11} = \frac{A_{11}^2 - A_{12}^2}{A_{11}}$$

$$\alpha_{12} = \frac{B_{16}(A_{11} + A_{12})}{A_{11}}$$

$$\alpha_{22} = \frac{D_{66}A_{11} - B_{16}^2}{A_{11}}$$

Substitution of Eq(s) 3, 6 and 14 into Eq 10 yields the following differential equation in β_x

$$(D_{66}A_{11} - B_{16}^2)\beta_{x,yy} - A_{44}A_{11}\beta_x = A_{44}A_{11}\frac{\theta}{L}(y+b) \tag{15}$$

which leads to

$$\beta_x = A_1 \sinh(sy) + A_2 \cosh(sy) + \frac{\theta}{L}(y+b) \tag{16}$$

where

$$s = \sqrt{\frac{A_{44}A_{11}}{(D_{66}A_{11} - B_{16}^2)}} \tag{17}$$

From the remaining boundary conditions at the laminate free edges

$$M_{xy}\big|_{y=\pm b} = 0 \tag{18}$$

and Eq 14, the even functions of y in the rotation β_x should vanish. As a result, the arbitrary constant A_2 in Eq 16 is zero. The axial strain, bending and twisting curvatures and the arbitrary constant A_1 are obtained from the end-loading and boundary conditions. The laminate is tested under uniaxial force, F. However, as is the case for the thrust bearing transducer and the rotating apparatus, an additional torsional restraining moment is induced.

These boundary conditions are expressed as

$$F = \int_{-b}^{b} N_{xx} dy$$

$$M = \int_{-b}^{b} M_{xx} dy = 0 \tag{19}$$

$$T = \int_{-b}^{b} (M_{xy} - Q_x y) dy = 2 \int_{-b}^{b} M_{xy} dy$$

where M and T denote bending and torsional restraining moment, respectively. Substituting for Eqs 13 and 14 into Eq 19 yields

$$\kappa = 0$$

$$F = 2\left[b\,\alpha_{11}\varepsilon_o + \frac{\theta}{L} b\,\alpha_{12} + \alpha_{12} A_1 \sinh(sb) \right] \tag{20}$$

$$T = 4\left[b\alpha_{12}\varepsilon_o + \alpha_{22} A_1 \sinh(sb) + \frac{\theta}{L}\alpha_{22} b \right]$$

where, from Eq 18,

$$A_1 = -\frac{1}{s\cosh(sb)}\left[\frac{\alpha_{12}}{\alpha_{22}}\varepsilon_o + \frac{\theta}{L} \right]. \tag{21}$$

Eliminating ε_o from Eq 20 yields the following equation for θ in terms of F and T.

$$\theta = \rho_1 T + \rho_2 F \tag{22}$$

where

$$\rho_1 = \frac{L\left(\alpha_{11}\alpha_{22} bs - \alpha_{12}^2 \tanh(sb)\right)}{8b\psi\,\alpha_{22}(bs - \tanh(sb))}$$

$$\rho_2 = \frac{-\alpha_{12} L}{4b\psi} \tag{23}$$

where

$$\psi = \alpha_{11}\alpha_{22} - \alpha_{12}^2 \tag{24}$$

It is worth noting that ρ_2 is independent of the characteristic root, s. That is, the shear deformation contribution to the twisting rotation is associated with torsional

restraining moment only. For the case of no torsional restraining moment, Eq 22 simplifies to

$$\frac{\theta}{L} = \frac{F}{4b}\left[\frac{B_{16}}{2B_{16}^2 - D_{66}(A_{11} - A_{12})}\right] \qquad (25)$$

The influence of shear deformation can be isolated by comparing the twisting rotation in Eq 22 with the Classical Lamination Theory (CLT) prediction. This is achieved by neglecting the transverse shear strain components γ_{xy} and γ_{yz} in Eq 3. In this case the rotations β_x and β_y are expressed as

$$\beta_x = \frac{\theta}{L}y$$
$$\beta_y = -W,_y \qquad (26)$$

and Eq 22 simplifies to

$$\frac{\theta}{L} = \frac{1}{4\psi b}\left[-\alpha_{12}F + \frac{\alpha_{12}}{2}T\right] = \frac{\left[-2B_{16}F + (A_{11} - A_{12})T\right]}{8b\left[D_{66}(A_{11} - A_{12}) - 2B_{16}^2\right]} \qquad (27)$$

The CLT solution violates the free edge boundary condition on the twisting moment given in Eq 18.

Finite Element Solution

A finite element solution was obtained using the finite element code ABAQUS. The discretization of the model was performed with a mesh containing 891 nodes and 800 quadrilateral shell elements. There are 5346 degrees of freedom for the model, generating a wave front width of 78. The material properties are given in Table 1 and the lamination sequence corresponds to the hygrothermally stable lay-up previously defined with $\alpha=30°$. An axial loading of 489 N was evenly distributed over the nodes at one end, 4.4 N at each node, while the boundary conditions at the opposite end correspond to a clamped condition. The angle of twist at the loaded end was indicated by the nodal rotations as 8.02 degrees. As a verification, the value was also computed using the nodal displacements, resulting in good agreement with the first value.

Testing Method and Instrumentation

The goals to be achieved by testing extension-twist coupled laminates are to verify the theoretical prediction of the relationship between axial force and twist.

Test Specimen

The specimen used for all the testing methods was manufactured from Ciba Geigy C30/922 graphite/epoxy unidirectional prepreg tape. The specimen dimensions are 246 mm X 22.9 mm X 0.91 mm. One end of the specimen has a built-in pin joint as shown in Fig. 2. The material constants E_{11}, E_{22}, G_{12}, v_{12}, and v_{21} were determined by measuring strains in $[0]_8$, $[90]_8$, and $[45]_8$ specimens. The subscripts 1 and 2 refer to the material principal directions. The modulus E_{11} and Poisson's ratio v_{12} are determined from the $[0]_8$

laminate. Similarly E_{22} and v_{21} are determined from the $[90]_8$ laminate measurements and G_{12} is found from the $[45]_8$ laminate measurements. The material properties are summarized in Table 1. The material symmetry property $(v_{12}E_{22}=v_{21}E_{11})$ is satisfied within 3.4%

Thrust Bearing Apparatus

The first apparatus uses a thrust bearing to achieve the free-rotating end condition as shown in Fig. 3. The load is applied via a universal testing machine, through the transducer, and the resultant twist of the laminate is measured by the change in voltage across a linear precision potentiometer mounted in the transducer. By measuring the twist angle and the applied load, the relationship between axial force and twist can be found. This design is easily produced, supplies repeatable results, and is easily interfaced with either a voltmeter or computer data acquisition system. However, due to friction of the thrust bearing in the transducer, the overall accuracy of the test changes throughout the loading sequence. Consequently, the measured twist is less than would occur in a truly free state.

The torsional restraining moment of the thrust bearing transducer was measured by applying an axial load to a rigid sample mounted between two like transducers. The sample was then loaded axially while the torque required to turn it was applied using a dead weight and pulley system. The weight at which the sample started rotating was used to calculate the torsional restraining moment. The results were then divided by two to account for only one of the transducers. The results of this calibration procedure are provided in Fig. 4. The restraining moment due to friction is small, but not negligible. The value at zero axial load is the restraining moment of the potentiometer itself.

The benefits of this method are that the testing procedure is no more complicated than the procedure used in a simple axial test. This allows for rapid testing of a large number of laminates if needed. With the use of different loading grips, the transducer can accommodate a variety of laminate geometries including closed sections.

The testing procedure for this apparatus follows in the same manner as a normal tension test. Once the laminate is clamped in the testing machine and transducer, load is applied manually. The resultant twist can then be measured by noting the change in output voltage from the transducer. The results from this test are shown in Fig. 5. The Shear Deformation Theory (SDT) prediction in Eq 25, which is identical to the Classical Lamination Theory (CLT), and finite element solution are shown with the data. The relative difference between the FEM prediction and the best line of fit of the data is 15%. For the SDT this difference is 33%. The difference between the analytical prediction and test data is due to the restraining moment induced by the thrust bearing transducer. This can be accommodated in the SDT prediction by including a twisting moment proportional to the applied load expressed as $T = -\xi F$. This moment is a result of modeling the friction of the thrust bearing as a torsional spring with a spring constant, ξ equal to the slope of the line provided in Fig. 4. A comparison between test data and SDT with and without friction appears in Fig. 6. The relative difference between the SDT with friction and the test data then drops to 1.9%. The SDT with friction is based on Eqs 22-24. The influence of shear deformation on the coupling can be assessed by comparing this prediction with Eq 27. The latter appears in Fig. 6 as CLT. It is of interest that the influence of shear deformation on the coupling is negligible for the lay-up and material system considered.

Rotating Frame Apparatus

The second testing apparatus uses a rotating testing frame as shown in Fig. 7. The major components of the apparatus are highlighted in the figure. The laminate under test is pinned at one end to a fixture which rotates in a vacuum chamber to eliminate aeroelastic effects. A mass is clamped to the other end of the laminate to provide the axial load when the load frame is rotating. The advantage to this testing method is that the outboard end of the laminate is unrestrained from twisting. However, failure testing using this method would be unsafe.

The testing procedure is the following. The testing chamber is evacuated to 724 mm Hg gage pressure. The angular speed of the rotating frame can then be increased from zero to a maximum of 5,000 rpm. The result of the increase in rpm is an increase in the axial load applied to the laminate. The rpm is monitored with a digital tachometer and maintained with a controller to within ± 1 rpm. The resultant load is calculated from the weight of the end mass, the rotational speed and the distance of the center of gravity of the weight to the axis of rotation. For the tests presented here the end mass is 69 grams, the radius of rotation of the mass is 239 mm, and the maximum rpm is 3,045. The resulting end load at maximum rpm is therefore 1,655 N. The rotation of the end mass was measured optically using a Questar telemicroscope mounted on an instrumented traverse and a strobe light. The results from this test are shown in Fig. 8 along with the SDT and CLT predictions. The CLT with applied torque, T equal to zero is indistguishable from the SDT and both are presented by the dashed linear curve. This prediction agrees with the test data at low rotation angles and axial loads, however, at higher rotations the linear approximation is no longer valid. This is due to the finite rotation of the end mass. As the mass twists, the resultant load is no longer purely axial as shown in Figs. 9a and 9b and induces a torsional moment which tends to return the laminate to the undeformed state.

This torsional moment is proportional to $\sin(2\theta)$ where θ is the twist angle of the end of the laminate. A derivation of T is provided in Appendix I. Upon substitution of T into Eq 22, the predicted extension-twist coupling becomes a non-linear function depicted by the solid line in Fig. 8.

Improved Thrust Bearing Apparatus

The third testing method proposed is an improved version of the thrust bearing transducer. The improvements include changing the bearing media and method of load application to ensure frictionless movement. The maximum load capacity of the improved apparatus is approximately 9 kN. The resolution of the output angle is $\pm 0.1°$ with a maximum hysteresis of $0.2°$. The high resolution is accomplished by using an optical measurement technique. The most significant difference from the thrust bearing transducer is that the accuracy of the improved method is unaffected by load. Therefore, failure testing can be achieved without friction.

The test procedure follows in the same manner as that described for the first thrust bearing apparatus with the difference in load application only. A differential pressure is applied to the improved transducer and the resultant load is measured by the testing machine load cell. The angle of twist can be read by either a digital display or a computer data acquisition system. Results from this test along with the laminated plate theory and finite element results are shown in Fig. 10. The relative difference between the line of best fit of the test data and the CLT, SDT is 17%. The relative difference for the FEM is 1.7%.

Comparison of Test Methods

Results for all the tests are shown in Fig. 11 with the finite element, and laminated plate theory solutions. The improved thrust bearing apparatus shows the greatest promise for future testing because of its ease of use when testing a large number of laminates. While the rotating frame apparatus guarantees that the end of the laminate under test is indeed free, using an inertial load results in parasitic effects once the laminate twists. As the laminate twists, the twisting of the end mass results in not only axial load, but a couple that tends to return the laminate to the undeformed state. The result is an apparent increase in stiffness of the laminate.

Conclusion

Three methods for testing extension-twist coupled laminates have been presented. Two of the methods yield results that follow the trend predicted by a finite element method and shear deformation laminated plate theory for axial loading. The rotating frame apparatus does not yield results that correspond with the predicted values due to the change in loading condition that occurs with finite twist of the end mass. This effect has been quantified by modeling the moment generated by the inertial load as the mass twists yielding good correlation with the experimental results. However, the maximum twist obtainable using this method asymptotically approaches a low finite value at low axial load.

Of the methods used in this work, the improved apparatus shows the most promise. With the restraining moment encountered in the thrust bearing apparatus significantly reduced, the results from the improved version correlate well with the theoretical predictions. The ease of use of this apparatus compared to the rotating frame also lead to this conclusion.

Although the appropriate theoretical predictions correlate well with each of the testing methods, the improved apparatus comes closest to the ideal testing condition. Because of its frictionless nature, the restraining moment of the grip is negligible. Likewise, the rotating frame apparatus ensures a frictionless and free end condition, but the inertial forces used to develop the axial load have a parasitic effect dependent on the displacement of the laminate. Therefore, while this method may not be perfectly suited for determining the extension twist coupling, it is ideally suited to isolating aeroelastic effects on the laminate response.

Appendix I

Derivation of Torsional moment for the rotating frame apparatus.

Consider the end mass connected to the specimen undergoing twisting rotation of magnitude θ as shown in Fig. 9b. For an element at a distance x, the centrifugal force denoted by F_c is given by

$$F_c = m\omega^2 R dx \qquad (28)$$

where m is the mass per unit length, R is the radial distance, and ω is the angular speed. The tangential component of F_c is given by

$$F_{ct} = m\omega^2 R \sin\beta dx = m\omega^2 x \cos\theta dx \qquad (29)$$

While the axial component of F_c is given by

$$F_{ca} = m\omega^2 R \cos\beta dx = m\omega^2 l dx \qquad (30)$$

The associated torque is

$$T = 2\omega^2 \sin\theta \cos\theta \int_d m x^2\, dx = \omega^2 \sin 2\theta \int_d m x^2\, dx \qquad (31)$$

and the associated bending moment is

$$M_B = \omega^2 l \sin\theta \int_d m x dx \qquad (32)$$

The mass is clamped to the specimen with two symmetrically located screws. They are treated as lumped masses at the proper locations. The symmetric variation of m along the positive x direction is given by

$$m_1 = 1.26 \, {}^g\!/_{mm}, \quad 0 \le x \le 15.3, \text{ and } 21.7 < x \le 24.8$$

$$m_2 = 1.77 \, {}^g\!/_{mm}, \quad 15.3 < x \le 21.7 \qquad (33)$$

The torque is then

$$T = 2\omega^2 \sin 2\theta \left[m_1 \int_0^{15.3} x^2\, dx + m_2 \int_{15.3}^{21.7} x^2\, dx + m_1 \int_{21.7}^{24.8} x^2\, dx \right] \qquad (34)$$

Due to the symmetry of the mass about the center, the bending moment in Eq 32 vanishes.

Acknowledgment

References

[1] Chandra, Stemple, and Chopra, "Thin Walled Composite Beams Under Bending, Torsional, and Extensional Load," *Journal of Aircraft,* Vol. 27, No. 7, July 1990.

[2] Armanios, E. A., Hooke, D., Kamat, M., Palmer, D., and Li, J., "Design and Testing of Composite Laminates for Optimum Extension-Twisting Coupling," *Composite Materials: Testing and Design (Eleventh Volume), ASTM STP 1206,* E. T. Camponeschi, Jr., Ed., American Society for Testing and Materials, Philadelphia, 1993, pp. 249-262.

[3] Armanios, E. A., and Li, J., " Interlaminar Fracture Analysis of Unsymmetrical Laminates," *Composite Materials: Fatigue and Fracture, Fourth Volume, ASTM STP 1156,* W. W. Stinchcomb and N. E. Ashbaugh, eds., American Society for Testing and Materials, Philadelphia, 1993, pp. 341-360.

[4] Winckler, S. I., "Hygrothermally Curvature Stable Laminates with Tension-Torsion Coupling," *Journal of the American Helicopter Society,* Vol. 31, No. 7, July 1985, pp. 56-58.

[5] Vinson, J. R. and Sierakowski, R. L. *The Behavior of Structures Composed of Composite Materials,* Martinus Nijhoff, Dordecht, The Netherlands, 1987, p. 54.

List of Tables

List of Figures

Table 1. Material Properties and Geometry

E_{11} = 134 GPa
E_{22} = 9.8 GPa
G_{12} = 7.45 GPa

ν_{12} = .35
Total Thickness = 0.9 mm
Width = 23 mm
Length = 224 mm
Number of Plies = 8
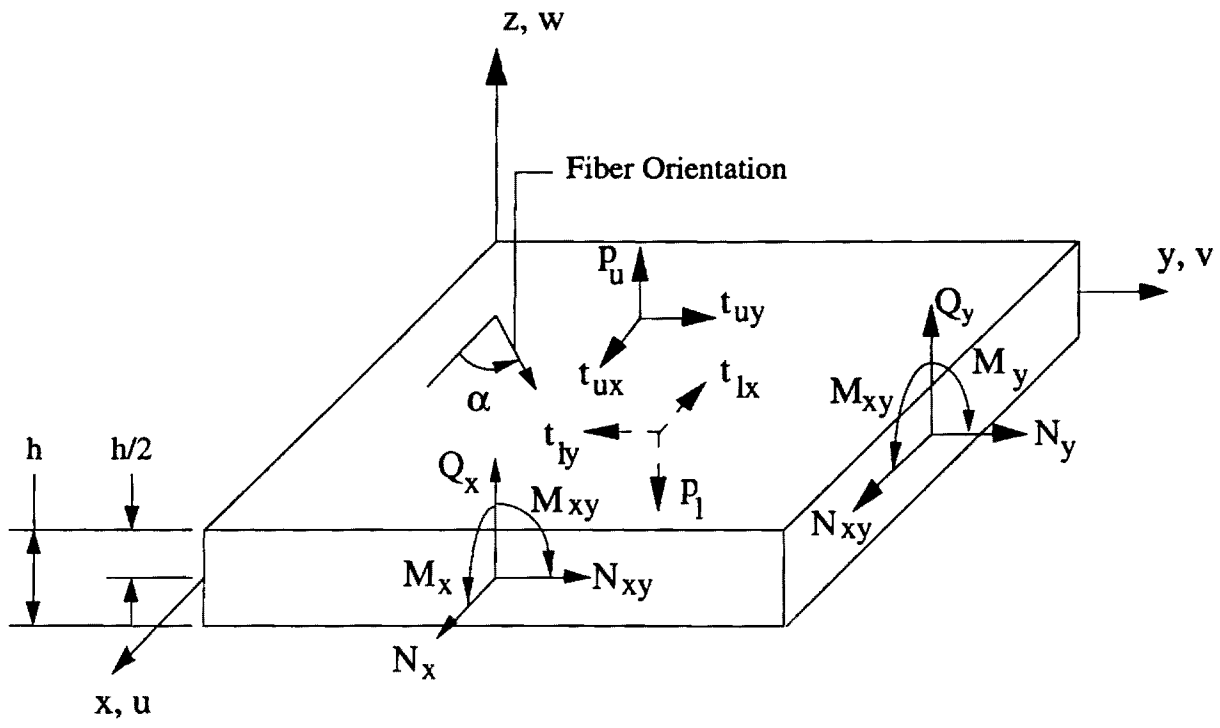
Figure 1. Generic Sublaminate
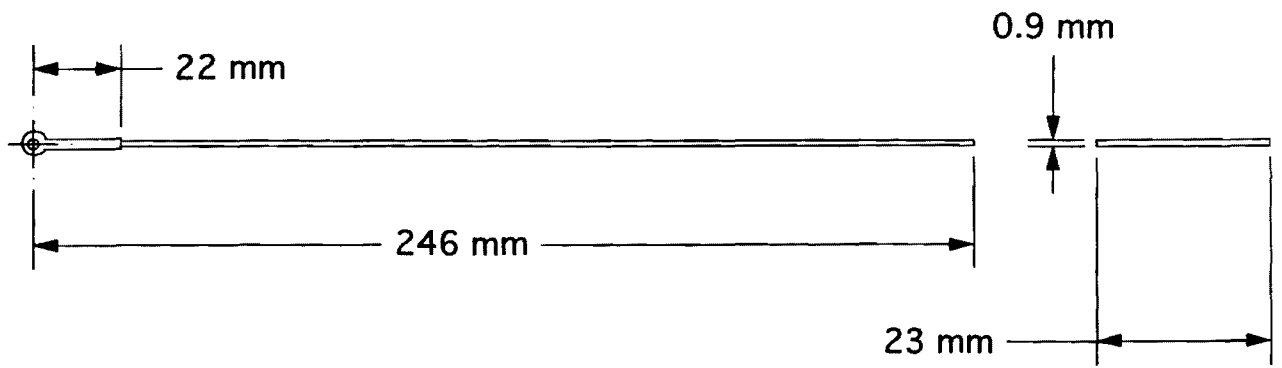
Figure 2. Specimen Design
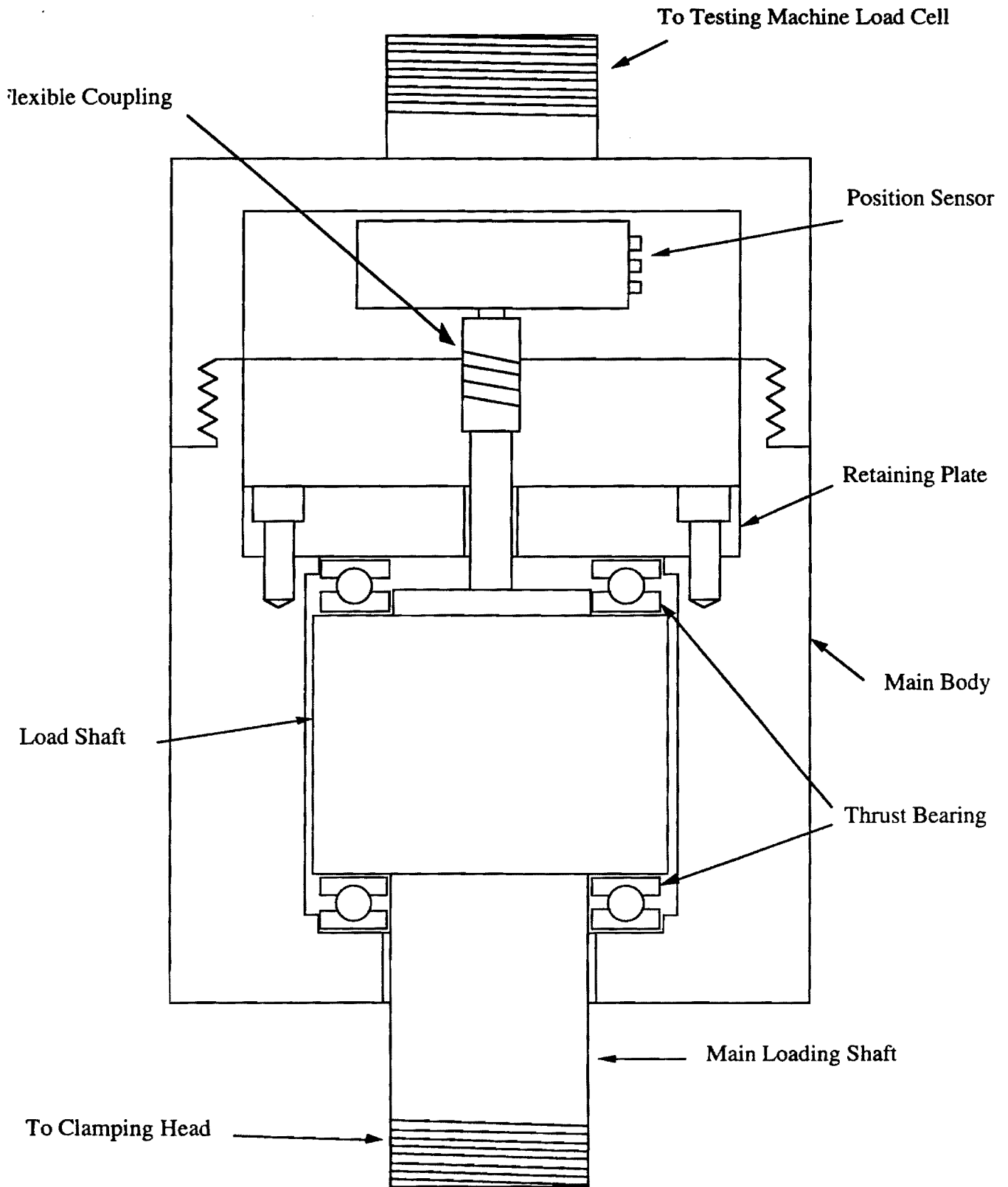
Figure 3. Schematic View of Thrust Bearing Apparatus
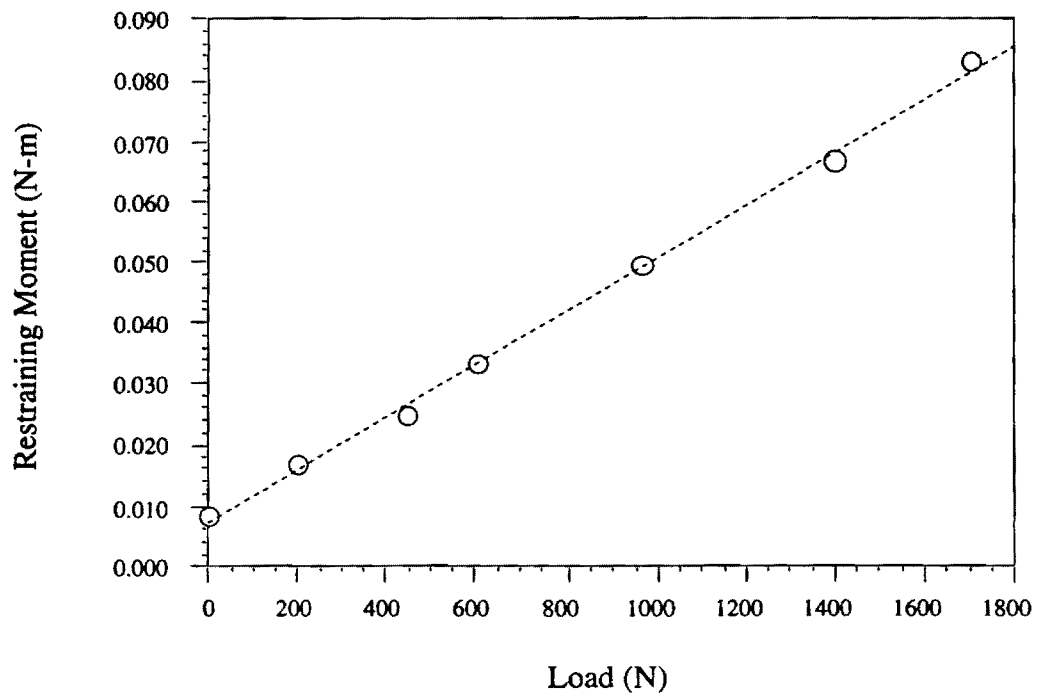
Figure 4. Restraining Moment for Thrust Bearing Transducer
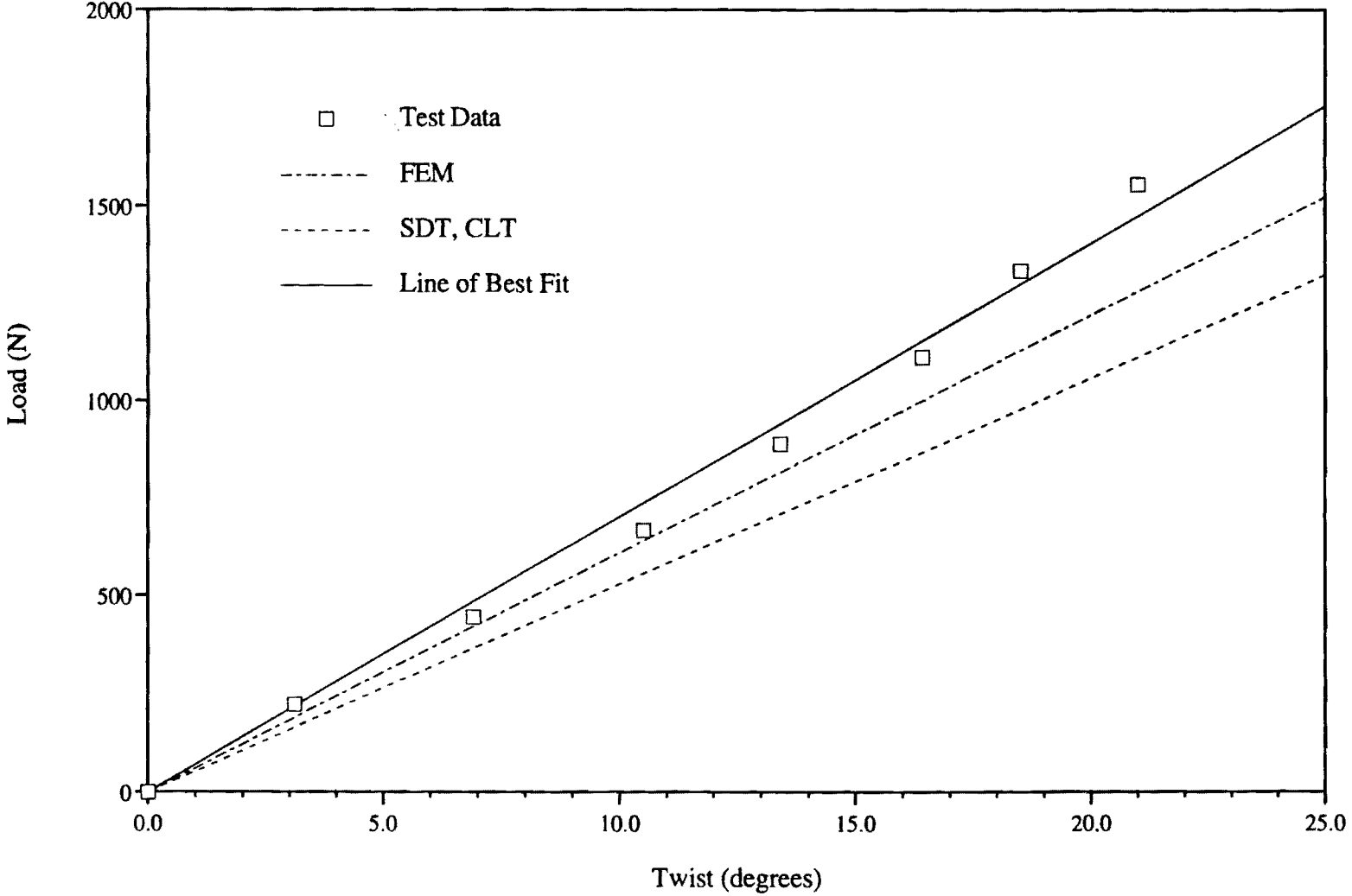
Figure 5. Experimental Results for Thrust Bearing Apparatus

Twist Trend for C30/922 Gr/Ep Laminate
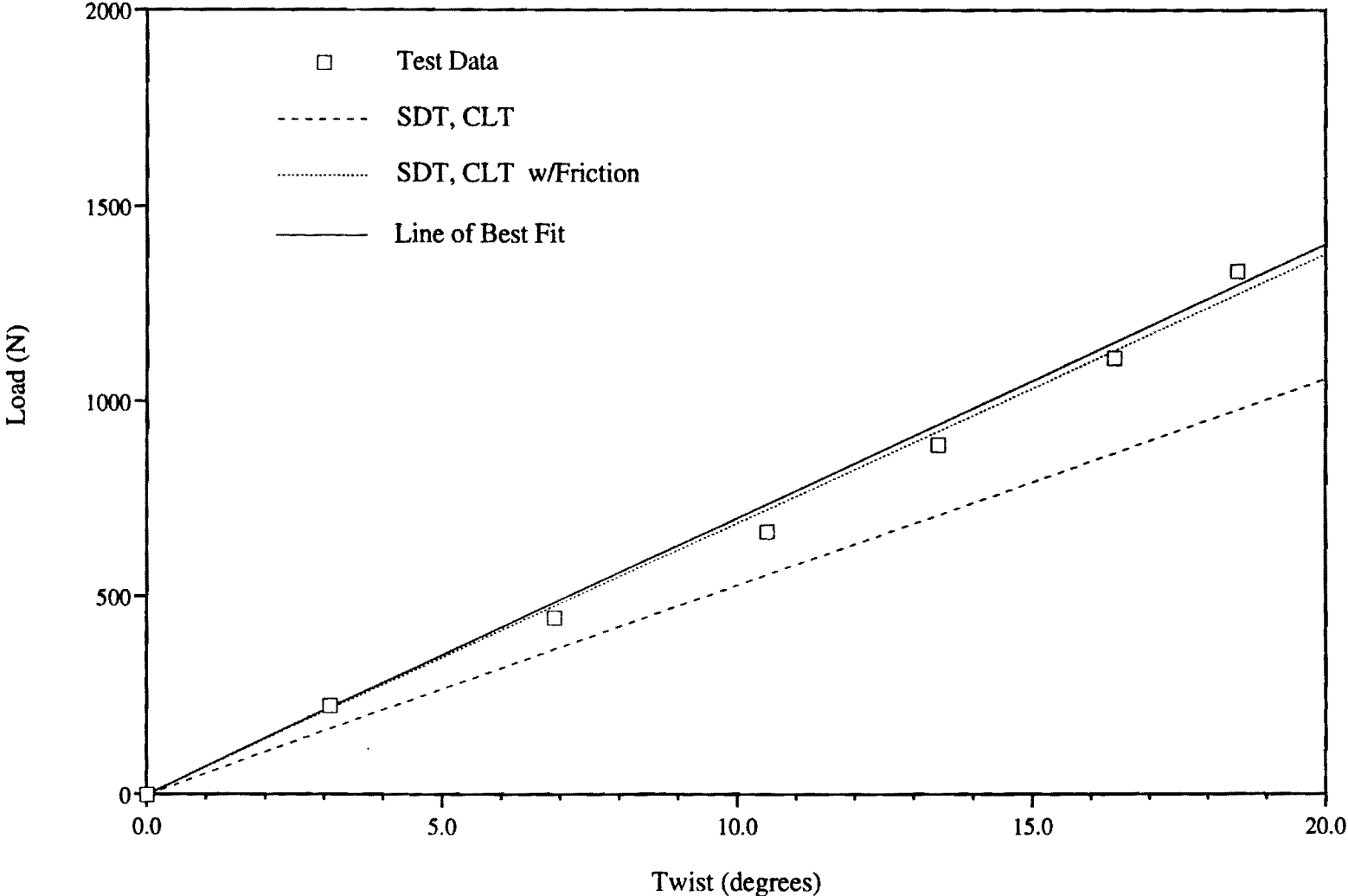
Figure 6. Thrust Bearing Results with Friction Added

Master Switch   Motor Controller   LCD Tachometer   End Mass   Strobe Trigger
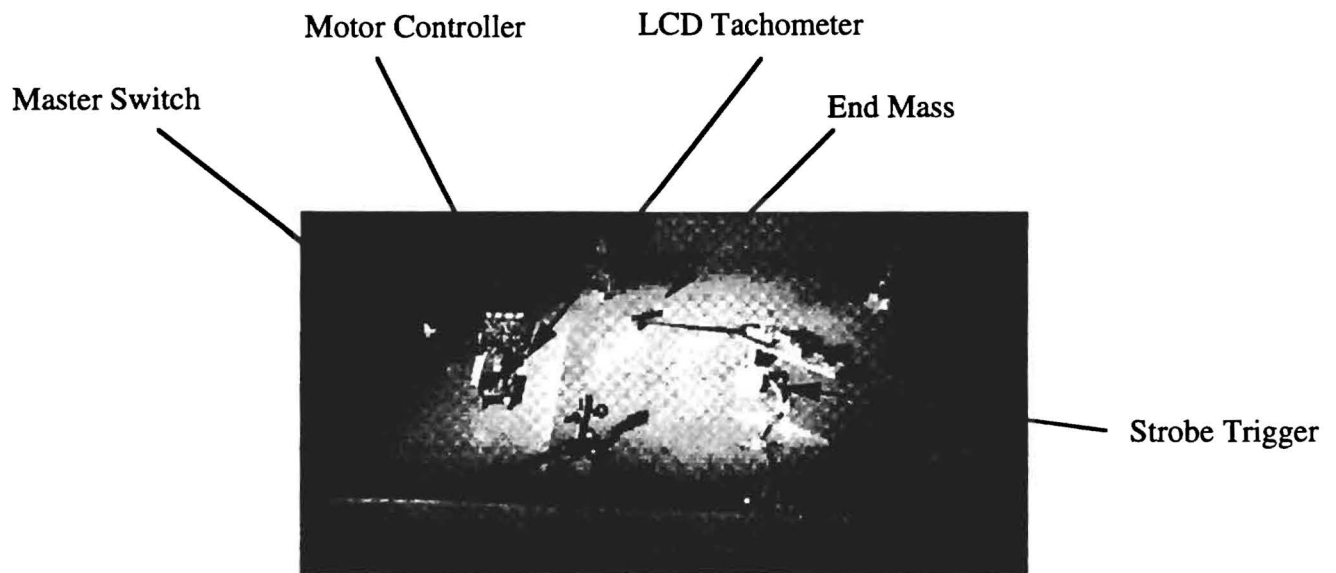
Figure 7. Rotating Frame Apparatus without Vacuum Dome

Twist Trend for C30/922 Gr/Ep Laminate
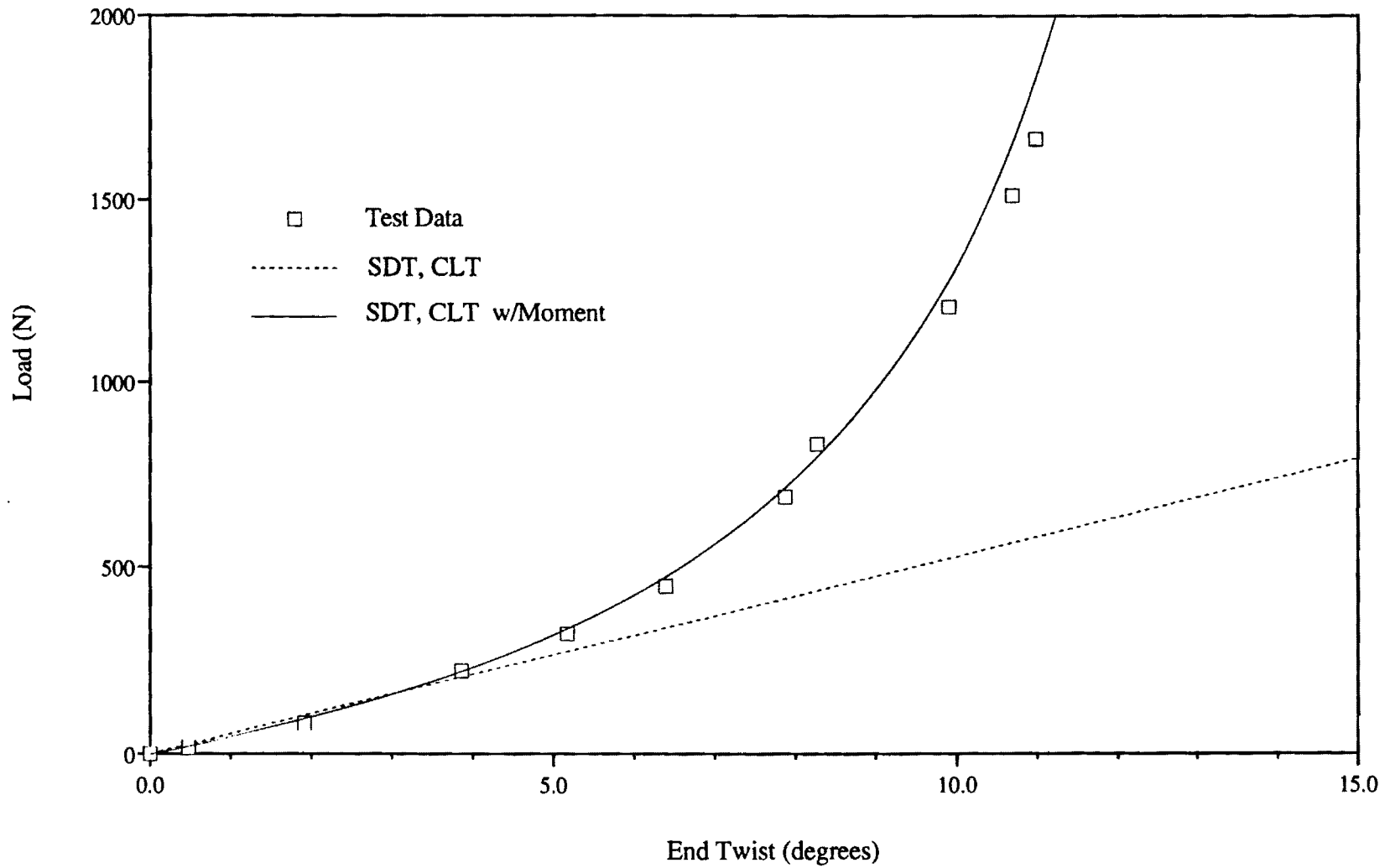
Figure 8. Experimental Results for Rotating Frame Apparatus
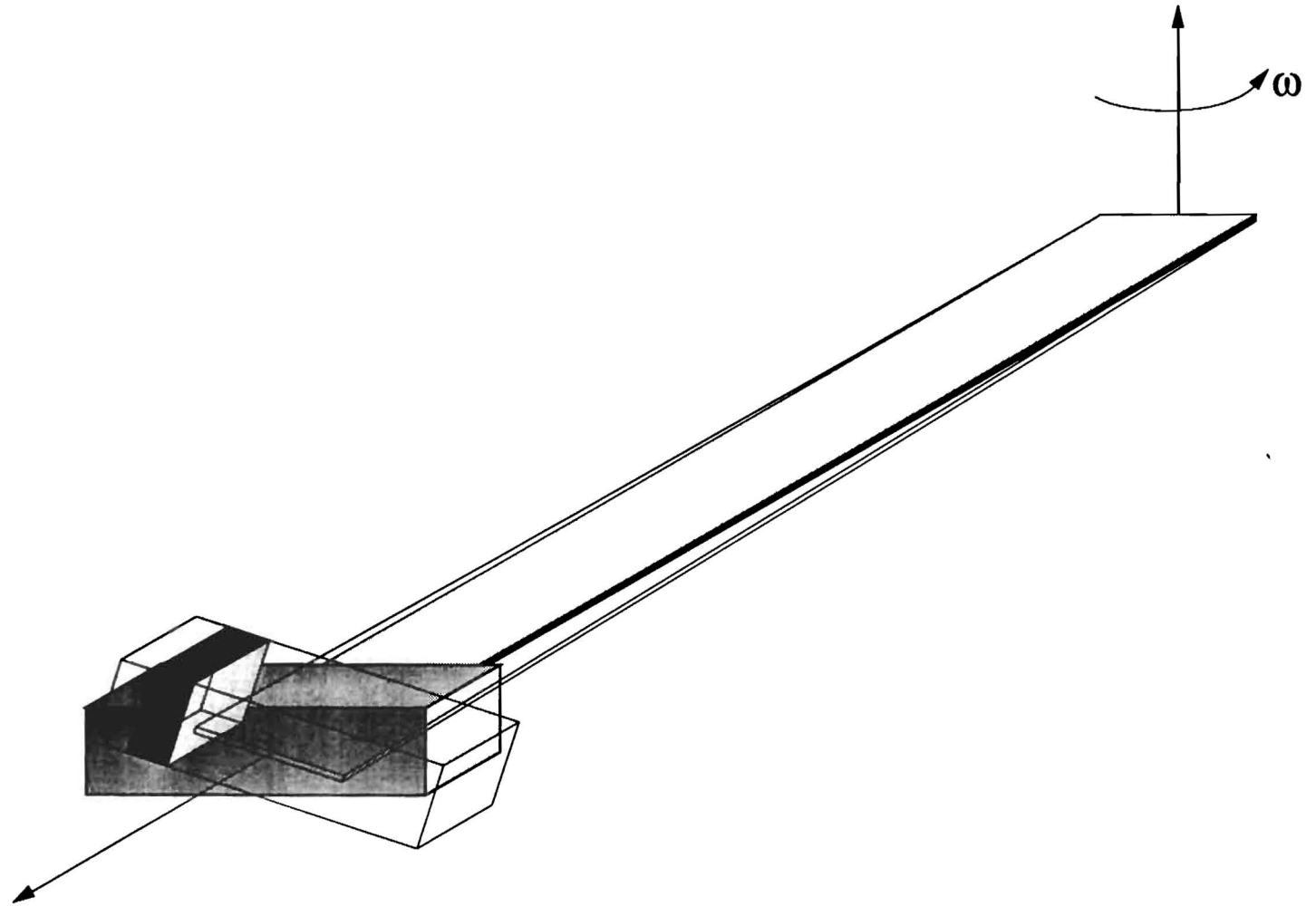
Figure 9a. Laminate in Undeformed and Deformed State

$$R^2 = l^2 + (x \cos \theta)^2$$

$$\tan \beta = \frac{x \cos \theta}{l}$$
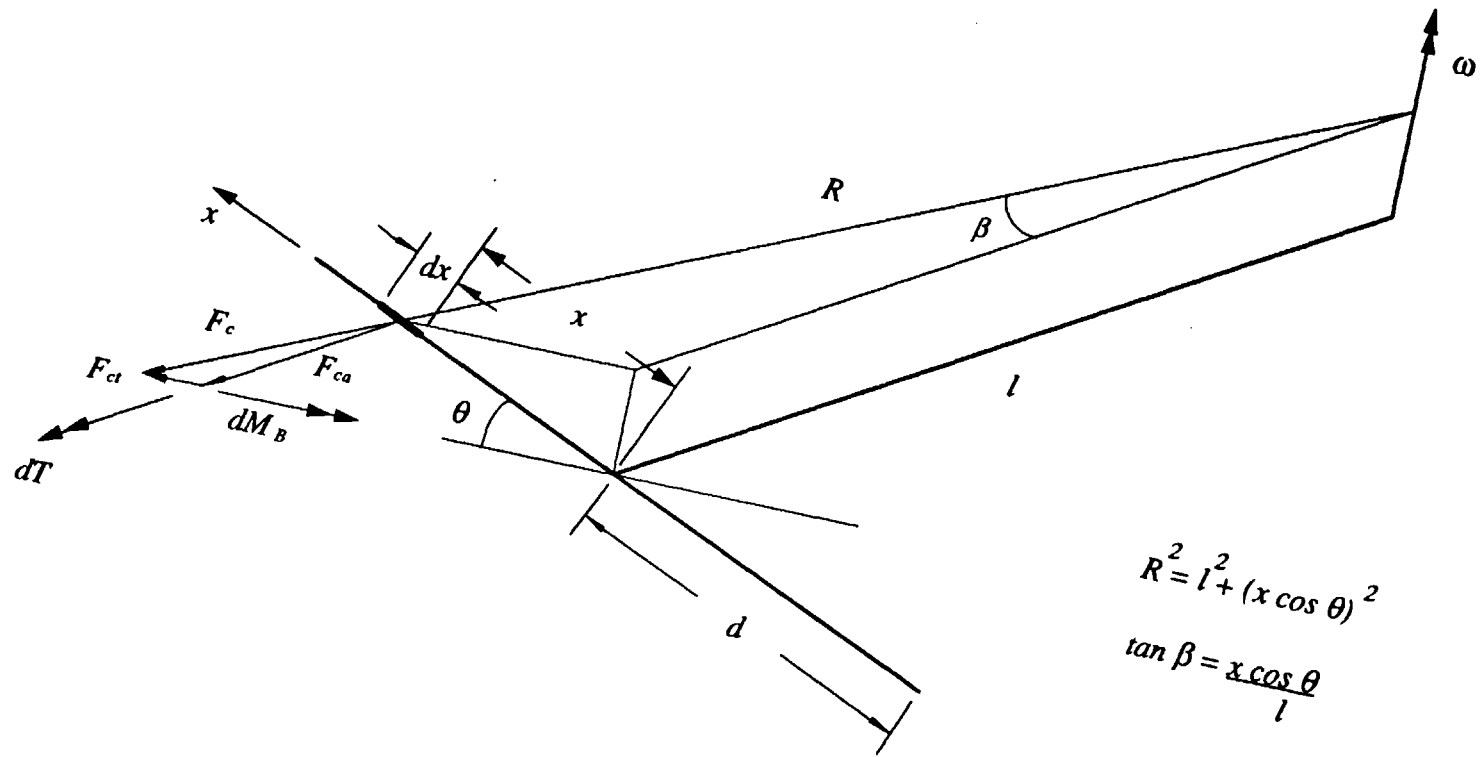
$$F_c = m\,dx\,\omega^2 R$$

$$F_{ct} = m\,dx\,\omega^2 R \sin \beta$$

$$F_{ca} = m\,dx\,\omega^2 R \cos \beta$$

$$dT = m\,dx\,\omega^2 R \sin \beta\, x \sin \theta$$

$$dM_B = m\,\omega^2 l x \sin \theta\, dx$$

Figure 9b. Decomposition of Inertial Forces

Twist Trend for C30/922 Gr/Ep Laminate
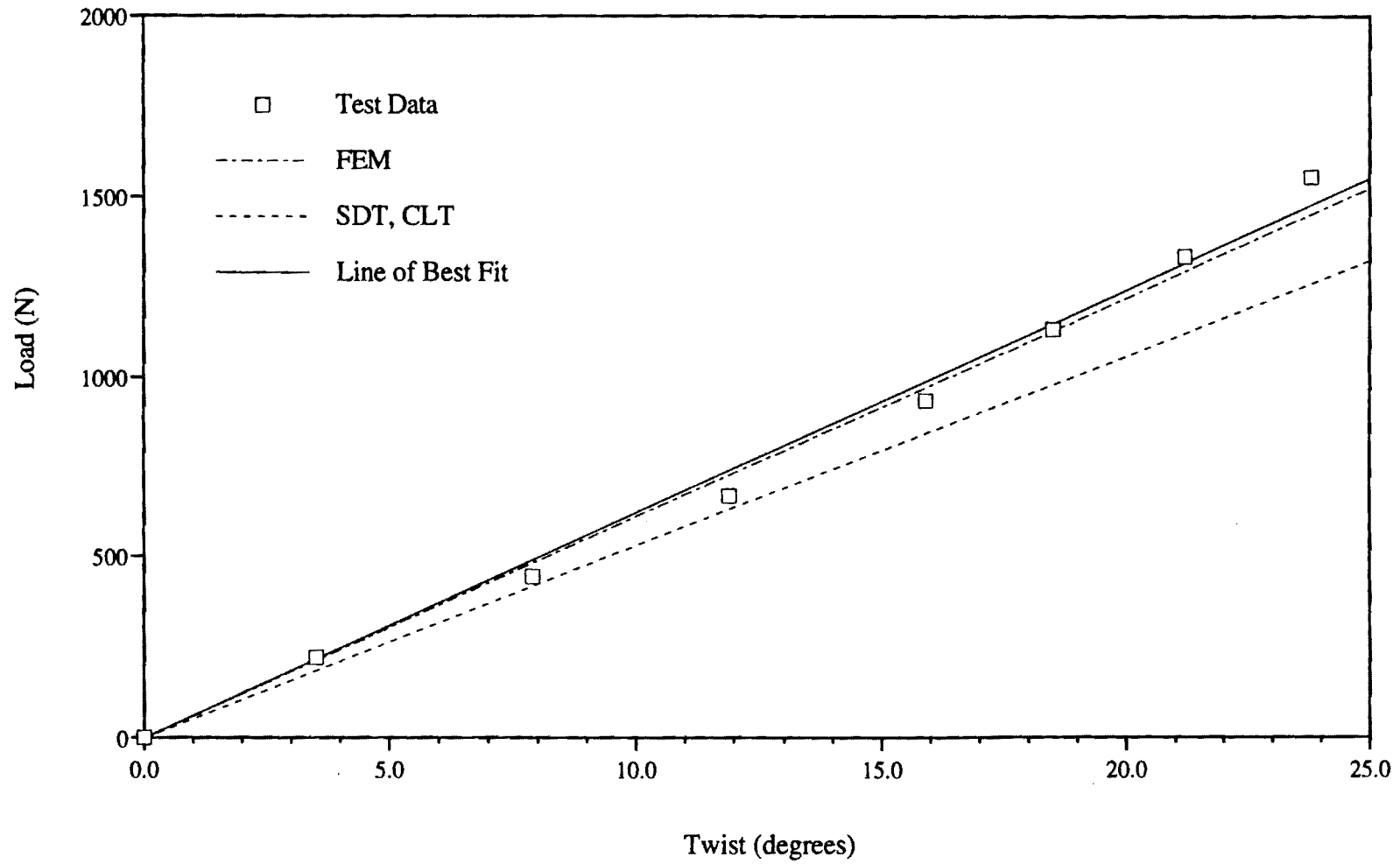
Figure 10. Experimental Results for Improved Thrust Bearing Apparatus

Twist Trend for C30/922 Gr/Ep Laminate
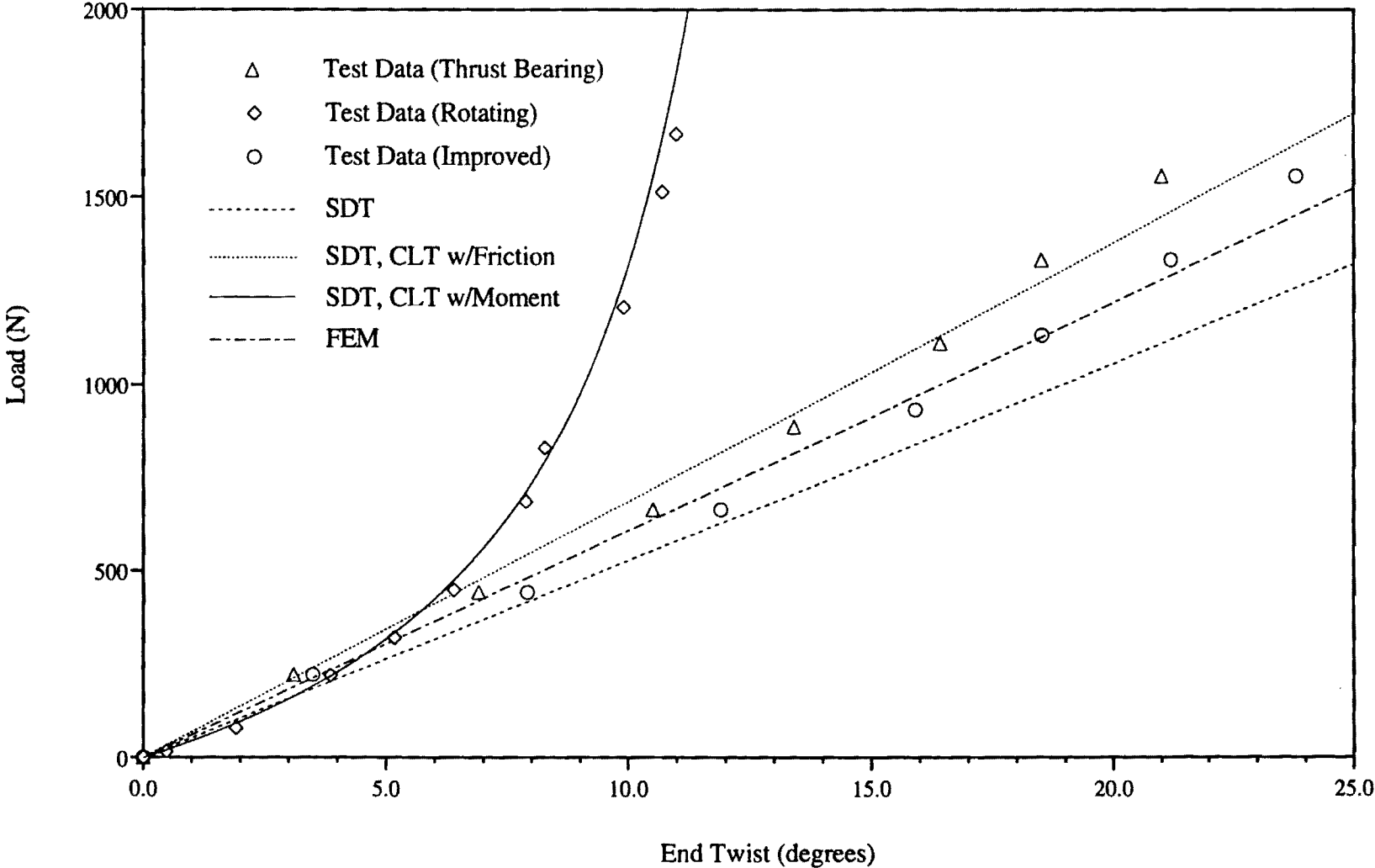
Figure 11. Experimental Results for All Testing Methods

STATUS REPORT

ADVANCED COMPOSITES AND SMART STRUCTURES RESEARCH

GRANT : DAAL03-92-G-380
GEORGIA TECH PROJECT: E16-X11

PRINCIPAL INVESTIGATOR
E. A. Armanios
School of Aerospace Engineering
Georgia Institute of Technology
Atlanta GA 30332-0150

Sponsor Technical Contact: DR. LEBONE MOETI
Clark Atlanta University
221 James P. Brawley Dr., S.W.
Atlanta, GA 30324

Problem studied

The primary objective of this research is the development of analytical tools, testing methods and smart concepts for advanced composite structures.

Progress during this reporting period

During this period an investigation of geometric and material non linear effects was performed. This investigation aimed at providing a model for the nonlinear behavior in extension-twist coupling data depicted in Figure 1. This nonlinear behavior could be a result of the finite twisting rotation at the specimen ends, the nonlinear shear stress/strain or initial warping associated with manufacturing tolerances and curing cycle. It was found that the nonlinear shear stress/strain behavior for the material system considered has a negligible influence on the extension-twist coupling. Also, the influence of initial twist as measured from the cured specimen did not result in any significant nonlinearity. However, the geometrically nonlinear model showed significant stiffening and over predicted the load associated with large twist rates.

An investigation of the finite element model appearing in Figure 1 is underway. The model is based on the ABAQUS code and allows for geometric nonlinearity. The specimen was discretized using 800 quadrilateral shell elements containing 891 nodes and 5346 degrees of freedom. The prediction of this model shows the best agreement with test data.
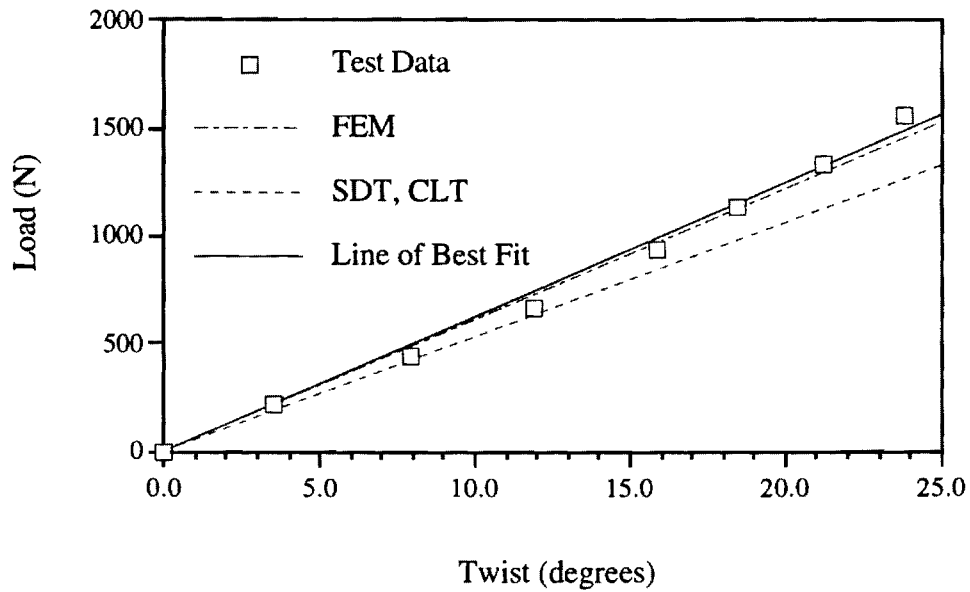
Figure 1. Comparison of analytical predictions with test data

Ongoing research

In addition to the finite element investigation, four specimens are being fabricated using a new material system in order to isolate the variability associated with manufacturing tolerances and cure cycle.

Work on the manufacturing of specimen with optimum extension-twist coupling is also planned.

STATUS REPORT

ADVANCED COMPOSITES AND SMART STRUCTURES RESEARCH

GRANT : DAAL03-92-G-380
GEORGIA TECH PROJECT: E16-X11
PRINCIPAL INVESTIGATOR
E. A. Armanios
School of Aerospace Engineering
Georgia Institute of Technology
Atlanta GA 30332-0150

Sponsor Technical Contact: DR. LEBONE MOETI
Clark Atlanta University
221 James P. Brawley Dr., S.W.
Atlanta, GA 30324

Problem studied

The primary objective of this research is the development of analytical tools, testing methods and smart concepts for advanced composite structures.

Progress during this reporting period

A new set of specimens exhibiting extension-twist coupling were fabricated and tested in order to resolve the nonlinear behavior outlined in the previous progress report.

Laminates were fabricated using the $[\theta/(\theta-90)_2/\theta/-\theta/(90-\theta)_2/-\theta]_T$ stacking sequence with $\theta = 20°$ and $30°$. Four specimens were fabricated for each value of θ. Each specimen was 1 in. wide and 11 in. long made of ICI Fiberite T300/954-3 Graphite/Cyanate prepreg material. All cured specimens had an initial twisting curvature. An investigation of the pretwist indicated that it was a result of the cure cycle provided by the manufacturer. Several trials were made in order to minimize initial warping by changing the cure cycle. The final modified cure cycle resulted in a -0.5° /in rate of pretwist which was considered acceptable. In order to determine the in-plane material properties, 0°, 90° and 45° unidirectional eight ply laminates were constructed and tested. The specimens were 1 in. wide and 11 in. long, and cured with the same modified cycle. A summary of the material properties is provided in the following table.

Properties of T300/954-3 Graphite/Cyanate Material System

$E_{11} = 135.6$ GPa (19.7 Msi)
$E_{22} = E_{33} = 9.9$ GPa (1.4 Msi)
$G_{12} = G_{13} = 4.2$ GPa (0.6 Msi)
$G_{23} = 2.5$ GPa (0.36 Msi)

$\nu_{12} = \nu_{13} = 0.3$

$\nu_{23} = 0.5$
Ply Thickness = 0.15 mm (0.006 in)
Laminate Semi Width = 12.6 mm (0.5 in)

The improved thrust bearing transducer developed earlier and described in Ref. *1* was used to measure the extension-twist coupling. The twist at the transducer end of the specimens was measured at load steps of 50 lbs. A plot of twist angle in degrees versus axial load in lbs appear in the attached figure for the $\theta = 30°$ laminate. Symbols 1 through 4 denote data from the four tested laminates. Three analytical predictions are plotted in the figure. The first, is the linear sublaminate shear deformation which is identical to the Classical lamination Theory prediction when the applied loading is purely axial with no restraining end moment. This prediction is denoted by CLT in the figure. The second, denoted by Flat in the figure, is a geometrically nonlinear analysis which accounts for the effect of finite twisting rotation. The solid line corresponds to the third prediction which is a geometrically nonlinear analysis that includes pretwist. A pretwist value of -0.5° /in is considered.

From the comparison provided in the figure, the following observations are worth noting:

1. A good correlation exists among the three analytical predictions and test data at low level of loading,
2. The nonlinear behavior exhibited by the data is a result of the finite cross sectional twisting rotation of the specimens as axial load is applied,
3. The linear CLT prediction introduces a softening effect, in the sense that less deformation is produced relative to the finite cross sectional twisting rotation prediction for a given applied axial load,
4. The influence of a negative pretwist increases this softening effect as more deformation (unwinding) is produced for a given load relative to a specimen with no initial pretwist,
5. The inclusion of the pretwist in the finite rotation theory leads to a prediction that is closer to test data trend.

Ongoing research

Documentation of the geometrically nonlinear analysis with and without pretwist is being prepared for publication. Comparison of predictions with nonlinear finite element simulations is being performed in order to provide further illustration of the accuracy of the model relative to numerical methods. This will enable the extension of the model to the investigation of their constrained optimum coupling and the influence of internal delamination on the coupling in unsymmterical laminates. Both tasks are currently being investigated under the ARO Center of Excellence in Rotorcraft Technology.

REFERENCE

[1] Hooke, D. and Armanios, E. A., " Examination of Three Methods for Testing Extension-Twist Coupled Laminates," presented at the *ASTM Twelfth Symposium on Composite Materials: Testing and Design*, Montreal, Quebec, May, 16-17, 1994. Also to be published as an ASTM STP.
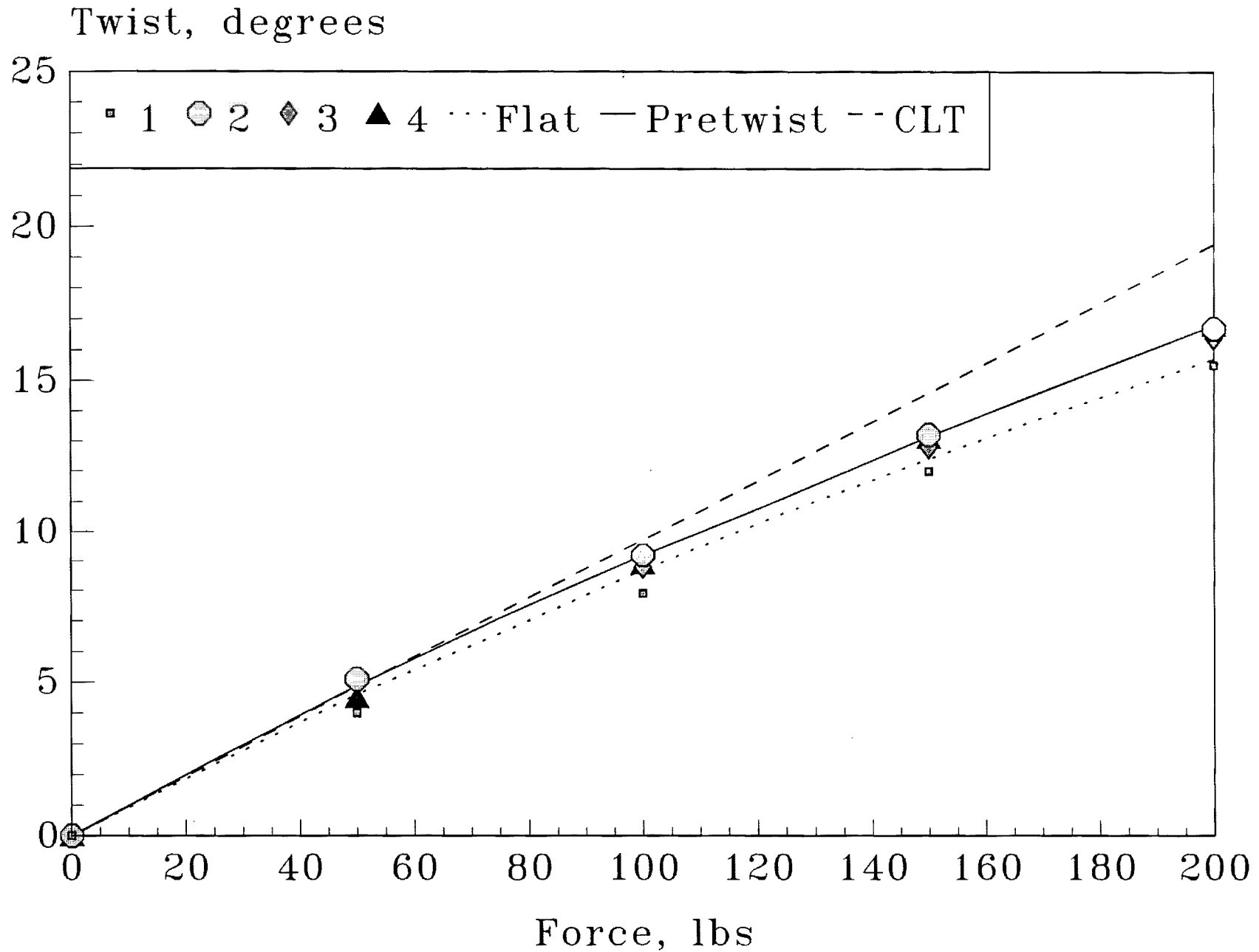
End Twist Data, CLT and Finite Deformation Theory Prediction, θ=30

STATUS REPORT

ADVANCED COMPOSITES AND SMART STRUCTURES RESEARCH

GRANT : DAAL03-92-G-380
GEORGIA TECH PROJECT: E16-X11
PRINCIPAL INVESTIGATOR
E. A. Armanios
School of Aerospace Engineering
Georgia Institute of Technology
Atlanta GA 30332-0150

Sponsor Technical Contact: DR. LEBONE MOETI
Clark Atlanta University
221 James P. Brawley Dr., S.W.
Atlanta, GA 30324

Problem studied

The primary objective of this research is the development of analytical tools, testing methods and smart concepts for advanced composite structures.

Progress during this reporting period

The geometrically nonlinear analysis with and without pretwist is under completion for publication. Also the effect of specimen width has been isolated. This could be of significance in simulating free-edge damage. Figure 1 shows a comparison of analytical twist predictions from three models with test data from four specimens. The first, referred to as Model (pretwisted), is the geometrically nonlinear model which accounts for the effect of initial pretwist resulting from the cure cycle. This pretwist amounted to -0.5°/in. The second, is the geometrically nonlinear model which neglects the effect of initial pretwist and is referred to as Model (flat) in figure 1. The third analytical model is a geometrically linear model of Reference 1. Figures 1 and 2 present the data from specimens with $[\theta/(\theta-90)_2/\theta/-\theta/(90-\theta)_2/-\theta]_T$ stacking sequence and $\theta = 20°$ and $30°$, respectively. the comparisons is figures 1 and 2 for both layups provides further verification to the observations made earlier for the case of $\theta = 30°$. These observations are restated in the following to underscore their significance:

1. A good correlation exists among the three analytical predictions and test data at low level of loading,
2. The nonlinear behavior exhibited by the data is a result of the finite cross sectional twisting rotation of the specimens as axial load is applied,
3. The linear CLT prediction introduces a softening effect, in the sense that more deformation is produced relative to the finite cross sectional twisting rotation prediction for a given applied axial load,
4. The influence of a negative pretwist decreases this softening effect as more deformation (unwinding) is produced for a given load relative to a specimen with no initial pretwist,
5. The inclusion of the pretwist in the finite rotation theory leads to a prediction that is closer to test data trend.

In order to investigate the influence of the width on the extension-twist coupling, one of the specimens, with a layup corresponding to $\theta = 30°$, was trimmed to half its width and tested. The linear theory of Reference 1 indicates that the twist versus extension relationship is linearly proportional to the width of the specimen. That is, a specimen trimmed to half its width should exhibit twice as much twist as the original specimen when subjected to the same load. The linear theory would therefore predict a twist versus applied stress relationship that is independent of the specimen width. A comparison of analytical prediction with test appears in Figure 3. The end twist is plotted against applied stress which is the applied load per unit cross sectional area. The comparison in figure 3 indicates that at stress level up to 15 MPa the end twist versus applied stress is independent of the specimen width. In contrast to the linear theory, higher level of applied stress shows a dependency of twist on the width of the specimen. Moreover, the predictions of geometrically nonlinear pretwist model are in very good agreement with test data

REFERENCE

[1] Hooke, D. and Armanios, E. A., " Examination of Three Methods for Testing Extension-Twist Coupled Laminates," presented at the *ASTM Twelfth Symposium on Composite Materials: Testing and Design*, Montreal, Quebec, May, 16-17, 1994. Also to be published as an ASTM STP.

[20/-70₂/20/-20/70₂/-20]_T laminate
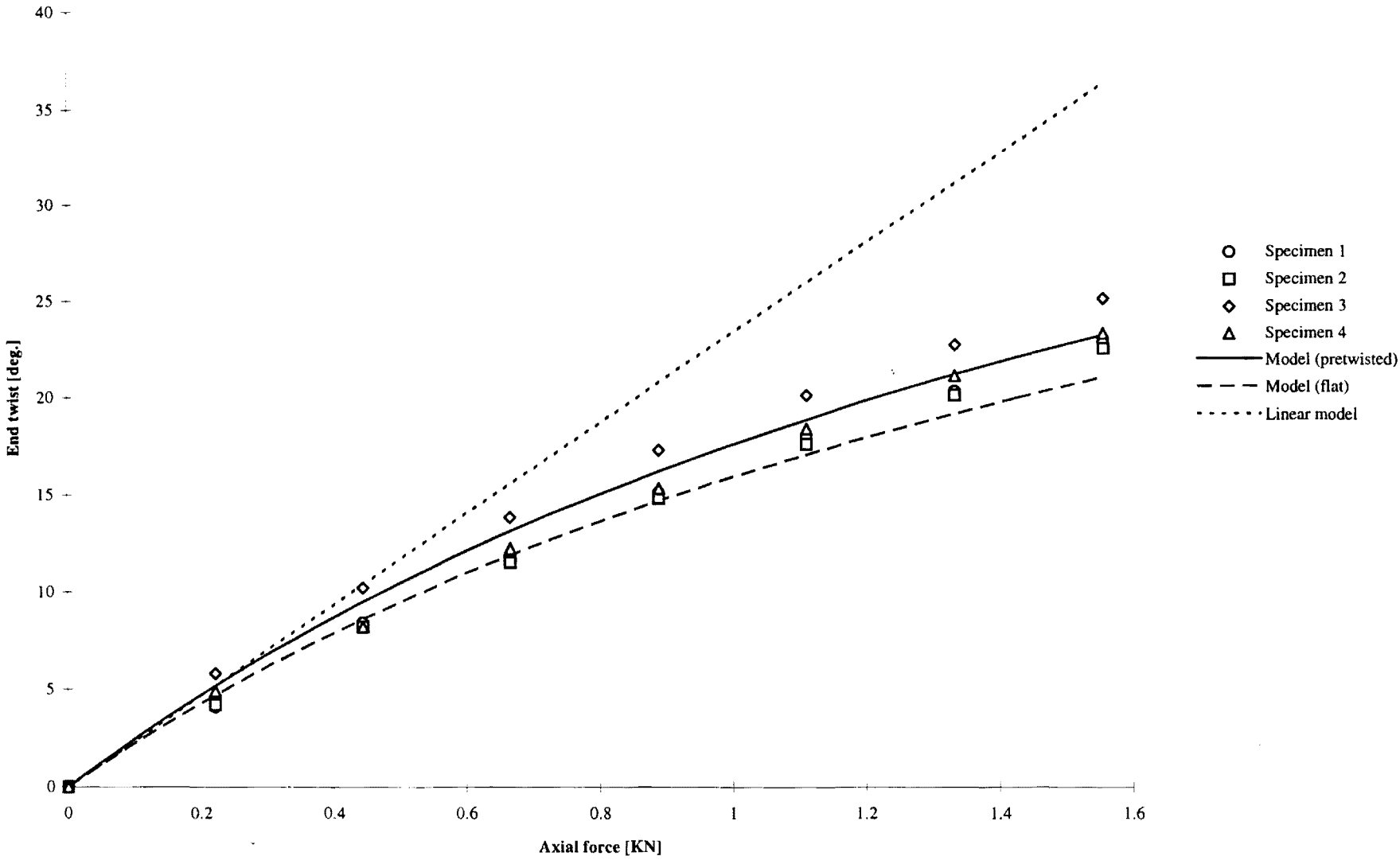
$[30/-60_2/30/-30/60_2/-30]_T$ laminate

Axial force [KN]

End twist [deg.]

Legend:
- ○ Specimen 1
- □ Specimen 2
- ◇ Specimen 3
- △ Specimen 4
- —— Model (pretwisted)
- – – – Model (flat)
- ······· Linear model

STATUS REPORT

ADVANCED COMPOSITES AND SMART STRUCTURES RESEARCH

GRANT : DAAL03-92-G-380
GEORGIA TECH PROJECT: E16-X11
PRINCIPAL INVESTIGATOR
E. A. Armanios
School of Aerospace Engineering
Georgia Institute of Technology
Atlanta GA 30332-0150

Sponsor Technical Contact: DR. LEBONE MOETI
Clark Atlanta University
221 James P. Brawley Dr., S.W.
Atlanta, GA 30324

Problem studied

The primary objective of this research is the development of analytical tools, testing methods and smart concepts for advanced composite structures.

Progress during this reporting period

The following is a summary of the analytical model for pretwisted composite strips undergoing finite displacement. Correlation with test data shows the accuracy of the extension-twist coupling predicted by the model. Correlation with predictions from finite element and other published numerical results is under way.

Displacement field

The displacement field is developed in three steps 3 accounting for a kinematic contribution. A finite rigid body twisting rotation is considered first. This is subsequently modified to include Saint Vénant's type warping where the transverse normal and "out-of-plane" shear strains are neglected. Finally, inplane extension, shear. bending and twisting curvatures are accounted for by superimposing a classical type small displacement field. A brief summary of key results is presented in the following.

Consider the laminated composite strip appearing in Fig. 1. Its thickness, h is small relative to the width $2b$ and its length L is large compared to the width.
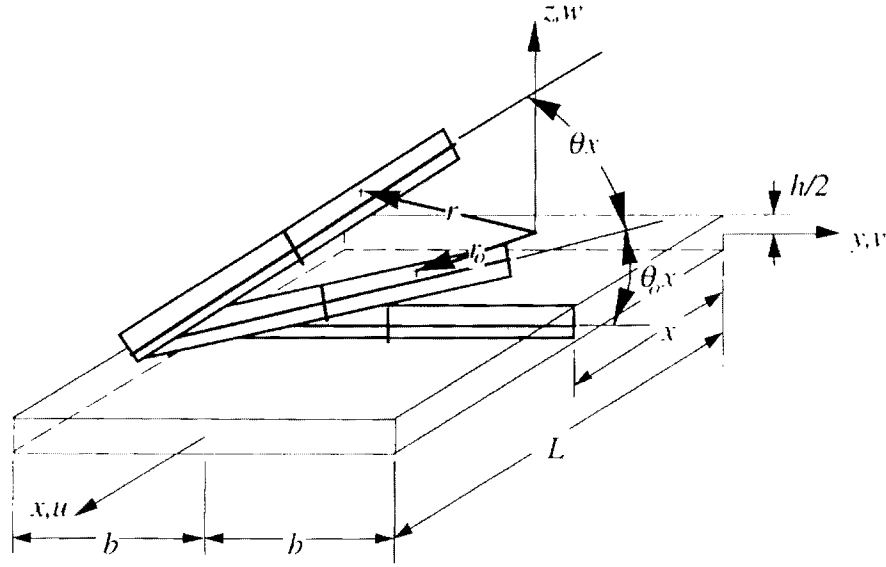
Fig. 1 Laminated strip geometry and coordinate system

† Graduate Research Assistant, School of Aerospace Engineering, Georgia Institute of Technology, Atlanta, Georgia, 30332-0150. Member AIAA.

The laminate has an initial twist rate, θ_o and is undergoing a constant elastic twist rate, θ about the x-axis and the associated strains are considered small and independent of x. The laminate material is considered linearly elastic. The position vector in the initial state is derived kinematically by considering a finite twist of the initially flat strip, assuming no "out-of-plane" strains, and keeping terms up to $O\left(\theta_o^2 y^2\right)$

$$\vec{r}_o = \left(x - \theta_o yz\right)\hat{i} + y\hat{e}_{20} + z\left[1 - \frac{1}{2}(\theta_o y)^2\right]\hat{e}_{30} \tag{1}$$

where the $\hat{e}_{20}$ and $\hat{e}_{30}$ denote the unit vectors in the plane of the cross section at the initial state. Consistent with the thin-walled strip geometry, the following bounds are imposed on the geometric and displacement variables

$$(\frac{h}{b})^2 = O(\varepsilon), \quad (\theta b)^2 = O(\varepsilon), \quad (\theta V),(\theta W) = O(\varepsilon^{3/2}),$$

$$\frac{\partial U}{\partial y}, \frac{\partial U}{\partial z}, \frac{\partial V}{\partial y}, \frac{\partial V}{\partial z}, \frac{\partial W}{\partial y}, \frac{\partial W}{\partial z} = O(\varepsilon) \tag{2}$$

where ε denotes the magnitude of the maximum strain and $U(y,z)$, $V(y,z)$ and $W(y,z)$ denote the displacement components along the x, y and z coordinates. Terms up to $O(\varepsilon)$ will be kept in the strain-displacement relationships. The position vector in the deformed configuration is

$$\vec{r} = \left[x\left(1 + \varepsilon_o\right) - \left(\theta + \theta_o\right)yz + U\right]\hat{i} + (y + V)\hat{e}_2 + \left\{z\left[1 - \frac{1}{2}(\theta + \theta_o)^2 y^2\right] + W\right\}\hat{e}_3 \tag{3}$$

where the $\hat{e}_2$ and $\hat{e}_3$ denote the unit vectors in the deformed cross section.

The Lagragian strain tensor components are defined as[1]

$$2\varepsilon_{ij} = g_{ij} - h_{ij} \tag{4}$$

where g_{ij} and h_{ij} are the metric tensor components associated with the final and initial states, respectively

$$g_{ij} = \frac{\partial \vec{r}}{\partial x^i} \cdot \frac{\partial \vec{r}}{\partial x^j}$$

$$h_{ij} = \frac{\partial \vec{r}_o}{\partial x^i} \cdot \frac{\partial \vec{r}_o}{\partial x^j} = \delta_{ij} \quad (x^1 = x, \ x^2 = y \ and \ x^3 = z) \tag{5}$$

Substitute Eqs. (1) and (3) into Eqs. (4) and (5) to get for the engineering strain components

$$\varepsilon_{xx} = \varepsilon_o + \frac{1}{2}\left(\theta^2 + 2\theta\theta_o\right)y^2, \quad \varepsilon_{yy} = \frac{\partial V_o}{\partial y} - z\frac{\partial V_I}{\partial y}, \quad \varepsilon_{zz} = -W_I$$

$$\gamma_{xy} = \frac{\partial U_o}{\partial y} - z\left(\frac{\partial U_I}{\partial y} + 2\theta\right), \quad \gamma_{xz} = -U_I, \quad \gamma_{yz} = -V_I + \frac{\partial W_o}{\partial y} \tag{6}$$

where $U_o(y)$, $V_o(y)$ and $W_o(y)$ are the mid-surface displacements along the x, y and z coordinates and $U_I(y)$ and $V_I(y)$ and W_I are the through-the-thickness average out-of-plane strain components $\gamma_{xz}(y)$, $\gamma_{yz}(y)$ and ε_{zz}, respectively. The average transverse normal strain is considered constant.

Equilibrium Equations

The equilibrium equations are derived using the principle of Virtual Work. For a strip whose lateral surfaces are traction free and ends subjected to an axial force F and torque T, the principle of virtual work is written as

$$\int_{-b}^{b}\int_{-h/2}^{h/2}(\sigma_{xx}\delta\varepsilon_{xx} + \sigma_{yy}\delta\varepsilon_{yy} + \sigma_{xx}\delta\varepsilon_{xx} + \sigma_{yz}\delta\gamma_{yz} + \sigma_{xz}\delta\gamma_{xz} + \sigma_{xy}\delta\gamma_{xy})\sqrt{g}dydz - T\delta\theta - F\delta\varepsilon_o = 0 \tag{7}$$

where σ_{ij} are the second Piola-Kirchoff stress tensor components. The contribution of σ_{zz} has been neglected in Eq.(7). The Jacobian $\sqrt{g}$ can be represented as

$$\sqrt{g} = \frac{\partial \vec{r}_o}{\partial x} \cdot \left(\frac{\partial \vec{r}_o}{\partial y} \times \frac{\partial \vec{r}_o}{\partial z}\right) = 1 \tag{8}$$

if terms of $O(\varepsilon)$ are neglected in comparison to unity. The force and moment resultants per unit middle surface length are defined as

$$(N_{xx}, N_{yy}, Q_y, Q_x, N_{xy}, M_{xx}, M_{yy}, M_{xy}) = \int_{-h/2}^{h/2} (\sigma_{xx}, \sigma_{yy}, \sigma_{yz}, \sigma_{xz}, \sigma_{xy}, z\sigma_{xx}, z\sigma_{yy}, z\sigma_{xy})\,dz$$

$$(9)$$

Substitute from Eqs.(6) and (8) into Eq.(7) and use Eq.(9) to get

$$N_{yy} = Q_y = N_{xy} = M_{yy} = M_{xx} = 0 \tag{10}$$

$$\frac{\partial M_{xy}}{\partial y} - Q_x = 0 \tag{11}$$

$$\int_{-b}^{b} N_{xx}\,dy = F \tag{12}$$

$$\int_{-b}^{b} \left[N_{xx}\, y^2(\theta + \theta_o) - 2M_{xy} \right] dy = T = 0 \tag{13}$$

Equation (10) satisfy the traction free conditions on the lateral surfaces. The term $N_{xx}\, y^2(\theta + \theta_o)$ in Eq.(13) represents the contribution of the axial force to the twisting moment in the deformed configuration and will be shown to have a significant contribution to the nonlinear behavior in the axial-force twist relationship.

Constitutive Relationships

The constitutive relationships for an antisymmetric angle ply laminate exhibiting extension-twist coupling can be expressed as

$$\begin{Bmatrix} N_{xx} \\ N_{yy} \\ M_{xy} \end{Bmatrix} = \begin{bmatrix} A_{11} & A_{12} & B_{16} \\ A_{12} & A_{22} & B_{26} \\ B_{16} & B_{26} & D_{66} \end{bmatrix} \begin{Bmatrix} \varepsilon_{xx}^o \\ \varepsilon_{yy}^o \\ -\kappa_{xy} \end{Bmatrix}$$

$$\begin{Bmatrix} N_{xy} \\ M_{xx} \\ M_{yy} \end{Bmatrix} = \begin{bmatrix} A_{11} & A_{12} & B_{16} \\ A_{12} & A_{22} & B_{26} \\ B_{16} & B_{26} & D_{66} \end{bmatrix} \begin{Bmatrix} \gamma_{xy}^o \\ -\kappa_{xx} \\ -\kappa_{yy} \end{Bmatrix} \tag{14}$$

$$\begin{Bmatrix} Q_y \\ Q_x \end{Bmatrix} = \begin{bmatrix} A_{44} & A_{45} \\ A_{45} & A_{55} \end{bmatrix} \begin{Bmatrix} \gamma_{yz}^o \\ \gamma_{xz}^o \end{Bmatrix} \tag{15}$$

Coefficients A_{ij}, B_{ij} and D_{ij}, are similar to the Classical Lamination Theory[2] in-plane, coupling and bending stiffness coefficients, respectively

Substitute from Eqs.(10) and (6), Eqs.(14) and (15) reduce to

$$\begin{Bmatrix} N_{xx} \\ M_{xx} \end{Bmatrix} = \begin{bmatrix} \alpha_{11} & \alpha_{12} \\ \alpha_{12} & \alpha_{22} \end{bmatrix} \begin{Bmatrix} \varepsilon_o + \frac{1}{2}\left(\theta^2 + 2\theta\theta_o\right)y^2 \\ -\frac{\partial U_I}{\partial y} - 2\theta \end{Bmatrix} \tag{16}$$

$$Q_x = -\beta U_I \tag{17}$$

$$\frac{\partial U_o}{\partial y} = \frac{\partial V_I}{\partial y} = 0 \tag{18}$$

where ε_o is the axial extensional strain and

$$\alpha_{11} = A_{11} - \frac{A_{12}^2}{A_{22}}, \quad \alpha_{22} = D_{66} - \frac{B_{26}^2}{A_{22}}, \quad \alpha_{12} = B_{16} - \frac{A_{12}B_{26}}{A_{22}}$$

$$\beta = A_{55} - \frac{A_{45}^2}{A_{55}} \tag{19}$$

Substitute Eqs.(16) and (17) into Eq.(11) to get

$$\alpha_{22}\frac{\partial^2 U_I}{\partial y^2} - \beta U_I = \alpha_{12}\left(\theta^2 + 2\theta\theta_o\right)y \tag{20}$$

Solve Eq.(20), enforce the free twisting moment conditions at the free edges to get the following expression for the warping function

$$U_I = \frac{\sinh sy}{\alpha_{22}s\cosh sb}\left[\alpha_{12}\varepsilon_o - 2\alpha_{22}\theta + \alpha_{12}\left(\frac{\alpha_{22}}{\beta} + \frac{b^2}{2}\right)\theta^2\right] - \frac{\alpha_{12}}{\beta}\left(\theta^2 + 2\theta\theta_o\right)y \tag{21}$$

where

$$s = \sqrt{\frac{\beta}{\alpha_{22}}} = \sqrt{\frac{A_{22}\left(A_{55}A_{44} - A_{45}^2\right)}{A_{44}\left(D_{66}A_{22} - B_{26}^2\right)}} \tag{22}$$

Substitute Eqs.(16) and (21) into Eqs.(12) and (13) and eliminate ε_o to get for the axial force-twist relationship

$$F\left(b_4 - \varphi - \varphi_o\right) = \left[b_1 + \left(\frac{4}{3}b_2 + 2b_3\varphi_o\right)\varphi_o\right]\varphi + \left(b_2 + 3b_3\varphi_o\right)\varphi^2 + b_3\varphi^3 \tag{23}$$

where

$$b_1 = \frac{8\psi k_1}{b\alpha_{11}k_3}, \quad b_2 = -\frac{6b\alpha_{12}}{L}(k_1 + k_2 k_4), \quad b_3 = \frac{b^3\alpha_{11}}{L^2}\left[k_4\left(k_3 - \frac{2}{15} - \frac{2\alpha_{12}^2 k_2}{\alpha_{11}\beta b^2}\right) - k_3\right]$$

$$b_4 = -\frac{2L}{b^2}\frac{\alpha_{12}k_1}{\alpha_{11}k_3}, \quad \psi = \alpha_{11}\alpha_{22} - \alpha_{12}^2, \quad k_1 = 1 - \frac{tanh(bs)}{bs},$$

$$k_3 = \frac{1}{3} - \frac{\alpha_{12}^2}{\alpha_{11}\alpha_{22}}\left(k_2 + \frac{1}{3}\right), \quad k_2 = \frac{2}{3} - k_1\left[1 + \frac{2}{(bs)^2}\right], \quad \varphi = -\theta L, \quad \varphi_o = -\theta_o L$$

(24)

Application

Equation (23) is applied to the prediction the twist associated with applied axial force for a laminated composite strip made of ICI Fiberite T300/954-3 Graphite/Cyanate material system with the following properties

$E_{11}= 135.6\ GPa,$ $E_{22}=9.9\ GPa,$ $G_{12}=4.2\ GPa$
$G_{23}= 2.5\ GPa,$ $n_{12}= 0.3,$
$n_{23}= 0.5$ (25)
Ply thickness = 0.15 mm (0.006 in.)

The laminate layup is antisymmetric and is given by

$$\left[\alpha/(90+\alpha)_2/\alpha/-\alpha/-(90+\alpha)_2/-\alpha\right]_T$$

(26)

The sequence consists of two $[0/90]_s$ laminates atop one another that have undergoing an opposing α degree rotation. Once rotated, the upper and lower halves produce opposing in-plane extension-shear coupling. Under extension. the opposing in-plane shear forces produce a twisting couple, and the laminate exhibits extension-twist coupling.

Two sets of four laminates each have been manufactured with $\alpha = 20°$ and $30°$, respectively. The laminates were 25.4 mm (1 in.) wide and 279.4 mm (11 in.) long and had a -0.20°/cm (-0.5°/in) of pretwist. A rotary transducer[3] based platform was used to collect twist data. The transducer fits into a universal testing machine and is clamped to one end of the laminate allowing for free end twist as an axial load is applied. In taking the experimental data, the twist at the transducer end of the laminate was recorded at load steps of 222.4 N (50 lbs).

Figures 2 and 3 present the results of the test data from the four laminates with $\alpha = 20°$ and $30°$, respectively. The four tested laminates are labeled Specimens 1-4 in the figures. The prediction of Eq. (23) are plotted in solid line and labeled nonlinear model. Also included in the figures is the prediction from the linear theory which corresponds to the classical lamination theory extension-twist coupling. The linear model prediction appearing as a dotted line is indistinguishable from the case where the contribution of the axial force to the twisting moment in the deformed state, is neglected. This indicate that this contribution, represented by the term $N_{xx}\ y^2(\theta + \theta_o)$ in Eq.(13) provides most of the

nonlinear behavior in the axial-force twist relationship for the material system and stacking sequence considered in this work.

References

1. Sokolnikoff, I. S., *Tensor Analysis*, John Wiley, 1951.
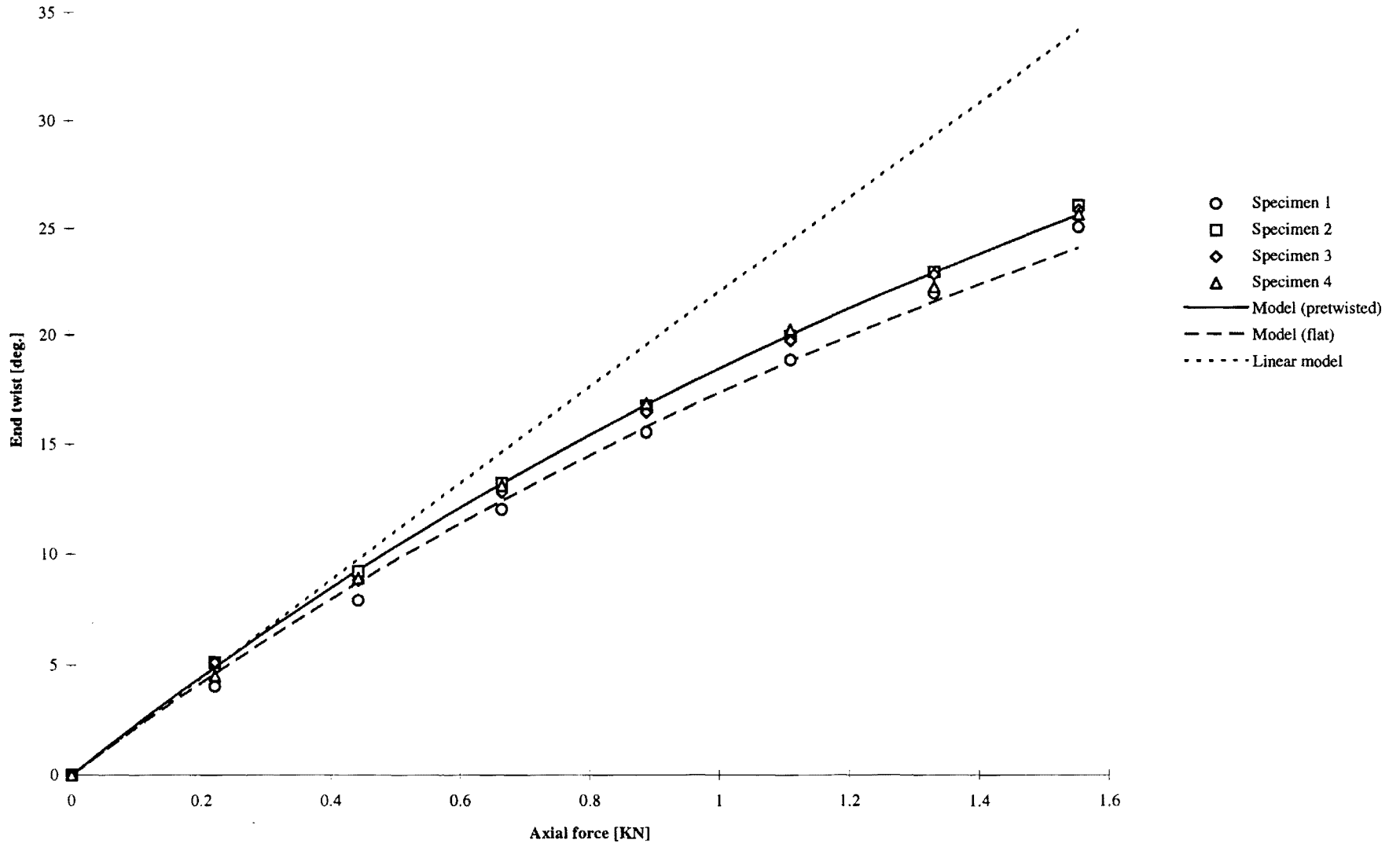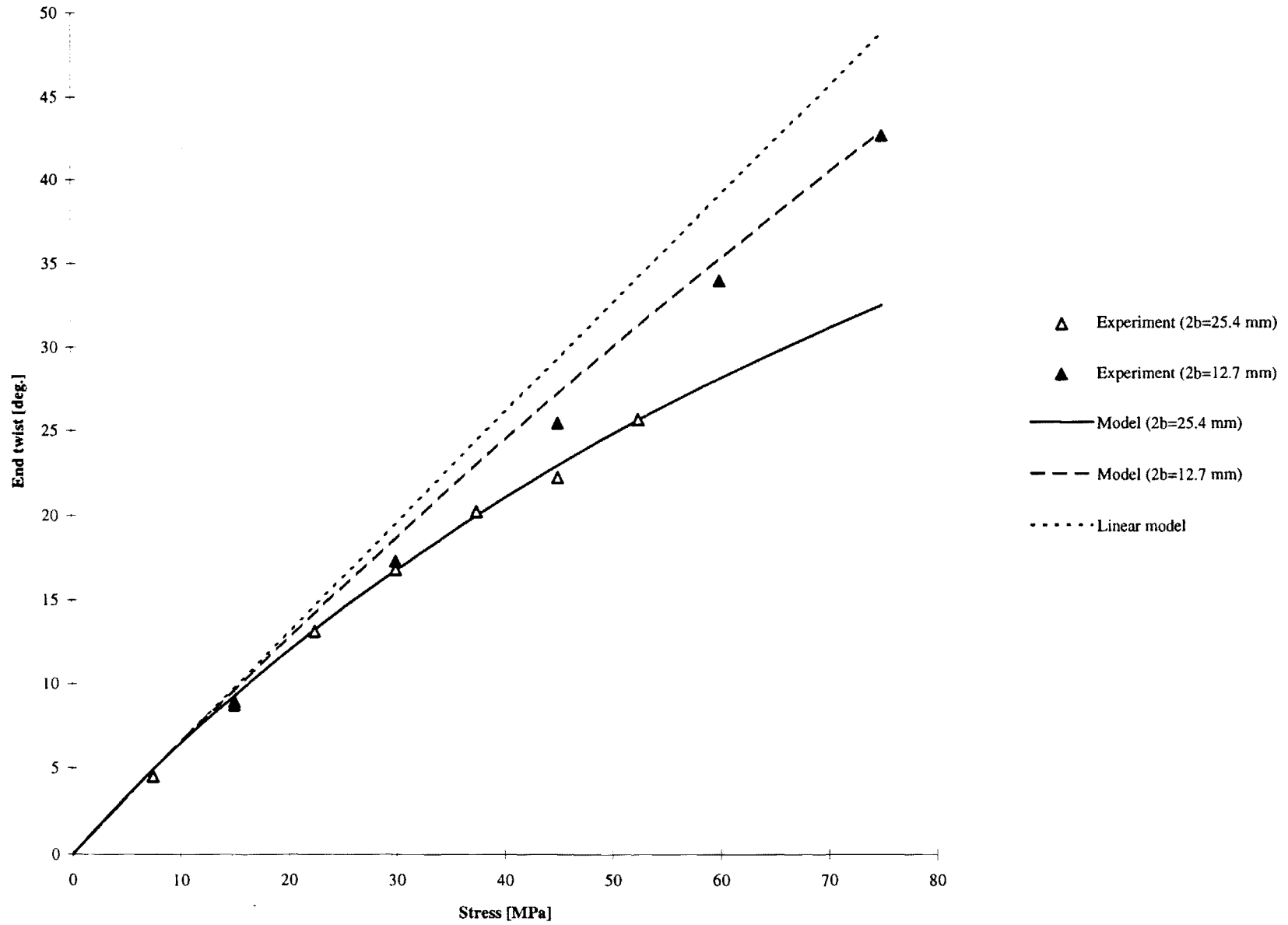2. Vinson, J. R. and Sierakowski, R. L., *The Behavior of Structures Composed of Composite Materials*, Martinus Nijhoff Publishers, 1986.
3. Hooke, D. A. and Armanios, E. A., "Examination of Three Methods for Testing Extension-twist Coupled Laminates," ASTM Twelfth Symposium on Composite Materials: Testing and Design, Montreal, Quebec, May 1994, to be published in an ASTM Special Technical Publication.

$[20/-70_2/20/-20/70_2/-20]_T$ laminate
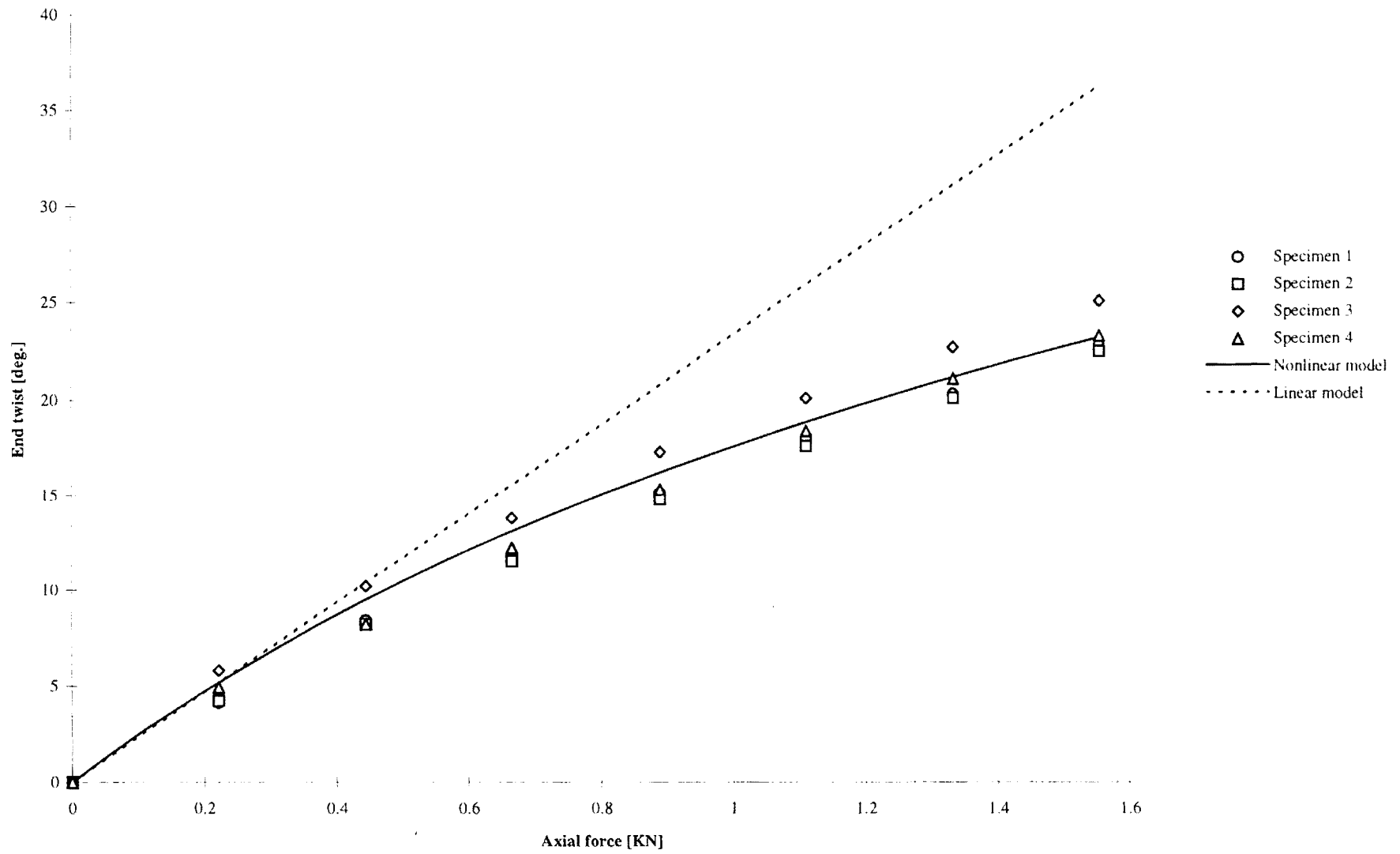
Figure 2. Comparison of twist prediction with test data

$[30/-60_2/30/-30/60_2/-30]_T$ laminate
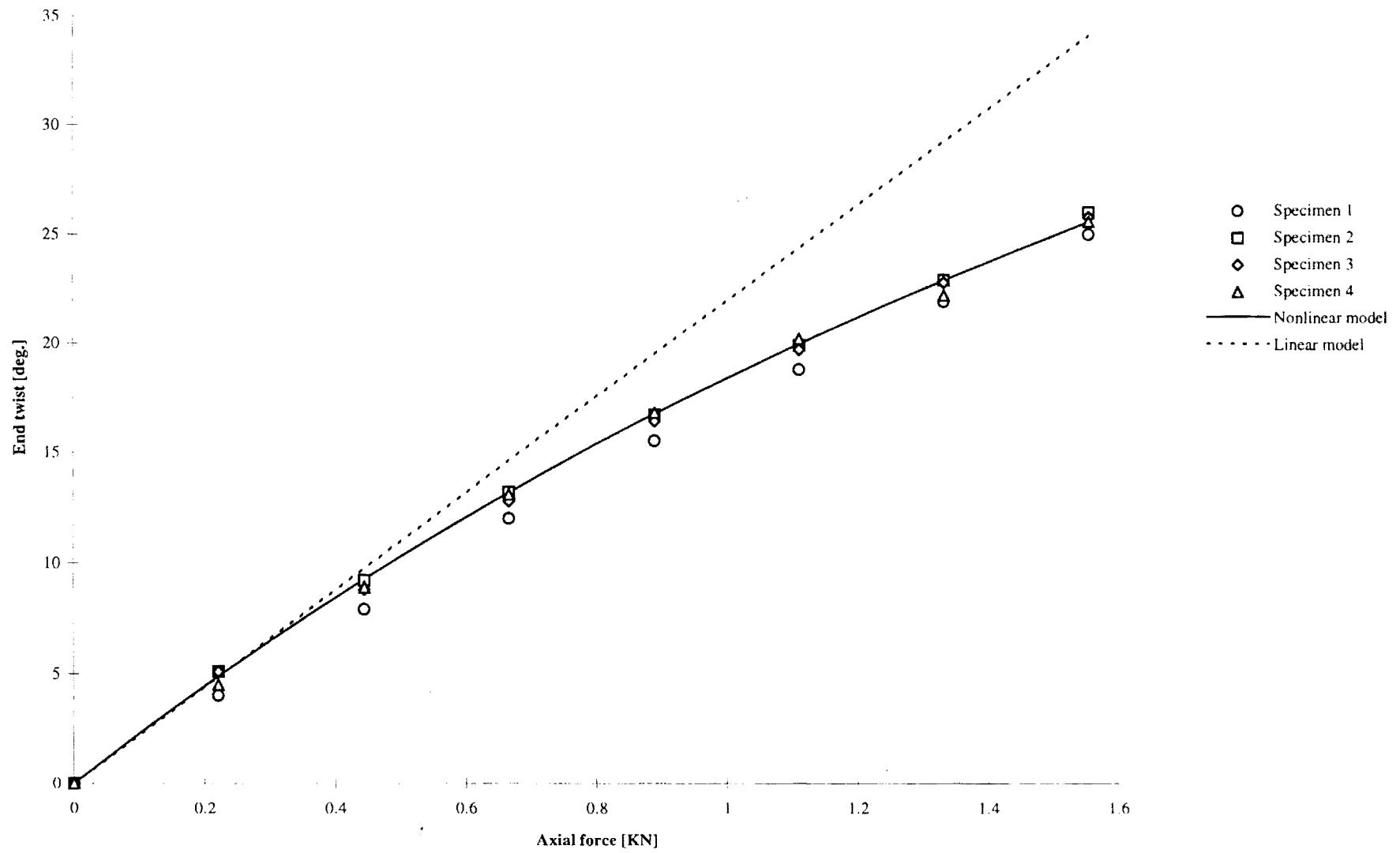
Figure 3. Comparison of twist prediction with test data

GEORGIA INSTITUTE OF TECHNOLOGY
A UNIT OF THE UNIVERSITY SYSTEM OF GEORGIA
SCHOOL OF AEROSPACE ENGINEERING
ATLANTA, GEORGIA 30332-0150

Dr. Erian Armanios (404) 894-8202
(404) 894-2760 (fax)
erian.armanios@ae.gatech.edu

October 20, 1996

Dr. Kofi Bota
Vice President for Research and Sponsored Programs
Clark Atlanta University
221 James P. Brawley Dr., S.W.
Atlanta, GA 30324

Dear Dr. Bota:

Enclosed, please find our final report on the work performed under the task entitled: " Advanced Composites and Smart Structures Research," Grant : Daal 03-92-G-380. Among the accomplishments achieved in this work, I would like to underscore two patents pending, a Ph.D. Thesis and two paper awards.

We look forward to a continuing collaboration between Clark Atlanta University and the School of Aerospace Engineering at Georgia Tech.

Sincerely,

Erian Armanios

FINAL REPORT

ADVANCED COMPOSITES AND SMART STRUCTURES RESEARCH

GRANT : DAAL03-92-G-380
GEORGIA TECH PROJECT: E16-X11

PRINCIPAL INVESTIGATOR
E. A. Armanios
School of Aerospace Engineering
Georgia Institute of Technology
Atlanta GA 30332-0150

Sponsor Technical Contact: Dr. Kofi Bota
Clark Atlanta University
221 James P. Brawley Dr., S.W.
Atlanta, GA 30324

Problem studied

The primary objective of this research is the development of analytical tools, testing methods and smart concepts for advanced composite structures.

Summary of Accomplishments:

1. Elastic tailoring

The work performed under this Grant focused on the implementation of elastic tailoring in composite structures. Elastically tailored composite laminates offer structural designers new degrees of freedom. With the use of materials that exhibit a coupled behavior such as extension-twist or bend-twist coupling, new, more efficient structural designs can be produced. However, a number of challenges associated with their analysis, manufacture and testing need to be addressed to make their implementation possible in practical applications. From the analytical standpoint the coupling adds more complexity to the resulting governing differential equations and solution procedures. Moreover, as shown by the results of the work performed under the current Grant, in the case of extension-twist coupling the relative magnitude of torsional to axial stiffness leads to finite twist which falls beyond the assumptions of small displacements (linear) theory. From a manufacturing standpoint, the unsymmetric nature of these laminates induces hygrothermal warping which has to be accounted for in the design in order to ensure the laminates integrity as they are subjected to the curing stresses and in the fabrication molds as well. From the testing standpoint, commonly available universal testing machines are not equipped to handle a second degree of freedom and bi-axial testing machines are quite expensive and less frequently available.

The work performed in this Grant addresses these technology barriers by designing and manufacturing three test apparatuses and methods [1.2]. These apparatuses have been evaluated through tests of flat hygrothermally stable laminates and pretwisted angle-ply laminates. One of the test apparatuses is the subject of a patent [3]. For the first time the nonlinear behavior of axial load versus twist response was isolated. This spurred the development of a nonlinear analytical model [4] under a National Rotorcraft Center of Excellence Grant. The source of the nonlinearity was geometric and found to be related to the finite twist. The main contribution was due to the twisting moment associated with the axial stress resultant in the deformed configuration. Closed-form expressions relating applied extension to twisting rotation were obtained and the contribution of axial force to the twisting moment was isolated. Three approximate models were derived and the influence of the free-edge conditions and Saint Vénant's assumptions were assessed. Based on this assessment a simple two-parameters model accounting for the axial force contribution to the twisting moment was proposed. Comparisons of analytical predictions with finite element simulations for both flat and pretwisted laminates illustrated the accuracy of the developed models. A set of pretwisted laminated composite strips made of a Graphite/Cyanate material system was manufactured and tested. Analytical predictions were is excellent agreement with test data.

An additional benefit to the investigation of unsymmetric laminate is the assessment of the damage tolerance of symmetric laminates. Damage initiated during laboratory testing and in service at stress raiser cites such as free-edges, holes, ply drop and impact events alter the initial symmetry of these laminates. An understanding of the unsymmetric behavior and resulting coupling is essential in designing damage tolerant composite structures.

A detailed description of the accomplishments achieved in design, manufacturing and testing of elastically tailored laminates with extension-twist coupling is provided in Ref. 2. A copy is included in the Appendix of this report.

2. Active materials

The performance of such elastically tailored laminate could be augmented by using a smart material concept. Rather than embedding actuators to provide active control, piezoelectric actuators will be used to effect flow control [5]. A novel approach in the use of active material actuators for flow control has been developed under the current Grant leading to a Patent application [6]. This approach takes into account the specific power and strain limitations of active material actuators and is aimed at circumventing this obstacle. In a departure from the traditional approaches, it uses active material actuators to modify the boundary conditions of the flow rather than the geometry of the boundary. The embodiment presented in Ref. 6, and shown in Fig. 1, stems from the observation that, in the case of airfoils with circulation control via blowing. the size of the blowing slot is of the same order of magnitude as the displacement produced by an active material actuator that can be housed within the airfoil. Evaluation of this concept has led to the

development of a circulation-control wing section with blowing intensity modulation via active material actuators.
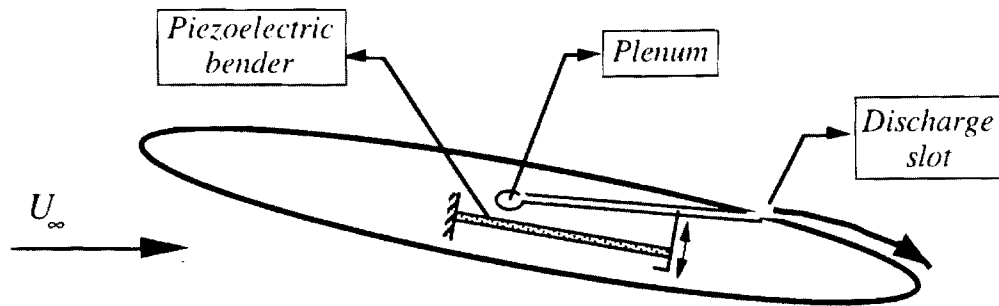
Figure 1. Schematic of a circulation control airfoil with piezoelectric blowing modulation.

Circulation control airfoils have been extensively investigated, with a large body of experimental work conducted at the David W. Taylor Naval Ship Research and Development Center. Experimental studies on unsteady circulation control airfoils are, however, very scarce. Reference 7 is one of the few examples. The unsteady blowing is achieved by the periodic modulation of plenum pressure by means of a rotating vane. One disadvantage of this solution consists in the difficulty to modulate the plenum pressure with an arbitrary signal, due to the pneumodynamic response of the system. Direct slot size modification using mechanisms allows for the blowing modulation with an arbitrary signal. However, this technical solution is characterized by increased complexity and, to our knowledge, it has not been used in any published investigation. The piezoelectric modulation of slot size makes it practical to generate an arbitrary modulation of blowing intensity at reduced system complexity

A proof-of-concept wing section, containing a constant pressure plenum and a piezoelectrically actuated discharge control mechanism, as shown in Fig. 1, has demonstrated the viability of the concept and the capacity of the system to rapidly and significantly modify the flow field. In the images of Figs. 2 and 3, captured during low-speed smoke tunnel testing of the wing section, the difference between the streakline patterns demonstrates the magnitude of flow field modification achieved. To our knowledge this is the first successful practical implementation of unsteady blowing using active material actuators.

Conclusion and recommendation

A solution to two technology barriers has been developed in this research. Each solution is the subject of a Patent [3,6]. The first solution, is a significant step towards the implementation of elastic tailoring concepts into composite structures. In this solution three test apparatuses and methods have been designed and manufacturing in order to measure extension-twist coupling. The second solution overcomes the specific

power and strain limitations of active material actuators and provides a means for their implementation at the full scale component level.
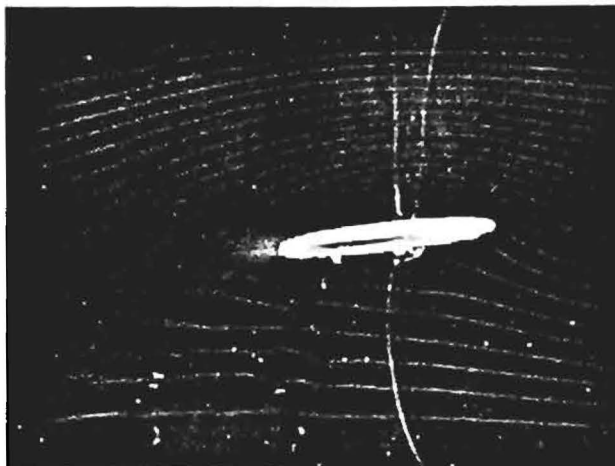
Figure 2. Streakline pattern at maximum blowing intensity during the cycle.
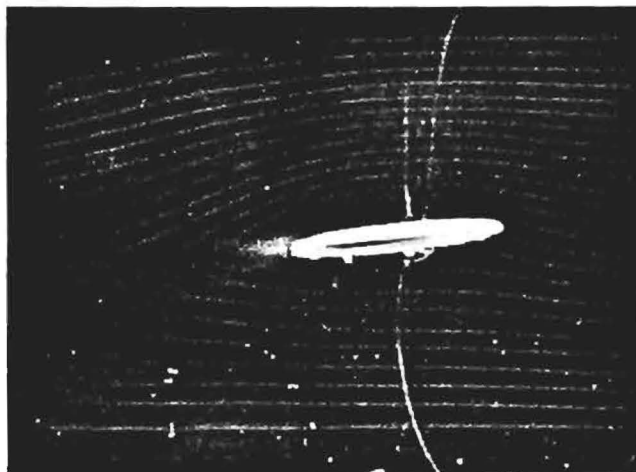
Figure 3. Streakline pattern at minimum blowing intensity during the cycle.

The findings of this research point to new areas of inquiries. An investigation of the influence of damage in geometrically nonlinear composites would be a positive step towards assessing the damage tolerance of elastically tailored composites. This is the subject of a research task under the National Rotorcraft Center of excellence at Georgia Tech.

A quantitative assessment of the circulation control airfoil by measuring the pressure distribution is needed. It is also recommended to implement the concept in Ref. 6 to vectored fluid flap and microturbulators in order to provide flow control over non-elliptical airfoil. These recommendations are the subject of a proposal to the Army Research Office [8].

4

References

[1] Hooke, D. A. and Armanios, E. A., "Design and Evaluation of Three Methods for Testing Extension-twist-Coupled Laminates," Composite Materials: Testing and Design (Twelfth Volume) ASTM STP 1274, C. R. Saff and R. B. Deo, Eds. American Society for Testing and Materials, 1996, pp. 340-357.

[2] Hooke, D. A., "Design and Evaluation of Test Apparatuses and Methods for Extension-Twist Coupled laminates," Ph.D. Thesis, School of Aerospace Engineering, Georgia Institute of Technology, Atlanta, Georgia, October 1996.

[3 Hooke, D. A. and Armanios, E. A., "Rotational Displacement Apparatus with Ultra-low Torque and High Thrust Capability," Patent Pending, US Patent and Trademark Office Serial No. 08/562,586.

[4] Armanios, E. A., Makeev, A., and Hooke, D. A., "Finite-Displacement Analysis of Laminated Composite Strips with Extension-twist Coupling" J. Aerosp. Engrg., ASCE, Vol. 9, No. 3, July 1996, pp. 81-91.

[5] Armanios , E. A., and Dancila, S., "Efficient Use of Piezoelectric Actuators for Unsteady Flow Control, " Second Workshop on Smart Structures and Materials, University of Maryland, College Park, MD., September 5-7, 1995.

[6] Dancila, D. S. and Armanios, E. A., "Apparatus and Method for Aerodynamic Blowing Control Using Smart Materials," Patent Pending, US Patent and Trademark Office Serial No. 08/517, 951.

[7] Gee, T. A. and Leishman, J. G., "Unsteady Circulation Control Aerodynamics of a Circular Cylinder with Periodic Jet Blowing." *AIAA Journal*, Volume 30, No. 2, February 1992, pp. 289-299.

[8] Armanios, E. A., "Rotor Flow Control Concepts Using Smart Materials Actuators," proposal submitted to the U. S. Army Research Office in response to Broad Agency Announcement, DAAH04-96-R-BAA1, October 1995.

APPENDIX

DESIGN AND EVALUATION OF TEST APPARATUSES AND METHODS FOR EXTENSION-TWIST COUPLED LAMINATES

A Thesis
Presented to
The Academic Faculty
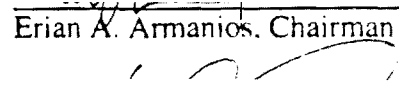
by
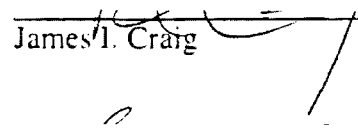
David A. Hooke

In Partial Fulfillment
of the Requirements for the Degree
Doctor of Philosophy
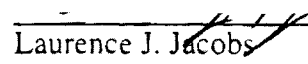
Georgia Institute of Technology
October 1996
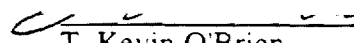
DESIGN AND EVALUATION OF TEST APPARATUSES AND METHODS FOR EXTENSION-TWIST COUPLED LAMINATES

Erian A. Armanios, Chairman

James I. Craig

Stanley C. Bailey

Laurence J. Jacobs

T. Kevin O'Brien

Date Approved by Chairman October 10, 1996

ii

ACKNOWLEDGMENTS

Words cannot fully illustrate my deepest gratitude to everyone who has helped me through my education. Indeed, it is very hard to put into words how I have been affected by the amount of nurturing and support I have received from my professors, friends, colleagues, and family. Dr. Erian Armanios, my thesis advisor and mentor, has shown me that science and engineering do not have to come at the expense of compassion, ethics, and understanding. This has made all the difference in the world. I would like to thank Dr. Craig and Dr. Bailey for helping so much when I was starting out in the laboratory. Their insight and fundamental knowledge as experimentalists are true gifts that have excited me. I would like to thank Dr. Jacobs and Dr. O'Brien for reading and commenting on my thesis. For that, I am grateful.

I would like to thank all my friends for their moral support along the way. I truly appreciate the hours Stefan Dancila has taken with me to explain technical issues and be a good friend.

I am most appreciative of my wife, Shelley, whose love, understanding, and encouragement have kept me focused on the important things life has to offer. I thank her parents, Carol and Brian, for all their support and love along the way.

I would especially like to thank my parents and brother for everything they have done for me. Through good times and bad, they have never left my side, and for that I am eternally indebted. Thank you. I love you all.

TABLE OF CONTENTS

LIST OF TABLES

LIST OF FIGURES

SUMMARY

Elastic tailoring of laminated composite materials is an enabling technology that has potential for significant weight and cost savings and reduced mechanical complexity with added design flexibility. The ability is available for engineers to prescribe complex deformation modes through material selection. stacking sequence. and component geometry. One such deformation mode is extension-twist coupling. As an axial load is applied. the component extends and twists. Verification of this behavior is needed to validate analytical tools. yet testing devices must not influence the behavior.

Three testing apparatuses have been developed and evaluated for testing extension-twist coupled laminated strips: a thrust bearing based apparatus. a free rotating frame apparatus. and an air bearing apparatus have been developed. An evaluation and comparison of the methods have shown that the air bearing apparatus best meets the demands for the accuracy. precision. and reliability needed of a testing method.

Furthermore. the accuracy of the air bearing apparatus has highlighted a geometrically nonlinear behavior of extension-twist coupled laminates that has been investigated and quantified.

CHAPTER 1

INTRODUCTION

Advanced composites enable designers to meet stiffness and strength requirements efficiently and economically. Elastically tailored composites exemplify these features. In addition to the development of analytical models that account for the inherent anisotropy of composites, an essential requirement for their validation and implementation in aircraft structures is the development of test methods that are accurate, reliable, and economical.

Traditional challenges to using composite materials for airframe construction are quality control and cost versus the long term benefits of high strength-to-weight and stiffness-to-weight ratios. While composite materials exhibit higher stiffness-to-weight ratios when compared to steel or titanium, the performance benefits come at the costs of the constituents of the composite material, the manufacturing of the composite part, and the maintenance throughout the life cycle.

Figure 1 shows a schematic of a typical life cycle cost curve during the design, manufacturing, and maintenance processes, which is commonly called the life cycle of the design[1].

1
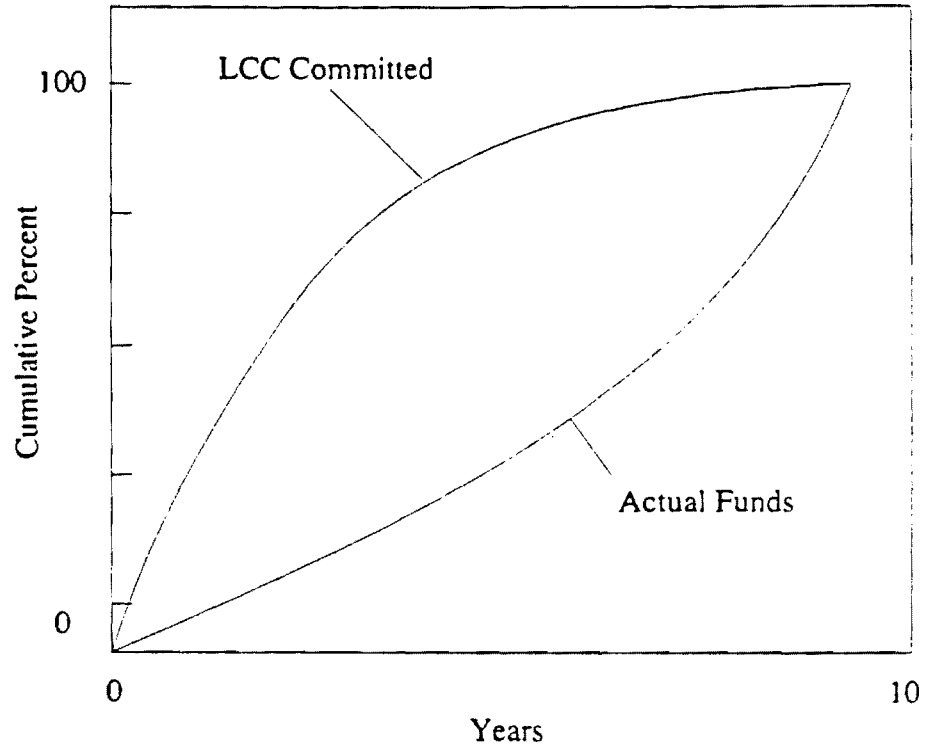
Figure 1. Life Cycle Cost Curve

It is preferable to reduce the costs of the design and preliminary testing stages of the product where large costs are encumbered in a relatively short time. Because this curve shows large life cycle costs committed at the beginning of the design cycle, there is ample reason to hedge against new or innovative designs in favor of proven technology. In the case of composite materials, if the costs of manufacturing and testing can be reduced, room for innovation will be made. Furthermore, intelligent use of all aspects of composite materials including material selection, stacking sequence, and geometry yields high performance dividends. Elastically tailored composite structures provide an extra degree of freedom to meet design requirements efficiently and economically. Elastically tailored structures reduce part count and weight and increase performance of the whole structure by replacing joints, linkages, and actuators with single components that perform the same function by coupling deformation modes.

Elastically tailoring composites offer designers the ability to develop structures that not only exhibit stiffness requirements for structural integrity, but also couple deformation states. This type of behavior is seen in bend-twist coupling and extension-twist coupling. In the first case, bending moments applied to a composite beam result in bending and twisting of the beam. In the second case, axial loads applied to the composite beam results in extension and twisting. Under certain circumstances, these behaviors can be seen in structural elements made from isotropic materials. For instance, bend-twist coupling is seen when a bending moment is applied to an unsymmetric beam through a location different than its shear center. Likewise, extension-twist coupling can be seen in pretwisted strips of material. As a tensile axial load is applied to the strip, it will untwist. Whereas structural elements made of isotropic materials need a specific cross section geometry or specific loading scheme to produce these results, the elastically tailored

3

composite counterpart requires only a specific material selection and orientation of the different layers of fibers.

Unidirectional composite laminates are strongest in the direction of their fibers; therefore, weights of components originally made of isotropic materials can be reduced using composites, either through alignment of fibers, redesign of the part, or a mixture of both. However, this use only takes advantage of the strength to weight ratio of the composite material. More important, there are a number of engineering applications that can benefit from the anisotropic behavior of laminated composites to a higher degree using elastic tailoring. Here, tailoring means the process of adapting the material, geometric, and stiffness characteristics to improve or create favorable deformation modes. Not only are the well-known extensional stiffnesses tailored, but off-axis stiffnesses are as well. The result of such a design is that out-of-plane response is possible through in-plane loading.

Practical use of elastic tailoring requires verification of the structural design tools used. This requires testing methods that, until this point, have not existed because homogeneous isotropic material behavior did not warrant such exhaustive techniques. However, as the engineering climate and design philosophy changes from "performance at any cost" to "cost-effective performance," the complete design and life cycle costs of a structure must be fully examined. Composite materials that exhibit coupling between deformation modes are inherently more difficult to test, thus less expensive testing procedures must be found to lower implementation costs. Within the framework of designing with the complete life cycle in mind, experimental methods play a significant role during the conceptual, manufacturing, and maintenance stages.

There is a need to produce testing methods for elastically tailored composites that can be standardized as are the established methods for testing isotropic materials. The

4

objective of this research is to design accurate, reliable, and cost effective means to test elastically tailored extension twist coupled laminates in order to 1) verify the accuracy of analytical models, 2) characterize the behavior of elastically tailored laminates at different load levels, and 3) provide a database of coupling parameters. New testing methods should allow the coupling between deformation modes to exist with minimal influence from the testing apparatus itself. The designed testing apparatuses strive to meet this need while minimizing cost through adaptability to existing test equipment. This adaptability results in minimal user training that, in turn, increases productivity while lowering operating costs.

An additional benefit to the development of test methods for elastically tailored laminates is the understanding and quantitative assessment of the role of coupling in unsymmetrical laminates. While symmetric configurations have desirable design and manufacturing features, the initial symmetry is often altered as a result of fabrication tolerances and service damage. An assessment of the influence of the coupling associated with this deviation from symmetry is key to designing damage tolerant structures.

CHAPTER II

LITERATURE SURVEY

A comprehensive literature search shows a limited number of works devoted to the development of test apparatuses and methods for measuring elastic coupling. This reflects the new nature of this emerging technology. In the following, a review of these works is presented in order to put the contribution of this work into proper context.

Some uses for elastic tailoring have been in aeroelastic tailoring of forward swept wings and structural tailoring of rotor blades to achieve an optimum compromise in design requirements. Nixon[2] studied a proposed rotor blade design subject to the constraints of aerodynamic performance, material strength, autorotation, and frequency. Once the loads were defined for the blade, the composite spar was "tuned" to meet the design criteria. However, at this point, elastic tailoring is intended as intelligent design for lowest weight. The author says that "an aerodynamic design must be developed prior to the structural design methodology." Therefore, no use is made of the elastic coupling phenomena of bend-twist, extension-twist or anticlastic curvature due to bending to enhance the aerodynamic properties of the rotor blade throughout the flight regime.

An important aspect of elastic tailoring makes use of coupling of deformation modes. Nixon[3] studied extension-twist coupling designed into composite tubes. Composite tubes can be incorporated with the rotor/propeller blades of tilt rotor aircraft. Optimum efficiency of the rotor system is achieved by using the extension-twist coupling to produce changes in the aerodynamic loads on the rotor system. As highlighted in the

paper, "there is a need for experimental data to confirm analytical predictions of twist deformation for axially loaded extension-twist coupled structures." In the study, a number of composite tubes were tested under tension/torsion loading. A ball thrust bearing was used to eliminate friction and to allow "free" twist of the tube under axial load. During the calibration tests on an aluminum tube, it is mentioned that "the thrust bearing had negligible torsional resistance." However, no quantitative data was presented to substantiate this statement. As seen in Armanios *et al.*[4], the torsional resistance of a thrust bearing increases with increasing axial load. While absolute values of torsional resistance may be small -- even at high loads -- their effects are dependent on the ratio of torsional rigidity of the test specimen to the torsional resistance of the testing apparatus.

Another important aspect of the study in Ref. 3 is that tension/torsion loading is performed. Ideally, there should be no torsional load applied so that the extension-twist coupling is isolated and its influence quantified accurately. The addition of torsional loading increases the complexity of the testing and analysis due to the problem of isolating, identifying, and quantifying the torsional resistance of the thrust bearing.

Chandra *et al.*[5] quantified extension-twist behavior using a one-pound extensional load. The beam under test was placed vertically in a testing apparatus and the tip load was applied through a thrust bearing and pulley system. The resultant twist of the beam was measured along the length of the specimen using a light beam reflected from a series of mirrors. The results of the test are very precise, as angles of twist were measured to a resolution of approximately 0.0006°, but the use of a suspended load and a thrust bearing to transmit the axial load prohibits testing to high loads because of the safety of large dead loads and the inaccuracies induced by friction in the thrust bearing.

While the literature search reveals a number of theoretical developments for

7

extension-twist coupling and other forms of elastic tailoring, very limited effort has been devoted to the development of testing methods appropriate to elastically tailored composites. In the majority of the work, the testing done was for proof-of-concept. No effort was made to design a test method that is both cost effective and adaptable while maintaining accuracy.

The need for designing and manufacturing apparatuses and test methods for measuring coupling in elastically tailored composites provides the main motivation of the work accomplished in this thesis. The next three chapters are devoted to the development of these testing apparatuses; namely the thrust bearing, rotating frame, and air bearing. An assessment of their use in quantifying extension-twist coupling is presented in Chapter VI. Of significance is the nonlinear behavior observed for the first time in twist versus axial load test measurements. Chapters VII and VIII elaborate on this finding. Conclusions and recommendations for future work based on the findings achieved in this work are provided in Chapter IX.

CHAPTER III

THRUST BEARING APPARATUS

An axial thrust bearing was initially chosen to be the means for allowing the free-end twist condition under axial load, which is how this apparatus is so aptly named. The apparatus in Figure 2 consists of an outer shell that contains the thrust bearing, load shaft, and 1 kΩ, one-turn potentiometer for angle measurement.

The load shaft is threaded to accept different loading heads that may be needed if the geometry of the specimen is changed. Similarly, the top of the apparatus is threaded to fit in a universal testing machine. To prevent binding effects caused by tolerance stack up or misalignment, a flexible coupling is used between the potentiometer and the load shaft. A one-turn potentiometer is used as the sensing element. This provides suitable accuracy for the expected twist range. A key aspect of the design was the means of instrumentation. A low cost means to get an accurate measure of twist was the key criterion. At the same time, the apparatus was to be connected to a 14 bit analog to digital (A/D) converter with an input range of zero to ten volts. With such a range, each bit represents 0.610 millivolts. Therefore, with the circuit shown in Figure 3, the measurement accuracy of the apparatus and the A/D converter is 0.02°, as shown in derivation of Equation 1. As the potentiometer's wiper jumps from wire to wire, there is a 4.89 millivolt change in output for an input voltage of ten volts. The true resolution of the apparatus is limited by this and is actually 0.18°. However, the wire wound potentiometer used needs less torque to turn than the equivalent continuous carbon strip based potentiometer.

9
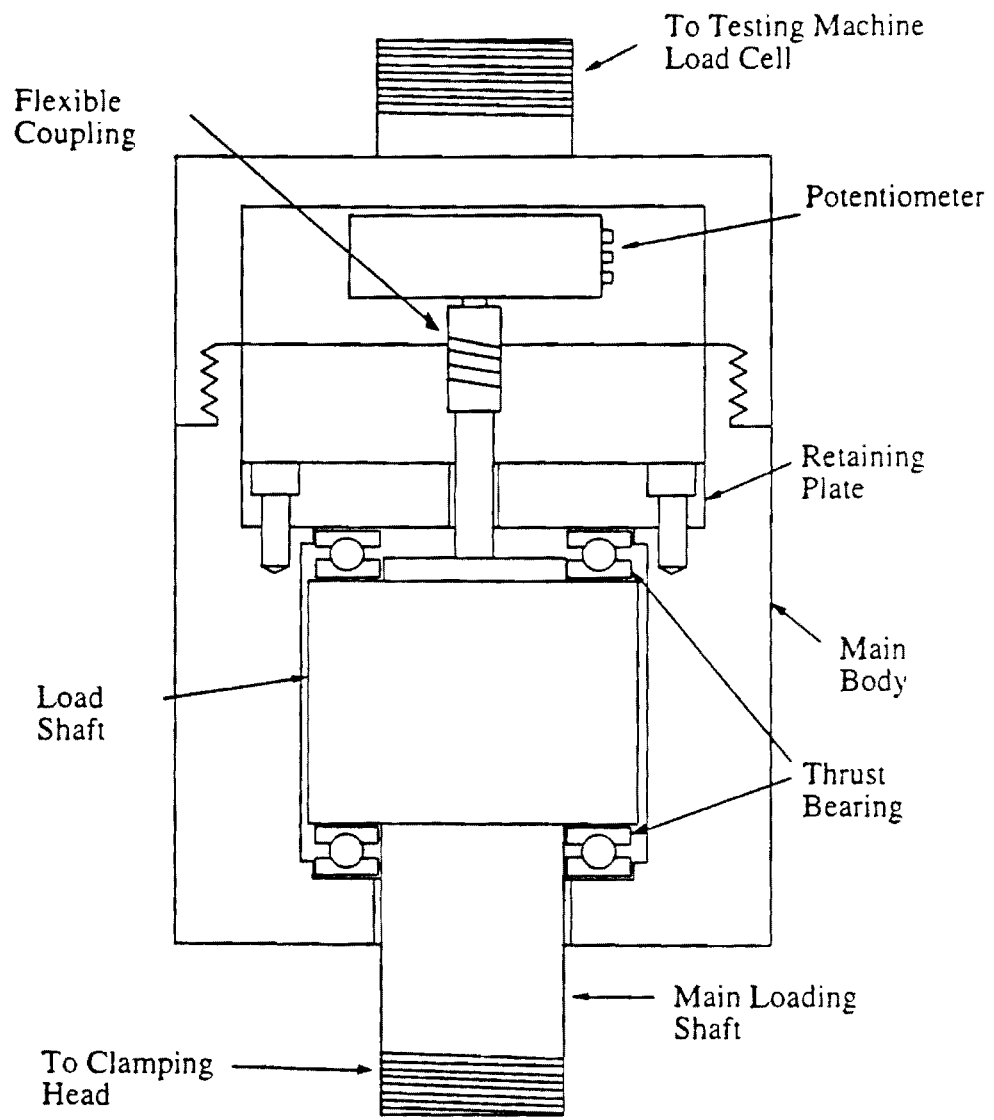
Figure 2. Schematic View of Thrust Bearing Apparatus
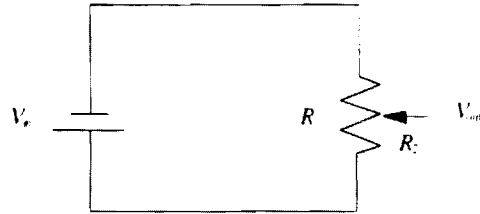
Figure 3. Circuit Schematic for Thrust Bearing Apparatus

$$V_{out} = \frac{V_{in} R_2}{R}$$

$$\frac{dV_{out}}{dR_2} = \frac{V_{in}}{R} = \frac{10V}{1000\Omega} = 0.01 \, V\!/\!\Omega$$

and for

$$\frac{1000\Omega}{360°} = 2.7 \, \Omega\!/\!°$$

then   (1)

$$0.01 \, V\!/\!\Omega \bullet 2.7 \, \Omega\!/\!° = 0.027 \, V\!/\!°$$

and

$$\frac{1}{0.027 \, V\!/\!°} \bullet 0.00061V = 0.02°$$

.

At this stage of the research, it was assumed that any friction in the thrust bearing under load would be negligible as stated in Ref. 3. Early tests using this apparatus showed the extension-twist coupling, however, there was an apparent stiffening of the test specimen at higher loads. During the development of the testing method, it was assumed that a linear theory was sufficient to fully understand the material behavior. It was in this vein that further investigations of friction were performed on the apparatus. Until all evidence of friction was removed from the testing technique, it was the main focus as the cause for the slight nonlinear response being observed in test data. While it is fully understood that there is friction in the thrust bearing as axial load is increased, a quantified measure of the friction had not been performed. The next step in the development was to quantify this friction.

The friction was measured by loading a rigid rod through two identical thrust bearings. Axial load was applied in a series of steps and the torque needed to rotate the rod was measured at each load step using a dead weight and pulley system. The results were then divided by two to account for only one of the bearings. The value at zero axial load is the restraining moment of the potentiometer itself. The results from this test are shown in Figure 4.
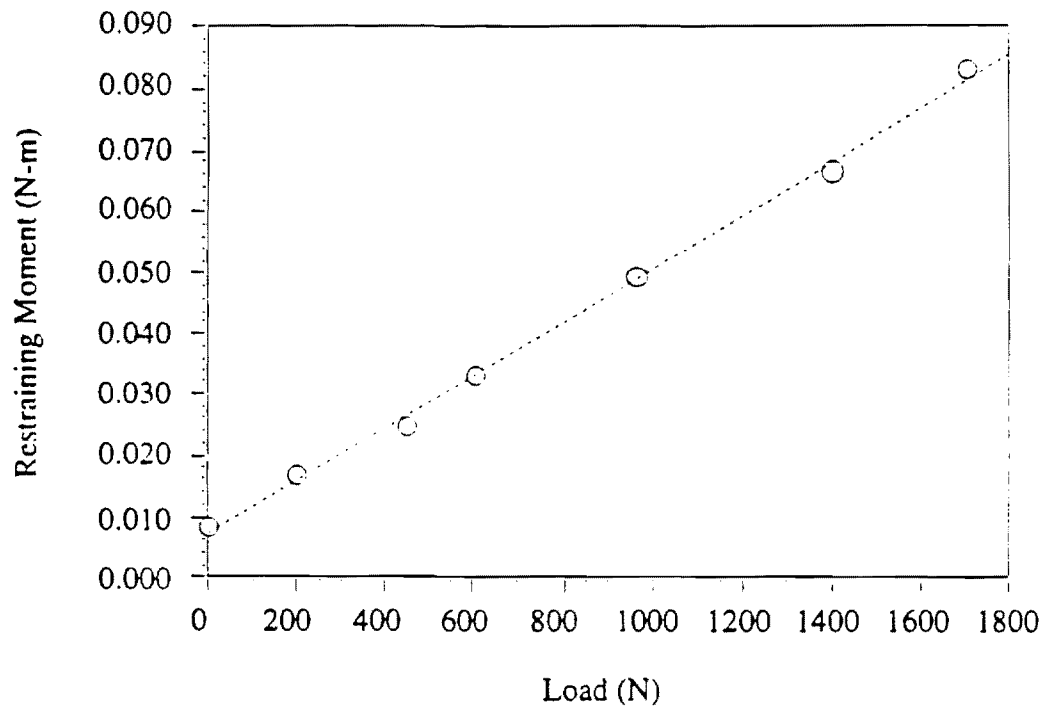
Figure 4. Restraining Moment for Thrust Bearing Apparatus

While friction is small, it is not negligible. Once the effect is known, however, it can be incorporated with the theoretical analysis. For simple cross-sections, this is handled with relative ease. Once the frictional effect was accounted for in the analysis as a torque dependent on axial load, the results were in better agreement with the theory of Ref. 4 and Chapter VI. However, the underlying nonlinear trend was still apparent.

The test setup is shown in Figure 5. The figure depicts the thrust bearing apparatus attached to the Instron universal testing machine. The test specimen is clamped at the lower end in a standard clamp and attached to the thrust bearing apparatus at the upper end with a clamp designed for the laminate cross-section geometry. The two coaxial cables attached to the apparatus carry the input and output voltages. The laminate in the picture is the evaluation specimen described in Chapter VI, with a special hinge joint at the lower end. The load applied in the picture is 1.557 kN. The resultant twist observed is 21°.

This design is easily produced, supplies repeatable results, and is easily interfaced with either a voltmeter or computer data acquisition system. However, due to friction of the thrust bearing in the transducer, the overall accuracy of the test changes throughout the loading sequence. Consequently, the measured twist is less than would occur in a truly free state.

The benefits of this method are that the testing procedure is no more complicated than the procedure used in a simple axial test. This allows for rapid testing of a large number of laminates if needed. With the use of different loading grips, the transducer can accommodate a variety of laminate geometries including closed sections. The testing procedure for this apparatus follows in the same manner as a normal tension test. Once the laminate is clamped in the testing machine and apparatus, load is applied manually. The resultant twist can then be measured by noting the change in output voltage from the

potentiometer. The results from this apparatus are discussed in Chapter VI.
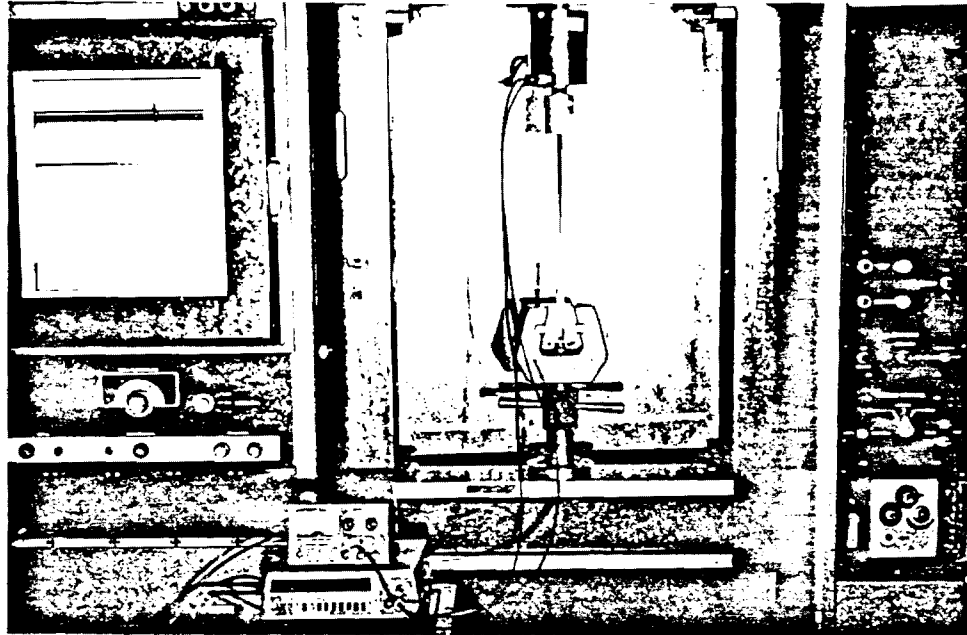
Figure 5. Thrust Bearing Apparatus in Testing Machine

CHAPTER IV

ROTATING FRAME APPARATUS

The basis for the design of a testing method and apparatus adopted here is that the apparatus have the least influence on the test specimen as possible. Above all else, the apparatus should not require an addition to the complexity of the analysis; it should provide as closely as possible the ideal loading. Because the thrust bearings had an influence on the coupling being measured, the next step in friction reduction was to remove any type of bearing altogether. The result of such a constraint was to design the rotating frame apparatus shown in Figure 6. The principal components shown in the figure are the laminate, the end weight, and the motor controller. The clamps visible in the figure are for the vacuum dome. The basis of this method is to change the conventional load frame where displacements are prescribed or loads applied via dead loading or hydraulic loads to an inertial loading frame. If the test specimen is spun around an axis at one end with a mass attached to the other, a load will be applied to the specimen and no frictional restraint will be present.

A one-quarter horsepower DC motor was used to drive the apparatus. A motor speed controller was used to maintain constant angular speed at prescribed intervals during the test. A light sensitive trigger was designed and a beam-breaking flag was mounted on the spinning shaft to control a strobe light and provide counting pulses to the tachometer. Accurate end twist angle measurements were taken by focusing a telemicroscope on the end mass and measuring the angle of inclination of a line scribed on it. The angular speed was increased until the load on the specimen was approximately 1.7 kN. The spinning shaft,

17

test specimen, end mass, and triggering system are enclosed in a vacuum chamber to significantly reduce any aeroelastic effects on the system as shown in Figure 7.

The testing procedure was the following. The testing chamber was evacuated to 724 mm Hg gage pressure. The angular speed of the rotating frame could then be increased from zero to a maximum of 5.000 rpm. The result of the increase in rpm was an increase in the axial load applied to the laminate. The rpm was monitored with a digital tachometer and maintained with a controller to within ± 1 rpm. The resultant load was calculated from the weight of the end mass, the rotational speed, and the distance of the center of gravity of the weight to the axis of rotation. For the tests presented here, the end mass was 69 grams, the radius of rotation of the mass was 239 mm, and the maximum rpm was 3.045. The resulting end load at maximum rpm was, therefore, 1.655 N. The rotation of the end mass was measured optically using a Questar telemicroscope mounted on an instrumented traverse and a strobe light. Figures 8 and 9 depict the test specimen at 1.370 RPM with an associated axial load of 339 N. A twist of 5.5° in the laminate is clearly seen.

As described in Chapter VI, the data showed a nonlinear behavior due to the distribution of the end mass. In addition, tests at higher loads are not safe. An alternative for negating friction is described in the next chapter.

Results from tests using the rotating apparatus are given in Chapter VI.
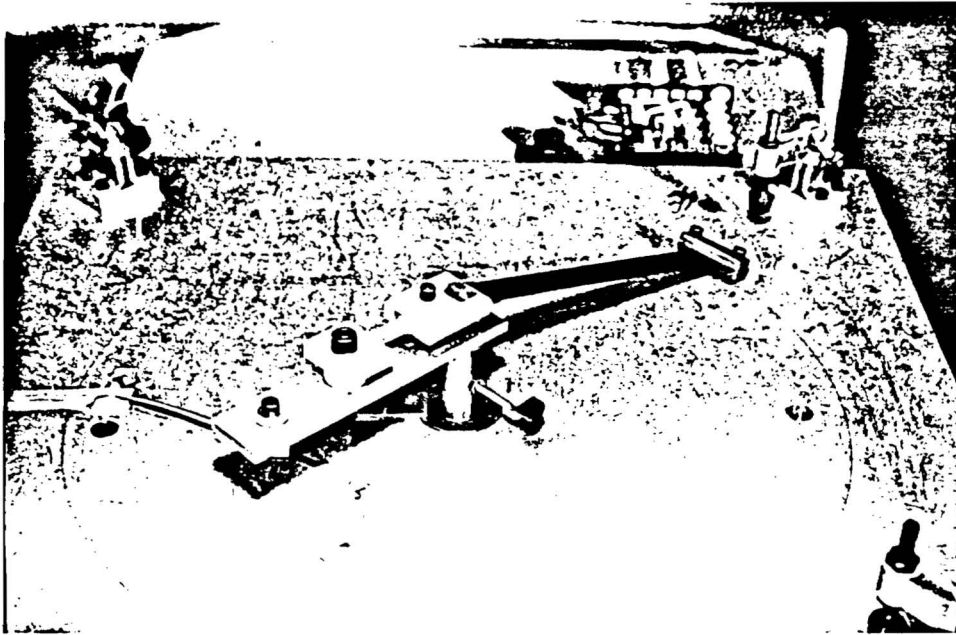
Figure 6. Rotating Frame Apparatus Components
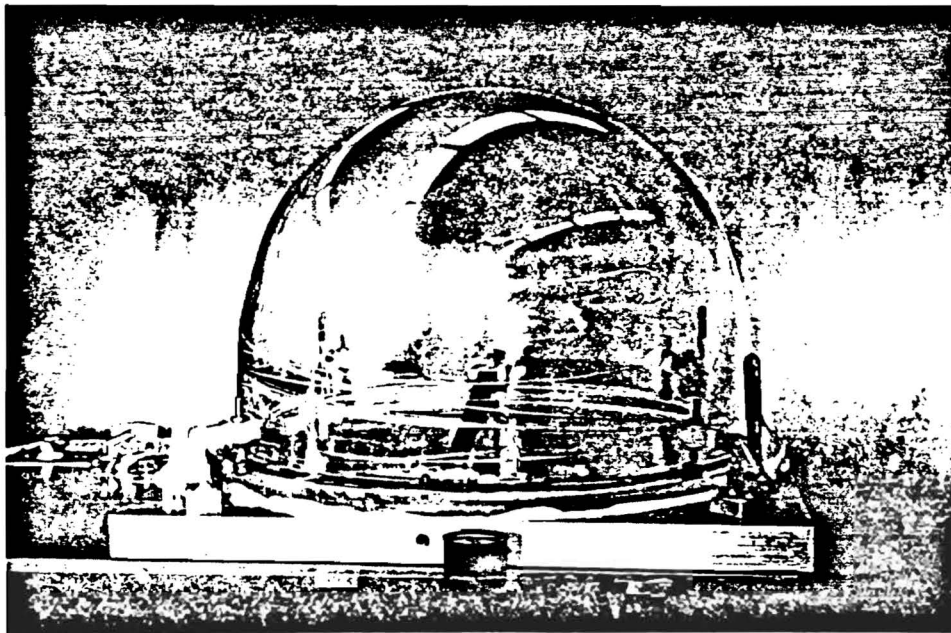
Figure 7. Complete Rotating Frame Apparatus with Dome
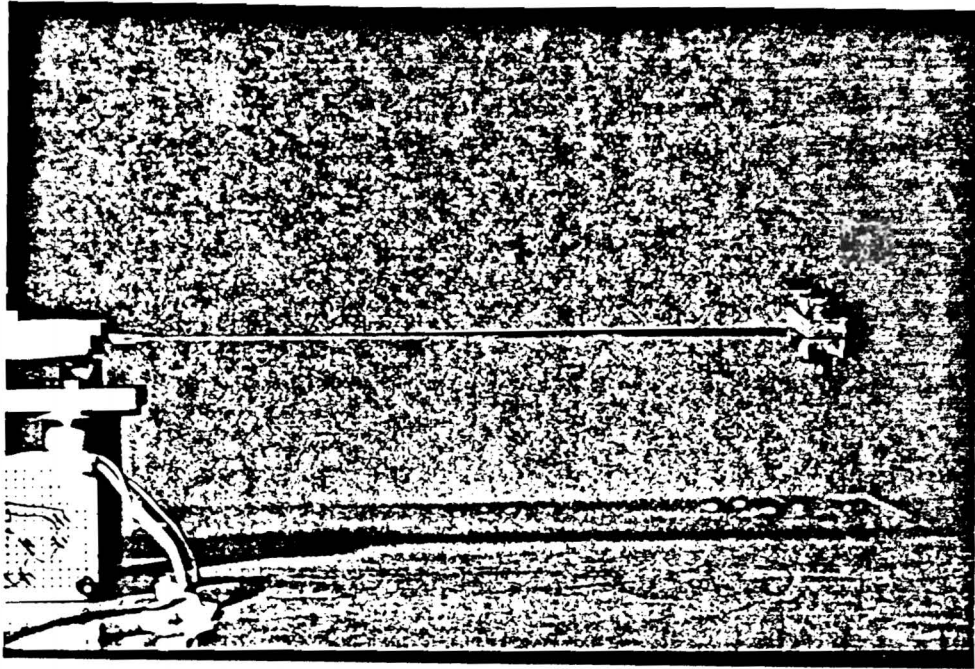
Figure 8. Laminate Under Test, 339 N, 1370 RPM
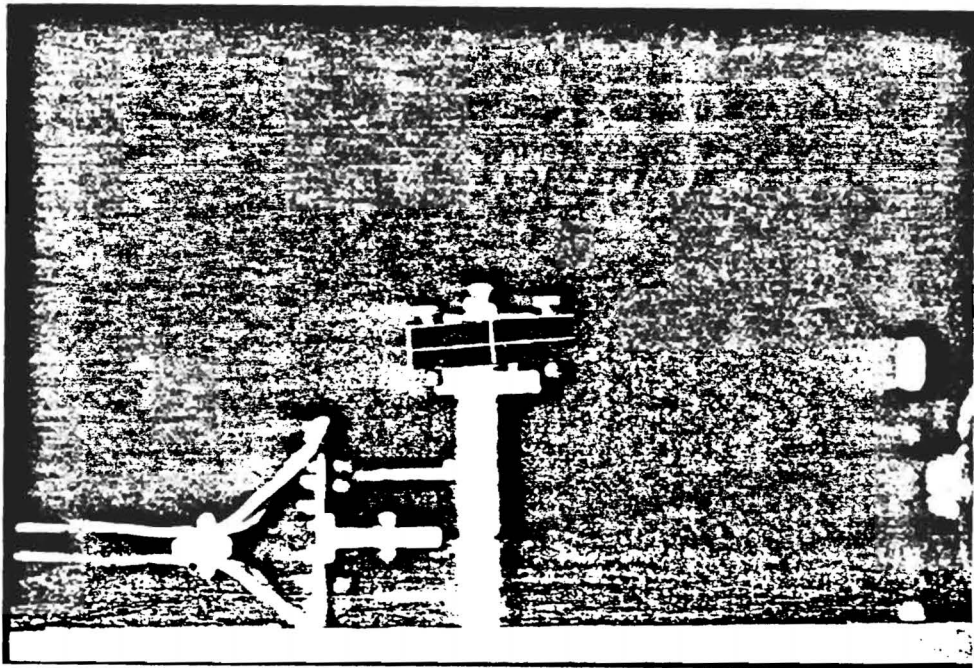
Figure 9. Laminate End Twist, 339 N, 1370 RPM

CHAPTER V

AIR BEARING APPARATUS

The results from the rotating frame apparatus initially forced the focus back to the thrust bearing apparatus. The basic question to be resolved was whether there was any way to remove friction from the thrust bearings themselves. Of course, lubricants could be used to minimize friction, but a constant verification of the actual friction would always be needed and as a result of the design, there would always be increasing friction with increasing load regardless of the lubricant used.

However, a non-contact method of applying a load would result in no friction. This is the case if a differential pressure is applied to a piston residing in a cylinder without any seals. Essentially, the air bearing apparatus is an exceptionally close tolerance air cylinder with no internal seals to cause friction. The basis of the design is a piston and piston rod precisely aligned in a cylinder with a wall clearance of two thousandths of an inch or less. Alignment of the piston is ensured by locating the piston rod in precision instrument bearings. When air pressure is applied to one side of the piston, it acts on the exposed area causing a resultant force. Because there is clearance at the wall, the pressure is bled to the other side which is open to the atmosphere. The differential pressure on the piston results in an axial load. Because the piston rod is journaled in radial bearings and there is no expected radial load, the friction inherent in the apparatus is negligible. The friction would be the amount of torque needed to rotate a radial bearing without any radial load applied to it. As the piston rod is free to slide in the radial bearings, no face loads are applied to the bearings either. The efficiency of such a device is dependant on the small

21

clearance between the piston and the cylinder. Accurate machining guarantees that this clearance is achieved.

The other source of friction in the thrust bearing apparatus was the potentiometer. The resolution of the potentiometer was also relatively low at 0.18°. A new means of angle measurement is employed in the air bearing apparatus. An optical encoder is used because it is a non-contact method of measuring angle. The optical encoder is mounted inside the apparatus and connected to the piston through a gear train with a ratio of 1: 1.8. This ratio is needed to obtain a resolution of 0.1°. The drive gear is connected to the piston through a hexagonal shaft. The mating hexagonal hole in the piston allows free movement of the piston up and down while transferring rotation. The encoder itself has 500 micro machined slots in a disk which passes through two sets of LED emitter-detector pairs. The output states of the detectors determine the angular displacement of the encoder. Four output logic state combinations are possible with the encoder: both high, both low, one high and one low, and one low and one high. Monitoring these states in quadrature increases the apparent output to two thousand lines per revolution. Using the gear ratio increases the output to 3600 lines per revolution of the piston which results in a resolution of 0.1°. Commercially available circuitry is used to monitor the output states of the detectors and drive an LCD panel. The test set-up using the air bearing transducer is shown in Figure 10. The figure shows the apparatus attached to the testing machine at the top. The test specimen is clamped in loading head at the apparatus and the lower grip of the testing machine. An axial load of 1.7 kN is applied to the specimen resulting in an end twist of 26.3°. A cross-section of the apparatus highlighting the key components is shown in Figure 11. Results from tests using this apparatus are in the following Chapter.

Because of the virtual elimination of friction as indicated by the repeatability of test results, this apparatus is the preferred means for testing. Its design was the subject of the pending patent, "Rotational Displacement Apparatus with Ultra-low Torque and High Thrust Capability," US Patent and Trademark Office Serial No. 08/562,586.
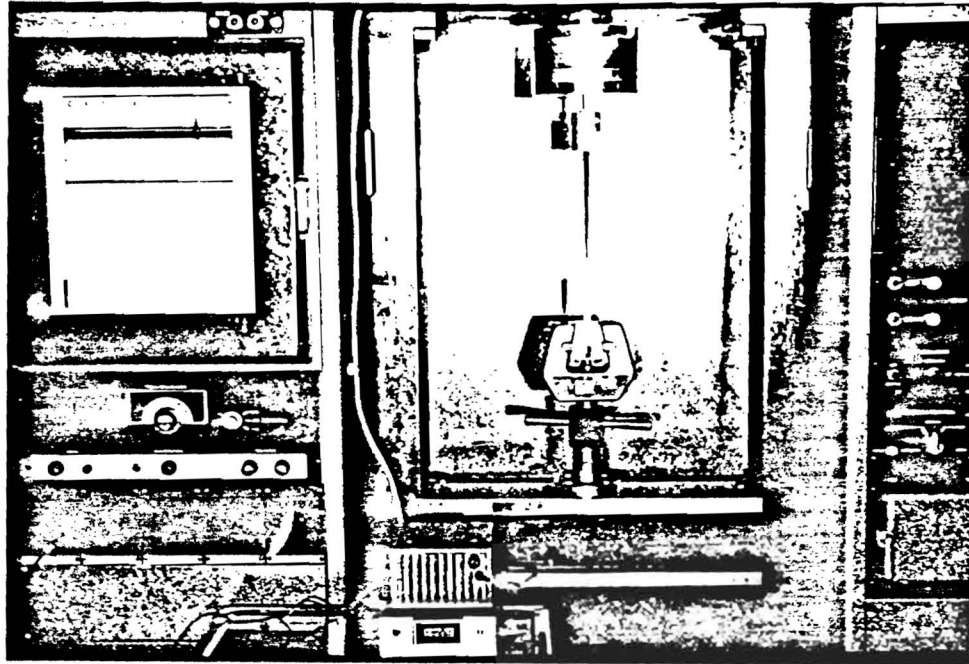
Figure 10. Air Bearing Apparatus
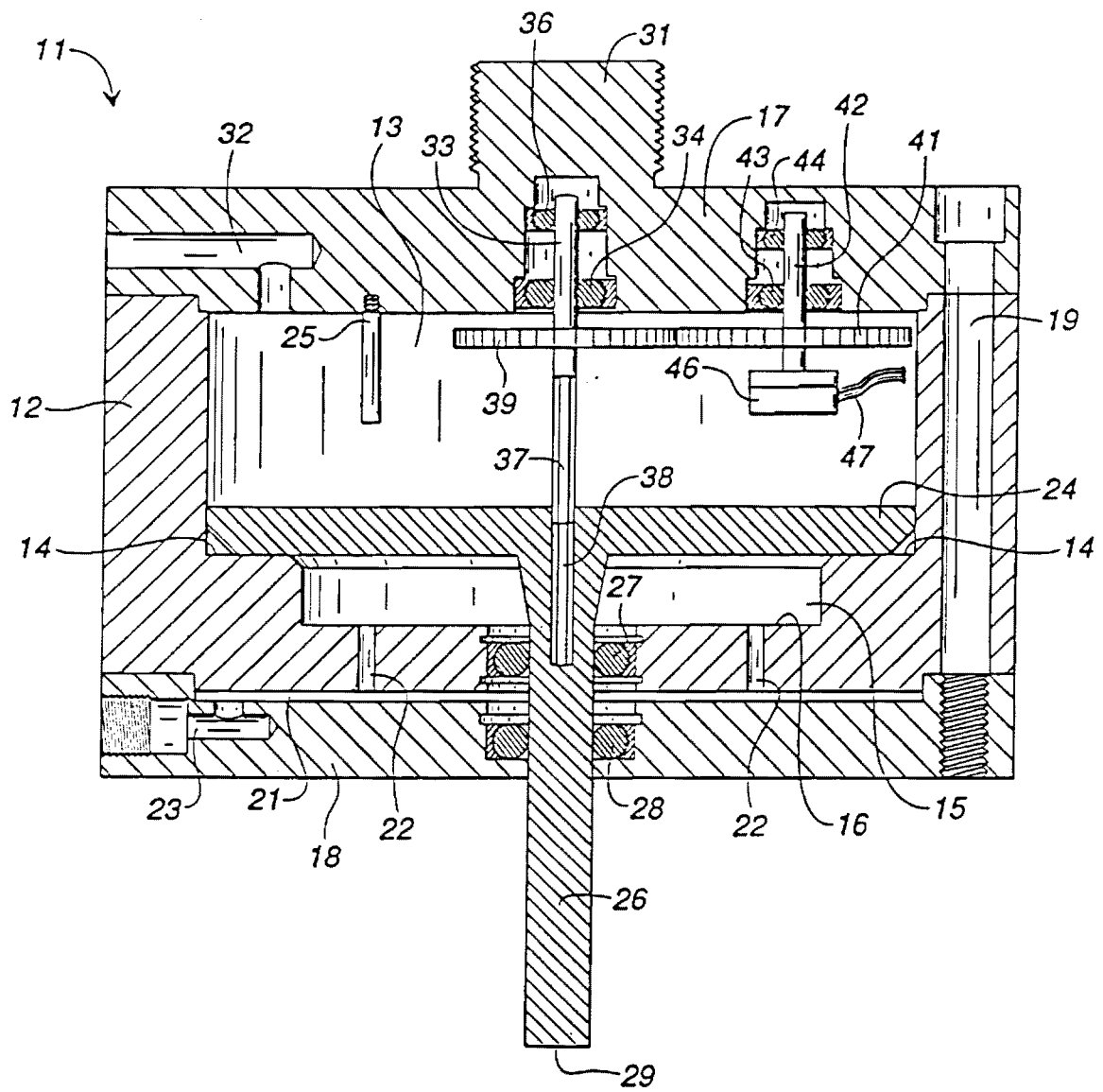
Figure 11. Cross-Section of Air Bearing Apparatus

CHAPTER VI

EVALUATION AND DISCUSSION OF TESTING METHODS

Test Specimen

The specimen used to compare the testing methods was manufactured from Ciba Geigy C30/922 graphite/epoxy unidirectional prepreg tape cured in an autoclave using the manufacturer's suggested cure cycle of 180°C for two hours at 586 kPa. The stacking sequence was $[30/-60_2/30/-30/60_2/-30]_T$. The specimen dimensions are 246 mm X 22.9 mm X 0.91 mm. One end of the laminate was designed with a built in hinge joint shown in Figure 12.

Table 1. Material Properties for Evaluation Test Specimen

E_{11}	134 GPa
E_{22}	9.8 GPa
G_{12}	7.45 GPa
v_{12}	0.35

In order to provide an estimate of axial force-twist range, the sublaminate shear deformation theory of Ref. 6 was applied to the prediction of twist versus axial load. The friction associated with the thrust bearing was also modeled. The theory is geometrically linear and is based on the small displacement assumption of Classical Lamination Theory. but the influence of shear deformation is accounted for. An outline of its development is presented in the following section.
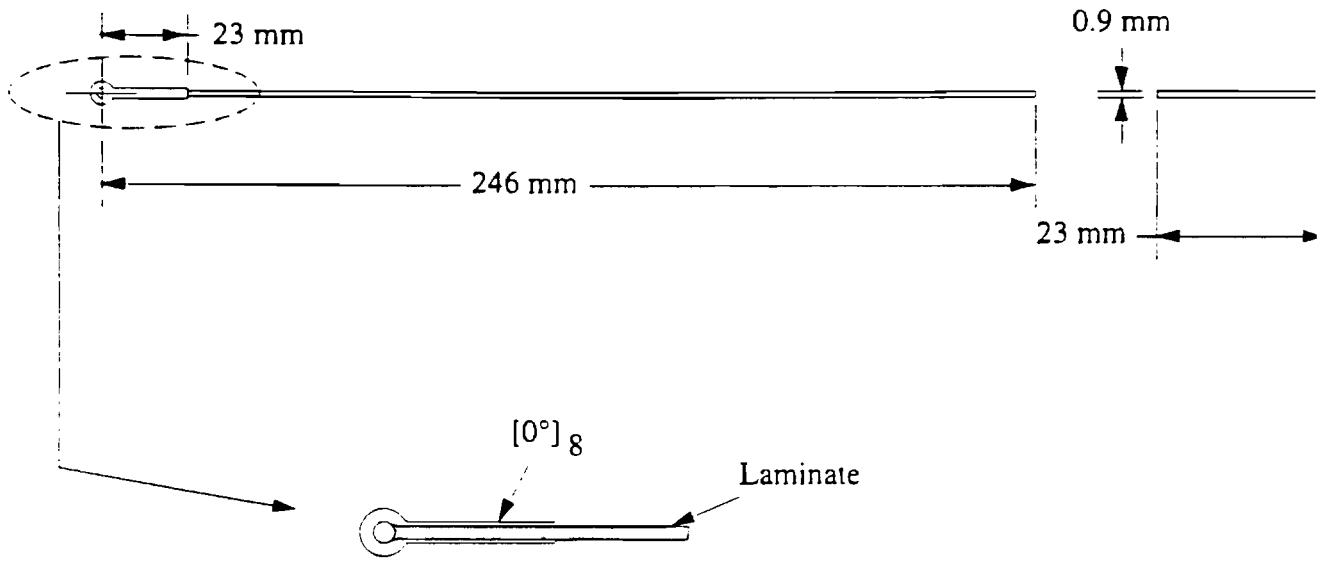
Figure 12. Specimen Design with Hinge Joint

Shear Deformation Laminated Plate Theory

The sublaminate shear deformation analysis of Ref. 4 is used to predict the twist associated with extension load in a $[\alpha/(\alpha-90)_2/\alpha/-\alpha/(90-\alpha)_2/-\alpha]_T$ laminate. This unsymmetrical lay-up ensures hygrothermal stability of the laminate[7] and eliminates initial warping that results from the curing stresses. A summary of the governing equations and solution procedure is presented for convenience. This development has been published in Ref. 4.

The governing equations are written for the generic sublaminate shown in Figure 13. A sublaminate is a ply or group of plies from the original laminate that is treated as a single laminated unit with equivalent effective properties. The in-plane stress resultants are denoted by N_{11}, N_{22}, and N_{12} while M_{11}, M_{22}, and M_{12} denote the bending in the x-z and y-z planes and the torsional moment respectively. The shear resultants in the y-z and x-z planes are denoted by Q_1 and Q_2 respectively. The interlaminar shear and peel stresses at the laminate upper and lower surfaces are denoted by t_{u1}, t_{u2}, p_u, and t_{l1}, t_{l2}, p_l respectively. In the present case the entire laminate cross section is modeled as one sublaminate. The displacement field is given by

$$u(x,y,z) = \varepsilon_0 x + \kappa xz + U(y) + z\beta_1(y)$$

$$v(x,y,z) = \frac{\theta}{L}xz + V(y) + z\beta_2(y) \tag{2}$$

$$w(x,y,z) = -\frac{\kappa}{2}x^2 - \frac{\theta}{L}xy + W(y)$$

where u, v, and w denote displacements relative to the x, y, and z axes, respectively. The origin of the Cartesian coordinate system coincides with the center of the laminate. The

laminate length is denoted by L and the axial extension strain is ε_o The twisting rotation

and bending curvature are denoted by θ and κ, respectively. These result from the

coupling effects associated with unsymmetrical lay-ups. Mid-plane displacements in the x.

y. and z directions are represented by $U(y)$, $V(y)$, and $W(y)$ respectively.

Shear deformation is recognized through the rotation β_x and β_y. Bending about the z axis is neglected since the laminate thickness is small compared to its width.

The corresponding strains are

$$\varepsilon_{xx} = \varepsilon_{xx}'' + z\kappa_{xx} \quad \varepsilon_{yy} = \varepsilon_{yy}'' + z\kappa_{yy} \quad \varepsilon_{zz} = 0$$

$$\gamma_{xy} = \gamma_{xy}'' + z\kappa_{xy} \quad \gamma_{yz} = \gamma_{yz}'' \quad \gamma_{xz} = \gamma_{xz}'' \tag{3}$$

The strain components associated with the reference surface are denoted by superscript o.

These and the associated curvatures are defined as

$$\varepsilon_{xx}'' = \varepsilon_o \quad \varepsilon_{yy}'' = V_{,y} \quad \gamma_{xy}'' = U_{,y}$$

$$\kappa_{xx} = \kappa \quad \kappa_{yy} = \beta_{y,y} \quad \kappa_{xy} = \beta_{x,y} + \frac{\theta}{L} \tag{4}$$

$$\gamma_{yz}'' = \beta_y + W_{,y} \qquad \gamma_{xz}'' = \beta_x - \frac{\theta}{L}y$$

where partial differentiation is denoted by a comma.

The constitutive relationships for the hygrothermally stable lay-up considered. take the

following uncoupled form:

$$\begin{Bmatrix} N_{xx} \\ N_{yy} \\ M_{xy} \end{Bmatrix} = \begin{bmatrix} A_{11} & A_{12} & B_{16} \\ A_{12} & A_{11} & -B_{16} \\ B_{16} & -B_{16} & D_{66} \end{bmatrix} \begin{Bmatrix} \varepsilon_{xx}'' \\ \varepsilon_{yy}'' \\ \kappa_{xy} \end{Bmatrix} \tag{5}$$

$$\left\{\begin{array}{c} N_{\iota\iota} \\ M_{\iota\iota} \\ M_{\gamma\gamma} \end{array}\right\} = \left[\begin{array}{ccc} A_{66} & B_{16} & -B_{16} \\ B_{16} & D_{11} & D_{12} \\ -B_{16} & D_{12} & D_{22} \end{array}\right] \left\{\begin{array}{c} \gamma''_{\iota\iota} \\ \kappa_{\iota\iota} \\ \kappa_{\gamma\gamma} \end{array}\right\} \tag{6}$$

$$\left\{\begin{array}{c} Q_{\iota} \\ Q_{\iota} \end{array}\right\} = \left[\begin{array}{cc} A_{44} & 0 \\ 0 & A_{44} \end{array}\right] \left\{\begin{array}{c} \gamma''_{\iota z} \\ \gamma''_{\iota z} \end{array}\right\} \tag{7}$$

For a sublaminate of thickness h, the stiffness coefficients are defined as

$$(A_{ij}, B_{ij}, D_{ij}) = \int_{-h/2}^{h/2} \overline{Q}_{ij}(1, z, z^2) dz \tag{8}$$

where $\overline{Q}_{ij}$ are the transformed reduced stiffnesses as defined in Ref. 5. Since the upper and lower surfaces of the sublaminate are stress free, the equilibrium equations reduce to

$$N_{\iota\iota,\iota} = N_{\gamma\gamma,\iota} = Q_{\iota,\iota} = 0 \tag{9}$$

$$M_{\iota\iota,\iota} - Q_{\iota} = 0 \tag{10}$$

$$M_{\iota\iota,\iota} - Q_{\iota} = 0 \tag{11}$$

From the boundary conditions

$$N_{\iota\iota}\big|_{\iota=\pm b} = N_{\iota\iota}\big|_{\iota=\pm b} = Q_{\iota}\big|_{\iota=\pm b} = M_{\iota\iota}\big|_{\iota=\pm b} = 0 \tag{12}$$

where b denotes the laminate semi-width, Eqs (9) and (10) reduce to

$$N_{\gamma\gamma} = N_{\iota\iota} = M_{\iota\iota} = Q_{\iota} = 0 \tag{13}$$

Substitution of Eqs (4) and (13) into Eqs (5) and (6) yields

$$M_{\iota\iota} = \frac{-B_{16}^2(D_{11} + D_{22} + 2D_{12}) + A_{66}(D_{11}D_{22} - D_{12}^2)}{D_{22}A_{66} - B_{16}^2} \kappa \tag{14}$$

$$\left\{ \begin{matrix} N_{\iota\iota} \\ M_{\iota\iota} \end{matrix} \right\} = \begin{bmatrix} \alpha_{11} & \alpha_{12} \\ \alpha_{12} & \alpha_{22} \end{bmatrix} \left\{ \begin{matrix} \varepsilon_{\iota} \\ \beta_{\iota,\iota} + \dfrac{\theta}{L} \end{matrix} \right\} \tag{15}$$

where

$$\alpha_{11} = \frac{A_{11}^2 - A_{12}^2}{A_{11}}$$

$$\alpha_{12} = \frac{B_{16}(A_{11} + A_{12})}{A_{11}}$$

$$\alpha_{22} = \frac{D_{66}A_{11} - B_{16}^2}{A_{11}}$$

Substitution of Eqs (4), (7) and (15) into Eq (11) yields the following differential equation in β

$$(D_{66}A_{11} - B_{16}^2)\beta_{\iota,yy} - A_{44}A_{11}\beta_\iota = -A_{44}A_{11}\frac{\theta}{L}y \tag{16}$$

which leads to

$$\beta_\iota = A_1 \, sinh(sy) + A_2 \, cosh(sy) + \frac{\theta}{L}y \tag{17}$$

where

$$s = \sqrt{\frac{A_{44}A_{11}}{(D_{66}A_{11} - B_{16}^2)}} \tag{18}$$

From the remaining boundary conditions at the laminate free edges

$$M_{\iota y}\Big|_{y=\pm b} = 0 \tag{19}$$

and Eq (15), the even functions of y in the rotation β_ι should vanish. As a result, the arbitrary constant A_2 in Eq (16) is zero. The axial strain, bending and twisting curvatures, and the arbitrary constant A_1 are obtained from the end-loading and boundary conditions. The laminate is tested under uniaxial force, F. However, as is the case for the thrust bearing transducer and the rotating apparatus, an additional torsional restraining moment is induced. In the thrust bearing apparatus, the torsional restraining moment is a result of the

31

bearing friction, while in the rotating frame apparatus, it is a result of the end mass distribution, as derived in Equation 32.

These boundary conditions are expressed as

$$F = \int_{-b}^{b} N_{xx} dy$$

$$M = \int_{-b}^{b} M_{xx} dy = 0 \quad\quad (20)$$

$$T = \int_{-b}^{b} (M_{xy} - Q_x y) dy = 2 \int_{-b}^{b} M_{xy} dy$$

where M and T denote bending and torsional restraining moment, respectively. Substituting for Eqs (14) and (15) into Eq (20) yields

$$\cdots h(sb) \Big] \quad\quad (21)$$

32

where, from Eq (19).

$$A_1 = -\frac{1}{s\cosh(sb)}\left[\frac{\alpha_{12}}{\alpha_{22}}\varepsilon_{\prime\prime} + \frac{2\theta}{L}\right]$$ (22)

Eliminating ε from Eq (20) yields the following equation for θ in terms of F and T.

$$\theta = \rho_1 T + \rho_2 F$$ (23)

where

$$\rho_1 = \frac{L(\alpha_{11}\alpha_{22}bs - \alpha_{12}^2\tanh(sb))}{8b\psi\alpha_{22}(bs - \tanh(sb))}$$ (24)

$$\rho_2 = \frac{-\alpha_{12}L}{4b\psi}$$

where

$$\psi = \alpha_{11}\alpha_{22} - \alpha_{12}^2$$ (25)

It is worth noting that ρ_2 is independent of the characteristic root, s. That is, the shear deformation contribution to the twisting rotation is associated with torsional restraining moment only. For the case of no torsional restraining moment, Eq (23) simplifies to

$$\beta_x = \frac{\theta}{L} y$$

$$\beta_y = -W_{,y}$$

(27)

and Eq (23) simplifies to

$$\frac{\theta}{L} = \frac{1}{4\psi b}\left[-\alpha_{12}F + \frac{\alpha_{11}}{2}T\right] = \frac{\left[-2B_{16}F + (A_{11} - A_{12})T\right]}{8b\left[D_{66}(A_{11} - A_{12}) - 2B_{16}^2\right]}$$

(28)

The CLT solution violates the free edge boundary condition on the twisting moment given in Eq (19).

·
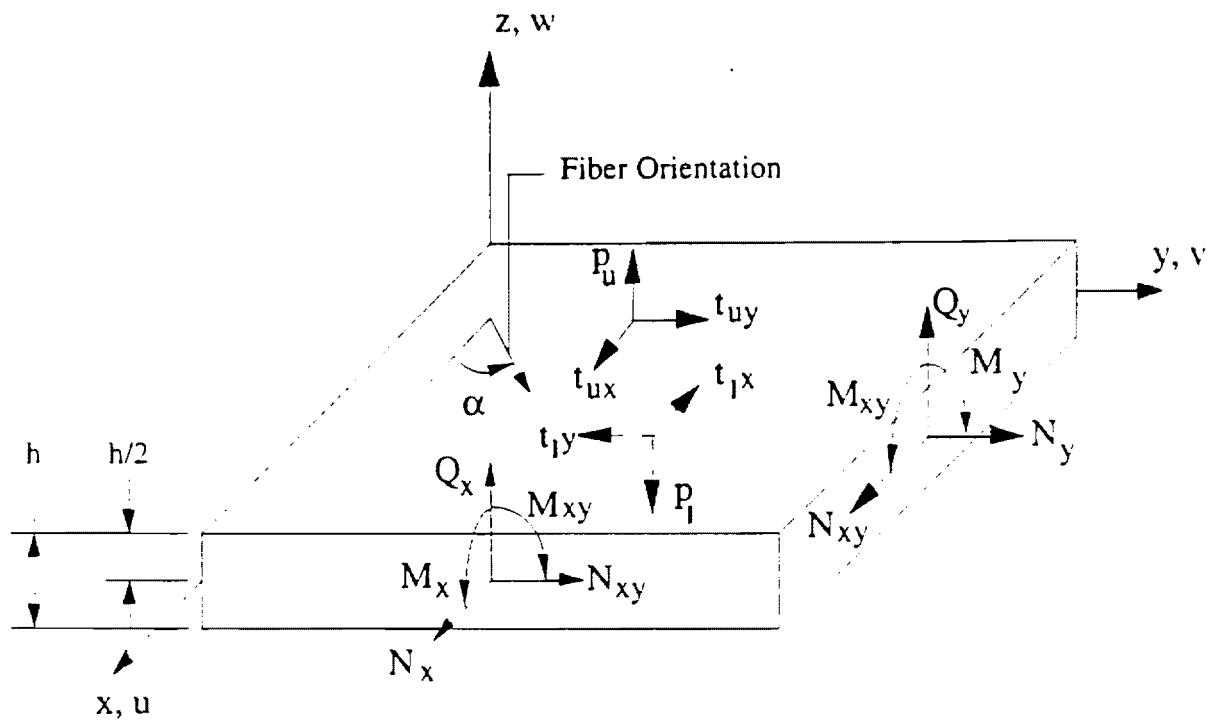
Figure 13. Generic Sublaminate

Thrust Bearing Apparatus Results

The results of the test on the evaluation specimen are shown in Figure 14. Data in tabular form is presented in Appendix I. The maximum load for the test is 1.6 kN. For the case of axial loading only, the Shear Deformation Theory (SDT) solution provided in Equations 23-25, is identical to the Classical Lamination Theory (CLT) solution (26) in the absence of torsional moment. The SDT and FEM solutions are plotted with the experimental data in Figure 13. The relative difference between the FEM prediction and the best line of fit of the data is 15%. For the SDT this difference is 33%. The finite element model uses 800 quadrilateral shell elements with 891 nodes. There are 5346 degrees of freedom for the model generating a wave front width of 78. The difference between the analytical prediction and test data is due to the restraining moment induced by the thrust bearing transducer. This can be accommodated in the SDT prediction by including an idealized twisting moment proportional to the applied load expressed as $T = -\xi F$. This moment is a result of modeling the friction of the thrust bearing simply as a steady behavior appearing in Figure 4. The constant ξ equals the slope of the least squares fit line through the data in the figure. A comparison between test data and SDT with and without friction appears in Figure 15. The relative difference between the SDT with friction and the test data then drops to 1.9%. It is of interest that the influence of shear deformation on the coupling is negligible for the lay-up and material system considered.
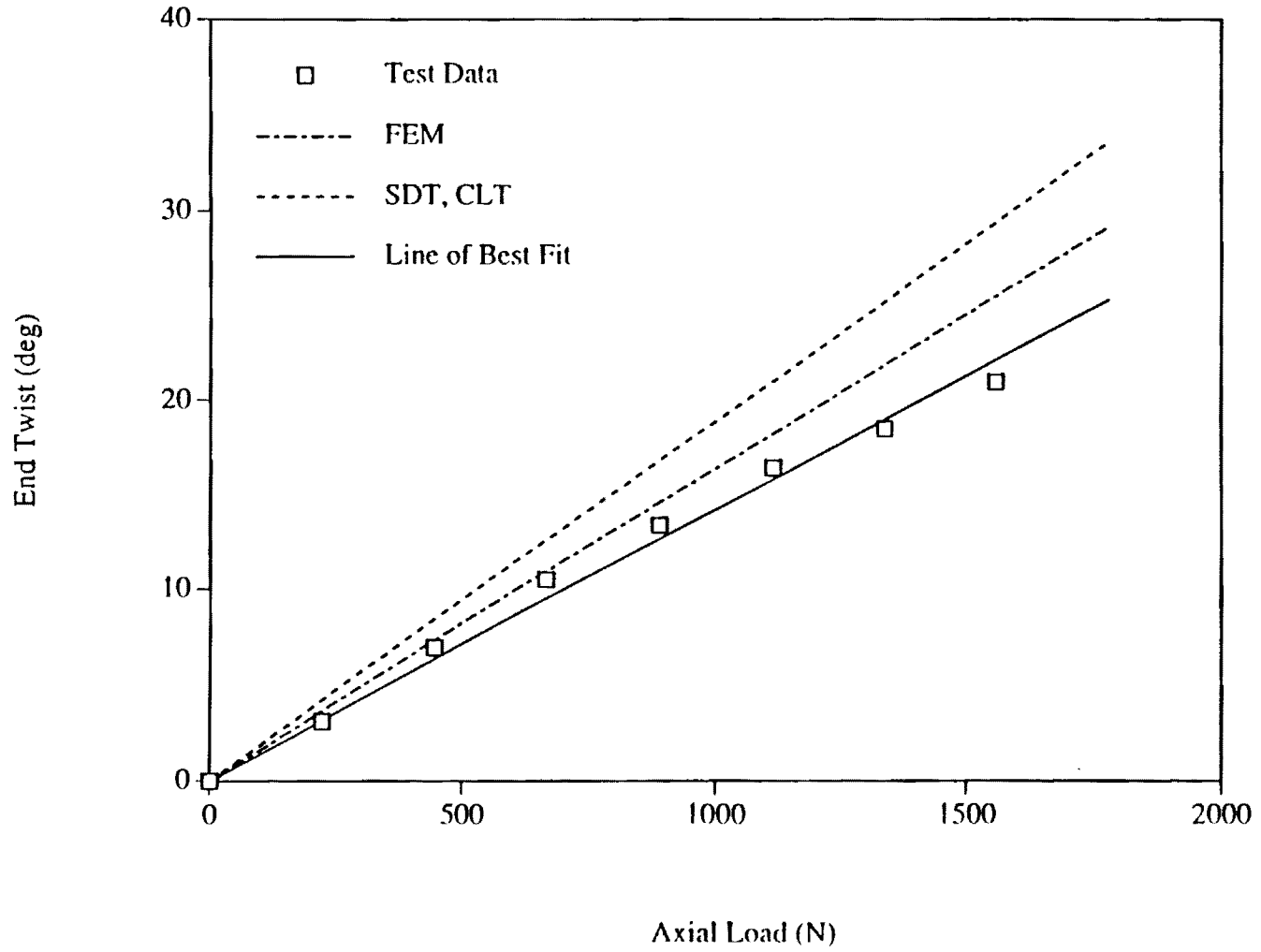
Figure 14. Experimental Results for Thrust Bearing Apparatus
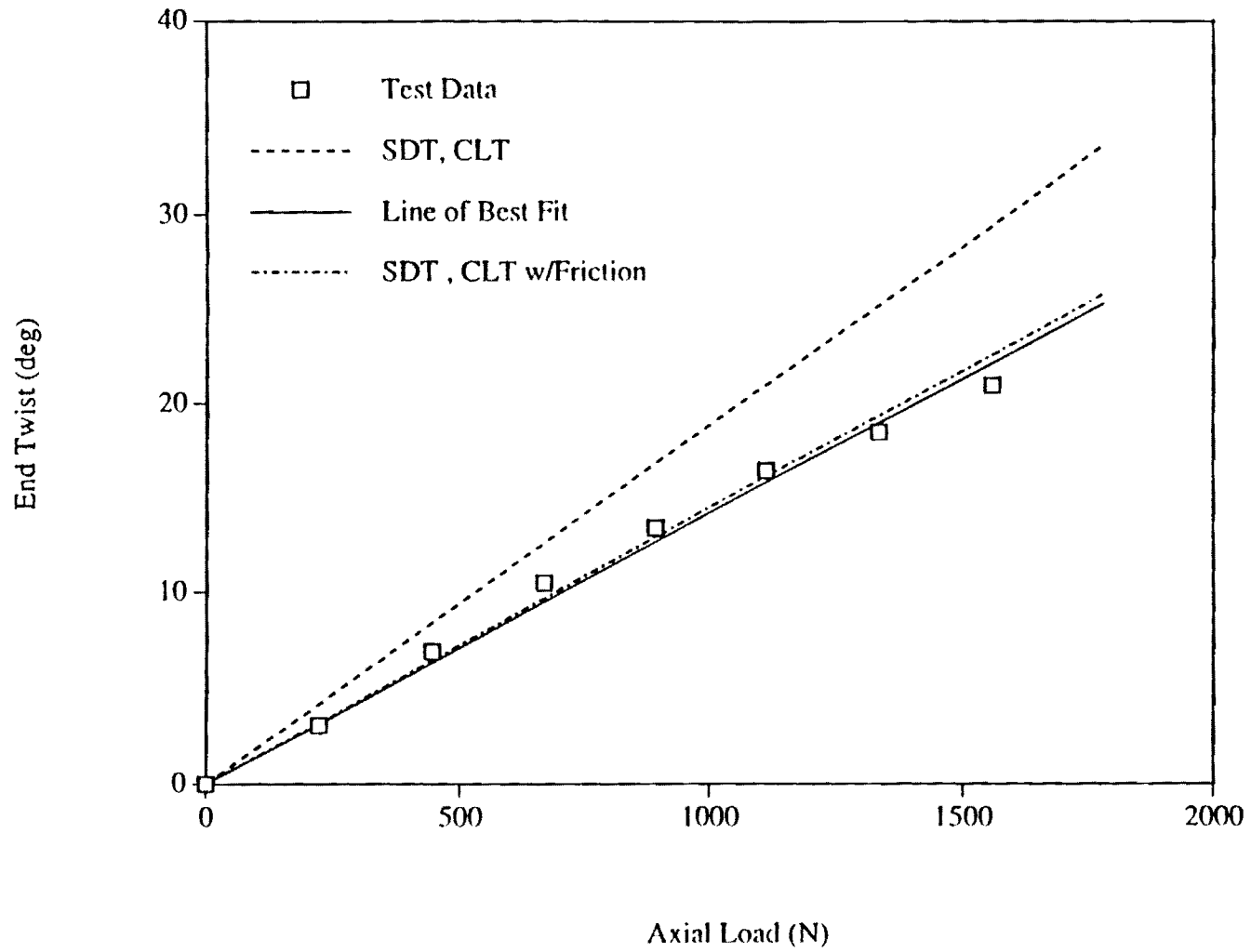
Figure 15. Experimental Results for Thrust Bearing Apparatus, Friction Added

Rotating Frame Apparatus

The results from the test on the evaluation specimen are shown in Figure 16. The test data in tabular form appears in Appendix I. Instead of an expected linear behavior, a very nonlinear behavior was observed. What was not accounted for in the initial design of the experiment was the complete set of inertial effects of the end mass. In addition to the axial load desired, a torque due to the end mass distribution is also produced as shown in Figure 17. The torque is derived in the following manner.

Consider the end mass connected to the specimen undergoing twisting rotation of magnitude θ as shown in Figure 16. For an element at a distance x, the centrifugal force denoted by F_c is given by

$$F_c = m \omega^2 R dx \tag{29}$$

where m is the mass per unit length, R is the radial distance, and ω is the angular speed. The tangential component of F_c is given by

$$F_{ct} = m \omega^2 R \sin \beta dx = m \omega^2 x \cos \theta dx \tag{30}$$

while the axial component of F_c is given by

$$F_{ca} = m \omega^2 R \cos \beta dx = m \omega^2 l dx \tag{31}$$

The associated torque is

$$T = 2 \omega^2 \sin \theta \cos \theta \int_d m x^2 dx = \omega^2 \sin 2\theta \int_d m x^2 dx \tag{32}$$

and the associated bending moment is

$$M_B = \omega^2 l \sin \theta \int_d m x dx \tag{33}$$

39

The mass is clamped to the specimen with two symmetrically located screws. They are treated as lumped masses at the proper locations. The symmetric variation of m along the positive x direction is given by

$$m_1 = 1.26 \ g/mm, \ 0 \le x \le 15.3 \ \text{mm}, \ and \ 21.7 < x \le 24.8 \ \text{mm} \qquad (34)$$
$$m_2 = 1.77 \ g/mm, \ 15.3 \ \text{mm} < x \le 21.7 \ \text{mm}$$

The torque is then

$$T = 2\,\omega^2 \sin 2\theta \left[m_1 \int_0^{15.3} x^2 dx + m_2 \int_{15.3}^{21.7} x^2 dx + m_1 \int_{21.7}^{24.8} x^2 dx \right] \qquad (35)$$

Due to the symmetry of the mass about the center, the bending moment vanishes.

Once this torque was included in the theoretical development, the theoretical curve is in excellent agreement with the test data. The CLT with applied torque, T equal to zero is indistinguishable from the SDT and both are presented by the dashed linear curve. This prediction agrees with the test data at low rotation angles and axial loads, however, at higher rotations the linear approximation is no longer valid. This is due to the finite rotation of the end mass. As the mass twists, the resultant load is no longer purely axial as shown in Figure 17 and it induces a torsional moment which tends to return the laminate to the undeformed state. This torsional moment is proportional to $sin(2\theta)$ where θ is the twist angle of the end of the laminate. Upon substitution of T from Equation 35 into Equation 23, the predicted extension-twist coupling becomes a nonlinear function depicted by the solid line in Figure 16. While unsafe for testing to failure, this test method closely

40

simulates a dynamic rotor and is suitable for isolating aeroelastic effects on closed sections.

One redeeming feature of the technique is that the free end condition is identically met. Features that detract from the method are the time consuming balancing process for the test specimen which is of the utmost importance as the assembly is spun up to 3,000 rpm: the danger of the end mass becoming separated from the test specimen at high rpm: a measurement technique that is time consuming and requires special equipment: and the additional torque associated with the end mass distribution that is a function of angle of twist.
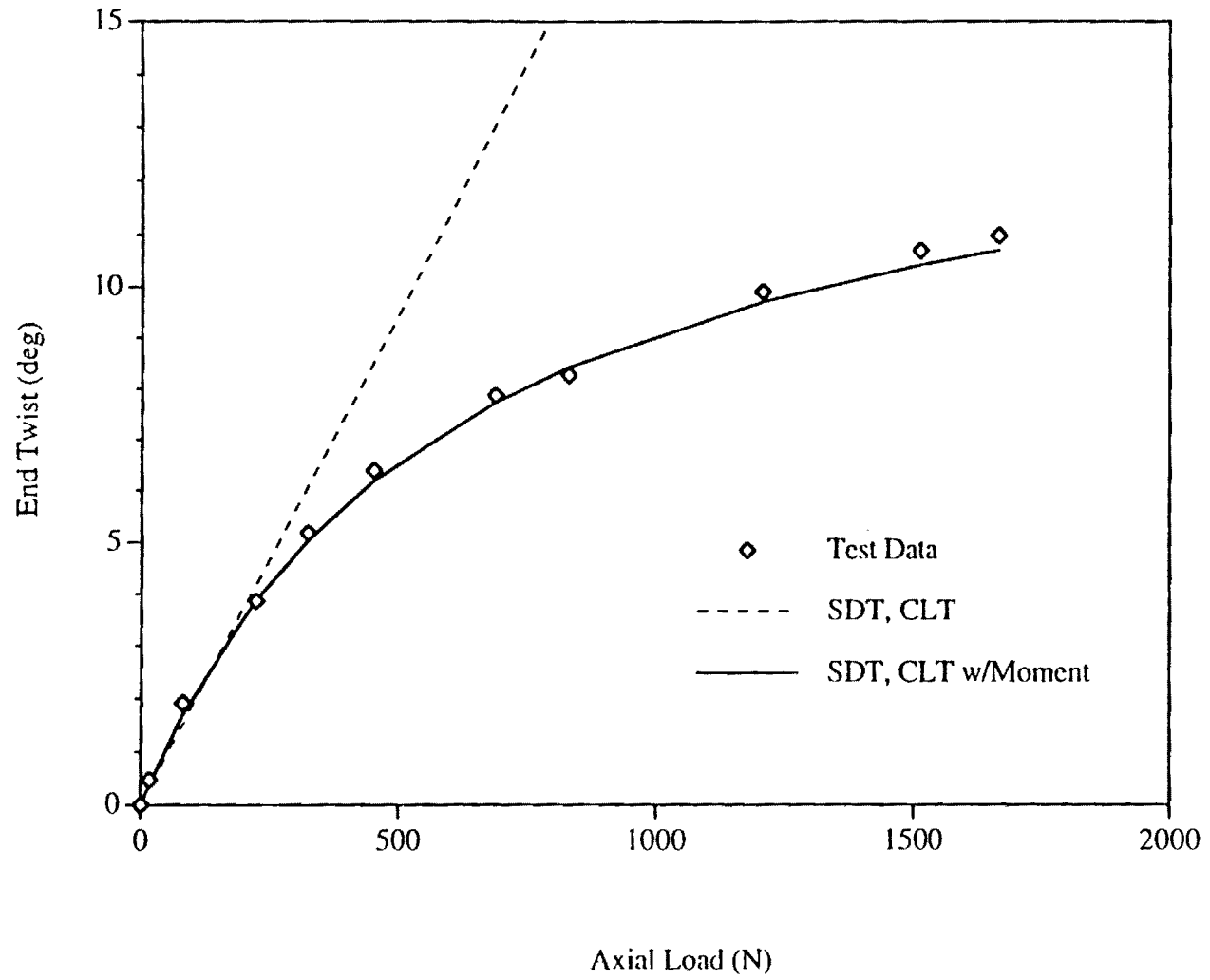
Figure 16. Experimental Results for Rotating Frame Apparatus
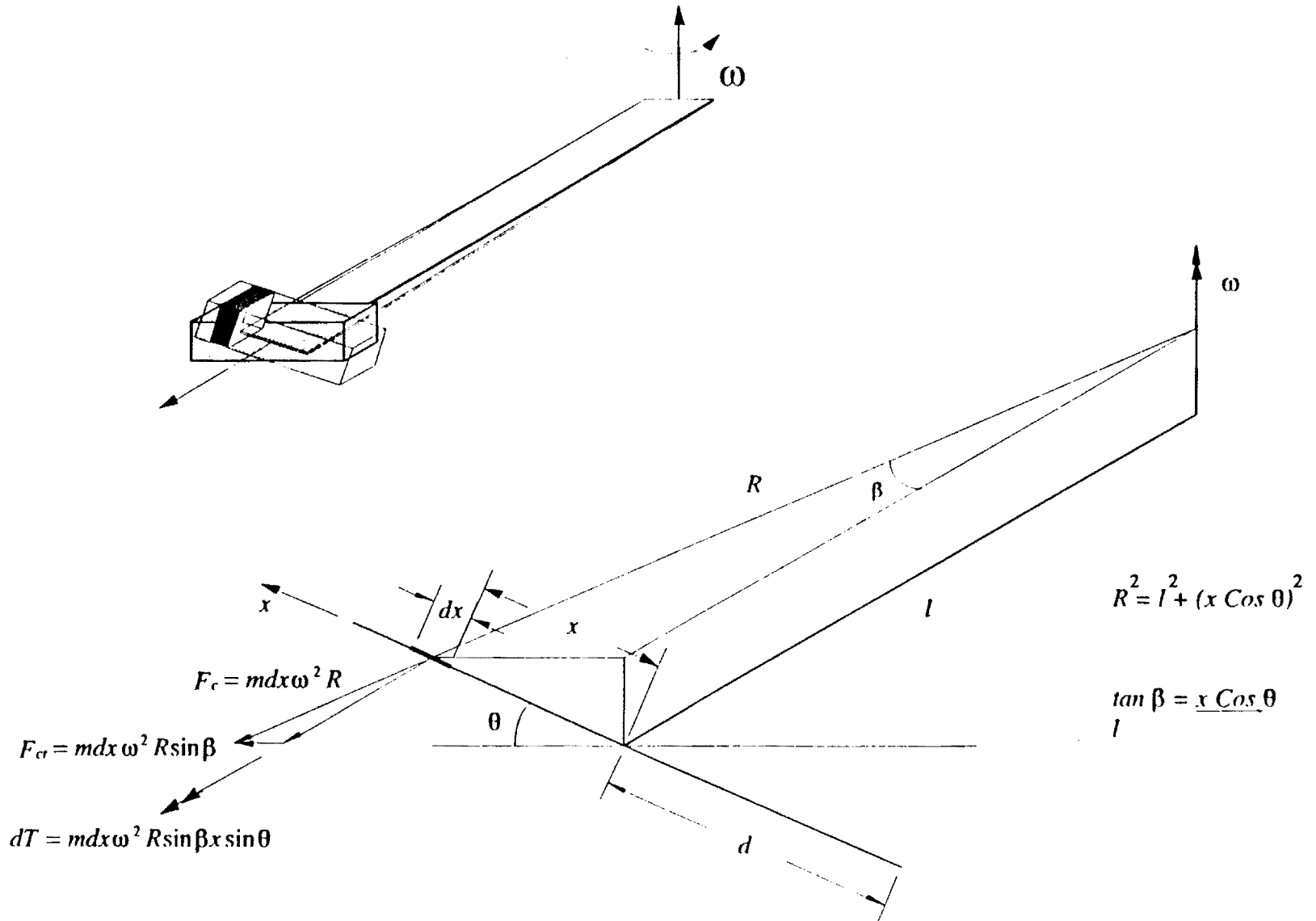
Figure 17. Decomposition of Inertial Forces

$$F_c = mdx\omega^2 R$$

$$F_{ct} = mdx\,\omega^2 R\sin\beta$$

$$dT = mdx\,\omega^2 R\sin\beta\,x\sin\theta$$

$$R^2 = l^2 + (x\,Cos\,\theta)^2$$

$$tan\,\beta = \frac{x\,Cos\,\theta}{l}$$

Air Bearing Apparatus

Results from the test of the evaluation specimen along with the laminated plate theory and FEM results are shown in Figure 18. Data in tabular form is provided in Appendix I. The relative difference between the line of best fit of the test data and the CLT. SDT is 17%. The relative difference for the FEM is 1.7%.
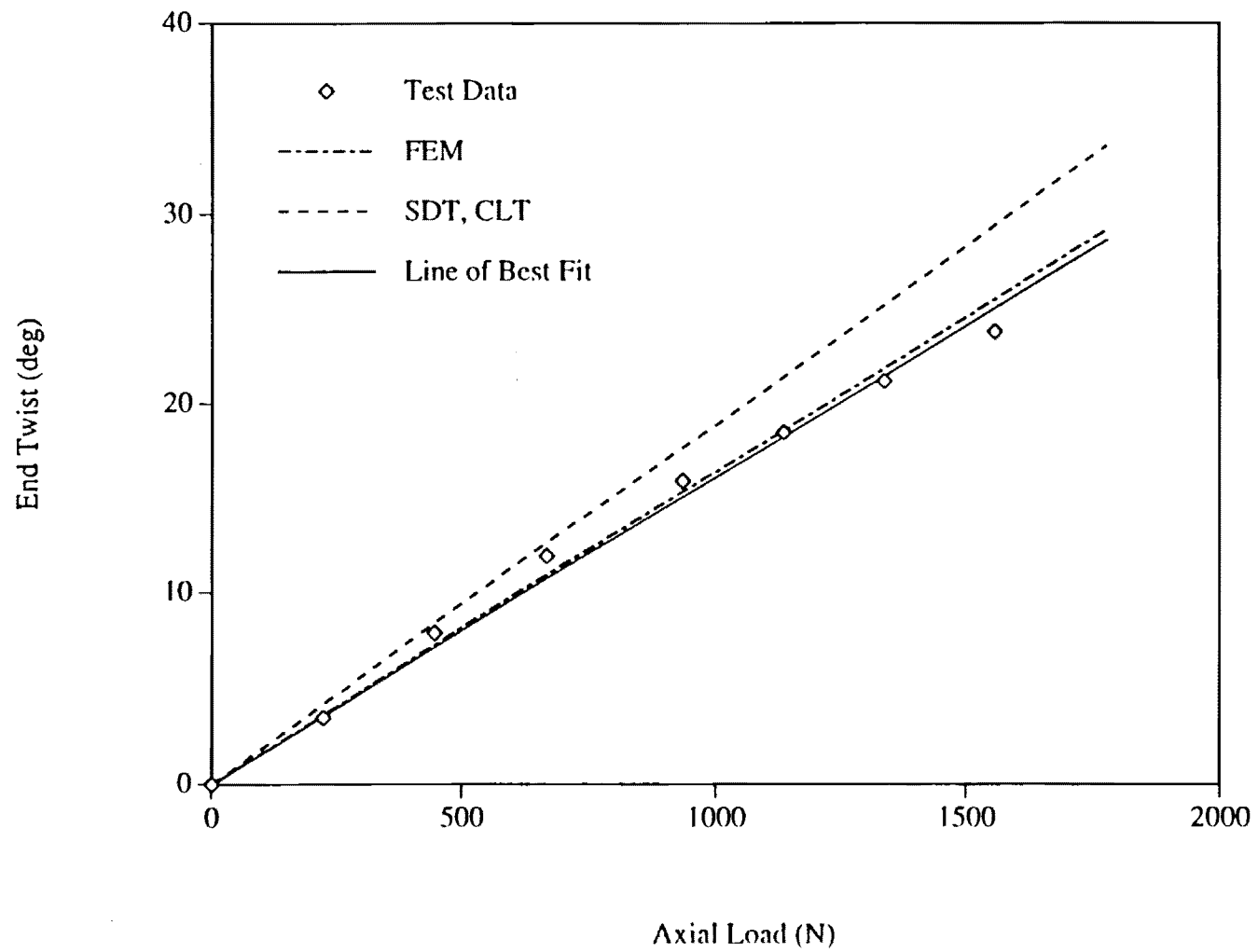
Figure 18. Experimental Results for Air Bearing Apparatus

Comparison of Testing Apparatuses

The experimental results for all the testing apparatuses are shown in Figure 19 with the linear finite element and closed form shear deformation analyses. The shift between the experimental data from the thrust bearing apparatus and the air bearing apparatus can be attributed to the friction of the thrust bearing. The highly nonlinear behavior of the rotating frame apparatus is attributed to inertial effects caused by the end mass distribution during loading. As the laminate twists, the twisting of the end mass results in not only axial load, but a couple which opposes the twist. The result is an apparent increase in stiffness of the laminate.

While a linear fit of the data provides satisfactory results, it is evident that the test specimen responds to the loading in a slightly nonlinear fashion. The nonlinearity is accurately and repeatably observed across tests using the thrust bearing apparatus and the air bearing apparatus. This nonlinear behavior not reported in Nixon[3] or Chandra et al.[5] has been observed for the first time in this work. The most plausible reason is the virtual elimination of friction. Another reason is the torsional rigidity of the laminated strips in comparison to the closed cells used in Refs. 3 and 5. The source of this nonlinearity will be investigated in Chapter VII.

46

40 ⟶ *(y-axis top)*

☐　Test Data (Thrust Bearing)

◇　Test Data (Rotating Frame)

○　Test Data (Air Bearing)

—·—·—　SDT, CLT

— — — —　SDT, CLT w/Friction

— — — —　SDT, CLT w/Moment

············　FEM

End Twist (deg)

Axial Load (N)

47
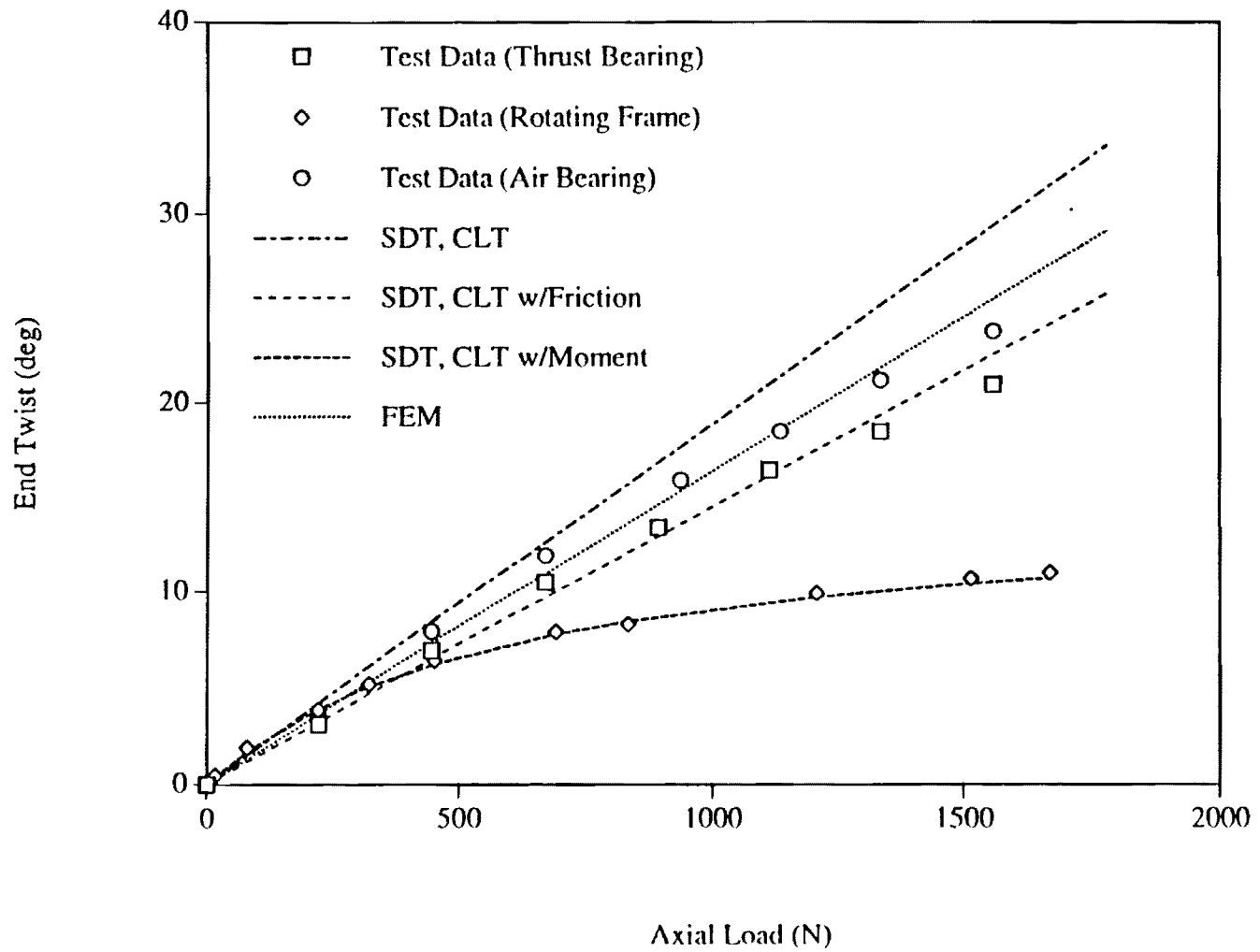
Figure 19. Comparison of Experimental Results for all Testing Apparatuses

CHAPTER VII

INVESTIGATION OF NONLINEAR BEHAVIOR

To confirm that the nonlinearity observed in the experimental data taken from the evaluation test specimen was not due to a manufacturing defect, a new set of laminates was manufactured from a different material system. Two sets of laminates were manufactured with a hygrothermally stable stacking sequence[7] of $\left[\theta/(\theta-90)_2/\theta/-\theta/(90-\theta)_2/-\theta\right]_T$

with $\theta=20°$ for one set and $\theta=30°$ for the other. Each set consisted of four laminates. A T300/954-3 graphite/cyanate system was used. The material properties were measured and are given in Table 2.

Table 2. Material Properties for T300/954-3 Material System

E_{11}	135.5 GPa
E_{22}	9.9 GPa
G_{12}	4.2 GPa
ν_{12}	0.3

After curing, each of the laminates exhibited a pretwist of $0.019°/\text{mm}$ likely due to uneven heating during the curing process. This warping effect has been investigated by Radford[8]. Volume fraction gradients through-the-thickness are a known cause of such warping. The resulting laminates are resin rich at the composite/tool interface and resin

poor at the laminate top surface where bleeding takes place. In an attempt to minimize the initial curvature, several trials were made in which the cure cycle was adjusted. A modified cure cycle, the temperature and pressure profiles of which are presented in Figure 20, was finally adopted. The laminates were trimmed to 298 mm X 25.4 mm X 1.23 mm.

The air bearing apparatus was used to measure the extension-twist coupling. The earlier evaluation of the testing apparatuses showed that the air bearing apparatus had the least influence on the test specimen of all methods. Results of these tests are shown in Figure 21 for the 20° cases and Figure 22 for the 30° cases. The data for each of the four specimens, denoted as Specimens 1-4, are shown in the figure.
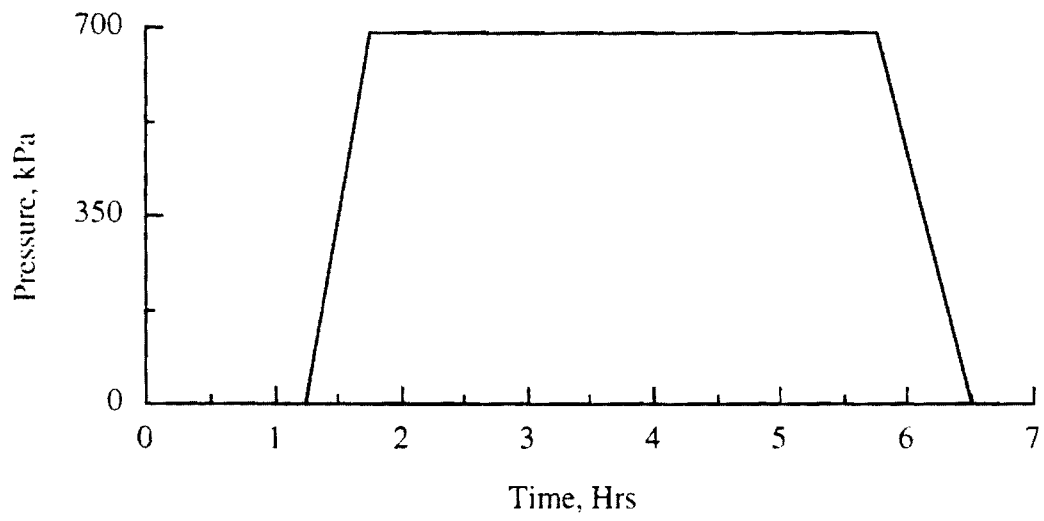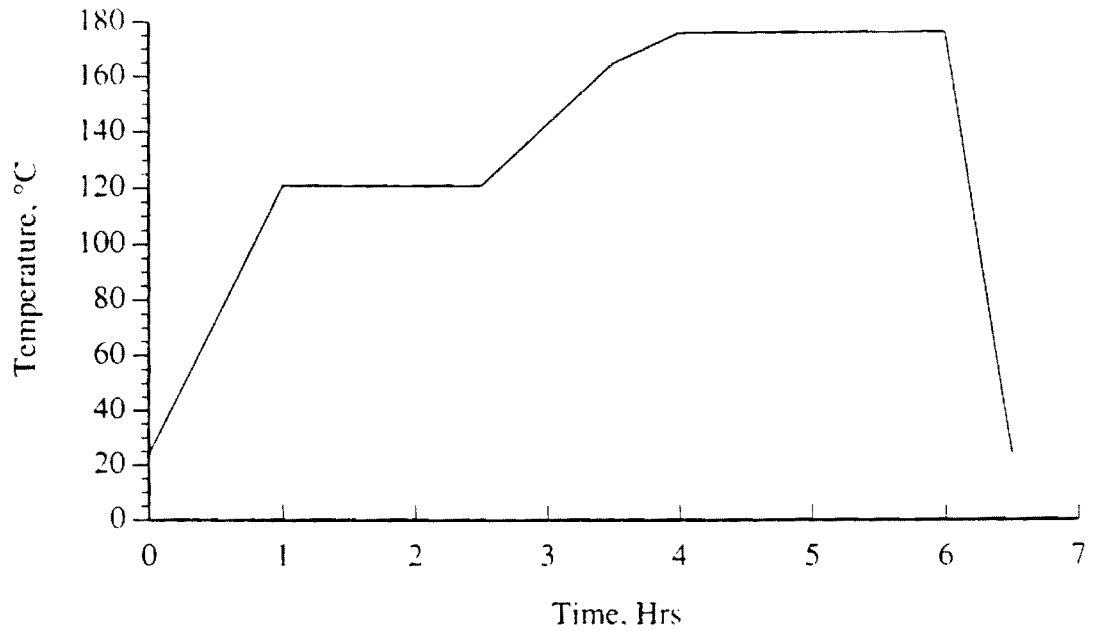
Figure 20. Modified Cure Cycle
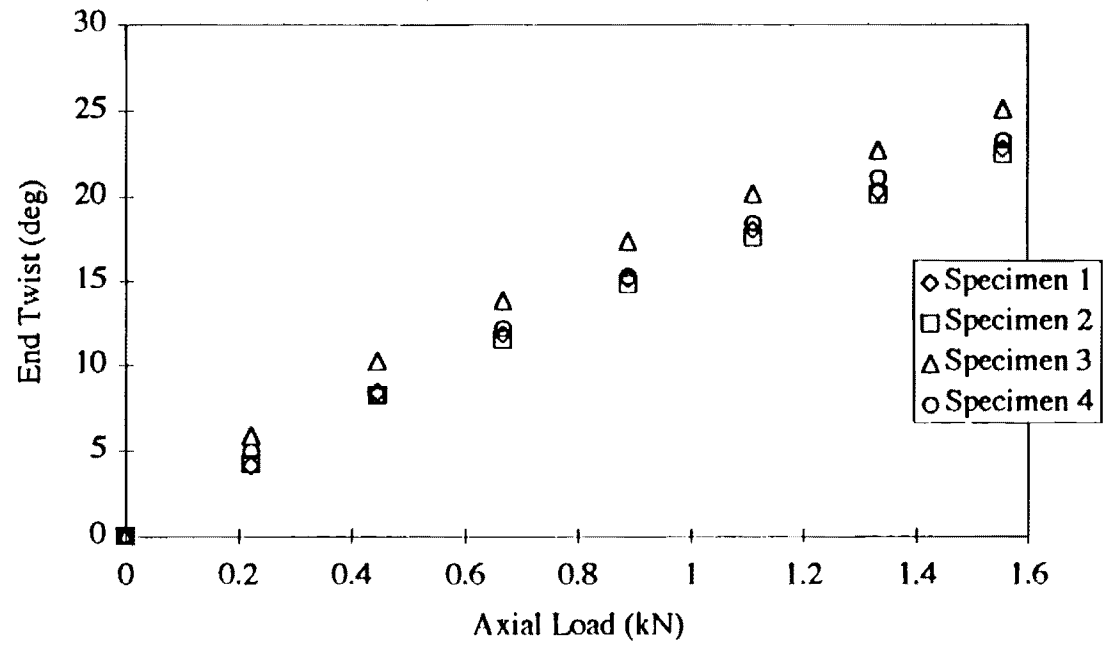
Figure 21. Experimental Results for [20/-70₂/20/-20/70₂/-20] Laminates
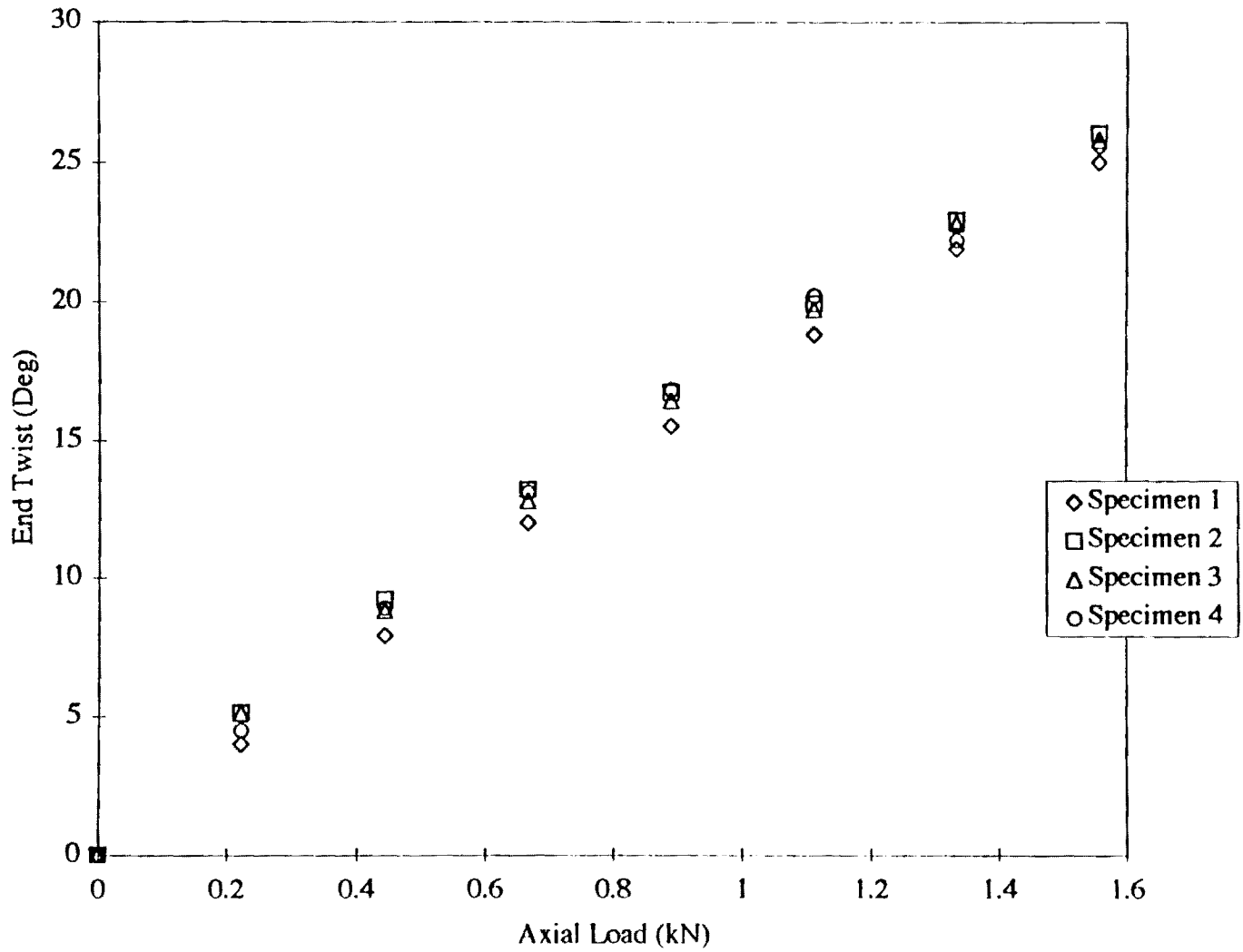
Figure 22. Experimental Results for [30/-60₂/30/-30/60₂/-30] Laminates

Data in tabular form is presented in Appendix 1. Clearly, the response is nonlinear. The nonlinear response may be caused by either a nonlinear material behavior or a nonlinear geometric behavior caused by finite twisting.

An FEM model of the laminate was constructed to investigate the effects of nonlinear geometric behavior. The model consisted of 891 nodes corresponding to 800 quadrilateral shell elements. In the ABAQUS code, this is represented as a S4R element. The analysis was performed using the ABAQUS nonlinear geometric routine. The prescribed end loads were varied from -2.2 kN to 1.65 kN. A negative preloading was applied to obtain the negative pre-twist observed from curing. The curves are then shifted so that the origin of the corrected curve is the point given by the amount of pre-twist on the original curve. This procedure has the advantage of eliminating the computation of the elastic constants along the initially pretwisted material coordinates.

The FEM curves are shown with the experimental data in Figures 23 and 24. The correlation coefficient, r^2, for the FEM solution with the data is 0.983 for the 20° case and 0.993 for the 30° case. It is clear from the FEM analysis that the behavior is geometrically nonlinear. This behavior has been verified in Ref. 9 with a closed form solution. Results including the closed form solution are shown in Figures 25 and 26. The correlation coefficients for the closed form solution are 0.995 and 0.997 for the 20° and 30° cases, respectively.
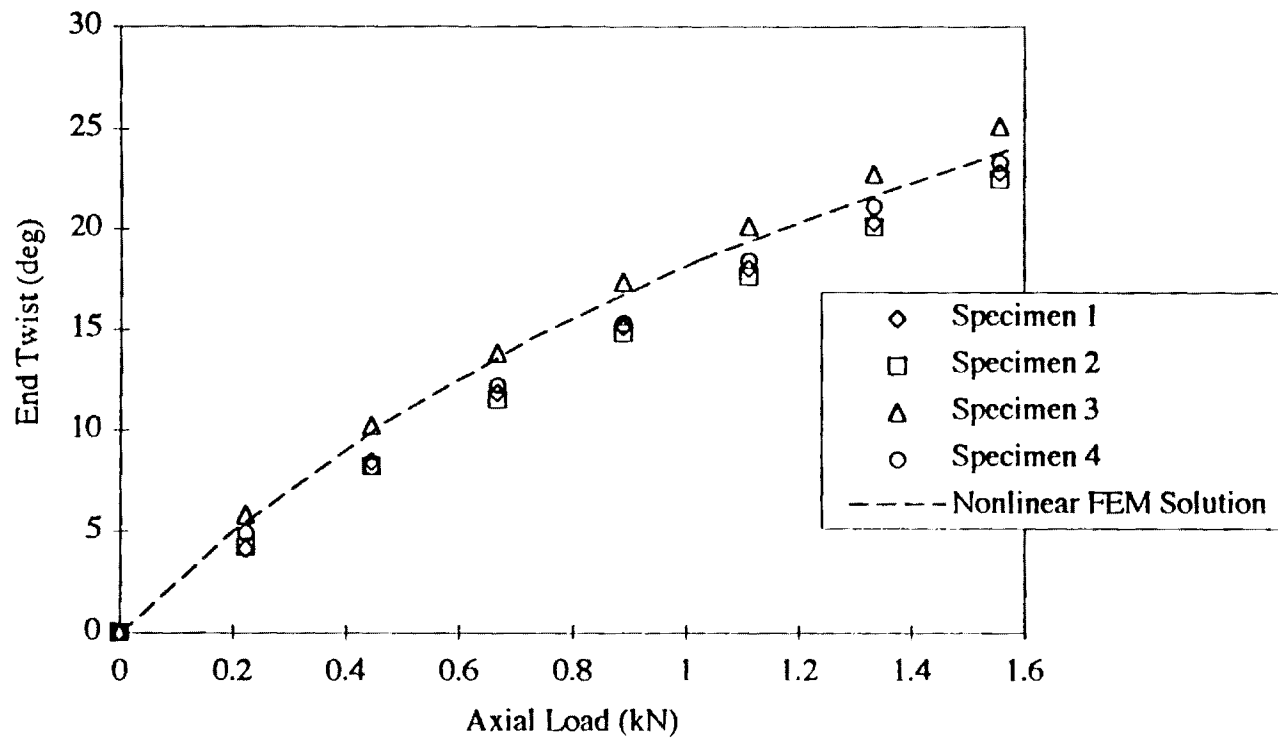
Figure 23. Experimental Results for [20/-70₂/20/-20/70₂/-20] Laminates with FEM
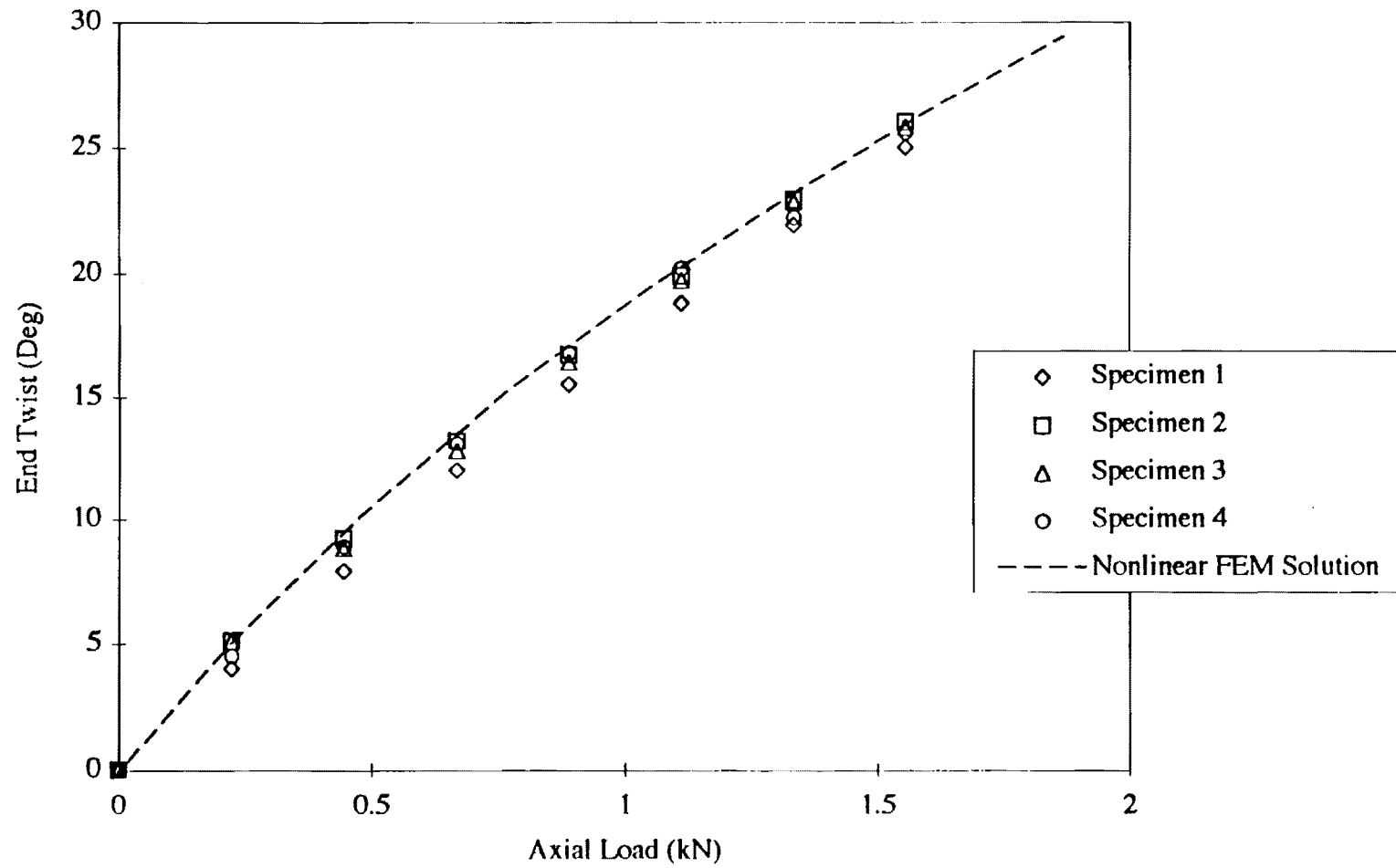
Figure 24. Experimental Results for [30/-60₂/30/-30/60₂/-30] Laminates with FEM
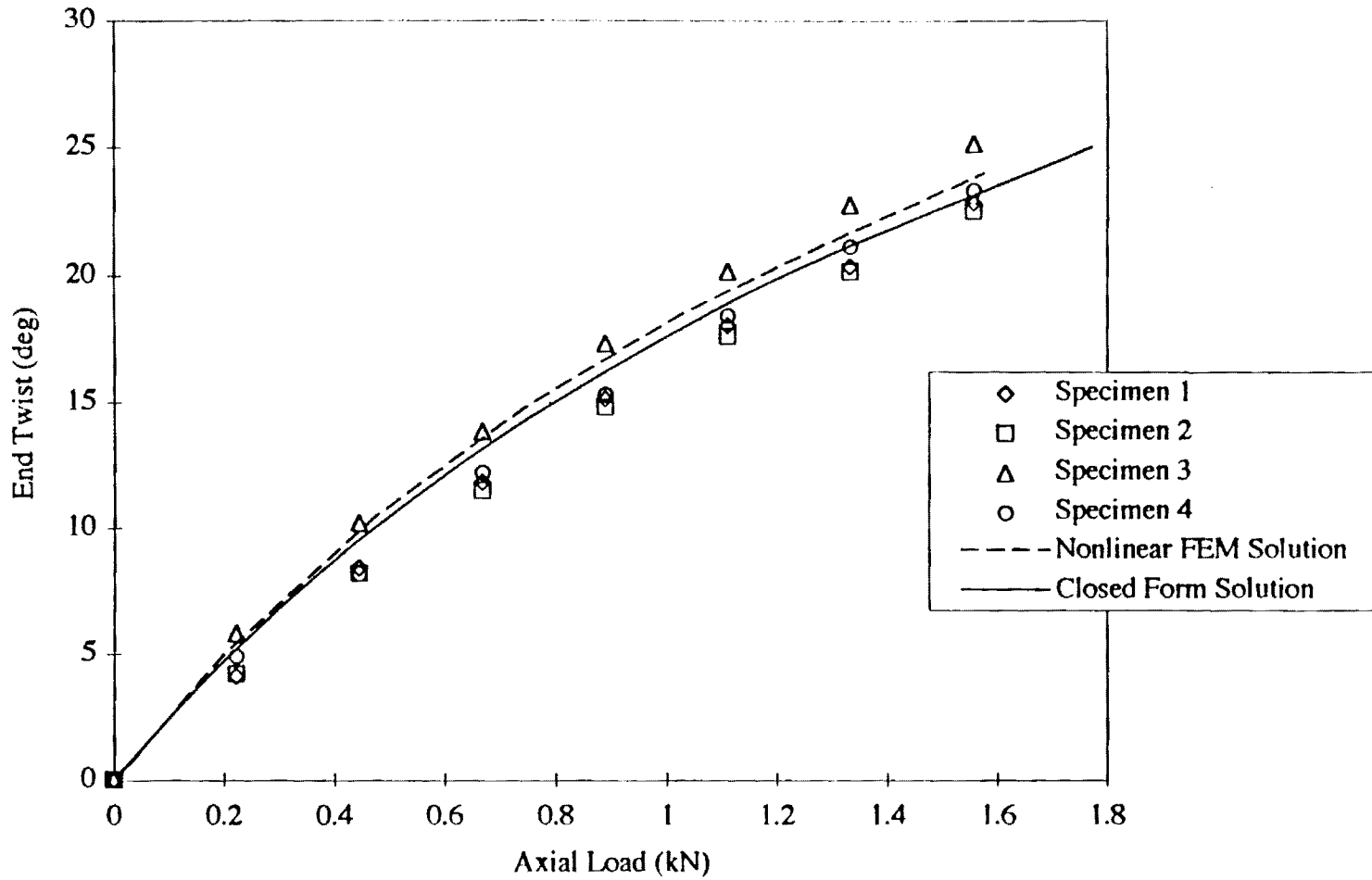
Figure 25. Experimental Results for [20/-70$_2$/20/-20/70$_2$/-20] Laminates with Closed Form Solution and FEM
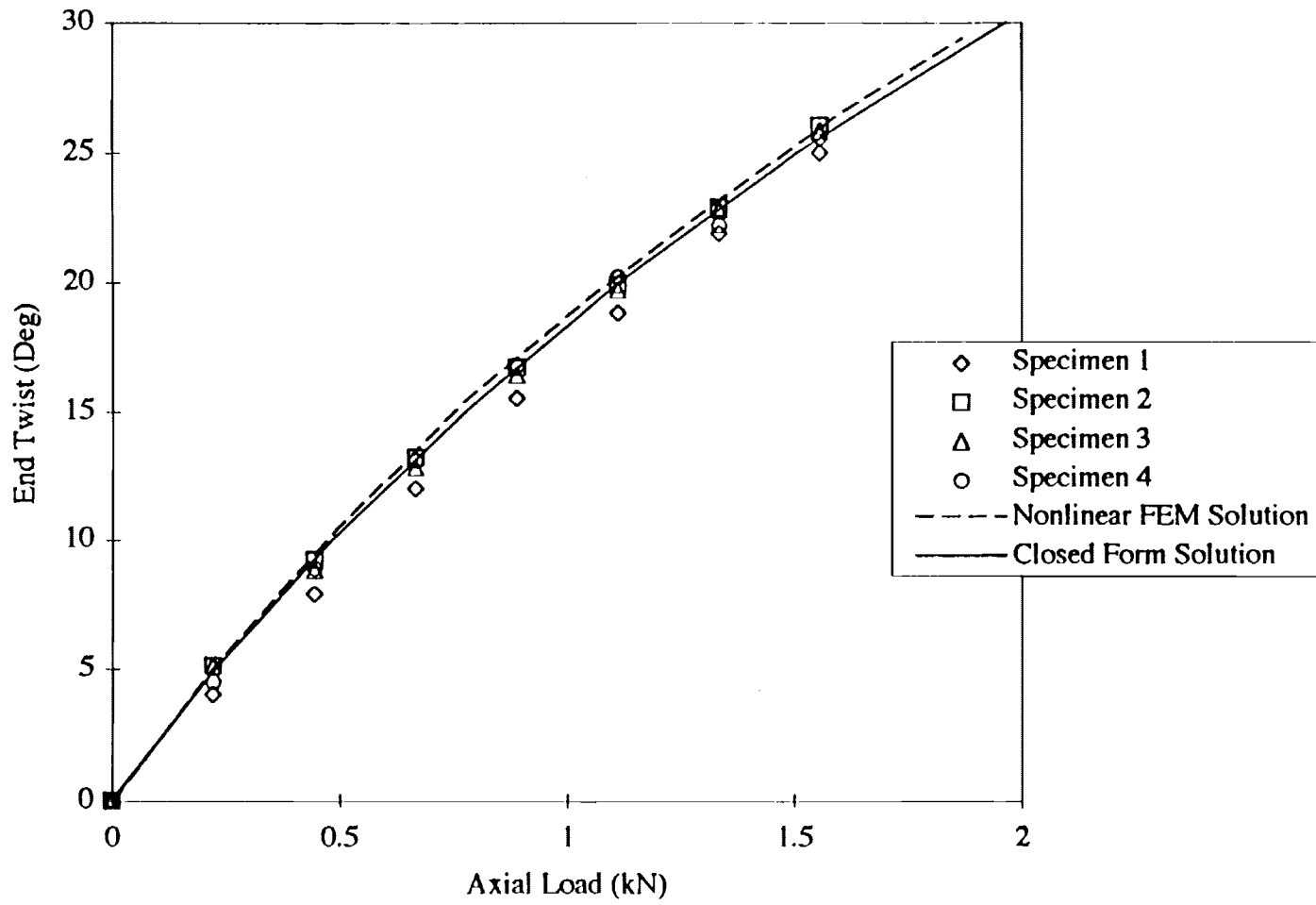
Figure 26. Experimental Results for [30/-60₂/30/-30/60₂/-30] Laminates with Closed Form Solution and FEM

CHAPTER VIII

INVESTIGATION OF ANGLE PLY LAMINATES

The majority of testing was performed on laminates designed to be initially flat and hygrothermally stable. However, there is a set of laminates in the antisymmetric class that exhibit higher extension-twist coupling at the expense of hygrothermal stability. These are the angle ply laminates. A set of three $\left[30_4/-30_4\right]_T$ laminates was manufactured from

T300/954-3 graphite/cyanate with material properties shown in Table 2.

After curing, the initial end twist due to curing stresses was measured. The values were 63.2°, 62.2°, and 64.9° of pretwist with an average value of 63.4°. The final dimensions were 298mm X 25.3mm X 0.56mm. In order to predict the pretwist due to curing stresses, the coefficients of thermal expansion along the material coordinate directions must be measured. One simple approach is to use a thermal-mechanical analyzer (TMA) where 0° and 90° coupons with dimensions of 25.4mm X 6.4mm are cut from unidirectional laminates and heated. The slope of the extension versus temperature curve is measured. The results of this method vary with the location of where the coupons are obtained from the laminate due to local variations in material properties. An alternative method developed in this work accurately accounts for the overall laminate properties. In this method, a 0° laminate and a 90° laminate are each bonded to a piece of steel shim stock with a known coefficient of thermal expansion. The bimaterial strip is then exposed to a change in temperature. The coefficient of thermal expansion for the composite laminate can then be determined using a simple beam theory and the measured tip displacement. A

nonlinear FEM analysis was performed with thermal and axial loading. A temperature decrement of 138°C was first applied in the analysis to represent the cooling process from cure temperature to room temperature and the resulting twist was computed to be 65.8°. The FEM prediction is within 3.6%. Axial load was then incremented in the analysis and end rotations were computed at specific intervals. Test results from the three laminates, FEM results, and the closed form solution[10] are shown in Figure 27. The correlation coefficients are 0.960 and 0.975 for the FEM and closed form solutions, respectively. Experimental data in tabular form is presented in Appendix I. One challenging feature for testing these highly pretwisted laminates is their stability. The closed form analysis in Refs. 9 and 10 indicate that the effective torsional rigidity depends on the axial strain. Therefore, the laminated strips are prone to torsional instability when axial load is applied. This is more significant in angle-ply laminates such as [30/-30] due to their relatively low axial stiffness. To eliminate any compressive preload, the air bearing apparatus was placed at the lower end of the laminate. The repeatability of the data illustrates the ability of the air bearing apparatus to accommodate such highly pretwisted laminates.
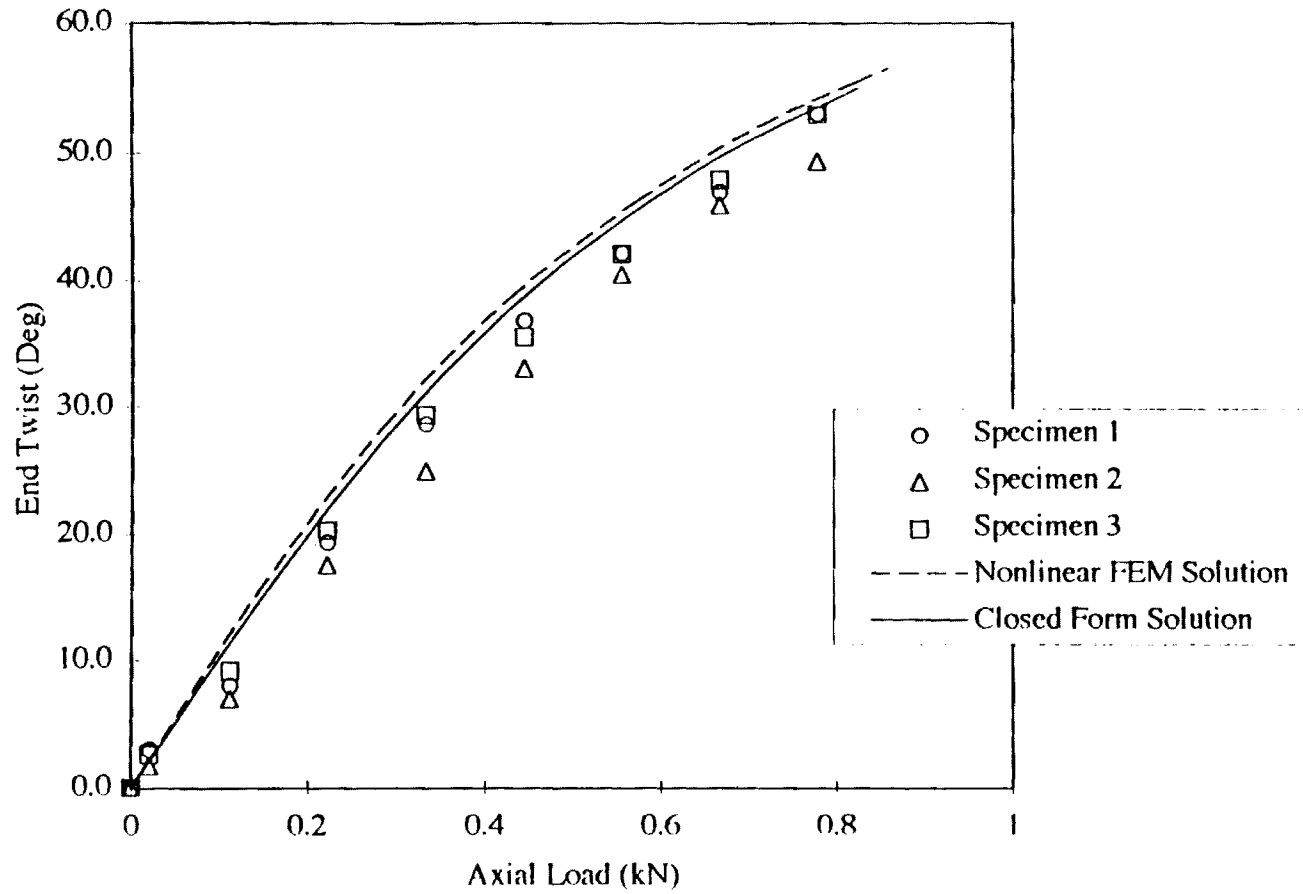
Figure 27. Experimental Results for $[30_4/-30_4]$ Laminates with Closed Form Solution and FEM

CHAPTER IX

CONCLUSIONS AND RECOMMENDATIONS

Three testing apparatuses have been developed to investigate extension-twist coupling in laminated composite strips. The first apparatus made was based on an axial thrust bearing with a linear one-turn potentiometer as a sensing element for twist angle. The device is simple and effective and provides accurate results if the friction is accounted for in theoretical predictions. The second apparatus was designed to eliminate friction altogether by spinning the laminate about one end with a mass attached to the other end. Friction was eliminated, but the mass distribution caused an additional inertial couple that resulted in a nonlinear response. The detrimental effects can be minimized by increasing the length of the test specimen and developing a mass distribution that reduces the inertial couple. This method has promise in studies of elastically tailored rotor blades. A larger test facility could accommodate larger test specimens and aeroelastic effects can be isolated in the vacuum chamber. The final design developed was the patent pending air bearing apparatus. It combines the ease of use of the thrust bearing apparatus with the frictionless nature of the rotating frame apparatus. Comparisons of the test data with FEM and closed form solutions show that if there is frictional resistance, it is inconsequential. The accuracy of this method is higher than the other methods developed and has proven to be reliable throughout all experiments. The three test apparatuses developed in this thesis are the subject of the work in Ref. 11.

The findings of this work point to new directions for further investigation. The recommendations encompass two elements. The first is concerned with improvement of

design of the apparatuses and alternatives. It is recommended that the air bearing apparatus is redesigned so that the operating medium is hydraulic oil. This task would necessitate changes to the shielding of the encoder and gear train on the interior of the apparatus and methods of capturing and reusing the hydraulic oil that is passed through the exit port at the top of the apparatus and through the clearances at the load shaft at the bottom of the apparatus. Adopting oil as the loading medium would allow for closed-loop control of the load using a servovalve and feedback sensors. Smaller piston diameters could also be used as a result of the higher hydraulic pressures available from standard hydraulic pumps. Other designs such as a thin film air bearing with a conical cup-and-cone cross-section could also eliminate the necessity for the lower radial thrust bearings without adding complexity to the design. Another alternative apparatus is a servo-motor controlled transducer that could insure that the zero torque end condition is met by precisely monitoring the torque at the end of the specimen and provide an error single to a controller that, in turn, would control a small motor that would twist the specimen until zero torque was applied. The level of complexity of this type of method is higher, but the benefits would be that testing to very high loads would be posssible. The challenge in this tye of method would be the design of a torsion load cell that could be very sensitive to torque while transmitting very high axial loads. Finally, a magnetic means of applying the axial load may be investigated. Early experiments using this method were not encouraging, however. The key challenges include the uniformity of the magnetic field and the bending rigidity of the laminate.

The second element of the recommendations is concerned with utilization of the air bearing apparatus for further testing. A number of areas need further investigation:

1)   Isolating the influence of free-edge and internal delamination

on extension-twist coupling.

2) Failure testing of extension-twist coupled laminates to establish design allowables.

3) Investigating the bending/torsional instability in elastically tailored laminates.

4) Testing extension-twist coupled closed cells with relatively high torsional rigidity.

In this work, thin elastically tailored strips have been investigated. Thick extension-twist coupled laminates, comparable with those found in flex-beam designs could be manufactured by stacking thin strips. However, an investigation of the durability of such designs is needed.

The results presented in this thesis show the excellent repeatability and accuracy of the test data. It is recommended that future work with these apparatuses include a sensitivity analysis of the parameters associated with a given apparatus to the measurement of load-twist data.

APPENDIX I

DATA IN TABULAR FORM

Table 3. Experimental Data for C30/922 [30/-60$_2$/30/-30/60$_2$/-30] Laminate
Using the Thrust Bearing Apparatus

Load (N)	Twist (deg)
0	0
222	3.1
445	6.9
667	10.5
890	13.4
1112	16.4
1335	18.5
1557	21

Table 4. Experimental Data for C30/922 [30/-60$_2$/30/-30/60$_2$/-30] Laminate
Using the Rotating Frame Apparatus

Load (N)	Twist (deg)
0	0
16.3	.5
79.2	1.9
221	3.9
321	5.2
450	6.4
689	7.9
831	8.3
1206	9.9
1513	10.7
1667	10.9

Table 5. Experimental Data for C30/922 [30/-60$_2$/30/-30/60$_2$/-30] Laminate
Using the Air Bearing Apparatus

Load (N)	Twist (deg)
0	0
222	3.5
445	7.9
667	11.9
934	15.9
1134	18.5
1335	21.2
1557	23.8

65

Table 6. Experimental Results for T300/954-3 [20/-70$_2$/20/-20/70$_2$/-20] Laminates

Load (kN)	Specimen 1 °	Specimen 2 °	Specimen 3 °	Specimen 4 °
0	0	0	0	0
.222	4.1	4.2	5.8	4.9
.445	8.4	8.2	10.2	8.2
.667	11.8	11.5	13.8	12.2
.889	15.1	14.8	17.3	15.3
1.112	18	17.6	20.1	18.4
1.334	20.3	20.1	22.7	21.1
1.557	22.8	22.5	25.1	23.3

Table 7. Analytical Results for T300/954-3 [20/-70$_2$/20/-20/70$_2$/-20] Laminates

FEM Load (kN)	FEM °	Closed Form Load (kN)	Closed Form °
0	0	0	0
.200	5	.214	5
.475	10.5	.473	10
.751	14.8	.798	15
1.026	18.4	1.216	20
1.300	21.3	1.772	25
1.5757	23.9		

Table 8. Experimental Results for T300/954-3 [30/-60$_2$/30/-30/60$_2$/-30] Laminates

Load (kN)	Specimen 1 °	Specimen 2 °	Specimen 3 °	Specimen 4 °
0	0	0	0	0
.222	4	5.1	5.1	4.5
.445	7.9	9.2	8.8	8.9
.667	12	13.2	12.8	13.1
.889	15.5	16.7	16.4	16.8
1.112	18.8	19.9	19.7	20.2
1.334	21.9	22.9	22.8	22.2
1.557	25	26	25.8	25.6

Table 9. Analytical Results for T300/954-3 [30/-60$_2$/30/-30/60$_2$/-30] Laminates

FEM Load (kN)	FEM °	Closed Form Load (kN)	Closed Form °
0	0	0	0
.2217	5	.227	5
.497	10.45	.484	10.0
.772	15.3	.777	15
1.047	19.4	1.114	20
1.322	23.0	1.506	25
1.597	26.4	1.967	30
1.872	29.4		

67

Table 10. Experimental Data for T300/954-3 [30$_4$/-30$_4$] Laminates

Load (kN)	Specimen 1 °	Specimen 2 °	Specimen 3 °
0	0	0	0
.02	3	1.7	2.6
.111	8	7	9.1
.222	19.3	17.5	20.2
.333	28.6	24.9	29.3
.444	36.8	33.0	35.5
.556	42.1	40.4	42.0
.667	46.9	45.9	47.8
.778	53.0	49.3	52.9

Table 11. Analytical Data for T300/954-3 [30$_4$/-30$_4$] Laminates

FEM Load (kN)	FEM °	Closed Form Load (kN)	Closed Form °
0	0	0	0
.143	15.3	.05	5
.286	28.4	.098	10
.429	38.6	.149	15
.572	46.2	.202	20
.715	52.1	.258	25
.858	56.5	.320	30
		.388	35
		.467	40
		.561	45
		.677	50
		.824	55

APPENDIX II

FINITE ELEMENT DATA FILES

Winckler 20° Input File

```
**
**
*HEADING
Extension-Twist Coupled Specimen
Run of 09/09/96
Winckler 20° Case
**
**
*PREPRINT, ECHO=YES, MODEL=NO, HISTORY=NO
**
**
*RESTART, FREQ=1, WRITE
**
**
*NODE
0100, 0.0, -12.600E-3, 0.0
1100, 0.0, 12.600E-3, 0.0
**
*NGEN, NSET=ROOT
0100, 1100, 100
**
**
*NODE
0180, 254.00E-3, -12.600E-3, 0.0
1180, 254.00E-3, 12.600E-3, 0.0
**
*NGEN, NSET=TIP
0180, 1180, 100
**
**
*NFILL, NSET=ALL
ROOT, TIP, 80, 1
**
**
**NSET, NSET=REF1
**0120, 0220, 0320,0420,0520,0620,0720,0820,0920,1020,1120
**
```

```
**
**NSET, NSET=REF2
**0160,  0260,  0360,0460,0560,0660,0760,0860,0960,1060,1160
**
**
*ELEMENT,TYPE=S4R,ELSET=BLADE
0100,  0100,  0101,  0201,  0200
*ELGEN,  ELSET=BLADE
0100,  10,  100,  100,  80,  1,  1
**
**
*BOUNDARY
ROOT,  1,  6
**
**
*MATERIAL,NAME=Carbon
*ELASTIC,TYPE=LAMINA
1.356E11,  9.9E9,  0.30,  4.2E9,  4.2E9,  2.5E9
**
**
*ORIENTATION,  NAME=ThirtyP
1.0,  0.0  ,0.0,  0.0,  1.0,  0.0
3,  30
**
**
*ORIENTATION,  NAME=ThirtyM
1.0,  0.0  ,0.0,  0.0,  1.0,  0.0
3,  -30
**
**
*ORIENTATION,  NAME=SixtyP
1.0,  0.0  ,0.0,  0.0,  1.0,  0.0
3,  60
**
**
*ORIENTATION,  NAME=SixtyM
1.0,  0.0  ,0.0,  0.0,  1.0,  0.0
3,  -60
**
**
*ORIENTATION,  NAME=TwentyP
1.0,  0.0  ,0.0,  0.0,  1.0,  0.0
3,  20
**
**
*ORIENTATION,  NAME=TwentyM
1.0,  0.0  ,0.0,  0.0,  1.0,  0.0
3,  -20
```

```
**
**
*ORIENTATION, NAME=SeventyP
1.0, 0.0 ,0.0, 0.0, 1.0, 0.0
3, 70
**
**
*ORIENTATION, NAME=SeventyM
1.0, 0.0 ,0.0, 0.0, 1.0, 0.0
3, -70
**
**
*ORIENTATION, NAME=Zero
1.0, 0.0 ,0.0, 0.0, 1.0, 0.0
3, 0
**
**
*SHELL SECTION, COMPOSITE, ELSET=BLADE
150.000E-6, 3,Carbon, TwentyP
150.000E-6, 3,Carbon, SeventyM
150.000E-6, 3,Carbon, SeventyM
150.000E-6, 3,Carbon, TwentyP
150.000E-6, 3,Carbon, TwentyM
150.000E-6, 3,Carbon, SeventyP
150.000E-6, 3,Carbon, SeventyP
150.000E-6, 3,Carbon, TwentyM
**
**
*STEP,NLGEOM
*STATIC
*CLOAD
TIP, 1, 25
*EL PRINT, FREQUENCY=0
**
**
*NODE PRINT, NSET=TIP
UR1
**
**
*END STEP
**
**
*STEP
*STATIC
*CLOAD
TIP, 1, 50
*EL PRINT, FREQUENCY=0
**
```

```
**
*NODE PRINT, NSET=TIP
UR1
**
**
*END STEP
**
**
*STEP
*STATIC
*CLOAD
TIP, 1, 75
*EL PRINT, FREQUENCY=0
**
**
*NODE PRINT, NSET=TIP
UR1
**
**
*END STEP
**
**
*STEP
*STATIC
*CLOAD
TIP, 1, 100
*EL PRINT, FREQUENCY=0
**
**
*NODE PRINT, NSET=TIP
UR1
**
**
*END STEP
**
**
*STEP
*STATIC
*CLOAD
TIP, 1, 125
*EL PRINT, FREQUENCY=0
**
**
*NODE PRINT, NSET=TIP
UR1
**
**
*END STEP
```

```
**
**
*STEP
*STATIC
*CLOAD
TIP, 1, 150
*EL PRINT, FREQUENCY=0
**
**
*NODE PRINT, NSET=TIP
UR1
**
**
*END STEP
```

Winckler 20° Output File

1

```
   AAAAAA      BBBBBBBBB     AAAAAA      QQQQQQQQ     U        U    SSSSSSSS
  A      A     B       B    A      A    Q        Q    U        U    S
  A      A     B       B    A      A    Q        Q    U        U    S
  A      A     B       B    A      A    Q        Q    U        U    S
  AAAAAAAAAA   BBBBBBBBB    AAAAAAAAAA  Q        Q    U        U    SSSSSSSS
  A      A     B       B    A      A    Q    Q   Q    U        U            S
  A      A     B       B    A      A    Q     Q  Q    U        U            S
  A      A     B       B    A      A    Q      Q Q    U        U            S
  A      A     BBBBBBBBB    A      A     QQQQQQQQ      UUUUUUUU    SSSSSSSS
                                               Q
```

```
       <|> <|> <|> <|> <|> <|> <|> <|> <|> <|>
       <|> <|> <|> <|> <|> <|> <|>  |   |   |
        |   |   |   |   |   |   |   <|> <|> <|>
       ------------------------------------------
       ------------------------------------------
        |  <|>  |  <|>  |   |  <|> <|> <|> <|>
        |  <|>  |   |   |   |   |  <|> <|> <|>
       <|>  |  <|>  |  <|> <|>  |  <|>  |  <|>
       <|>  |  <|> <|> <|> <|> <|> <|>  |   |
       <|> <|> <|> <|> <|> <|> <|>  |  <|>  |
       <|> <|> <|> <|> <|> <|> <|>  |  <|> <|>
```

73

<|> <|> <|> <|> <|> <|> <|> <|> <|> <|>

THIS PROGRAM HAS BEEN DEVELOPED BY

HIBBITT, KARLSSON AND SORENSEN, INC.
1080 MAIN STREET
PAWTUCKET, R.I. 02860

THIS IS AN ACADEMIC LICENSE OF ABAQUS AND IS MADE
AVAILABLE FOR INTERNAL USE AT GEORGIA INSTITUTE OF TECHNOLOGY.

SUPPORT OF YOUR USAGE IS NOT INCLUDED IN THE LICENSE
PRICE. TO PURCHASE SUPPORT, OR SEND INFORMATION TO HKS
ABOUT A SUSPECTED ERROR, PLEASE FOLLOW THE PROCEDURES
DESCRIBED IN THE ABAQUS ACADEMIC SUPPORT INSTRUCTIONS
DOCUMENT. A COPY OF THIS DOCUMENT HAS BEEN SENT TO THE
DESIGNATED USER AT YOUR SITE. ADDITIONAL COPIES CAN BE
OBTAINED BY CONTACTING HKS OR YOUR LOCAL HKS
REPRESENTATIVE.

SHOULD YOU HAVE ANY QUESTIONS CONCERNING THE TERMS OF
THIS ACADEMIC LICENSE, PLEASE CONTACT THE DESIGNATED
USER AT YOUR UNIVERSITY, DAVID MCDOWELL.

ON MACHINE 7274A507,
YOU ARE AUTHORIZED TO RUN
STANDARD, AQUA, AND POST UNTIL JUNE 30, 1997

YOUR SITE ID IS: 08GIT


```
*  *  *  *  *  *  *  *  *  *  *  *  *  *  *  *  *  *  *  *  *  *  *  *  *  *  *  *  *
*                                                                               *
*                      ******************                                       *
*                      *  N O T I C E  *                                        *
*                      ******************                                       *
*                                                                               *
*                                                                               *
*                 THIS IS ABAQUS VERSION 5.5-1                                   *
*                                                                               *
*                                                                               *
*   PLEASE MAKE SURE YOU ARE USING VERSION 5.5 MANUALS                           *
*   PLUS THE NOTES ACCOMPANYING THIS RELEASE. THESE NOTES                        *
*   CAN BE OBTAINED BY USING THE INFORMATION OPTION ON THE                       *
*   ABAQUS COMMAND LINE.                                                         *
*                                                                               *
```

```
   *RESTART, FREQ=1, WRITE
1
```

   ABAQUS VERSION 5.5-1   DATE 10-SEP-96   TIME
22:59:21   PAGE   2
   FOR USE AT GEORGIA INSTITUTE OF TECHNOLOGY UNDER ACADEMIC LICENSE FROM HKS, INC.

                                     A B A Q U S   I N P U T   E C H O

                           5   10   15   20   25   30   35   40   45   50   55   60   65
70   75   80

                           **
                           **
                     *HEADING
                     Extension-Twist Coupled Specimen
        CARD   5   Run of 09/09/96
                     DWP Thesis Data
                           **
                           **
                     *PREPRINT, ECHO=YES, MODEL=NO, HISTORY=NO
        CARD   10   **
                           **
                     *RESTART, FREQ=1, WRITE
                           **
                           **
        CARD   15   *NODE
                     0100, 0.0, -12.600E-3, 0.0
                     1100, 0.0, 12.600E-3, 0.0
                           **
                     *NGEN, NSET=ROOT
        CARD   20   0100, 1100, 100
                           **
                           **
                     *NODE
                     0180, 254.00E-3, -12.600E-3, 0.0
        CARD   25   1180, 254.00E-3, 12.600E-3, 0.0
                           **
                     *NGEN, NSET=TIP
                     0180, 1180, 100
```

```
                    **
CARD    30          **
                    *NFILL, NSET=ALL
                    ROOT, TIP, 80, 1
                    **
                    **
CARD    35          **NSET, NSET=REF1
                    **0120, 0220, 0320,0420,0520,0620,0720,0820,0920,1020,1120
                    **
                    **
                    **NSET, NSET=REF2
CARD    40          **0160, 0260, 0360,0460,0560,0660,0760,0860,0960,1060,1160
                    **
                    **
                    *ELEMENT,TYPE=S4R,ELSET=BLADE
                    0100, 0100, 0101, 0201, 0200
CARD    45          *ELGEN, ELSET=BLADE
                    0100, 10, 100, 100, 80, 1, 1
                    **
                    **
                    *BOUNDARY
CARD    50          ROOT, 1, 6
                    **
                    **
                    *MATERIAL,NAME=Carbon
                    *ELASTIC,TYPE=LAMINA
CARD    55          1.356E11, 9.9E9, 0.30, 4.2E9, 4.2E9, 2.5E9
                    **
                    **
                    *ORIENTATION, NAME=ThirtyP
                    1.0, 0.0 ,0.0, 0.0, 1.0, 0.0
CARD    60          3, 30
                    **
                    **
                    *ORIENTATION, NAME=ThirtyM
                    1.0, 0.0 ,0.0, 0.0, 1.0, 0.0
CARD    65          3, -30
                    **
                    **
                    *ORIENTATION, NAME=SixtyP
                    1.0, 0.0 ,0.0, 0.0, 1.0, 0.0
CARD    70          3, 60
                    **
                    **
                    *ORIENTATION, NAME=SixtyM
                    1.0, 0.0 ,0.0, 0.0, 1.0, 0.0
CARD    75          3, -60
                    **
                    **
                    *ORIENTATION, NAME=TwentyP
                    1.0, 0.0 ,0.0, 0.0, 1.0, 0.0
CARD    80          3, 20
```

```
              **
              **
              *ORIENTATION, NAME=TwentyM
              1.0, 0.0 ,0.0, 0.0, 1.0, 0.0
CARD    85    3, -20
              **
              **
              *ORIENTATION, NAME=SeventyP
              1.0, 0.0 ,0.0, 0.0, 1.0, 0.0
CARD    90    3, 70
              **
              **
              *ORIENTATION, NAME=SeventyM
              1.0, 0.0 ,0.0, 0.0, 1.0, 0.0
CARD    95    3, -70
              **
              **
              *ORIENTATION, NAME=Zero
              1.0, 0.0 ,0.0. 0.0, 1.0, 0.0
CARD    100   3, 0
              **
              **
              *SHELL SECTION, COMPOSITE, ELSET=BLADE
              150.000E-6, 3,Carbon, TwentyP
CARD    105   150.000E-6, 3,Carbon, SeventyM
              150.000E-6, 3,Carbon, SeventyM
              150.000E-6, 3,Carbon, TwentyP
              150.000E-6, 3,Carbon, TwentyM
              150.000E-6, 3,Carbon, SeventyP
CARD    110   150.000E-6, 3,Carbon, SeventyP
              150.000E-6, 3,Carbon, TwentyM
              **
              **
              *STEP,NLGEOM
CARD    115   *STATIC
              *CLOAD
              TIP, 1, 25
              *EL PRINT, FREQUENCY=0
              **
CARD    120   **
              *NODE PRINT, NSET=TIP
              UR1
              **
              **
CARD    125   *END STEP
              **
              **
              *STEP
              *STATIC
CARD    130   *CLOAD
              TIP, 1, 50
              *EL PRINT, FREQUENCY=0
```

```
               **
               **
CARD   135     *NODE PRINT, NSET=TIP
               UR1
               **
               **
               *END STEP
CARD   140     **
               **
               *STEP
               *STATIC
               *CLOAD
CARD   145     TIP, 1, 75
               *EL PRINT, FREQUENCY=0
               **
               **
               *NODE PRINT, NSET=TIP
CARD   150     UR1
               **
               **
               *END STEP
               **
CARD   155     **
               *STEP
               *STATIC
               *CLOAD
               TIP, 1, 100
CARD   160     *EL PRINT, FREQUENCY=0
               **
               **
               *NODE PRINT, NSET=TIP
               UR1
CARD   165     **
               **
               *END STEP
               **
               **
CARD   170     *STEP
               *STATIC
               *CLOAD
               TIP, 1, 125
               *EL PRINT, FREQUENCY=0
CARD   175     **
               **
               *NODE PRINT, NSET=TIP
               UR1
               **
CARD   180     **
               *END STEP
               **
               **
               *STEP
```

78

```
        CARD    185      *STATIC
                         *CLOAD
                         TIP, 1, 150
                         *EL PRINT, FREQUENCY=0
                         **
        CARD    190      **
                         *NODE PRINT, NSET=TIP
                         UR1
                         **
                         **
        CARD    195      *END STEP
```

```
        -------------------------------------------------------------
-------------
                   5    10   15   20   25   30   35   40   45   50   55   60   65
70   75   80
        -------------------------------------------------------------
-------------
```

        OPTIONS BEING PROCESSED
        ****

***WARNING: ALL CARDS BEFORE THE FIRST KEYWORD CARD ARE IGNORED
 *HEADING
          Extension-Twist Coupled Specimen
          Run of 09/09/96
          DWP Thesis Data
 *NODE
 *NGEN, NSET=ROOT
 *NODE
 *NGEN, NSET=TIP
 *NFILL, NSET=ALL
 *ELEMENT,TYPE=S4R,ELSET=BLADE
 *ELGEN, ELSET=BLADE
 *MATERIAL,NAME=Carbon
 *ELASTIC,TYPE=LAMINA
 *ORIENTATION, NAME=ThirtyP
 *ORIENTATION, NAME=ThirtyM
 *ORIENTATION, NAME=SixtyP
 *ORIENTATION, NAME=SixtyM
 *ORIENTATION, NAME=TwentyP
 *ORIENTATION, NAME=TwentyM
 *ORIENTATION, NAME=SeventyP
 *ORIENTATION, NAME=SeventyM
 *ORIENTATION, NAME=Zero
 *SHELL SECTION, COMPOSITE, ELSET=BLADE
 *SHELL SECTION, COMPOSITE, ELSET=BLADE
 *STEP,NLGEOM

79

```
*STATIC
*EL PRINT, FREQUENCY=0
*END STEP
*STEP
*STATIC
*EL PRINT, FREQUENCY=0
*END STEP

***WARNING: THE NLGEOM FLAG IS ACTIVATED BECAUSE IT WAS ACTIVE IN THE PREVIOUS
            STEP.
*STEP
*STATIC
*EL PRINT, FREQUENCY=0
*END STEP

***WARNING: THE NLGEOM FLAG IS ACTIVATED BECAUSE IT WAS ACTIVE IN THE PREVIOUS
            STEP.
*STEP
*STATIC
*EL PRINT, FREQUENCY=0
*END STEP

***WARNING: THE NLGEOM FLAG IS ACTIVATED BECAUSE IT WAS ACTIVE IN THE PREVIOUS
            STEP.
*STEP
*STATIC
*EL PRINT, FREQUENCY=0
*END STEP

***WARNING: THE NLGEOM FLAG IS ACTIVATED BECAUSE IT WAS ACTIVE IN THE PREVIOUS
            STEP.
*STEP
*STATIC
*EL PRINT, FREQUENCY=0
*END STEP

***WARNING: THE NLGEOM FLAG IS ACTIVATED BECAUSE IT WAS ACTIVE IN THE PREVIOUS
            STEP.
*BOUNDARY
*STEP,NLGEOM
*STATIC
*CLOAD
*NODE PRINT, NSET=TIP
*END STEP
*STEP
*STATIC
*CLOAD
*NODE PRINT, NSET=TIP
*END STEP
*STEP
*STATIC
*CLOAD
```

```
*NODE PRINT, NSET=TIP
*END STEP
*STEP
*STATIC
*CLOAD
*NODE PRINT, NSET=TIP
*END STEP
*STEP
*STATIC
*CLOAD
*NODE PRINT, NSET=TIP
*END STEP
*STEP
*STATIC
*CLOAD
*NODE PRINT, NSET=TIP
*END STEP
```

W A V E F R O N T   M I N I M I Z A T I O N

NUMBER OF NODES   891
NUMBER OF ELEMENTS   800
ORIGINAL MAXIMUM D.O.F WAVEFRONT ESTIMATED AS   498
ORIGINAL RMS D.O.F WAVEFRONT ESTIMATED AS   452

PERIPHERAL DIAMETER IS DEFINED BY NODES   100   580

WAVEFRONT OPTIMIZED BY CHOOSING   180 AS THE STARTING NODE

MINIMUM WAVEFRONT OBTAINED USING METHOD 1.   USE
*WAVEFRONT MINIMIZATION, NODES, METHOD=1
     100,   580
TO REDUCE THE CPU TIME ON SUBSEQUENT JOBS USING THIS SAME MESH.

P R O B L E M   S I Z E

NUMBER OF ELEMENTS IS   800
NUMBER OF NODES IS   891
NUMBER OF NODES DEFINED BY THE USER   891
TOTAL NUMBER OF VARIABLES IN THE MODEL   5346
(DEGREES OF FREEDOM PLUS ANY LAGRANGE MULTIPLIER VARIABLES)
MAXIMUM D.O.F. WAVEFRONT ESTIMATED AS   78
RMS WAVEFRONT ESTIMATED AS   78

FILE SIZES - THESE VALUES ARE CONSERVATIVE UPPER BOUNDS

    UNIT   WORDS   MEGABYTES

81

```
        21        603200         4.83
        22        603200         4.83
     -------      ----------     ----------
     TOTAL        1206400         9.65


        IF THE RESTART FILE IS WRITTEN ITS LENGTH WILL BE APPROXIMATELY

                                                          WORDS     MEGABYTES
                                                          ----------  ----------
        WRITTEN IN THE ANALYSIS PREPROCESSOR              133654        1.07
        PLUS WRITTEN AT THE BEGINNING OF EACH STEP         80080        0.64
        PLUS FOR EACH INCREMENT WRITTEN TO THE RESTART FILE  710617      5.68



        ALLOCATED WORKSPACE                                1371681




                            END OF USER INPUT PROCESSING



        JOB TIME SUMMARY
          USER TIME   =   6.9900
          SYSTEM TIME =   1.0400
          TOTAL TIME  =   8.0300
   1
```

```
     Extension-Twist Coupled Specimen
STEP    1  INCREMENT    1

TIME COMPLETED IN THIS STEP     0.


               S T E P      1     S T A T I C    A N A L Y S I S



        AUTOMATIC TIME CONTROL WITH -
             A SUGGESTED INITIAL TIME INCREMENT OF          1.00
             AND A TOTAL TIME PERIOD OF                     1.00
             THE MINIMUM TIME INCREMENT ALLOWED IS          1.000E-05
             THE MAXIMUM TIME INCREMENT ALLOWED IS          1.00

             LARGE DISPLACEMENT THEORY WILL BE USED
```

INCREMENT   1 SUMMARY

TIME INCREMENT COMPLETED   1.00   , FRACTION OF STEP COMPLETED   1.00
STEP TIME COMPLETED   1.00   , TOTAL TIME COMPLETED   1.00

N O D E   O U T P U T

THE FOLLOWING TABLE IS PRINTED FOR NODESET   TIP

   NODE FOOT-   UR1
        NOTE

    180   -9.2306E-02
    280   -9.2585E-02
    380   -9.1905E-02
    480   -9.2525E-02
    580   -9.1721E-02
    680   -9.2486E-02
    780   -9.1721E-02
    880   -9.2525E-02
    980   -9.1905E-02
   1080   -9.2585E-02
   1180   -9.2306E-02

MAXIMUM   -9.1721E-02
AT NODE   780

MINIMUM   -9.2585E-02
AT NODE   1080
1

   ABAQUS VERSION 5.5-1   DATE 10-SEP-96   TIME
22:59:34   PAGE   2
   FOR USE AT GEORGIA INSTITUTE OF TECHNOLOGY UNDER ACADEMIC LICENSE FROM HKS, INC.

     Extension-Twist Coupled Specimen
STEP   2 INCREMENT   1

TIME COMPLETED IN THIS STEP   0.

              S T E P   2   S T A T I C   A N A L Y S I S

AUTOMATIC TIME CONTROL WITH -
          A SUGGESTED INITIAL TIME INCREMENT OF   1.00
          AND A TOTAL TIME PERIOD OF   1.00
          THE MINIMUM TIME INCREMENT ALLOWED IS   1.000E-05
          THE MAXIMUM TIME INCREMENT ALLOWED IS   1.00

          LARGE DISPLACEMENT THEORY WILL BE USED

                          INCREMENT   1 SUMMARY

TIME INCREMENT COMPLETED   1.00   , FRACTION OF STEP COMPLETED   1.00
STEP TIME COMPLETED   1.00   , TOTAL TIME COMPLETED   2.00

                     N O D E   O U T P U T

THE FOLLOWING TABLE IS PRINTED FOR NODESET   TIP

    NODE FOOT-   UR1
         NOTE

     180   -0.1699
     280   -0.1704
     380   -0.1690
     480   -0.1702
     580   -0.1685
     680   -0.1701
     780   -0.1685
     880   -0.1702
     980   -0.1690
    1080   -0.1704
    1180   -0.1699

MAXIMUM   -0.1685
AT NODE   580

MINIMUM   -0.1704
AT NODE   1080
1

Extension-Twist Coupled Specimen
STEP   3   INCREMENT   1

TIME COMPLETED IN THIS STEP   0.

                        S T E P   3   S T A T I C   A N A L Y S I S

        AUTOMATIC TIME CONTROL WITH -
                A SUGGESTED INITIAL TIME INCREMENT OF   1.00
                AND A TOTAL TIME PERIOD OF   1.00
                THE MINIMUM TIME INCREMENT ALLOWED IS   1.000E-05
                THE MAXIMUM TIME INCREMENT ALLOWED IS   1.00

        LARGE DISPLACEMENT THEORY WILL BE USED

                        INCREMENT   1 SUMMARY

TIME INCREMENT COMPLETED   1.00   ,   FRACTION OF STEP COMPLETED   1.00
STEP TIME COMPLETED   1.00   ,   TOTAL TIME COMPLETED   3.00

                        N O D E   O U T P U T

    THE FOLLOWING TABLE IS PRINTED FOR NODESET   TIP

    NODE FOOT-   UR1
         NOTE

        180   -0.2235
        280   -0.2244
        380   -0.2222
        480   -0.2241
        580   -0.2213
        680   -0.2238
        780   -0.2213
        880   -0.2241
        980   -0.2222
       1080   -0.2244
       1180   -0.2235

                                85

```
MAXIMUM       -0.2213
AT NODE        780

MINIMUM       -0.2244
AT NODE       1080
1
```

    Extension-Twist Coupled Specimen
STEP   4 INCREMENT   1

TIME COMPLETED IN THIS STEP   0.

                     S T E P   4   S T A T I C   A N A L Y S I S

         AUTOMATIC TIME CONTROL WITH -
             A SUGGESTED INITIAL TIME INCREMENT OF   1.00
             AND A TOTAL TIME PERIOD OF   1.00
             THE MINIMUM TIME INCREMENT ALLOWED IS   1.000E-05
             THE MAXIMUM TIME INCREMENT ALLOWED IS   1.00

         LARGE DISPLACEMENT THEORY WILL BE USED

                        INCREMENT   1 SUMMARY

TIME INCREMENT COMPLETED   1.00   , FRACTION OF STEP COMPLETED   1.00
STEP TIME COMPLETED   1.00   , TOTAL TIME COMPLETED   4.00

                        N O D E   O U T P U T

    THE FOLLOWING TABLE IS PRINTED FOR NODESET   TIP

      NODE FOOT-   UR1
           NOTE

       180   -0.2797

```
280      -0.2809
380      -0.2778
480      -0.2803
580      -0.2766
680      -0.2800
780      -0.2766
880      -0.2803
980      -0.2778
1080     -0.2809
1180     -0.2797


MAXIMUM   -0.2766
AT NODE      780


MINIMUM   -0.2809
AT NODE      280
1
```

ABAQUS VERSION 5.5-1   DATE 10-SEP-96   TIME
22:59:34   PAGE   5
  FOR USE AT GEORGIA INSTITUTE OF TECHNOLOGY UNDER ACADEMIC LICENSE FROM HKS, INC.

    Extension-Twist Coupled Specimen
STEP   5 INCREMENT   1

TIME COMPLETED IN THIS STEP   0.

                  S T E P   5   S T A T I C   A N A L Y S I S

        AUTOMATIC TIME CONTROL WITH -
              A SUGGESTED INITIAL TIME INCREMENT OF   1.00
              AND A TOTAL TIME PERIOD OF   1.00
              THE MINIMUM TIME INCREMENT ALLOWED IS   1.000E-05
              THE MAXIMUM TIME INCREMENT ALLOWED IS   1.00

        LARGE DISPLACEMENT THEORY WILL BE USED

                        INCREMENT   1 SUMMARY

TIME INCREMENT COMPLETED   1.00   , FRACTION OF STEP COMPLETED   1.00
STEP TIME COMPLETED   1.00   , TOTAL TIME COMPLETED   5.00

                        N O D E   O U T P U T

                                 87

THE FOLLOWING TABLE IS PRINTED FOR NODESET   TIP

    NODE FOOT-   UR1
         NOTE

     180   -0.3264
     280   -0.3279
     380   -0.3240
     480   -0.3271
     580   -0.3223
     680   -0.3266
     780   -0.3223
     880   -0.3271
     980   -0.3240
    1080   -0.3279
    1180   -0.3264

 MAXIMUM   -0.3223
 AT NODE   780

 MINIMUM   -0.3279
 AT NODE   1080
1

    ABAQUS VERSION 5.5-1   DATE 10-SEP-96   TIME
22:59:34   PAGE   6
    FOR USE AT GEORGIA INSTITUTE OF TECHNOLOGY UNDER ACADEMIC LICENSE FROM HKS, INC.

    Extension-Twist Coupled Specimen
STEP   6 INCREMENT   1

TIME COMPLETED IN THIS STEP   0.

                    S T E P   6   S T A T I C   A N A L Y S I S

       AUTOMATIC TIME CONTROL WITH -
            A SUGGESTED INITIAL TIME INCREMENT OF   1.00
            AND A TOTAL TIME PERIOD OF   1.00
            THE MINIMUM TIME INCREMENT ALLOWED IS   1.000E-05
            THE MAXIMUM TIME INCREMENT ALLOWED IS   1.00

            LARGE DISPLACEMENT THEORY WILL BE USED

TIME INCREMENT COMPLETED   1.00   , FRACTION OF STEP COMPLETED   1.00
STEP TIME COMPLETED   1.00   , TOTAL TIME COMPLETED   6.00

N O D E   O U T P U T

THE FOLLOWING TABLE IS PRINTED FOR NODESET   TIP

NODE	FOOT- NOTE	UR1
180		-0.3656
280		-0.3674
380		-0.3627
480		-0.3664
580		-0.3606
680		-0.3657
780		-0.3606
880		-0.3664
980		-0.3627
1080		-0.3674
1180		-0.3656

MAXIMUM	-0.3606
AT NODE	780

MINIMUM	-0.3674
AT NODE	1080

THE ANALYSIS HAS BEEN COMPLETED

ANALYSIS COMPLETE
WITH   6 WARNING MESSAGES ON THE DAT FILE
AND   2 WARNING MESSAGES ON THE MSG FILE
         2 WARNINGS ARE FOR NEGATIVE EIGENVALUES

JOB TIME SUMMARY
   USER TIME   =   437.07
   SYSTEM TIME =   28.790

TOTAL TIME =   465.86

Winckler 30° Input File

```
**
**
*HEADING
Extension-Twist Coupled Specimen
Run of 09/10/96
Winkler 30° Case
**
**
*PREPRINT, ECHO=YES, MODEL=NO, HISTORY=NO
**
**
*RESTART, FREQ=1, WRITE
**
**
*NODE
0100, 0.0, -12.600E-3, 0.0
1100, 0.0, 12.600E-3, 0.0
**
*NGEN, NSET=ROOT
0100, 1100, 100
**
**
*NODE
0180, 254.00E-3, -12.600E-3, 0.0
1180, 254.00E-3, 12.600E-3, 0.0
**
*NGEN, NSET=TIP
0180, 1180, 100
**
**
*NFILL, NSET=ALL
ROOT, TIP, 80, 1
**
**
**NSET, NSET=REF1
**0120, 0220, 0320,0420,0520,0620,0720,0820,0920,1020,1120
**
**
**NSET, NSET=REF2
**0160, 0260, 0360,0460,0560,0660,0760,0860,0960,1060,1160
**
**
*ELEMENT,TYPE=S4R,ELSET=BLADE
0100, 0100, 0101, 0201, 0200
*ELGEN, ELSET=BLADE
0100, 10, 100, 100, 80, 1, 1
```

```
**
**
*BOUNDARY
ROOT, 1, 6
**
**
*MATERIAL,NAME=Carbon
*ELASTIC,TYPE=LAMINA
1.356E11, 9.9E9, 0.30, 4.2E9, 4.2E9, 2.5E9
**
**
*ORIENTATION, NAME=ThirtyP
1.0, 0.0 ,0.0, 0.0, 1.0, 0.0
3, 30
**
**
*ORIENTATION, NAME=ThirtyM
1.0, 0.0 ,0.0, 0.0, 1.0, 0.0
3, -30
**
**
*ORIENTATION, NAME=SixtyP
1.0, 0.0 ,0.0, 0.0, 1.0, 0.0
3, 60
**
**
*ORIENTATION, NAME=SixtyM
1.0, 0.0 ,0.0, 0.0, 1.0, 0.0
3, -60
**
**
*ORIENTATION, NAME=TwentyP
1.0, 0.0 ,0.0, 0.0, 1.0, 0.0
3, 20
**
**
*ORIENTATION, NAME=TwentyM
1.0, 0.0 ,0.0, 0.0, 1.0, 0.0
3, -20
**
**
*ORIENTATION, NAME=SeventyP
1.0, 0.0 ,0.0, 0.0, 1.0, 0.0
3, 70
**
**
*ORIENTATION, NAME=SeventyM
1.0, 0.0 ,0.0, 0.0, 1.0, 0.0
```

92

```
3, -70
**
**
*ORIENTATION, NAME=Zero
1.0, 0.0 ,0.0, 0.0, 1.0, 0.0
3, 0
**
**
*SHELL SECTION, COMPOSITE, ELSET=BLADE
150.000E-6, 3,Carbon, ThirtyP
150.000E-6, 3,Carbon, SixtyM
150.000E-6, 3,Carbon, SixtyM
150.000E-6, 3,Carbon, ThirtyP
150.000E-6, 3,Carbon, ThirtyM
150.000E-6, 3,Carbon, SixtyP
150.000E-6, 3,Carbon, SixtyP
150.000E-6, 3,Carbon, ThirtyM
**
**
*STEP,NLGEOM
*STATIC
*CLOAD
TIP, 1, 25
*EL PRINT, FREQUENCY=0
**
**
*NODE PRINT, NSET=TIP
UR1
**
**
*END STEP
**
**
*STEP
*STATIC
*CLOAD
TIP, 1, 50
*EL PRINT, FREQUENCY=0
**
**
*NODE PRINT, NSET=TIP
UR1
**
**
*END STEP
**
**
*STEP
```

93

```
*STATIC
*CLOAD
TIP, 1, 75
*EL PRINT, FREQUENCY=0
**
**
*NODE PRINT, NSET=TIP
UR1
**
**
*END STEP
**
**
*STEP
*STATIC
*CLOAD
TIP, 1, 100
*EL PRINT, FREQUENCY=0
**
**
*NODE PRINT, NSET=TIP
UR1
**
**
*END STEP
**
**
*STEP
*STATIC
*CLOAD
TIP, 1, 125
*EL PRINT, FREQUENCY=0
**
**
*NODE PRINT, NSET=TIP
UR1
**
**
*END STEP
**
**
*STEP
*STATIC
*CLOAD
TIP, 1, 150
*EL PRINT, FREQUENCY=0
**
**
```

```
*NODE PRINT, NSET=TIP
U
**
**
*END STEP
```

Winckler 30° Output File

```
1
```

```
    AAAAAA       BBBBBBBBB      AAAAAA       QQQQQQQQ     U          U     SSSSSSSS
   A      A     B         B    A      A     Q        Q   U          U    S
   A      A     B         B   A        A    Q        Q   U          U    S
   A      A     B         B   A        A    Q        Q   U          U    S
   AAAAAAAAAA   BBBBBBBBB     AAAAAAAAAA     Q        Q   U          U    SSSSSSSS
   A      A     B         B   A        A    Q    Q   Q   U          U           S
   A      A     B         B   A        A    Q     Q  Q   U          U           S
   A      A     B         B   A        A    Q      Q Q   U          U           S
   A      A     BBBBBBBBB     A        A     QQQQQQQQ      UUUUUUUU     SSSSSSSS
                                                     Q
```

```
    <|> <|> <|> <|> <|> <|> <|> <|> <|> <|>
    <|> <|> <|> <|> <|> <|> <|>  |   |   |
     |   |   |   |   |   |   |   <|> <|> <|>
   ----------------------------------------
   ----------------------------------------
    |   <|>  |   <|>  |   |   <|> <|> <|> <|>
    |   <|>  |   |   |   |   |   <|> <|> <|>
   <|>  |   <|>  |   <|> <|>  |   <|>  |   <|>
   <|>  |   <|> <|> <|> <|> <|> <|>  |   |
   <|> <|> <|> <|> <|> <|> <|>  |   <|>  |
   <|> <|> <|> <|> <|> <|> <|>  |   <|> <|>
   <|> <|> <|> <|> <|> <|> <|> <|> <|> <|>
```

 *RESTART, FREQ=1, WRITE
1

   ABAQUS VERSION 5.5-1   DATE 11-SEP-96   TIME

                                    A B A Q U S   I N P U T   E C H O

                        5   10   15   20   25   30   35   40   45   50   55   60   65
70   75   80

                    **
                    **
                    *HEADING
                    Extension-Twist Coupled Specimen
      CARD   5   Run of 09/10/96
                    DWP Thesis Data 30° flat
                    **
                    **
                    *PREPRINT, ECHO=YES, MODEL=NO, HISTORY=NO
      CARD   10   **
                    **
                    *RESTART, FREQ=1, WRITE
                    **
                    **
      CARD   15   *NODE
                    0100, 0.0, -12.600E-3, 0.0
                    1100, 0.0, 12.600E-3, 0.0
                    **
                    *NGEN, NSET=ROOT
      CARD   20   0100, 1100, 100
                    **
                    **
                    *NODE
                    0180, 254.00E-3, -12.600E-3, 0.0
      CARD   25   1180, 254.00E-3, 12.600E-3, 0.0
                    **
                    *NGEN, NSET=TIP
                    0180, 1180, 100
                    **
      CARD   30   **
                    *NFILL, NSET=ALL
                    ROOT, TIP, 80, 1
                    **
                    **
      CARD   35   **NSET, NSET=REF1
                    **0120, 0220, 0320,0420,0520,0620,0720,0820,0920,1020,1120
                    **
                    **
                    **NSET, NSET=REF2
      CARD   40   **0160, 0260, 0360,0460,0560,0660,0760,0860,0960,1060,1160

```
                      **
                      **
                      *ELEMENT,TYPE=S4R,ELSET=BLADE
                      0100, 0100, 0101, 0201, 0200
CARD     45           *ELGEN, ELSET=BLADE
                      0100, 10, 100, 100, 80, 1, 1
                      **
                      **
                      *BOUNDARY
CARD     50           ROOT, 1, 6
                      **
                      **
                      *MATERIAL,NAME=Carbon
                      *ELASTIC,TYPE=LAMINA
CARD     55           1.356E11, 9.9E9, 0.30, 4.2E9, 4.2E9, 2.5E9
                      **
                      **
                      *ORIENTATION, NAME=ThirtyP
                      1.0, 0.0 ,0.0, 0.0, 1.0, 0.0
CARD     60           3, 30
                      **
                      **
                      *ORIENTATION, NAME=ThirtyM
                      1.0, 0.0 ,0.0, 0.0, 1.0, 0.0
CARD     65           3, -30
                      **
                      **
                      *ORIENTATION, NAME=SixtyP
                      1.0, 0.0 ,0.0, 0.0, 1.0, 0.0
CARD     70           3, 60
                      **
                      **
                      *ORIENTATION, NAME=SixtyM
                      1.0, 0.0 ,0.0, 0.0, 1.0, 0.0
CARD     75           3, -60
                      **
                      **
                      *ORIENTATION, NAME=TwentyP
                      1.0, 0.0 ,0.0, 0.0, 1.0, 0.0
CARD     80           3, 20
                      **
                      **
                      *ORIENTATION, NAME=TwentyM
                      1.0, 0.0 ,0.0, 0.0, 1.0, 0.0
CARD     85           3, -20
                      **
                      **
                      *ORIENTATION, NAME=SeventyP
                      1.0, 0.0 ,0.0, 0.0, 1.0, 0.0
CARD     90           3, 70
                      **
                      **
```

```
                *ORIENTATION, NAME=SeventyM
                1.0, 0.0 ,0.0, 0.0, 1.0, 0.0
CARD    95      3, -70
                **
                **
                *ORIENTATION, NAME=Zero
                1.0, 0.0 ,0.0, 0.0, 1.0, 0.0
CARD    100     3, 0
                **
                **
                *SHELL SECTION, COMPOSITE, ELSET=BLADE
                150.000E-6, 3,Carbon, ThirtyP
CARD    105     150.000E-6, 3,Carbon, SixtyM
                150.000E-6, 3,Carbon, SixtyM
                150.000E-6, 3,Carbon, ThirtyP
                150.000E-6, 3,Carbon, ThirtyM
                150.000E-6, 3,Carbon, SixtyP
CARD    110     150.000E-6, 3,Carbon, SixtyP
                150.000E-6, 3,Carbon, ThirtyM
                **
                **
                *STEP,NLGEOM
CARD    115     *STATIC
                *CLOAD
                TIP, 1, 25
                *EL PRINT, FREQUENCY=0
                **
CARD    120     **
                *NODE PRINT, NSET=TIP
                UR1
                **
                **
CARD    125     *END STEP
                **
                **
                *STEP
                *STATIC
CARD    130     *CLOAD
                TIP, 1, 50
                *EL PRINT, FREQUENCY=0
                **
                **
CARD    135     *NODE PRINT, NSET=TIP
                UR1
                **
                **
                *END STEP
CARD    140     **
                **
                *STEP
                *STATIC
                *CLOAD
```

```
CARD    145     TIP, 1, 75
                *EL PRINT, FREQUENCY=0
                **
                **
                *NODE PRINT, NSET=TIP
CARD    150     UR1
                **
                **
                *END STEP
                **
CARD    155     **
                *STEP
                *STATIC
                *CLOAD
                TIP, 1, 100
CARD    160     *EL PRINT, FREQUENCY=0
                **
                **
                *NODE PRINT, NSET=TIP
                UR1
CARD    165     **
                **
                *END STEP
                **
                **
CARD    170     *STEP
                *STATIC
                *CLOAD
                TIP, 1, 125
                *EL PRINT, FREQUENCY=0
CARD    175     **
                **
                *NODE PRINT, NSET=TIP
                UR1
                **
CARD    180     **
                *END STEP
                **
                **
                *STEP
CARD    185     *STATIC
                *CLOAD
                TIP, 1, 150
                *EL PRINT, FREQUENCY=0
                **
CARD    190     **
                *NODE PRINT, NSET=TIP
                U
                **
                **
CARD    195     *END STEP
```

100

```
--------------                 ----------------------------------------------------------------
                        5   10   15   20   25   30   35   40   45   50   55   60   65
70   75   80
                               ----------------------------------------------------------------
--------------
```

         OPTIONS BEING PROCESSED
         ****

   *HEADING
           Extension-Twist Coupled Specimen
           Run of 09/10/96
           DWP Thesis Data 30° flat
   *NODE
   *NGEN, NSET=ROOT
   *NODE
   *NGEN, NSET=TIP
   *NFILL, NSET=ALL
   *ELEMENT,TYPE=S4R,ELSET=BLADE
   *ELGEN, ELSET=BLADE
   *MATERIAL,NAME=Carbon
   *ELASTIC,TYPE=LAMINA
   *ORIENTATION, NAME=ThirtyP
   *ORIENTATION, NAME=ThirtyM
   *ORIENTATION, NAME=SixtyP
   *ORIENTATION, NAME=SixtyM
   *ORIENTATION, NAME=TwentyP
   *ORIENTATION, NAME=TwentyM
   *ORIENTATION, NAME=SeventyP
   *ORIENTATION, NAME=SeventyM
   *ORIENTATION, NAME=Zero
   *SHELL SECTION, COMPOSITE, ELSET=BLADE
   *SHELL SECTION, COMPOSITE, ELSET=BLADE
   *STEP,NLGEOM
   *STATIC
   *EL PRINT, FREQUENCY=0
   *END STEP
   *STEP
   *STATIC
   *EL PRINT, FREQUENCY=0
   *END STEP

   ***WARNING: THE NLGEOM FLAG IS ACTIVATED BECAUSE IT WAS ACTIVE IN THE PREVIOUS
               STEP.
   *STEP
   *STATIC
   *EL PRINT, FREQUENCY=0
   *END STEP

101

```
***WARNING: THE NLGEOM FLAG IS ACTIVATED BECAUSE IT WAS ACTIVE IN THE PREVIOUS
            STEP.
*STEP
*STATIC
*EL PRINT, FREQUENCY=0
*END STEP

***WARNING: THE NLGEOM FLAG IS ACTIVATED BECAUSE IT WAS ACTIVE IN THE PREVIOUS
            STEP.
*STEP
*STATIC
*EL PRINT, FREQUENCY=0
*END STEP

***WARNING: THE NLGEOM FLAG IS ACTIVATED BECAUSE IT WAS ACTIVE IN THE PREVIOUS
            STEP.
*STEP
*STATIC
*EL PRINT, FREQUENCY=0
*END STEP

***WARNING: THE NLGEOM FLAG IS ACTIVATED BECAUSE IT WAS ACTIVE IN THE PREVIOUS
            STEP.
*BOUNDARY
*STEP,NLGEOM
*STATIC
*CLOAD
*NODE PRINT, NSET=TIP
*END STEP
*STEP
*STATIC
*CLOAD
*NODE PRINT, NSET=TIP
*END STEP
*STEP
*STATIC
*CLOAD
*NODE PRINT, NSET=TIP
*END STEP
*STEP
*STATIC
*CLOAD
*NODE PRINT, NSET=TIP
*END STEP
*STEP
*STATIC
*CLOAD
*NODE PRINT, NSET=TIP
*END STEP
*STEP
*STATIC
```

*CLOAD
*NODE PRINT, NSET=TIP
*END STEP

                    W A V E F R O N T   M I N I M I Z A T I O N

    NUMBER OF NODES   891
    NUMBER OF ELEMENTS   800
    ORIGINAL MAXIMUM D.O.F WAVEFRONT ESTIMATED AS   498
    ORIGINAL RMS D.O.F WAVEFRONT ESTIMATED AS   452

    PERIPHERAL DIAMETER IS DEFINED BY NODES   100   580

    WAVEFRONT OPTIMIZED BY CHOOSING   180 AS THE STARTING NODE

    MINIMUM WAVEFRONT OBTAINED USING METHOD 1.   USE
    *WAVEFRONT MINIMIZATION, NODES, METHOD=1
          100,   580
    TO REDUCE THE CPU TIME ON SUBSEQUENT JOBS USING THIS SAME MESH.

                         P R O B L E M   S I Z E

        NUMBER OF ELEMENTS IS   800
        NUMBER OF NODES IS   891
        NUMBER OF NODES DEFINED BY THE USER   891
        TOTAL NUMBER OF VARIABLES IN THE MODEL   5346
        (DEGREES OF FREEDOM PLUS ANY LAGRANGE MULTIPLIER VARIABLES)
        MAXIMUM D.O.F. WAVEFRONT ESTIMATED AS   78
        RMS WAVEFRONT ESTIMATED AS   78

        FILE SIZES - THESE VALUES ARE CONSERVATIVE UPPER BOUNDS

           UNIT   WORDS   MEGABYTES

            21   603200   4.83
            22   603200   4.83
         -------   ----------   ----------
          TOTAL   1206400   9.65

        IF THE RESTART FILE IS WRITTEN ITS LENGTH WILL BE APPROXIMATELY

                                                      WORDS   MEGABYTES
                                                    ---------- ----------
        WRITTEN IN THE ANALYSIS PREPROCESSOR   133654   1.07
        PLUS WRITTEN AT THE BEGINNING OF EACH STEP   80080   0.64
        PLUS FOR EACH INCREMENT WRITTEN TO THE RESTART FILE   710617   5.68

                                  103

END OF USER INPUT PROCESSING

```
     JOB TIME SUMMARY
        USER TIME    =    7.9000
        SYSTEM TIME  =    1.2900
        TOTAL TIME   =    9.1900
1
```

ABAQUS VERSION 5.5-1   DATE 11-SEP-96   TIME
18:51:05   PAGE   1
   FOR USE AT GEORGIA INSTITUTE OF TECHNOLOGY UNDER ACADEMIC LICENSE FROM HKS, INC.

     Extension-Twist Coupled Specimen
STEP   1 INCREMENT   1

TIME COMPLETED IN THIS STEP   0.

S T E P   1   S T A T I C   A N A L Y S I S

```
     AUTOMATIC TIME CONTROL WITH -
          A SUGGESTED INITIAL TIME INCREMENT OF            1.00
          AND A TOTAL TIME PERIOD OF                       1.00
          THE MINIMUM TIME INCREMENT ALLOWED IS            1.000E-05
          THE MAXIMUM TIME INCREMENT ALLOWED IS            1.00

     LARGE DISPLACEMENT THEORY WILL BE USED
```

INCREMENT   1 SUMMARY

```
TIME INCREMENT COMPLETED   1.00   ,  FRACTION OF STEP COMPLETED   1.00
STEP TIME COMPLETED        1.00   ,  TOTAL TIME COMPLETED         1.00
```

N O D E   O U T P U T

THE FOLLOWING TABLE IS PRINTED FOR NODESET   TIP

```
   NODE FOOT-    UR1
        NOTE

    180     -9.1417E-02
    280     -9.1603E-02
    380     -9.1030E-02
    480     -9.1464E-02
    580     -9.0837E-02
    680     -9.1401E-02
    780     -9.0837E-02
    880     -9.1464E-02
    980     -9.1030E-02
   1080     -9.1603E-02
   1180     -9.1417E-02


 MAXIMUM     -9.0837E-02
 AT NODE         580


 MINIMUM     -9.1603E-02
 AT NODE        1080
1
```

   FOR USE AT GEORGIA INSTITUTE OF TECHNOLOGY UNDER ACADEMIC LICENSE FROM HKS, INC.

      Extension-Twist Coupled Specimen
STEP   2 INCREMENT   1

TIME COMPLETED IN THIS STEP   0.

                    S T E P   2   S T A T I C   A N A L Y S I S

      AUTOMATIC TIME CONTROL WITH -
            A SUGGESTED INITIAL TIME INCREMENT OF   1.00
            AND A TOTAL TIME PERIOD OF   1.00
            THE MINIMUM TIME INCREMENT ALLOWED IS   1.000E-05
            THE MAXIMUM TIME INCREMENT ALLOWED IS   1.00

      LARGE DISPLACEMENT THEORY WILL BE USED

                         INCREMENT   1 SUMMARY

                                   105

```
TIME INCREMENT COMPLETED  0.250   ,  FRACTION OF STEP COMPLETED  0.250
STEP TIME COMPLETED       0.250   ,  TOTAL TIME COMPLETED        1.25
```

N O D E   O U T P U T

THE FOLLOWING TABLE IS PRINTED FOR NODESET   TIP

```
    NODE FOOT-    UR1
         NOTE

     180        -0.1125
     280        -0.1128
     380        -0.1120
     480        -0.1126
     580        -0.1117
     680        -0.1125
     780        -0.1117
     880        -0.1126
     980        -0.1120
    1080        -0.1128
    1180        -0.1125


MAXIMUM        -0.1117
AT NODE         580

MINIMUM        -0.1128
AT NODE        1080
```

INCREMENT   2 SUMMARY

```
TIME INCREMENT COMPLETED  0.250   ,  FRACTION OF STEP COMPLETED  0.500
STEP TIME COMPLETED       0.500   ,  TOTAL TIME COMPLETED        1.50
```

N O D E   O U T P U T

THE FOLLOWING TABLE IS PRINTED FOR NODESET   TIP

```
NODE FOOT-    UR1
     NOTE

 180        -0.1329
 280        -0.1333
 380        -0.1323
 480        -0.1330
 580        -0.1319
 680        -0.1329
 780        -0.1319
 880        -0.1330
 980        -0.1323
1080        -0.1333
1180        -0.1329


MAXIMUM     -0.1319
AT NODE        580


MINIMUM     -0.1333
AT NODE       1080
```

INCREMENT   3 SUMMARY

TIME INCREMENT COMPLETED 0.375   , FRACTION OF STEP COMPLETED 0.875
STEP TIME COMPLETED   0.875   , TOTAL TIME COMPLETED   1.88

N O D E   O U T P U T

THE FOLLOWING TABLE IS PRINTED FOR NODESET   TIP


```
NODE FOOT-    UR1
     NOTE

 180        -0.1625
 280        -0.1629
 380        -0.1617
 480        -0.1626
 580        -0.1612
 680        -0.1624
 780        -0.1612
 880        -0.1626
 980        -0.1617
1080        -0.1629
1180        -0.1625
```

```
MAXIMUM      -0.1612
AT NODE         780

MINIMUM      -0.1629
AT NODE        1080
```

INCREMENT   4 SUMMARY

```
TIME INCREMENT COMPLETED  0.125   ,  FRACTION OF STEP COMPLETED   1.00
STEP TIME COMPLETED        1.00   ,  TOTAL TIME COMPLETED         2.00
```

N O D E   O U T P U T

THE FOLLOWING TABLE IS PRINTED FOR NODESET   TIP

```
NODE FOOT-    UR1
     NOTE

 180      -0.1720
 280      -0.1725
 380      -0.1712
 480      -0.1722
 580      -0.1706
 680      -0.1720
 780      -0.1706
 880      -0.1722
 980      -0.1712
1080      -0.1725
1180      -0.1720

MAXIMUM   -0.1706
AT NODE       780

MINIMUM   -0.1725
AT NODE      1080
1
```

     Extension-Twist Coupled Specimen
STEP   3 INCREMENT   1

TIME COMPLETED IN THIS STEP   0.

                    S T E P   3   S T A T I C   A N A L Y S I S

       AUTOMATIC TIME CONTROL WITH -
              A SUGGESTED INITIAL TIME INCREMENT OF   1.00
              AND A TOTAL TIME PERIOD OF   1.00
              THE MINIMUM TIME INCREMENT ALLOWED IS   1.000E-05
              THE MAXIMUM TIME INCREMENT ALLOWED IS   1.00

       LARGE DISPLACEMENT THEORY WILL BE USED

                        INCREMENT   1 SUMMARY

TIME INCREMENT COMPLETED 1.00   , FRACTION OF STEP COMPLETED   1.00
STEP TIME COMPLETED   1.00   , TOTAL TIME COMPLETED   3.00

                        N O D E   O U T P U T

   THE FOLLOWING TABLE IS PRINTED FOR NODESET   TIP

     NODE FOOT-   UR1
          NOTE

      180   -0.2436
      280   -0.2442
      380   -0.2422
      480   -0.2436
      580   -0.2413
      680   -0.2433
      780   -0.2413
      880   -0.2436
      980   -0.2422
     1080   -0.2442
     1180   -0.2436

   MAXIMUM   -0.2413
   AT NODE   580

                              109

```
MINIMUM      -0.2442
AT NODE       1080
1
```

    Extension-Twist Coupled Specimen
STEP   4 INCREMENT   1

TIME COMPLETED IN THIS STEP   0.

                    S T E P   4   S T A T I C   A N A L Y S I S

        AUTOMATIC TIME CONTROL WITH -
            A SUGGESTED INITIAL TIME INCREMENT OF   1.00
            AND A TOTAL TIME PERIOD OF   1.00
            THE MINIMUM TIME INCREMENT ALLOWED IS   1.000E-05
            THE MAXIMUM TIME INCREMENT ALLOWED IS   1.00

        LARGE DISPLACEMENT THEORY WILL BE USED

                        INCREMENT   1 SUMMARY

TIME INCREMENT COMPLETED   1.00   , FRACTION OF STEP COMPLETED   1.00
STEP TIME COMPLETED   1.00   , TOTAL TIME COMPLETED   4.00

                        N O D E   O U T P U T

    THE FOLLOWING TABLE IS PRINTED FOR NODESET   TIP

    NODE FOOT-   UR1
         NOTE

        180   -0.3071
        280   -0.3079
        380   -0.3051
        480   -0.3069
        580   -0.3038

```
    680      -0.3064
    780      -0.3038
    880      -0.3069
    980      -0.3051
   1080      -0.3079
   1180      -0.3071


MAXIMUM      -0.3038
AT NODE        580


MINIMUM      -0.3079
AT NODE       1080
1
```

Extension-Twist Coupled Specimen
STEP   5 INCREMENT   1

TIME COMPLETED IN THIS STEP   0.

                      S T E P   5   S T A T I C   A N A L Y S I S

       AUTOMATIC TIME CONTROL WITH -
            A SUGGESTED INITIAL TIME INCREMENT OF   1.00
            AND A TOTAL TIME PERIOD OF   1.00
            THE MINIMUM TIME INCREMENT ALLOWED IS   1.000E-05
            THE MAXIMUM TIME INCREMENT ALLOWED IS   1.00

       LARGE DISPLACEMENT THEORY WILL BE USED

                       INCREMENT   1 SUMMARY

TIME INCREMENT COMPLETED   1.00   , FRACTION OF STEP COMPLETED   1.00
STEP TIME COMPLETED   1.00   , TOTAL TIME COMPLETED   5.00

                          N O D E   O U T P U T

   THE FOLLOWING TABLE IS PRINTED FOR NODESET   TIP

```
NODE FOOT-     UR1
     NOTE

  180      -0.3662
  280      -0.3672
  380      -0.3637
  480      -0.3658
  580      -0.3619
  680      -0.3651
  780      -0.3619
  880      -0.3658
  980      -0.3637
 1080      -0.3672
 1180      -0.3662

MAXIMUM      -0.3619
AT NODE          580

MINIMUM      -0.3672
AT NODE          280
1
```

Extension-Twist Coupled Specimen
STEP   6   INCREMENT   1

TIME COMPLETED IN THIS STEP   0.

                  S T E P   6   S T A T I C   A N A L Y S I S

     AUTOMATIC TIME CONTROL WITH -
          A SUGGESTED INITIAL TIME INCREMENT OF   1.00
          AND A TOTAL TIME PERIOD OF   1.00
          THE MINIMUM TIME INCREMENT ALLOWED IS   1.000E-05
          THE MAXIMUM TIME INCREMENT ALLOWED IS   1.00

     LARGE DISPLACEMENT THEORY WILL BE USED

                           INCREMENT   1 SUMMARY

TIME INCREMENT COMPLETED   1.00   ,   FRACTION OF STEP COMPLETED   1.00

                                  112

STEP TIME COMPLETED   1.00   , TOTAL TIME COMPLETED   6.00

N O D E   O U T P U T

THE FOLLOWING TABLE IS PRINTED FOR NODESET   TIP

NODE	FOOT-NOTE	U1	U2	U3	UR1	UR2	UR3
180		5.3362E-04	1.0973E-03	5.0567E-03	-0.4189	-2.4783E-02	2.2631E-02
280		4.9733E-04	8.5943E-04	4.0401E-03	-0.4201	-1.0377E-02	2.4214E-04
380		5.1780E-04	6.4746E-04	3.0229E-03	-0.4158	-1.1706E-02	3.7881E-03
480		4.9859E-04	4.2633E-04	2.0129E-03	-0.4183	-4.2205E-03	8.4231E-04
580		5.1464E-04	2.1436E-04	1.0053E-03	-0.4134	-3.4948E-03	9.4025E-04
680		4.9901E-04	0.	0.	-0.4174	0.	0.
760		5.1464E-04	-2.1436E-04	-1.0053E-03	-0.4134	3.4948E-03	-9.4025E-04
880		4.9859E-04	-4.2633E-04	-2.0129E-03	-0.4183	4.2205E-03	-8.4231E-04
980		5.1780E-04	-6.4746E-04	-3.0229E-03	-0.4158	1.1706E-02	-3.7881E-03
1080		4.9733E-04	-8.5943E-04	-4.0401E-03	-0.4201	1.0377E-02	-2.4214E-04
1180		5.3362E-04	-1.0973E-03	-5.0567E-03	-0.4189	2.4783E-02	-2.2631E-02
MAXIMUM		5.3362E-04	1.0973E-03	5.0567E-03	-0.4134	2.4783E-02	2.2631E-02
AT NODE		180	180	180	780	1180	180
MINIMUM		4.9733E-04	-1.0973E-03	-5.0567E-03	-0.4201	-2.4783E-02	-2.2631E-02
AT NODE		280	1180	1180	280	180	1180

THE ANALYSIS HAS BEEN COMPLETED

ANALYSIS COMPLETE
WITH   5 WARNING MESSAGES ON THE DAT FILE
AND   3 WARNING MESSAGES ON THE MSG FILE
          2 WARNINGS ARE FOR NEGATIVE EIGENVALUES

JOB TIME SUMMARY
   USER TIME   =   698.50
   SYSTEM TIME =   39.530
   TOTAL TIME =   738.03

[30/-30] Input File
**
**
*HEADING
Extension-Twist Coupled Specimen - Temperature Variation
Run of 09/17/96
+30/-30 case
**
**
*PREPRINT, ECHO=NO, MODEL=NO, HISTORY=NO
**
**
**RESTART, FREQ=1, WRITE
**
**
*NODE
0100, 0.0, -12.65E-3, 0.0
1100, 0.0, 12.65E-3, 0.0
**
*NGEN, NSET=ROOT
0100, 1100, 100
**
**
*NODE
0180, 298.45E-3, -12.65E-3, 0.0
1180, 298.452E-3, 12.65E-3, 0.0
**
*NGEN, NSET=TIP
0180, 1180, 100
**
**
*NFILL, NSET=ALL
ROOT, TIP, 80, 1
**
**
*NSET, NSET=REF1
0120, 0220, 0320,0420,0520,0620,0720,0820,0920,1020,1120
**
**
*NSET, NSET=REF2
0160, 0260, 0360,0460,0560,0660,0760,0860,0960,1060,1160
**
**
*ELEMENT,TYPE=S8R,ELSET=BLADE
0100, 0100, 0102, 0302, 0300, 0101, 0202, 0301, 0200
*ELGEN, ELSET=BLADE
0100, 5, 200, 100, 40, 2, 1
**

```
**
*BOUNDARY
ROOT,1,6
**
**
*MATERIAL,NAME=Carbon
*ELASTIC,TYPE=LAMINA
1.38254E11, 9.092E9, 0.304, 4.609E9, 4.609E9, 2.627E9
*EXPANSION, TYPE=ORTHO
4.34E-6, 37.0E-6, 37.0E-6
**
**
*ORIENTATION, NAME=ThirtyP
1.0, 0.0 ,0.0, 0.0, 1.0, 0.0
3, 30
**
**
*ORIENTATION, NAME=ThirtyM
1.0, 0.0 ,0.0, 0.0, 1.0, 0.0
3, -30
**
**
*ORIENTATION, NAME=Zero
1.0, 0.0 ,0.0, 0.0, 1.0, 0.0
3, 0
**
**
*ORIENTATION, NAME=SixtyP
1.0, 0.0 ,0.0, 0.0, 1.0, 0.0
3, 60
**
**
*ORIENTATION, NAME=SixtyM
1.0, 0.0 ,0.0, 0.0, 1.0, 0.0
3, -60
**
**
*SHELL SECTION, COMPOSITE, ELSET=BLADE
285.00E-6, 9,Carbon, ThirtyP
285.00E-6, 9,Carbon, ThirtyM
**
**
*STEP,NLGEOM, INC=100
*STATIC
*TEMPERATURE
ALL,-138
*EL PRINT, FREQUENCY=0
**
```

```
**
*NODE PRINT, NSET=TIP
U
**NODE PRINT, NSET=REF1
**U
**NODE PRINT, NSET=REF2
**U
**
**
*END STEP
**
**
*STEP,NLGEOM, INC=100
*STATIC
*CLOAD
TIP, 1, 13
*EL PRINT, FREQUENCY=0
**
**
*NODE PRINT, NSET=TIP
U
**
**
*END STEP
**
**
*STEP, NLGEOM, INC=100
*STATIC
*CLOAD
TIP, 1, 26
*EL PRINT, FREQUENCY=0
**
**
*NODE PRINT, NSET=TIP
U
**
**
*END STEP
**
**
*STEP, NLGEOM, INC=100
*STATIC
*CLOAD
TIP, 1, 39
*EL PRINT, FREQUENCY=0
**
**
*NODE PRINT, NSET=TIP
```

116

```
U
**
**
*END STEP
**
**
*STEP, NLGEOM, INC=100
*STATIC
*CLOAD
TIP, 1, 52
*EL PRINT, FREQUENCY=0
**
**
*NODE PRINT, NSET=TIP
U
**
**
*END STEP
**
**
*STEP, NLGEOM, INC=100
*STATIC
*CLOAD
TIP, 1, 65
*EL PRINT, FREQUENCY=0
**
**
*NODE PRINT, NSET=TIP
U
**
**
*END STEP
**
**
*STEP, NLGEOM, INC=100
*STATIC
*CLOAD
TIP, 1, 78
*EL PRINT, FREQUENCY=0
**
**
*NODE PRINT, NSET=TIP
U
**
**
*END STEP
```

[30/-30] Output File

1

```
   AAAAAA      BBBBBBBBB      AAAAAA      QQQQQQQQ      U         U    SSSSSSSS
  A      A    B         B    A       A    Q        Q    U         U   S
 A        A   B         B   A         A   Q        Q    U         U   S
 A        A   B         B   A         A   Q        Q    U         U   S
 AAAAAAAAAA   BBBBBBBBB     AAAAAAAAAA    Q        Q    U         U    SSSSSSSS
 A        A   B         B   A         A   Q    Q   Q    U         U            S
 A        A   B         B   A         A   Q      Q Q    U         U            S
 A        A   B         B   A         A   Q       Q Q   U         U            S
 A        A   BBBBBBBBB     A         A   QQQQQQQQ      UUUUUUUU    SSSSSSSS
                                                Q
```

```
 <|> <|> <|> <|> <|> <|> <|> <|> <|> <|>
 <|> <|> <|> <|> <|> <|> <|>   |    |    |
  |   |   |   |   |   |   |   <|> <|> <|>
 ------------------------------------------
 ------------------------------------------
  |   <|>  |   <|>  |   |   <|> <|> <|> <|>
  |   <|>  |   |    |   |   |   <|> <|> <|>
 <|>  |   <|>  |   <|> <|>  |   <|>  |   <|>
 <|>  |   <|> <|> <|> <|> <|> <|>  |    |
 <|> <|> <|> <|> <|> <|> <|>  |   <|>  |
 <|> <|> <|> <|> <|> <|> <|>  |   <|> <|>
 <|> <|> <|> <|> <|> <|> <|> <|> <|> <|>
```

OPTIONS BEING PROCESSED
****

*HEADING
        Extension-Twist Coupled Specimen - Temperature Variation

119

```
          Run of 09 17/96
          +30 -30 case
*NODE
*NGEN, NSET=ROOT
*NODE
*NGEN, NSET=TIP
*NFILL, NSET=ALL
*NSET, NSET=REF1
*NSET, NSET=REF2
*ELEMENT,TYPE=S8R,ELSET=BLADE
*ELGEN, ELSET=BLADE
*MATERIAL,NAME=Carbon
*ELASTIC,TYPE=LAMINA
*EXPANSION, TYPE=ORTHO
*ORIENTATION, NAME=ThirtyP
*ORIENTATION, NAME=ThirtyM
*ORIENTATION, NAME=Zero
*ORIENTATION, NAME=SixtyP
*ORIENTATION, NAME=SixtyM
*SHELL SECTION, COMPOSITE, ELSET=BLADE
*SHELL SECTION, COMPOSITE, ELSET=BLADE
*STEP,NLGEOM, INC=100
*STATIC
*EL PRINT, FREQUENCY=0
*END STEP
*STEP,NLGEOM, INC=100
*STATIC
*EL PRINT, FREQUENCY=0
*END STEP
*STEP, NLGEOM, INC=100
*STATIC
*EL PRINT, FREQUENCY=0
*END STEP
*STEP, NLGEOM, INC=100
*STATIC
*EL PRINT, FREQUENCY=0
*END STEP
*STEP, NLGEOM, INC=100
*STATIC
*EL PRINT, FREQUENCY=0
*END STEP
*STEP, NLGEOM, INC=100
*STATIC
*EL PRINT, FREQUENCY=0
*END STEP
*STEP, NLGEOM, INC=100
*STATIC
*EL PRINT, FREQUENCY=0
*END STEP
*BOUNDARY
*STEP,NLGEOM, INC=100
*STATIC
```

*TEMPERATURE
*NODE PRINT, NSET=TIP
*END STEP
*STEP,NLGEOM, INC=100
*STATIC
*CLOAD
*NODE PRINT, NSET=TIP
*END STEP
*STEP, NLGEOM, INC=100
*STATIC
*CLOAD
*NODE PRINT, NSET=TIP
*END STEP
*STEP, NLGEOM, INC=100
*STATIC
*CLOAD
*NODE PRINT, NSET=TIP
*END STEP
*STEP, NLGEOM, INC=100
*STATIC
*CLOAD
*NODE PRINT, NSET=TIP
*END STEP
*STEP, NLGEOM, INC=100
*STATIC
*CLOAD
*NODE PRINT, NSET=TIP
*END STEP
*STEP, NLGEOM, INC=100
*STATIC
*CLOAD
*NODE PRINT, NSET=TIP
*END STEP

W A V E F R O N T   M I N I M I Z A T I O N

NUMBER OF NODES   691
NUMBER OF ELEMENTS   200
ORIGINAL MAXIMUM D.O.F WAVEFRONT ESTIMATED AS   516
ORIGINAL RMS D.O.F WAVEFRONT ESTIMATED AS   434

PERIPHERAL DIAMETER IS DEFINED BY NODES   100   480

WAVEFRONT OPTIMIZED BY CHOOSING   179 AS THE STARTING NODE

MINIMUM WAVEFRONT OBTAINED USING METHOD 1. USE
*WAVEFRONT MINIMIZATION, NODES, METHOD=1
      100,   480
TO REDUCE THE CPU TIME ON SUBSEQUENT JOBS USING THIS SAME MESH.

PROBLEM SIZE

```
NUMBER OF ELEMENTS IS                                      200
NUMBER OF NODES IS                                         691
NUMBER OF NODES DEFINED BY THE USER                        691
TOTAL NUMBER OF VARIABLES IN THE MODEL                    4146
(DEGREES OF FREEDOM PLUS ANY LAGRANGE MULTIPLIER VARIABLES)
MAXIMUM D.O.F. WAVEFRONT ESTIMATED AS                      96
RMS WAVEFRONT ESTIMATED AS                                 95
```

FILE SIZES - THESE VALUES ARE CONSERVATIVE UPPER BOUNDS

UNIT	WORDS	MEGABYTES
21	442000	3.54
22	442000	3.54
-------	----------	----------
TOTAL	884000	7.07

IF THE RESTART FILE IS WRITTEN ITS LENGTH WILL BE APPROXIMATELY

	WORDS	MEGABYTES
WRITTEN IN THE ANALYSIS PREPROCESSOR	83080	0.66
PLUS WRITTEN AT THE BEGINNING OF EACH STEP	38940	0.31
PLUS FOR EACH INCREMENT WRITTEN TO THE RESTART FILE	526539	4.21

```
ALLOCATED WORKSPACE                                       1109742
```

END OF USER INPUT PROCESSING

```
    JOB TIME SUMMARY
       USER TIME   =   3.7600
       SYSTEM TIME =   0.57000
       TOTAL TIME  =   4.3300
1
```

    Extension-Twist Coupled Specimen - Temperature Variation
STEP   1 INCREMENT   1

TIME COMPLETED IN THIS STEP   0.

                      S T E P   1   S T A T I C   A N A L Y S I S

        AUTOMATIC TIME CONTROL WITH -
              A SUGGESTED INITIAL TIME INCREMENT OF   1.00
              AND A TOTAL TIME PERIOD OF   1.00
              THE MINIMUM TIME INCREMENT ALLOWED IS   1.000E-05
              THE MAXIMUM TIME INCREMENT ALLOWED IS   1.00

        LARGE DISPLACEMENT THEORY WILL BE USED

                          INCREMENT   1 SUMMARY

TIME INCREMENT COMPLETED 0.250   , FRACTION OF STEP COMPLETED 0.250
STEP TIME COMPLETED   0.250   , TOTAL TIME COMPLETED   0.250

                          N O D E   O U T P U T

        THE FOLLOWING TABLE IS PRINTED FOR NODESET   TIP

NODE	FOOT-NOTE	U1	U2	U3	UR1	UR2	UR3
180		-6.7515E-05	1.0503E-03	-5.0206E-03	0.4084	1.8395E-02	3.5869E-03
280		-6.6988E-05	8.4016E-04	-4.0168E-03	0.4084	1.4819E-02	2.8667E-03
380		-6.6523E-05	6.3011E-04	-3.0129E-03	0.4084	1.1196E-02	2.1493E-03
480		-6.6167E-05	4.2008E-04	-2.0087E-03	0.4085	7.5125E-03	1.4389E-03
580		-6.5946E-05	2.1004E-04	-1.0044E-03	0.4085	3.7679E-03	7.2011E-04
680		-6.5871E-05	2.1974E-11	-1.4819E-10	0.4085	3.2426E-08	-3.5627E-08
780		-6.5946E-05	-2.1005E-04	1.0044E-03	0.4085	-3.7678E-03	-7.2010E-04
880		-6.6167E-05	-4.2008E-04	2.0087E-03	0.4085	-7.5124E-03	-1.4390E-03
980		-6.6523E-05	-6.3012E-04	3.0129E-03	0.4084	-1.1196E-02	-2.1493E-03
1080		-6.6989E-05	-8.4017E-04	4.0168E-03	0.4084	-1.4819E-02	-2.8668E-03
1180		-6.7516E-05	-1.0503E-03	5.0206E-03	0.4084	-1.8395E-02	-3.5869E-03
MAXIMUM		-6.5871E-05	1.0503E-03	5.0206E-03	0.4085	1.8395E-02	3.5869E-03
AT NODE		680	180	1180	680	180	180

```
MINIMUM      -6.7516E-05 -1.0503E-03 -5.0206E-03  0.4084     -1.8395E-02 -3.5869E-03
AT NODE         1180        1180        180         180         1180        1180
```

                              INCREMENT   2 SUMMARY


```
TIME INCREMENT COMPLETED  7.812E-03,  FRACTION OF STEP COMPLETED  0.258
STEP TIME COMPLETED       0.258    ,  TOTAL TIME COMPLETED        0.258
```


                         N O D E   O U T P U T

THE FOLLOWING TABLE IS PRINTED FOR NODESET   TIP

NODE	FOOT-NOTE	U1	U2	U3	UR1	UR2	UR3
180		-6.9876E-05	1.1091E-03	-5.1537E-03	0.4199	1.8953E-02	3.8020E-03
280		-6.9316E-05	8.8726E-04	-4.1233E-03	0.4199	1.5270E-02	3.0387E-03
380		-6.8821E-05	6.6543E-04	-3.0928E-03	0.4199	1.1538E-02	2.2784E-03
480		-6.8442E-05	4.4362E-04	-2.0620E-03	0.4200	7.7425E-03	1.5254E-03
580		-6.8207E-05	2.2182E-04	-1.0311E-03	0.4200	3.8833E-03	7.6341E-04
680		-6.8127E-05	2.7659E-11	-1.8126E-10	0.4200	3.4786E-08	-3.5882E-08
780		-6.8207E-05	-2.2182E-04	1.0311E-03	0.4200	-3.8833E-03	-7.6339E-04
880		-6.8442E-05	-4.4362E-04	2.0620E-03	0.4200	-7.7425E-03	-1.5255E-03
980		-6.8821E-05	-6.6544E-04	3.0928E-03	0.4199	-1.1538E-02	-2.2784E-03
1080		-6.9316E-05	-8.8727E-04	4.1233E-03	0.4199	-1.5270E-02	-3.0389E-03
1180		-6.9877E-05	-1.1091E-03	5.1538E-03	0.4199	-1.8953E-02	-3.8020E-03

```
MAXIMUM      -6.8127E-05  1.1091E-03  5.1538E-03  0.4200      1.8953E-02  3.8020E-03
AT NODE          680         180        1180        680         180         180

MINIMUM      -6.9877E-05 -1.1091E-03 -5.1537E-03  0.4199     -1.8953E-02 -3.8020E-03
AT NODE         1180        1180        180         180         1180        1180
```


                              INCREMENT   3 SUMMARY


```
TIME INCREMENT COMPLETED  7.812E-03,  FRACTION OF STEP COMPLETED  0.266
STEP TIME COMPLETED       0.266    ,  TOTAL TIME COMPLETED        0.266
```


                         N O D E   O U T P U T

THE FOLLOWING TABLE IS PRINTED FOR NODESET   TIP

NODE	FOOT-NOTE	U1	U2	U3	UR1	UR2	UR3
180		-7.2211E-05	1.1682E-03	-5.2833E-03	0.4312	1.9508E-02	4.0205E-03
280		-7.1617E-05	9.3448E-04	-4.2269E-03	0.4312	1.5718E-02	3.2134E-03
380		-7.1091E-05	7.0085E-04	-3.1705E-03	0.4312	1.1878E-02	2.4094E-03
480		-7.0690E-05	4.6723E-04	-2.1138E-03	0.4312	7.9713E-03	1.6133E-03
580		-7.0440E-05	2.3362E-04	-1.0570E-03	0.4313	3.9981E-03	8.0735E-04
680		-7.0355E-05	2.1575E-11	-1.4379E-10	0.4313	3.6740E-08	-3.6085E-08
780		-7.0440E-05	-2.3362E-04	1.0570E-03	0.4313	-3.9980E-03	-8.0733E-04
880		-7.0690E-05	-4.6723E-04	2.1138E-03	0.4312	-7.9713E-03	-1.6134E-03
980		-7.1092E-05	-7.0085E-04	3.1705E-03	0.4312	-1.1878E-02	-2.4094E-03
1080		-7.1617E-05	-9.3449E-04	4.2270E-03	0.4312	-1.5718E-02	-3.2136E-03
1180		-7.2212E-05	-1.1682E-03	5.2833E-03	0.4312	-1.9509E-02	-4.0205E-03

| MAXIMUM | | -7.0355E-05 | 1.1682E-03 | 5.2833E-03 | 0.4313 | 1.9508E-02 | 4.0205E-03 |
| AT NODE | | 680 | 180 | 1180 | 680 | 180 | 180 |

| MINIMUM | | -7.2212E-05 | -1.1682E-03 | -5.2833E-03 | 0.4312 | -1.9509E-02 | -4.0205E-03 |
| AT NODE | | 1180 | 1180 | 180 | 180 | 1180 | 1180 |

INCREMENT   4 SUMMARY

TIME INCREMENT COMPLETED 1.172E-02, FRACTION OF STEP COMPLETED 0.277
STEP TIME COMPLETED   0.277   , TOTAL TIME COMPLETED   0.277

N O D E   O U T P U T

THE FOLLOWING TABLE IS PRINTED FOR NODESET   TIP

NODE	FOOT-NOTE	U1	U2	U3	UR1	UR2	UR3
180		-7.5743E-05	1.2590E-03	-5.4754E-03	0.4480	2.0337E-02	4.3583E-03
280		-7.5095E-05	1.0072E-03	-4.3806E-03	0.4480	1.6386E-02	3.4833E-03
380		-7.4523E-05	7.5534E-04	-3.2858E-03	0.4480	1.2382E-02	2.6112E-03
480		-7.4084E-05	5.0355E-04	-2.1907E-03	0.4480	8.3105E-03	1.7485E-03
580		-7.3812E-05	2.5178E-04	-1.0954E-03	0.4481	4.1688E-03	8.7519E-04

680	-7.3719E-05	2.0745E-11	-1.3958E-10	0.4481	4.0266E-08	-3.6247E-08
780	-7.3812E-05	-2.5178E-04	1.0954E-03	0.4481	-4.1667E-03	-8.7517E-04
880	-7.4084E-05	-5.0355E-04	2.1907E-03	0.4480	-8.3105E-03	-1.7485E-03
980	-7.4523E-05	-7.5534E-04	3.2858E-03	0.4480	-1.2382E-02	-2.6112E-03
1080	-7.5096E-05	-1.0072E-03	4.3807E-03	0.4480	-1.6387E-02	-3.4835E-03
1180	-7.5744E-05	-1.2590E-03	5.4754E-03	0.4480	-2.0337E-02	-4.3583E-03
MAXIMUM	-7.3719E-05	1.2590E-03	5.4754E-03	0.4481	2.0337E-02	4.3583E-03
AT NODE	680	180	1180	680	180	180
MINIMUM	-7.5744E-05	-1.2590E-03	-5.4754E-03	0.4480	-2.0337E-02	-4.3583E-03
AT NODE	1180	1180	180	180	1180	1180

INCREMENT   5 SUMMARY

TIME INCREMENT COMPLETED 1.758E-02, FRACTION OF STEP COMPLETED 0.295
STEP TIME COMPLETED   0.295   , TOTAL TIME COMPLETED   0.295

N O D E   O U T P U T

THE FOLLOWING TABLE IS PRINTED FOR NODESET   TIP

NODE	FOOT-NOTE	U1	U2	U3	UR1	UR2	UR3
180		-8.1051E-05	1.3988E-03	-5.7557E-03	0.4728	2.1573E-02	4.8853E-03
280		-8.0319E-05	1.1189E-03	-4.6049E-03	0.4728	1.7385E-02	3.9046E-03
380		-7.9673E-05	8.3917E-04	-3.4540E-03	0.4728	1.3138E-02	2.9271E-03
480		-7.9177E-05	5.5943E-04	-2.3028E-03	0.4728	8.8195E-03	1.9601E-03
580		-7.8868E-05	2.7972E-04	-1.1515E-03	0.4728	4.4241E-03	9.8109E-04
680		-7.8764E-05	4.0089E-11	-2.1337E-10	0.4729	4.6539E-08	-3.6193E-08
780		-7.8868E-05	-2.7972E-04	1.1515E-03	0.4728	-4.4240E-03	-9.8107E-04
880		-7.9177E-05	-5.5943E-04	2.3028E-03	0.4728	-8.8195E-03	-1.9602E-03
980		-7.9673E-05	-8.3917E-04	3.4540E-03	0.4728	-1.3138E-02	-2.9271E-03
1080		-8.0320E-05	-1.1190E-03	4.6049E-03	0.4728	-1.7385E-02	-3.9048E-03
1180		-8.1052E-05	-1.3988E-03	5.7558E-03	0.4728	-2.1574E-02	-4.8853E-03
MAXIMUM		-7.8764E-05	1.3988E-03	5.7558E-03	0.4729	2.1573E-02	4.8853E-03
AT NODE		680	180	1180	680	180	180
MINIMUM		-8.1052E-05	-1.3988E-03	-5.7557E-03	0.4728	-2.1574E-02	-4.8853E-03
AT NODE		1180	1180	180	180	1180	1180

126

INCREMENT   6 SUMMARY

TIME INCREMENT COMPLETED 2.637E-02, FRACTION OF STEP COMPLETED 0.321
STEP TIME COMPLETED   0.321   , TOTAL TIME COMPLETED   0.321

N O D E   O U T P U T

THE FOLLOWING TABLE IS PRINTED FOR NODESET   TIP

NODE	FOOT-NOTE	U1	U2	U3	UR1	UR2	UR3
180		-8.9024E-05	1.6153E-03	-6.1587E-03	0.5090	2.3409E-02	5.7185E-03
280		-8.8158E-05	1.2921E-03	-4.9272E-03	0.5090	1.8867E-02	4.5704E-03
380		-8.7391E-05	9.6900E-04	-3.6957E-03	0.5090	1.4260E-02	3.4259E-03
480		-8.6804E-05	6.4597E-04	-2.4640E-03	0.5090	9.5746E-03	2.2945E-03
580		-8.6438E-05	3.2298E-04	-1.2320E-03	0.5090	4.8026E-03	1.1483E-03
680		-8.6314E-05	4.2340E-11	-2.1504E-10	0.5090	5.5345E-08	-3.5637E-08
780		-8.6438E-05	-3.2298E-04	1.2320E-03	0.5090	-4.8026E-03	-1.1483E-03
880		-8.6804E-05	-6.4597E-04	2.4640E-03	0.5090	-9.5746E-03	-2.2946E-03
980		-8.7392E-05	-9.6901E-04	3.6957E-03	0.5090	-1.4260E-02	-3.4259E-03
1080		-8.8158E-05	-1.2921E-03	4.9273E-03	0.5090	-1.8867E-02	-4.5706E-03
1180		-8.9025E-05	-1.6153E-03	6.1587E-03	0.5090	-2.3410E-02	-5.7185E-03
MAXIMUM		-8.6314E-05	1.6153E-03	6.1587E-03	0.5090	2.3409E-02	5.7185E-03
AT NODE		680	180	1180	680	180	180
MINIMUM		-8.9025E-05	-1.6153E-03	-6.1587E-03	0.5090	-2.3410E-02	-5.7185E-03
AT NODE		1180	1180	180	380	1180	1180

INCREMENT   7 SUMMARY

TIME INCREMENT COMPLETED 3.955E-02, FRACTION OF STEP COMPLETED 0.361
STEP TIME COMPLETED   0.361   , TOTAL TIME COMPLETED   0.361

N O D E   O U T P U T

THE FOLLOWING TABLE IS PRINTED FOR NODESET   TIP

NODE	FOOT-NOTE	U1	U2	U3	UR1	UR2	UR3
180		-1.0097E-04	1.9524E-03	-6.7245E-03	0.5611	2.6119E-02	7.0566E-03
280		-9.9886E-05	1.5617E-03	-5.3799E-03	0.5611	2.1053E-02	5.6389E-03
380		-9.8923E-05	1.1711E-03	-4.0352E-03	0.5611	1.5913E-02	4.2258E-03
480		-9.8184E-05	7.8068E-04	-2.6902E-03	0.5611	1.0687E-02	2.8305E-03
580		-9.7725E-05	3.9032E-04	-1.3452E-03	0.5611	5.3599E-03	1.4162E-03
680		-9.7569E-05	4.3919E-11	-2.0855E-10	0.5611	6.9736E-08	-3.3506E-08
780		-9.7725E-05	-3.9032E-04	1.3452E-03	0.5611	-5.3598E-03	-1.4162E-03
880		-9.8185E-05	-7.8068E-04	2.6902E-03	0.5611	-1.0687E-02	-2.8306E-03
980		-9.8924E-05	-1.1711E-03	4.0352E-03	0.5611	-1.5913E-02	-4.2258E-03
1080		-9.9886E-05	-1.5617E-03	5.3799E-03	0.5611	-2.1053E-02	-5.6391E-03
1180		-1.0097E-04	-1.9524E-03	6.7246E-03	0.5611	-2.6119E-02	-7.0567E-03
MAXIMUM		-9.7569E-05	1.9524E-03	6.7246E-03	0.5611	2.6119E-02	7.0566E-03
AT NODE		680	180	1180	1080	180	180
MINIMUM		-1.0097E-04	-1.9524E-03	-6.7245E-03	0.5611	-2.6119E-02	-7.0567E-03
AT NODE		1180	1180	180	680	1180	1180

INCREMENT   8 SUMMARY

TIME INCREMENT COMPLETED 3.955E-02, FRACTION OF STEP COMPLETED 0.400
STEP TIME COMPLETED   0.400   , TOTAL TIME COMPLETED   0.400

N O D E   O U T P U T

THE FOLLOWING TABLE IS PRINTED FOR NODESET   TIP

NODE	FOOT-NOTE	U1	U2	U3	UR1	UR2	UR3
180		-1.1287E-04	2.3003E-03	-7.2462E-03	0.6108	2.8774E-02	8.4905E-03
280		-1.1154E-04	1.8399E-03	-5.7971E-03	0.6108	2.3192E-02	6.7825E-03
380		-1.1036E-04	1.3797E-03	-4.3480E-03	0.6107	1.7530E-02	5.0809E-03
480		-1.0945E-04	9.1964E-04	-2.8988E-03	0.6107	1.1774E-02	3.4032E-03
580		-1.0889E-04	4.5978E-04	-1.4494E-03	0.6107	5.9038E-03	1.7023E-03
680		-1.0870E-04	4.3306E-11	-1.9818E-10	0.6106	8.5419E-08	-2.9839E-08
780		-1.0889E-04	-4.5978E-04	1.4494E-03	0.6107	-5.9037E-03	-1.7022E-03
880		-1.0946E-04	-9.1964E-04	2.8988E-03	0.6107	-1.1774E-02	-3.4033E-03
980		-1.1036E-04	-1.3797E-03	4.3480E-03	0.6108	-1.7530E-02	-5.0810E-03

128

1080	-1.1154E-04	-1.8399E-03	5.7972E-03	0.6108	-2.3192E-02	-6.7827E-03
1180	-1.1287E-04	-2.3003E-03	7.2462E-03	0.6108	-2.8774E-02	-8.4906E-03
MAXIMUM	-1.0870E-04	2.3003E-03	7.2462E-03	0.6108	2.8774E-02	8.4905E-03
AT NODE	680	180	1180	1180	180	180
MINIMUM	-1.1287E-04	-2.3003E-03	-7.2462E-03	0.6106	-2.8774E-02	-8.4906E-03
AT NODE	1180	1180	180	680	1180	1180

INCREMENT   9 SUMMARY

TIME INCREMENT COMPLETED 3.955E-02, FRACTION OF STEP COMPLETED 0.440
STEP TIME COMPLETED   0.440   , TOTAL TIME COMPLETED   0.440

N O D E   O U T P U T

THE FOLLOWING TABLE IS PRINTED FOR NODESET   TIP

NODE	FOOT-NOTE	U1	U2	U3	UR1	UR2	UR3
180		-1.2468E-04	2.6552E-03	-7.7262E-03	0.6582	3.1374E-02	1.0010E-02
280		-1.2308E-04	2.1237E-03	-6.1811E-03	0.6581	2.5284E-02	7.9927E-03
380		-1.2167E-04	1.5924E-03	-4.6359E-03	0.6580	1.9108E-02	5.9846E-03
480		-1.2058E-04	1.0614E-03	-3.0906E-03	0.6579	1.2835E-02	4.0081E-03
580		-1.1991E-04	5.3061E-04	-1.5453E-03	0.6578	6.4340E-03	2.0041E-03
680		-1.1968E-04	3.9592E-11	-1.8168E-10	0.6578	1.0220E-07	-2.4671E-08
780		-1.1991E-04	-5.3061E-04	1.5453E-03	0.6578	-6.4338E-03	-2.0040E-03
880		-1.2058E-04	-1.0614E-03	3.0906E-03	0.6579	-1.2835E-02	-4.0082E-03
980		-1.2167E-04	-1.5924E-03	4.6359E-03	0.6580	-1.9108E-02	-5.9846E-03
1080		-1.2308E-04	-2.1237E-03	6.1811E-03	0.6582	-2.5284E-02	-7.9929E-03
1180		-1.2468E-04	-2.6553E-03	7.7263E-03	0.6582	-3.1374E-02	-1.0010E-02
MAXIMUM		-1.1968E-04	2.6552E-03	7.7263E-03	0.6582	3.1374E-02	1.0010E-02
AT NODE		680	180	1180	1180	180	180
MINIMUM		-1.2468E-04	-2.6553E-03	-7.7262E-03	0.6578	-3.1374E-02	-1.0010E-02
AT NODE		1180	1180	180	680	1180	1180

INCREMENT   10 SUMMARY

TIME INCREMENT COMPLETED 3.955E-02, FRACTION OF STEP COMPLETED 0.479

129

STEP TIME COMPLETED   0.479   , TOTAL TIME COMPLETED   0.479

N O D E   O U T P U T

THE FOLLOWING TABLE IS PRINTED FOR NODESET   TIP

NODE	FOOT-NOTE	U1	U2	U3	UR1	UR2	UR3
180		-1.3638E-04	3.0142E-03	-8.1675E-03	0.7033	3.3919E-02	1.1605E-02
280		-1.3450E-04	2.4107E-03	-6.5340E-03	0.7033	2.7329E-02	9.2618E-03
380		-1.3283E-04	1.8074E-03	-4.9005E-03	0.7031	2.0648E-02	6.9308E-03
480		-1.3155E-04	1.2046E-03	-3.2669E-03	0.7029	1.3869E-02	4.6411E-03
580		-1.3075E-04	6.0220E-04	-1.6334E-03	0.7028	6.9503E-03	2.3196E-03
680		-1.3049E-04	3.1938E-11	-1.5969E-10	0.7027	1.1990E-07	-1.8057E-08
780		-1.3075E-04	-6.0221E-04	1.6334E-03	0.7028	-6.9501E-03	-2.3195E-03
880		-1.3155E-04	-1.2046E-03	3.2669E-03	0.7030	-1.3869E-02	-4.6412E-03
980		-1.3283E-04	-1.8075E-03	4.9005E-03	0.7031	-2.0648E-02	-6.9308E-03
1080		-1.3450E-04	-2.4107E-03	6.5341E-03	0.7033	-2.7329E-02	-9.2621E-03
1180		-1.3638E-04	-3.0143E-03	8.1676E-03	0.7033	-3.3920E-02	-1.1605E-02
MAXIMUM		-1.3049E-04	3.0142E-03	8.1676E-03	0.7033	3.3919E-02	1.1605E-02
AT NODE		680	180	1180	1180	180	180
MINIMUM		-1.3638E-04	-3.0143E-03	-8.1675E-03	0.7027	-3.3920E-02	-1.1605E-02
AT NODE		1180	1180	180	680	1180	1180

INCREMENT   11 SUMMARY

TIME INCREMENT COMPLETED 3.955E-02, FRACTION OF STEP COMPLETED 0.519
STEP TIME COMPLETED   0.519   , TOTAL TIME COMPLETED   0.519

N O D E   O U T P U T

THE FOLLOWING TABLE IS PRINTED FOR NODESET   TIP

NODE	FOOT-NOTE	U1	U2	U3	UR1	UR2	UR3

130

NODE						
180	-1.4795E-04	3.3750E-03	-8.5731E-03	0.7464	3.6409E-02	1.3269E-02
280	-1.4576E-04	2.6990E-03	-6.8584E-03	0.7464	2.9327E-02	1.0583E-02
380	-1.4383E-04	2.0235E-03	-5.1436E-03	0.7461	2.2149E-02	7.9141E-03
480	-1.4234E-04	1.3485E-03	-3.4289E-03	0.7459	1.4871E-02	5.2960E-03
580	-1.4142E-04	6.7409E-04	-1.7144E-03	0.7456	7.4464E-03	2.6442E-03
680	-1.4111E-04	1.7944E-11	-1.2969E-10	0.7456	1.3816E-07	-1.0115E-08
780	-1.4142E-04	-6.7409E-04	1.7144E-03	0.7456	-7.4462E-03	-2.6441E-03
880	-1.4234E-04	-1.3485E-03	3.4289E-03	0.7459	-1.4871E-02	-5.2961E-03
980	-1.4383E-04	-2.0235E-03	5.1436E-03	0.7461	-2.2149E-02	-7.9141E-03
1080	-1.4577E-04	-2.6991E-03	6.8584E-03	0.7464	-2.9327E-02	-1.0583E-02
1180	-1.4795E-04	-3.3750E-03	8.5732E-03	0.7464	-3.6409E-02	-1.3269E-02
MAXIMUM	-1.4111E-04	3.3750E-03	8.5732E-03	0.7464	3.6409E-02	1.3269E-02
AT NODE	680	180	1180	1180	180	180
MINIMUM	-1.4795E-04	-3.3750E-03	-8.5731E-03	0.7456	-3.6409E-02	-1.3269E-02
AT NODE	1180	1180	180	680	1180	1180

INCREMENT   12 SUMMARY

TIME INCREMENT COMPLETED 3.955E-02,   FRACTION OF STEP COMPLETED 0.559
STEP TIME COMPLETED   0.559   ,   TOTAL TIME COMPLETED   0.559

N O D E   O U T P U T

THE FOLLOWING TABLE IS PRINTED FOR NODESET   TIP

NODE	FOOT-NOTE	U1	U2	U3	UR1	UR2	UR3
180		-1.5939E-04	3.7357E-03	-8.9457E-03	0.7876	3.8846E-02	1.4995E-02
280		-1.5688E-04	2.9873E-03	-7.1563E-03	0.7875	3.1278E-02	1.1951E-02
380		-1.5466E-04	2.2394E-03	-5.3670E-03	0.7872	2.3613E-02	8.9302E-03
480		-1.5295E-04	1.4923E-03	-3.5777E-03	0.7869	1.5852E-02	5.9743E-03
580		-1.5189E-04	7.4591E-04	-1.7887E-03	0.7866	7.9337E-03	2.9810E-03
680		-1.5154E-04	-1.1061E-12	-9.3458E-11	0.7865	1.5739E-07	-6.9400E-10
780		-1.5189E-04	-7.4591E-04	1.7887E-03	0.7866	-7.9335E-03	-2.9809E-03
880		-1.5295E-04	-1.4923E-03	3.5777E-03	0.7869	-1.5852E-02	-5.9744E-03
980		-1.5466E-04	-2.2394E-03	5.3670E-03	0.7872	-2.3613E-02	-8.9302E-03
1080		-1.5688E-04	-2.9873E-03	7.1564E-03	0.7875	-3.1278E-02	-1.1951E-02
1180		-1.5939E-04	-3.7357E-03	8.9458E-03	0.7876	-3.8846E-02	-1.4995E-02
MAXIMUM		-1.5154E-04	3.7357E-03	8.9458E-03	0.7876	3.8846E-02	1.4995E-02

AT NODE	680	180	1180	1180	180	180
MINIMUM	-1.5939E-04	-3.7357E-03	-8.9457E-03	0.7865	-3.8846E-02	-1.4995E-02
AT NODE	1180	1180	180	660	1180	1180

INCREMENT   13 SUMMARY

TIME INCREMENT COMPLETED 5.933E-02, FRACTION OF STEP COMPLETED 0.618
STEP TIME COMPLETED   0.618   , TOTAL TIME COMPLETED   0.618

N O D E   O U T P U T

THE FOLLOWING TABLE IS PRINTED FOR NODESET   TIP

NODE	FOOT-NOTE	U1	U2	U3	UR1	UR2	UR3
180		-1.7630E-04	4.2735E-03	-9.4487E-03	0.8461	4.2406E-02	1.7687E-02
280		-1.7327E-04	3.4170E-03	-7.5585E-03	0.8461	3.4124E-02	1.4081E-02
380		-1.7058E-04	2.5612E-03	-5.6684E-03	0.8456	2.5744E-02	1.0509E-02
480		-1.6853E-04	1.7065E-03	-3.7785E-03	0.8452	1.7277E-02	7.0269E-03
580		-1.6725E-04	8.5292E-04	-1.8891E-03	0.8447	8.6409E-03	3.5033E-03
680		-1.6683E-04	5.8492E-11	-2.6264E-10	0.8445	1.8904E-07	1.5857E-08
780		-1.6725E-04	-8.5292E-04	1.8891E-03	0.8447	-8.6406E-03	-3.5032E-03
880		-1.6853E-04	-1.7065E-03	3.7785E-03	0.8452	-1.7277E-02	-7.0270E-03
980		-1.7058E-04	-2.5612E-03	5.6684E-03	0.8456	-2.5744E-02	-1.0509E-02
1080		-1.7327E-04	-3.4170E-03	7.5585E-03	0.8461	-3.4124E-02	-1.4081E-02
1180		-1.7630E-04	-4.2736E-03	9.4488E-03	0.8461	-4.2406E-02	-1.7687E-02
MAXIMUM		-1.6683E-04	4.2735E-03	9.4488E-03	0.8461	4.2406E-02	1.7687E-02
AT NODE		680	180	1180	1180	180	180
MINIMUM		-1.7630E-04	-4.2736E-03	-9.4487E-03	0.8445	-4.2406E-02	-1.7687E-02
AT NODE		1180	1180	180	680	1180	1180

INCREMENT   14 SUMMARY

TIME INCREMENT COMPLETED 5.933E-02, FRACTION OF STEP COMPLETED 0.677
STEP TIME COMPLETED   0.677   , TOTAL TIME COMPLETED   0.677

132

NODE OUTPUT

THE FOLLOWING TABLE IS PRINTED FOR NODESET   TIP

NODE	FOOT-NOTE	U1	U2	U3	UR1	UR2	UR3
180		-1.9289E-04	4.8046E-03	-9.8918E-03	0.9012	4.5855E-02	2.0489E-02
280		-1.8930E-04	3.8412E-03	-7.9127E-03	0.9011	3.6874E-02	1.6292E-02
380		-1.8613E-04	2.8788E-03	-5.9338E-03	0.9005	2.7798E-02	1.2144E-02
480		-1.8370E-04	1.9179E-03	-3.9553E-03	0.8999	1.8649E-02	8.1152E-03
580		-1.8220E-04	9.5846E-04	-1.9774E-03	0.8992	9.3200E-03	4.0425E-03
680		-1.8169E-04	1.5371E-11	-2.2025E-10	0.8990	2.1875E-07	3.4533E-08
780		-1.8220E-04	-9.5846E-04	1.9774E-03	0.8992	-9.3196E-03	-4.0422E-03
880		-1.8370E-04	-1.9179E-03	3.9553E-03	0.8999	-1.8649E-02	-8.1153E-03
980		-1.8613E-04	-2.8788E-03	5.9338E-03	0.9005	-2.7798E-02	-1.2144E-02
1080		-1.8931E-04	-3.8412E-03	7.9127E-03	0.9011	-3.6875E-02	-1.6293E-02
1180		-1.9290E-04	-4.8047E-03	9.8919E-03	0.9012	-4.5856E-02	-2.0489E-02
MAXIMUM		-1.8169E-04	4.8046E-03	9.8919E-03	0.9012	4.5855E-02	2.0489E-02
AT NODE		680	180	1180	1180	180	180
MINIMUM		-1.9290E-04	-4.8047E-03	-9.8918E-03	0.8990	-4.5856E-02	-2.0489E-02
AT NODE		1180	1180	180	680	1180	1180

INCREMENT   15 SUMMARY

TIME INCREMENT COMPLETED 5.933E-02, FRACTION OF STEP COMPLETED 0.737
STEP TIME COMPLETED   0.737   ,   TOTAL TIME COMPLETED   0.737

NODE OUTPUT

THE FOLLOWING TABLE IS PRINTED FOR NODESET   TIP

NODE	FOOT-NOTE	U1	U2	U3	UR1	UR2	UR3
180		-2.0919E-04	5.3267E-03	-1.0282E-02	0.9532	4.9200E-02	2.3388E-02
280		-2.0501E-04	4.2581E-03	-8.2247E-03	0.9530	3.9535E-02	1.8574E-02
380		-2.0130E-04	3.1908E-03	-6.1676E-03	0.9523	2.9779E-02	1.3826E-02

133

480	-1.9848E-04	2.1255E-03	-4.1110E-03	0.9514	1.9970E-02	9.2337E-03
580	-1.9674E-04	1.0621E-03	-2.0552E-03	0.9506	9.9725E-03	4.5955E-03
680	-1.9615E-04	-5.3292E-11	-1.6246E-10	0.9503	2.4816E-07	5.5276E-08
780	-1.9674E-04	-1.0621E-03	2.0552E-03	0.9506	-9.9721E-03	-4.5953E-03
880	-1.9848E-04	-2.1255E-03	4.1110E-03	0.9514	-1.9970E-02	-9.2338E-03
980	-2.0130E-04	-3.1908E-03	6.1676E-03	0.9523	-2.9779E-02	-1.3826E-02
1080	-2.0501E-04	-4.2582E-03	8.2248E-03	0.9530	-3.9535E-02	-1.8574E-02
1180	-2.0919E-04	-5.3268E-03	1.0282E-02	0.9532	-4.9201E-02	-2.3389E-02
MAXIMUM	-1.9615E-04	5.3267E-03	1.0282E-02	0.9532	4.9200E-02	2.3388E-02
AT NODE	680	180	1180	1180	180	180
MINIMUM	-2.0919E-04	-5.3268E-03	-1.0282E-02	0.9503	-4.9201E-02	-2.3389E-02
AT NODE	1180	1180	180	680	1180	1180

INCREMENT   16 SUMMARY

TIME INCREMENT COMPLETED 5.933E-02, FRACTION OF STEP COMPLETED 0.796
STEP TIME COMPLETED   0.796   . TOTAL TIME COMPLETED   0.796

N O D E   O U T P U T

THE FOLLOWING TABLE IS PRINTED FOR NODESET   TIP

NODE	FOOT-NOTE	U1	U2	U3	UR1	UR2	UR3
180		-2.2520E-04	5.8384E-03	-1.0626E-02	1.002	5.2445E-02	2.6374E-02
280		-2.2038E-04	4.6666E-03	-8.4995E-03	1.002	4.2110E-02	2.0917E-02
380		-2.1613E-04	3.4963E-03	-6.3735E-03	1.001	3.1691E-02	1.5549E-02
480		-2.1289E-04	2.3287E-03	-4.2481E-03	1.000	2.1244E-02	1.0378E-02
580		-2.1089E-04	1.1635E-03	-2.1237E-03	0.9991	1.0600E-02	5.1603E-03
680		-2.1022E-04	-1.5843E-10	-7.9533E-11	0.9988	2.7661E-07	7.7674E-08
780		-2.1089E-04	-1.1635E-03	2.1237E-03	0.9991	-1.0600E-02	-5.1600E-03
880		-2.1289E-04	-2.3287E-03	4.2482E-03	1.000	-2.1244E-02	-1.0378E-02
980		-2.1613E-04	-3.4964E-03	6.3735E-03	1.001	-3.1692E-02	-1.5549E-02
1080		-2.2039E-04	-4.6667E-03	8.4996E-03	1.002	-4.2110E-02	-2.0918E-02
1180		-2.2520E-04	-5.8385E-03	1.0626E-02	1.002	-5.2446E-02	-2.6375E-02
MAXIMUM		-2.1022E-04	5.8384E-03	1.0626E-02	1.002	5.2445E-02	2.6374E-02
AT NODE		680	180	1180	1180	180	180
MINIMUM		-2.2520E-04	-5.8385E-03	-1.0626E-02	0.9988	-5.2446E-02	-2.6375E-02
AT NODE		1180	1180	180	680	1180	1180

INCREMENT   17 SUMMARY

TIME INCREMENT COMPLETED 5.933E-02, FRACTION OF STEP COMPLETED 0.855
STEP TIME COMPLETED   0.855   , TOTAL TIME COMPLETED   0.855

N O D E   O U T P U T

THE FOLLOWING TABLE IS PRINTED FOR NODESET   TIP

NODE	FOOT-NOTE	U1	U2	U3	UR1	UR2	UR3
180		-2.4094E-04	6.3388E-03	-1.0929E-02	1.049	5.5597E-02	2.9439E-02
280		-2.3546E-04	5.0660E-03	-8.7415E-03	1.049	4.4605E-02	2.3316E-02
380		-2.3061E-04	3.7950E-03	-6.5547E-03	1.048	3.3540E-02	1.7307E-02
480		-2.2695E-04	2.5273E-03	-4.3689E-03	1.046	2.2474E-02	1.1544E-02
580		-2.2468E-04	1.2626E-03	-2.1840E-03	1.045	1.1205E-02	5.7352E-03
680		-2.2393E-04	-3.0439E-10	1.5751E-11	1.045	3.0372E-07	1.0136E-07
780		-2.2468E-04	-1.2626E-03	2.1840E-03	1.045	-1.1204E-02	-5.7349E-03
880		-2.2695E-04	-2.5273E-03	4.3689E-03	1.046	-2.2473E-02	-1.1544E-02
980		-2.3062E-04	-3.7950E-03	6.5548E-03	1.048	-3.3540E-02	-1.7307E-02
1080		-2.3546E-04	-5.0661E-03	8.7415E-03	1.049	-4.4606E-02	-2.3317E-02
1180		-2.4094E-04	-6.3389E-03	1.0929E-02	1.049	-5.5598E-02	-2.9439E-02

MAXIMUM		-2.2393E-04	6.3388E-03	1.0929E-02	1.049	5.5597E-02	2.9439E-02
AT NODE		680	180	1180	1180	180	180
MINIMUM		-2.4094E-04	-6.3389E-03	-1.0929E-02	1.045	-5.5598E-02	-2.9439E-02
AT NODE		1180	1180	180	680	1180	1180

INCREMENT   18 SUMMARY

TIME INCREMENT COMPLETED 8.899E-02, FRACTION OF STEP COMPLETED 0.944
STEP TIME COMPLETED   0.944   , TOTAL TIME COMPLETED   0.944

N O D E   O U T P U T

135

THE FOLLOWING TABLE IS PRINTED FOR NODESET   TIP

NODE	FOOT-NOTE	U1	U2	U3	UR1	UR2	UR3
180		-2.6407E-04	7.0674E-03	-1.1315E-02	1.115	6.0159E-02	3.4167E-02
280		-2.5753E-04	5.6472E-03	-9.0506E-03	1.115	4.8208E-02	2.7004E-02
380		-2.5176E-04	4.2294E-03	-6.7864E-03	1.113	3.6200E-02	2.0002E-02
480		-2.4741E-04	2.8161E-03	-4.5231E-03	1.112	2.4241E-02	1.3329E-02
580		-2.4473E-04	1.4067E-03	-2.2611E-03	1.110	1.2071E-02	6.6135E-03
680		-2.4384E-04	-6.2021E-10	1.7863E-10	1.109	3.4063E-07	1.3830E-07
780		-2.4473E-04	-1.4067E-03	2.2611E-03	1.110	-1.2071E-02	-6.6131E-03
880		-2.4741E-04	-2.8161E-03	4.5231E-03	1.112	-2.4241E-02	-1.3330E-02
980		-2.5177E-04	-4.2295E-03	6.7864E-03	1.113	-3.6201E-02	-2.0002E-02
1080		-2.5753E-04	-5.6473E-03	9.0506E-03	1.115	-4.8208E-02	-2.7005E-02
1180		-2.6408E-04	-7.0675E-03	1.1315E-02	1.115	-6.0161E-02	-3.4167E-02
MAXIMUM		-2.4384E-04	7.0674E-03	1.1315E-02	1.115	6.0159E-02	3.4167E-02
AT NODE		680	180	1180	1180	180	180
MINIMUM		-2.6408E-04	-7.0675E-03	-1.1315E-02	1.109	-6.0161E-02	-3.4167E-02
AT NODE		1180	1180	180	680	1180	1180

INCREMENT   19 SUMMARY

TIME INCREMENT COMPLETED 5.579E-02, FRACTION OF STEP COMPLETED   1.00
STEP TIME COMPLETED   1.00   , TOTAL TIME COMPLETED   1.00

N O D E   O U T P U T

THE FOLLOWING TABLE IS PRINTED FOR NODESET   TIP

NODE	FOOT-NOTE	U1	U2	U3	UR1	UR2	UR3
180		-2.7831E-04	7.5105E-03	-1.1521E-02	1.154	6.2925E-02	3.7204E-02
280		-2.7107E-04	6.0005E-03	-9.2155E-03	1.154	5.0386E-02	2.9366E-02
380		-2.6469E-04	4.4934E-03	-6.9100E-03	1.152	3.7805E-02	2.1723E-02
480		-2.5989E-04	2.9914E-03	-4.6055E-03	1.150	2.5305E-02	1.4468E-02
580		-2.5694E-04	1.4941E-03	-2.3022E-03	1.148	1.2592E-02	7.1725E-03
680		-2.5596E-04	-9.0758E-10	3.1977E-10	1.148	3.6041E-07	1.6163E-07
780		-2.5694E-04	-1.4941E-03	2.3022E-03	1.148	-1.2591E-02	-7.1720E-03

136

880	-2.5989E-04	-2.9915E-03	4.6055E-03	1.150	-2.5305E-02 -1.4468E-02
980	-2.6469E-04	-4.4935E-03	6.9100E-03	1.152	-3.7805E-02 -2.1723E-02
1080	-2.7107E-04	-6.0006E-03	9.2155E-03	1.154	-5.0387E-02 -2.9367E-02
1180	-2.7831E-04	-7.5106E-03	1.1521E-02	1.154	-6.2926E-02 -3.7204E-02

```
MAXIMUM      -2.5596E-04  7.5105E-03  1.1521E-02  1.154    6.2925E-02  3.7204E-02
AT NODE          680         180        1180       1180       180         180


MINIMUM      -2.7831E-04 -7.5106E-03 -1.1521E-02  1.148   -6.2926E-02 -3.7204E-02
AT NODE         1180        1180         180        680      1180        1180
1
```

   FOR USE AT GEORGIA INSTITUTE OF TECHNOLOGY UNDER ACADEMIC LICENSE FROM HKS, INC.

   Extension-Twist Coupled Specimen - Temperature Variation
STEP   2 INCREMENT   1

TIME COMPLETED IN THIS STEP   0.

                    S T E P   2   S T A T I C   A N A L Y S I S

        AUTOMATIC TIME CONTROL WITH -
             A SUGGESTED INITIAL TIME INCREMENT OF   1.00
             AND A TOTAL TIME PERIOD OF   1.00
             THE MINIMUM TIME INCREMENT ALLOWED IS   1.000E-05
             THE MAXIMUM TIME INCREMENT ALLOWED IS   1.00

        LARGE DISPLACEMENT THEORY WILL BE USED

                          INCREMENT   1 SUMMARY

    TIME INCREMENT COMPLETED 0.500 , FRACTION OF STEP COMPLETED 0.500
    STEP TIME COMPLETED   0.500 , TOTAL TIME COMPLETED   1.50

                        N O D E   O U T P U T

    THE FOLLOWING TABLE IS PRINTED FOR NODESET   TIP

NODE	FOOT-NOTE	U1	U2	U3	UR1	UR2	UR3
180		-1.9161E-04	5.7707E-03	-1.0568E-02	0.9971	4.9246E-02	2.5166E-02
280		-1.8805E-04	4.6087E-03	-8.4511E-03	0.9977	3.9062E-02	1.9463E-02
380		-1.8414E-04	3.4490E-03	-6.3348E-03	0.9958	2.8826E-02	1.3932E-02
480		-1.8119E-04	2.2951E-03	-4.2210E-03	0.9937	1.8989E-02	9.1449E-03
580		-1.7934E-04	1.1459E-03	-2.1096E-03	0.9916	9.3413E-03	4.5126E-03
680		-1.7884E-04	3.8232E-08	-8.0682E-08	0.9911	1.9482E-06	5.3070E-07
780		-1.7934E-04	-1.1459E-03	2.1094E-03	0.9916	-9.3377E-03	-4.5112E-03
880		-1.8118E-04	-2.2950E-03	4.2208E-03	0.9937	-1.8986E-02	-9.1440E-03
980		-1.8413E-04	-3.4489E-03	6.3347E-03	0.9958	-2.8823E-02	-1.3931E-02
1080		-1.8804E-04	-4.6087E-03	8.4510E-03	0.9977	-3.9059E-02	-1.9463E-02
1180		-1.9161E-04	-5.7707E-03	1.0568E-02	0.9971	-4.9243E-02	-2.5165E-02
MAXIMUM		-1.7884E-04	5.7707E-03	1.0568E-02	0.9977	4.9246E-02	2.5166E-02
AT NODE		680	180	1180	1080	180	180
MINIMUM		-1.9161E-04	-5.7707E-03	-1.0568E-02	0.9911	-4.9243E-02	-2.5165E-02
AT NODE		180	1180	180	680	1180	1180

INCREMENT   2 SUMMARY

TIME INCREMENT COMPLETED 0.125   , FRACTION OF STEP COMPLETED 0.625
STEP TIME COMPLETED   0.625   , TOTAL TIME COMPLETED   1.62

N O D E   O U T P U T

THE FOLLOWING TABLE IS PRINTED FOR NODESET   TIP

NODE	FOOT-NOTE	U1	U2	U3	UR1	UR2	UR3
180		-1.7131E-04	5.3714E-03	-1.0295E-02	0.9587	4.6309E-02	2.2834E-02
280		-1.6849E-04	4.2893E-03	-8.2326E-03	0.9596	3.6724E-02	1.7588E-02
380		-1.6503E-04	3.2094E-03	-6.1705E-03	0.9576	2.6970E-02	1.2451E-02
480		-1.6241E-04	2.1354E-03	-4.1112E-03	0.9555	1.7691E-02	8.1423E-03
580		-1.6076E-04	1.0661E-03	-2.0546E-03	0.9533	8.6722E-03	4.0135E-03
680		-1.6035E-04	1.6635E-08	-1.2467E-08	0.9529	1.9207E-06	7.2094E-07
780		-1.6076E-04	-1.0661E-03	2.0545E-03	0.9533	-8.6686E-03	-4.0117E-03
880		-1.6241E-04	-2.1354E-03	4.1111E-03	0.9556	-1.7687E-02	-8.1411E-03
980		-1.6503E-04	-3.2094E-03	6.1705E-03	0.9576	-2.6967E-02	-1.2449E-02
1080		-1.6849E-04	-4.2893E-03	8.2326E-03	0.9596	-3.6721E-02	-1.7587E-02
1180		-1.7131E-04	-5.3714E-03	1.0295E-02	0.9587	-4.6307E-02	-2.2833E-02

138

	MAXIMUM	-1.6035E-04	5.3714E-03	1.0295E-02	0.9596	4.6309E-02	2.2834E-02
	AT NODE	680	180	1180	1080	180	180
	MINIMUM	-1.7131E-04	-5.3714E-03	-1.0295E-02	0.9529	-4.6307E-02	-2.2833E-02
	AT NODE	1180	1180	180	680	1180	1180

INCREMENT   3 SUMMARY

TIME INCREMENT COMPLETED 0.125   ,   FRACTION OF STEP COMPLETED   0.750
STEP TIME COMPLETED   0.750   ,   TOTAL TIME COMPLETED   1.75

N O D E   O U T P U T

THE FOLLOWING TABLE IS PRINTED FOR NODESET   TIP

NODE	FOOT-NOTE	U1	U2	U3	UR1	UR2	UR3
180		-1.5158E-04	4.9900E-03	-1.0013E-02	0.9211	4.3531E-02	2.0728E-02
280		-1.4945E-04	3.9843E-03	-8.0067E-03	0.9222	3.4548E-02	1.5908E-02
380		-1.4640E-04	2.9808E-03	-6.0007E-03	0.9202	2.5243E-02	1.1122E-02
480		-1.4407E-04	1.9830E-03	-3.9977E-03	0.9181	1.6486E-02	7.2466E-03
580		-1.4259E-04	9.8990E-04	-1.9977E-03	0.9158	8.0513E-03	3.5684E-03
680		-1.4226E-04	1.5527E-08	-1.2434E-08	0.9155	1.9656E-06	6.9007E-07
780		-1.4259E-04	-9.8987E-04	1.9977E-03	0.9158	-8.0477E-03	-3.5667E-03
880		-1.4407E-04	-1.9830E-03	3.9977E-03	0.9181	-1.6482E-02	-7.2454E-03
980		-1.4640E-04	-2.9808E-03	6.0007E-03	0.9202	-2.5240E-02	-1.1121E-02
1080		-1.4945E-04	-3.9844E-03	8.0067E-03	0.9222	-3.4545E-02	-1.5908E-02
1180		-1.5159E-04	-4.9900E-03	1.0013E-02	0.9211	-4.3529E-02	-2.0727E-02

	MAXIMUM	-1.4226E-04	4.9900E-03	1.0013E-02	0.9222	4.3531E-02	2.0728E-02
	AT NODE	680	180	1180	1080	180	180
	MINIMUM	-1.5159E-04	-4.9900E-03	-1.0013E-02	0.9155	-4.3529E-02	-2.0727E-02
	AT NODE	1180	1180	180	680	1180	1180

INCREMENT   4 SUMMARY

TIME INCREMENT COMPLETED 0.125   ,   FRACTION OF STEP COMPLETED   0.875
STEP TIME COMPLETED   0.875   ,   TOTAL TIME COMPLETED   1.88

N O D E   O U T P U T

THE FOLLOWING TABLE IS PRINTED FOR NODESET   TIP

NODE	FOOT-NOTE	U1	U2	U3	UR1	UR2	UR3
180		-1.3237E-04	4.6255E-03	-9.7218E-03	0.8840	4.0902E-02	1.8826E-02
280		-1.3087E-04	3.6929E-03	-7.7734E-03	0.8853	3.2524E-02	1.4403E-02
380		-1.2819E-04	2.7623E-03	-5.8254E-03	0.8833	2.3636E-02	9.9290E-03
480		-1.2612E-04	1.8374E-03	-3.8806E-03	0.8813	1.5368E-02	6.4460E-03
580		-1.2478E-04	9.1713E-04	-1.9391E-03	0.8789	7.4754E-03	3.1716E-03
680		-1.2452E-04	1.4456E-08	-1.2360E-08	0.8786	1.9896E-06	6.4944E-07
780		-1.2478E-04	-9.1710E-04	1.9391E-03	0.8789	-7.4716E-03	-3.1699E-03
880		-1.2612E-04	-1.8374E-03	3.8806E-03	0.8813	-1.5364E-02	-6.4449E-03
980		-1.2819E-04	-2.7623E-03	5.8254E-03	0.8833	-2.3633E-02	-9.9276E-03
1080		-1.3087E-04	-3.6930E-03	7.7734E-03	0.8853	-3.2521E-02	-1.4403E-02
1180		-1.3237E-04	-4.6255E-03	9.7218E-03	0.8840	-4.0899E-02	-1.8825E-02
MAXIMUM		-1.2452E-04	4.6255E-03	9.7218E-03	0.8853	4.0902E-02	1.8826E-02
AT NODE		680	180	1180	1080	180	180
MINIMUM		-1.3237E-04	-4.6255E-03	-9.7218E-03	0.8786	-4.0899E-02	-1.8825E-02
AT NODE		1180	1180	180	680	1180	1180

INCREMENT   5 SUMMARY

TIME INCREMENT COMPLETED	0.125	,	FRACTION OF STEP COMPLETED	1.00
STEP TIME COMPLETED	1.00	,	TOTAL TIME COMPLETED	2.00

N O D E   O U T P U T

THE FOLLOWING TABLE IS PRINTED FOR NODESET   TIP

NODE	FOOT-NOTE	U1	U2	U3	UR1	UR2	UR3
180		-1.1365E-04	4.2783E-03	-9.4229E-03	0.8475	3.8408E-02	1.7110E-02

140

```
   280    -1.1276E-04   3.4154E-03  -7.5341E-03   0.8491        3.0640E-02   1.3055E-02
   380    -1.1040E-04   2.5543E-03  -5.6456E-03   0.8470        2.2142E-02   8.8584E-03
   480    -1.0856E-04   1.6988E-03  -3.7605E-03   0.8451        1.4336E-02   5.7335E-03
   580    -1.0735E-04   8.4785E-04  -1.8790E-03   0.8426        6.9439E-03   2.8193E-03
   680    -1.0716E-04   1.3426E-08  -1.2244E-08   0.8424        1.9950E-06   6.0118E-07
   780    -1.0735E-04  -8.4783E-04   1.8789E-03   0.8426       -6.9402E-03  -2.8177E-03
   880    -1.0856E-04  -1.6988E-03   3.7605E-03   0.8451       -1.4332E-02  -5.7325E-03
   980    -1.1040E-04  -2.5543E-03   5.6456E-03   0.8471       -2.2139E-02  -8.8571E-03
  1080    -1.1276E-04  -3.4154E-03   7.5342E-03   0.8491       -3.0637E-02  -1.3055E-02
  1180    -1.1365E-04  -4.2784E-03   9.4229E-03   0.8476       -3.8405E-02  -1.7109E-02

MAXIMUM   -1.0716E-04   4.2783E-03   9.4229E-03   0.8491        3.8408E-02   1.7110E-02
AT NODE       680          180         1180        1080            180         180


MINIMUM   -1.1365E-04  -4.2784E-03  -9.4229E-03   0.8424       -3.8405E-02  -1.7109E-02
AT NODE      1180         1180          180         680           1180        1180
1
```

    Extension-Twist Coupled Specimen - Temperature Variation
STEP   3 INCREMENT   1

TIME COMPLETED IN THIS STEP   0.

            S T E P   3   S T A T I C   A N A L Y S I S

        AUTOMATIC TIME CONTROL WITH -
            A SUGGESTED INITIAL TIME INCREMENT OF   1.00
            AND A TOTAL TIME PERIOD OF   1.00
            THE MINIMUM TIME INCREMENT ALLOWED IS   1.000E-05
            THE MAXIMUM TIME INCREMENT ALLOWED IS   1.00

        LARGE DISPLACEMENT THEORY WILL BE USED

                INCREMENT   1 SUMMARY

TIME INCREMENT COMPLETED   1.00   , FRACTION OF STEP COMPLETED   1.00
STEP TIME COMPLETED   1.00   , TOTAL TIME COMPLETED   3.00

            N O D E   O U T P U T

THE FOLLOWING TABLE IS PRINTED FOR NODESET   TIP

NODE	FOOT-NOTE	U1	U2	U3	UR1	UR2	UR3
180		1.9858E-05	2.1291E-03	-6.9265E-03	0.5838	2.2264E-02	8.3677E-03
280		1.6910E-05	1.6984E-03	-5.5376E-03	0.5872	1.9448E-02	6.3225E-03
380		1.7493E-05	1.2683E-03	-4.1474E-03	0.5851	1.3284E-02	3.4515E-03
480		1.8143E-05	8.4270E-04	-2.7607E-03	0.5840	8.2906E-03	2.2006E-03
580		1.8774E-05	4.2019E-04	-1.3786E-03	0.5809	3.8321E-03	1.1021E-03
680		1.8561E-05	6.9474E-09	-1.0271E-08	0.5813	1.7422E-06	1.7759E-07
780		1.8774E-05	-4.2018E-04	1.3785E-03	0.5809	-3.8289E-03	-1.1011E-03
880		1.8143E-05	-8.4269E-04	2.7607E-03	0.5840	-8.2873E-03	-2.2004E-03
980		1.7493E-05	-1.2683E-03	4.1474E-03	0.5851	-1.3282E-02	-3.4507E-03
1080		1.6910E-05	-1.6984E-03	5.5376E-03	0.5872	-1.9446E-02	-6.3228E-03
1180		1.9859E-05	-2.1291E-03	6.9266E-03	0.5838	-2.2261E-02	-8.3672E-03
MAXIMUM		1.9859E-05	2.1291E-03	6.9266E-03	0.5872	2.2264E-02	8.3677E-03
AT NODE		1180	180	1180	1080	180	180
MINIMUM		1.6910E-05	-2.1291E-03	-6.9265E-03	0.5809	-2.2261E-02	-8.3672E-03
AT NODE		280	1180	180	580	1180	1180

1

ABAQUS VERSION 5.5-1   DATE 01-OCT-96   TIME 11:36:13   PAGE   4
FOR USE AT GEORGIA INSTITUTE OF TECHNOLOGY UNDER ACADEMIC LICENSE FROM HKS, INC.

Extension-Twist Coupled Specimen - Temperature Variation
STEP   4 INCREMENT   1

TIME COMPLETED IN THIS STEP   0.

S T E P   4   S T A T I C   A N A L Y S I S

AUTOMATIC TIME CONTROL WITH -
       A SUGGESTED INITIAL TIME INCREMENT OF   1.00
       AND A TOTAL TIME PERIOD OF   1.00
       THE MINIMUM TIME INCREMENT ALLOWED IS   1.000E-05
       THE MAXIMUM TIME INCREMENT ALLOWED IS   1.00

       LARGE DISPLACEMENT THEORY WILL BE USED

INCREMENT 1 SUMMARY

TIME INCREMENT COMPLETED 1.00 , FRACTION OF STEP COMPLETED 1.00
STEP TIME COMPLETED   1.00 , TOTAL TIME COMPLETED   4.00

N O D E   O U T P U T

THE FOLLOWING TABLE IS PRINTED FOR NODESET   TIP

NODE	FOOT-NOTE	U1	U2	U3	UR1	UR2	UR3
180		1.3005E-04	9.4190E-04	-4.6266E-03	0.3752	1.0650E-02	5.0845E-03
280		1.2415E-04	7.5066E-04	-3.7013E-03	0.3805	1.2822E-02	3.7179E-03
380		1.2372E-04	5.5954E-04	-2.7720E-03	0.3787	8.0813E-03	1.2291E-03
480		1.2375E-04	3.7158E-04	-1.8443E-03	0.3789	4.8960E-03	8.3633E-04
580		1.2415E-04	1.8515E-04	-9.2033E-04	0.3756	2.0959E-03	4.8249E-04
680		1.2365E-04	3.2188E-09	-7.4412E-09	0.3767	1.2856E-06	-1.4936E-07
780		1.2415E-04	-1.8514E-04	9.2032E-04	0.3756	-2.0935E-03	-4.8202E-04
880		1.2375E-04	-3.7158E-04	1.8443E-03	0.3789	-4.8936E-03	-8.3666E-04
980		1.2372E-04	-5.5954E-04	2.7720E-03	0.3787	-8.0793E-03	-1.2286E-03
1080		1.2415E-04	-7.5067E-04	3.7013E-03	0.3805	-1.2821E-02	-3.7188E-03
1180		1.3005E-04	-9.4191E-04	4.6266E-03	0.3752	-1.0648E-02	-5.0844E-03

MAXIMUM	1.3005E-04	9.4190E-04	4.6266E-03	0.3805	1.2822E-02	5.0845E-03
AT NODE	1180	180	1180	1080	280	180

MINIMUM	1.2365E-04	-9.4191E-04	-4.6266E-03	0.3752	-1.2821E-02	-5.0844E-03
AT NODE	680	1180	180	180	1080	1180

1

  Extension-Twist Coupled Specimen - Temperature Variation
STEP   5 INCREMENT   1

TIME COMPLETED IN THIS STEP   0.

S T E P   5   S T A T I C   A N A L Y S I S

```
AUTOMATIC TIME CONTROL WITH -
        A SUGGESTED INITIAL TIME INCREMENT OF          1.00
        AND A TOTAL TIME PERIOD OF                     1.00
        THE MINIMUM TIME INCREMENT ALLOWED IS          1.000E-05
        THE MAXIMUM TIME INCREMENT ALLOWED IS          1.00

        LARGE DISPLACEMENT THEORY WILL BE USED


                        INCREMENT    1 SUMMARY


TIME INCREMENT COMPLETED   1.00   ,  FRACTION OF STEP COMPLETED   1.00
STEP TIME COMPLETED        1.00   ,  TOTAL TIME COMPLETED         5.00




                        N O D E   O U T P U T



        THE FOLLOWING TABLE IS PRINTED FOR NODESET      TIP


        NODE FOOT-   U1          U2          U3          UR1       UR2          UR3
             NOTE


         180    2.2489E-04  3.7283E-04 -2.7540E-03  0.2161   1.6697E-03  4.4616E-03
         280    2.1639E-04  2.9610E-04 -2.2088E-03  0.2234   8.7619E-03  2.8908E-03
         380    2.1523E-04  2.1971E-04 -1.6562E-03  0.2220   4.9111E-03  3.4059E-04
         480    2.1484E-04  1.4606E-04 -1.1020E-03  0.2240   2.9603E-03  3.4410E-04
         580    2.1513E-04  7.2807E-05 -5.4947E-04  0.2207   1.1160E-03  2.9884E-04
         680    2.1439E-04  1.3335E-09 -4.6635E-09  0.2225   8.0666E-07 -3.5675E-07
         780    2.1513E-04 -7.2805E-05  5.4946E-04  0.2207  -1.1145E-03 -2.9866E-04
         880    2.1484E-04 -1.4606E-04  1.1020E-03  0.2240  -2.9588E-03 -3.4481E-04
         980    2.1523E-04 -2.1971E-04  1.6562E-03  0.2220  -4.9099E-03 -3.4042E-04
        1080    2.1639E-04 -2.9610E-04  2.2088E-03  0.2234  -8.7612E-03 -2.8921E-03
        1180    2.2490E-04 -3.7284E-04  2.7540E-03  0.2161  -1.6683E-03 -4.4619E-03

MAXIMUM      2.2490E-04  3.7283E-04  2.7540E-03  0.2240   8.7619E-03  4.4616E-03
AT NODE       1180        180        1180         880       280         180

MINIMUM      2.1439E-04 -3.7284E-04 -2.7540E-03  0.2161  -8.7612E-03 -4.4619E-03
AT NODE        680       1180         180         180      1080        1180
1
```

Extension-Twist Coupled Specimen - Temperature Variation
STEP   6 INCREMENT   1

TIME COMPLETED IN THIS STEP   0.

                        S T E P   6   S T A T I C   A N A L Y S I S

        AUTOMATIC TIME CONTROL WITH -
            A SUGGESTED INITIAL TIME INCREMENT OF   1.00
            AND A TOTAL TIME PERIOD OF   1.00
            THE MINIMUM TIME INCREMENT ALLOWED IS   1.000E-05
            THE MAXIMUM TIME INCREMENT ALLOWED IS   1.00

        LARGE DISPLACEMENT THEORY WILL BE USED

                        INCREMENT   1 SUMMARY

TIME INCREMENT COMPLETED   1.00   , FRACTION OF STEP COMPLETED   1.00
STEP TIME COMPLETED   1.00   , TOTAL TIME COMPLETED   6.00

                        N O D E   O U T P U T

    THE FOLLOWING TABLE IS PRINTED FOR NODESET   TIP

NODE	FOOT-NOTE	U1	U2	U3	UR1	UR2	UR3
180		3.1044E-04	1.4051E-04	-1.2874E-03	9.4272E-02	-5.6914E-03	5.1711E-03
280		2.9949E-04	1.0959E-04	-1.0420E-03	0.1035	6.2209E-03	2.8355E-03
380		2.9772E-04	7.9867E-05	-7.8569E-04	0.1027	2.9233E-03	1.0928E-05
480		2.9699E-04	5.3372E-05	-5.2363E-04	0.1066	1.8580E-03	1.9694E-04
580		2.9721E-04	2.6732E-05	-2.6081E-04	0.1034	5.6416E-04	2.8366E-04
680		2.9622E-04	5.2184E-10	-2.2437E-09	0.1060	3.5343E-07	-4.8176E-07
780		2.9721E-04	-2.6731E-05	2.6081E-04	0.1034	-5.6345E-04	-2.8364E-04
880		2.9699E-04	-5.3372E-05	5.2362E-04	0.1066	-1.8574E-03	-1.9788E-04
980		2.9772E-04	-7.9867E-05	7.8569E-04	0.1027	-2.9228E-03	-1.0870E-05
1080		2.9949E-04	-1.0959E-04	1.0420E-03	0.1035	-6.2210E-03	-2.8371E-03
1180		3.1044E-04	-1.4052E-04	1.2874E-03	9.4273E-02	5.6923E-03	-5.1716E-03
MAXIMUM		3.1044E-04	1.4051E-04	1.2874E-03	0.1066	6.2209E-03	5.1711E-03

                                145

```
AT NODE        1180        180        1180        880        280        180

MINIMUM        2.9622E-04 -1.4052E-04 -1.2874E-03  9.4272E-02 -6.2210E-03 -5.1716E-03
AT NODE         680        1180        180        180        1080        1180
1
```

   Extension-Twist Coupled Specimen - Temperature Variation
STEP   7 INCREMENT   1

TIME COMPLETED IN THIS STEP   0.

S T E P   7   S T A T I C   A N A L Y S I S

   AUTOMATIC TIME CONTROL WITH -
      A SUGGESTED INITIAL TIME INCREMENT OF   1.00
      AND A TOTAL TIME PERIOD OF   1.00
      THE MINIMUM TIME INCREMENT ALLOWED IS   1.000E-05
      THE MAXIMUM TIME INCREMENT ALLOWED IS   1.00

   LARGE DISPLACEMENT THEORY WILL BE USED

INCREMENT   1 SUMMARY

TIME INCREMENT COMPLETED 0.250   , FRACTION OF STEP COMPLETED 0.250
STEP TIME COMPLETED   0.250   , TOTAL TIME COMPLETED   6.25

N O D E   O U T P U T

THE FOLLOWING TABLE IS PRINTED FOR NODESET   TIP

NODE	FOOT-NOTE	U1	U2	U3	UR1	UR2	UR3
180		3.3085E-04	1.1388E-04	-9.7396E-04	6.8275E-02	-7.3514E-03	5.4743E-03
280		3.1930E-04	8.7945E-05	-7.9295E-04	7.7949E-02	5.7498E-03	2.8850E-03
380		3.1739E-04	6.3498E-05	-6.0006E-04	7.7396E-02	2.5516E-03	-2.7253E-05

NODE						
480	3.1658E-04	4.2521E-05	-4.0043E-04	8.1803E-02	1.6692E-03	1.8574E-04
580	3.1678E-04	2.1352E-05	-1.9936E-04	7.8556E-02	4.7036E-04	2.9203E-04
680	3.1574E-04	4.2567E-10	-1.7011E-09	8.1375E-02	2.4567E-07	-5.0405E-07
780	3.1678E-04	-2.1351E-05	1.9935E-04	7.8556E-02	-4.6986E-04	-2.9203E-04
880	3.1658E-04	-4.2521E-05	4.0043E-04	8.1803E-02	-1.6687E-03	-1.8673E-04
980	3.1739E-04	-6.3497E-05	6.0006E-04	7.7397E-02	-2.5512E-03	2.7295E-05
1080	3.1931E-04	-8.7945E-05	7.9295E-04	7.7950E-02	-5.7501E-03	-2.8866E-03
1180	3.3085E-04	-1.1388E-04	9.7396E-04	6.8276E-02	7.3522E-03	-5.4748E-03

```
MAXIMUM       3.3085E-04   1.1388E-04   9.7396E-04   8.1803E-02   7.3522E-03   5.4743E-03
AT NODE       1180         180          1180         880          1180         180

MINIMUM       3.1574E-04  -1.1388E-04  -9.7396E-04   6.8275E-02  -7.3514E-03  -5.4748E-03
AT NODE       680          1180         180          180          180          1180
```

INCREMENT   2 SUMMARY

```
TIME INCREMENT COMPLETED  0.250    ,  FRACTION OF STEP COMPLETED  0.500
STEP TIME COMPLETED       0.500    ,  TOTAL TIME COMPLETED        6.50
```

N O D E   O U T P U T

THE FOLLOWING TABLE IS PRINTED FOR NODESET   TIP

NODE	FOOT-NOTE	U1	U2	U3	UR1	UR2	UR3
180		3.5095E-04	9.6113E-05	-6.7885E-04	4.3772E-02	-8.9527E-03	5.8142E-03
280		3.3882E-04	7.3323E-05	-5.5858E-04	5.3935E-02	5.3311E-03	2.9510E-03
380		3.3676E-04	5.2346E-05	-4.2549E-04	5.3552E-02	2.2189E-03	-5.4201E-05
480		3.3587E-04	3.5123E-05	-2.8462E-04	5.8463E-02	1.5072E-03	1.8068E-04
580		3.3606E-04	1.7690E-05	-1.4160E-04	5.5249E-02	3.9016E-04	3.0322E-04
680		3.3496E-04	3.6090E-10	-1.1823E-09	5.8276E-02	1.4022E-07	-5.2355E-07
780		3.3606E-04	-1.7689E-05	1.4160E-04	5.5249E-02	-3.8985E-04	-3.0324E-04
880		3.3587E-04	-3.5123E-05	2.8462E-04	5.8464E-02	-1.5069E-03	-1.8171E-04
980		3.3677E-04	-5.2346E-05	4.2549E-04	5.3552E-02	-2.2187E-03	5.4233E-05
1080		3.3882E-04	-7.3323E-05	5.5858E-04	5.3935E-02	-5.3316E-03	-2.9527E-03
1180		3.5096E-04	-9.6116E-05	6.7885E-04	4.3772E-02	8.9534E-03	-5.8147E-03

```
MAXIMUM       3.5096E-04   9.6113E-05   6.7885E-04   5.8464E-02   8.9534E-03   5.8142E-03
AT NODE       1180         180          1180         880          1180         180

MINIMUM       3.3496E-04  -9.6116E-05  -6.7885E-04   4.3772E-02  -8.9527E-03  -5.8147E-03
AT NODE       680          1180         180          180          180          1180
```

INCREMENT   3 SUMMARY

TIME INCREMENT COMPLETED 0.375   , FRACTION OF STEP COMPLETED 0.875
STEP TIME COMPLETED   0.875   , TOTAL TIME COMPLETED   6.88

N O D E   O U T P U T

THE FOLLOWING TABLE IS PRINTED FOR NODESET   TIP

NODE	FOOT-NOTE	U1	U2	U3	UR1	UR2	UR3
180		3.8062E-04	8.3125E-05	-2.6771E-04	9.5448E-03	-1.1256E-02	6.3823E-03
280		3.6760E-04	6.2213E-05	-2.3225E-04	2.0443E-02	4.7898E-03	3.0743E-03
380		3.6534E-04	4.3648E-05	-1.8257E-04	2.0323E-02	1.7847E-03	-7.8232E-05
480		3.6433E-04	2.9335E-05	-1.2355E-04	2.6000E-02	1.3078E-03	1.8166E-04
580		3.6450E-04	1.4837E-05	-6.1287E-05	2.2837E-02	2.9199E-04	3.2391E-04
680		3.6331E-04	3.1339E-10	-4.4754E-10	2.6179E-02	-1.3169E-08	-5.4825E-07
780		3.6450E-04	-1.4837E-05	6.1286E-05	2.2837E-02	-2.9196E-04	-3.2394E-04
880		3.6433E-04	-2.9335E-05	1.2355E-04	2.6000E-02	-1.3078E-03	-1.8273E-04
980		3.6534E-04	-4.3648E-05	1.8257E-04	2.0323E-02	-1.7848E-03	7.8255E-05
1080		3.6760E-04	-6.2213E-05	2.3225E-04	2.0443E-02	-4.7906E-03	-3.0761E-03
1180		3.8062E-04	-8.3127E-05	2.6771E-04	9.5443E-03	1.1257E-02	-6.3830E-03
MAXIMUM		3.8062E-04	8.3125E-05	2.6771E-04	2.6179E-02	1.1257E-02	6.3823E-03
AT NODE		1180	180	1180	680	1180	180
MINIMUM		3.6331E-04	-8.3127E-05	-2.6771E-04	9.5443E-03	-1.1256E-02	-6.3830E-03
AT NODE		680	1180	180	1180	180	1180

INCREMENT   4 SUMMARY

TIME INCREMENT COMPLETED 0.125   , FRACTION OF STEP COMPLETED 1.00
STEP TIME COMPLETED   1.00   , TOTAL TIME COMPLETED   7.00

N O D E   O U T P U T

148

THE FOLLOWING TABLE IS PRINTED FOR NODESET   TIP

NODE	FOOT-NOTE	U1	U2	U3	UR1	UR2	UR3
180		3.9039E-04	8.1871E-05	-1.3850E-04	-1.2415E-03	-1.2001E-02	6.5852E-03
280		3.7708E-04	6.0943E-05	-1.2975E-04	9.9025E-03	4.6303E-03	3.1207E-03
380		3.7475E-04	4.2552E-05	-1.0631E-04	9.8708E-03	1.6554E-03	-8.2738E-05
480		3.7370E-04	2.8597E-05	-7.2996E-05	1.5805E-02	1.2518E-03	1.8374E-04
580		3.7386E-04	1.4479E-05	-3.6089E-05	1.2661E-02	2.6448E-04	3.3158E-04
680		3.7264E-04	3.0880E-10	-2.1423E-10	1.6108E-02	-6.3261E-08	-5.5542E-07
780		3.7386E-04	-1.4478E-05	3.6088E-05	1.2661E-02	-2.6454E-04	-3.3162E-04
880		3.7370E-04	-2.8596E-05	7.2996E-05	1.5805E-02	-1.2519E-03	-1.8483E-04
980		3.7475E-04	-4.2552E-05	1.0631E-04	9.8708E-03	-1.6555E-03	8.2760E-05
1080		3.7708E-04	-6.0944E-05	1.2975E-04	9.9021E-03	-4.6312E-03	-3.1225E-03
1180		3.9039E-04	-8.1874E-05	1.3849E-04	-1.2422E-03	1.2001E-02	-6.5859E-03
MAXIMUM		3.9039E-04	8.1871E-05	1.3849E-04	1.6108E-02	1.2001E-02	6.5852E-03
AT NODE		1180	180	1180	680	1180	180
MINIMUM		3.7264E-04	-8.1874E-05	-1.3850E-04	-1.2422E-03	-1.2001E-02	-6.5859E-03
AT NODE		680	1180	180	1180	180	1180

THE ANALYSIS HAS BEEN COMPLETED

ANALYSIS COMPLETE
WITH   28 WARNING MESSAGES ON THE MSG FILE
        23 WARNINGS ARE FOR NEGATIVE EIGENVALUES

JOB TIME SUMMARY
    USER TIME   =   2200.6
    SYSTEM TIME =   88.210
    TOTAL TIME =   2288.8

BIBLIOGRAPHY

1.   Schrage, D.P. and Meyer, S.A., "Logistics Supportability Considerations During Conceptual and Preliminary Design", *Vertiflite*, Vol. 32. No. 2, March-April 1986, pp.48-51.

2.   Mark W. Nixon, "Preliminary Design of Composite Main Rotor Blades for Minimum Weight," NASA Technical Paper 2730, AVSCOM Technical Memorandum 87-B-6, July 1987.

3.   Mark W. Nixon, "Extension-Twist Coupling of Composite Circular Tubes with Application to Tilt Rotor Blade Design," AIAA. 1987.

4.   Armanios, E. A., Hooke, D., Kamat, M., Palmer, D., and Li, J., "Design and Testing of Composite Laminates for Optimum Extension-Twisting Coupling." *Composite Materials: Testing and Design (Eleventh Volume). ASTM STP 1206*, E. T. Camponeschi, Jr., Ed., American Society for Testing and Materials. Philadelphia, 1993, pp. 249-262.

5.   Chandra, R., Stemple, A., Chopra, I, "Thin-Walled Composite Beams Under Bending, Torsional, and Extensional Loads." *Journal of Aircraft*, Vol. 27, No. 7, July 1990, pp 619-626.

150

6. Armanios, E. A., and Li, J., "Interlaminar Fracture Analysis of Unsymmetrical Laminates," *Composite Materials: Fatigue and Fracture. Fourth Volume. ASTM STP 1156*, W. W. Stinchcomb and N. E. Ashbaugh, eds., American Society for Testing and Materials, Philadelphia, 1993, pp. 341-360.

7. Winckler, S. I., "Hygrothermally Curvature Stable Laminates with Tension-Torsion Coupling," *Journal of the American Helicopter Society*, Vol. 31, No. 7, July 1985, pp. 56-58.

8. Radford, D. W. (1993), "Cure shrinkage induced Warpage in flat uni-axial Composites," *J. of Composites Technology & Research*, Vol. 15 N. 4, Winter 1993, pp. 290-296.

9. Armanios, Erian A., Makeev, Andrew, and Hooke, David, "Finite-Displacement Analysis of Laminated Composite Strips with Extension-Twist Coupling," *Journal of Aerospace Engineering*, Vol.9, No. 3, July 1996, pp. 80-91.

10. Armanios, E. A., Hooke, D., and Makeev, A., "Geometrically Nonlinear Analysis and Testing of Extension-Twist Coupled Laminates With Hygrothermal Effects," *ASTM thirteenth Symposium on Composite Materials: Testing and Design*, Orlando, Fl, May 19-21, 1996.

11. Hooke, D.A. and Armanios, E.A.,"Design and Evaluation of Three Methods for

Testing Extension-Twist-Coupled Laminates." *Composite Materials: Testing and Design (Twelfth Volume), ASTM STP 1274,* R.B. Deo and C.R. Saff. Eds., American Society for Testing and Materials, 1996, pp. 340-357.

VITA

David A. Hooke was born on January 19, 1967 in Easton, Pennsylvania. He attended The Hill School in Pottstown, Pennsylavania, graduating in 1985. He then attended the Georgia Institute of Technology in Atlanta, Georgia, graduating with High Honor in 1989 with a Bachelor of Aerospace Engineering Degree. He continued his education in the school of Aerospace at Georgia Tech, earning a Master of Science degree in 1990. While at Georgia Tech, he married Shelley Jones in 1996.